PRODUCTION AND ANALYSIS OF BEAMS OF SYNTHETIC POLYMERS BY MASS SPECTROMETRY

Julie Elizabeth Varney

Submitted for the qualification of Doctor of Philosophy

UNIVERSITY OF WARWICK
DEPARTMENT OF CHEMISTRY

OCTOBER 1997

To
My Mother

ACKNOWLEDGEMENTS

I would like to thank my supervisor Professor Peter Derrick for his guidance and encouragement throughout my time at Warwick University.

I am grateful to Dr. Karoly Vekey and Zoltan Szilagyi for their enthusiasm, hospitality and help during my stay in Hungary.

All of the members of the MMM group both past and present have been good companions and a constant source of encouragement and humour.

British Petroleum Chemicals at Sunbury part funded this research and I am grateful to both of my industrial supervisors, Dr. Martin Smith and Dr. Phil McDowell for their support and also to Dr. P. Lyne who initially organised funding. I would also like to thank the University of Warwick for the other part of my funding, especially Professor Terry Kemp, who was instrumental in securing my place at Warwick. I would like to thank Andrea Mahon for her help with SEC measurements.

My friends and family have been extremely supportive throughout my research. I particularly wish to thank my mother, Judith Henstone, for her continuous encouragement throughout my education and the use of her computer. Finally, I am grateful to my partner Stephen Cooper, for his patience, understanding and the occasional use of his printer.

DECLARATION

I hereby declare that this thesis is my own work and that, to the best of my knowledge and belief, it contains no material previously published or written by another nor material which to sustantial extent has been accepted for an award of any other degree or diploma of a university or other institute of higher learning except where due acknowledgment is made in the text of this thesis.

Julie Elizabeth Varney

ABSTRACT

The conditions under which poly(styrene) standards up to m/z = 12 000 can be analysed by matrix-assisted laser desorption/ionisation (MALDI) have been optimised using 9-nitroanthracene as the matrix material in conjunction with silver tri-fluoroacetate addition. The development of such conditions permitted the analysis of a range of polymeric materials including poly(sulfide) samples and novel poly(isobutylene)samples containing aromatic ring functions of molecular masses up to 1000 Da. A series of calculations were carried out in order to assess the accuracy of molecular mass statistics for a range of PMMA and poly(styrene) standards of low poly(dispersity) values up to masses of 12 000 Da obtained by MALDI. It was found that data obtained were in good agreement with those derived from size exclusion chromatography measurements. Electrospray sample preparation was investigated as a method of increasing reproducibilities and signal-to-noise values in MALDI experiments. Electrospraying low mass poly(styrene) samples (up to 3000 Da) increased intensities, however, higher mass samples could not be detected using this method. Moreover, the traditional spotting method worked much better at higher masses.

Post-source decay (PSD) experiments have been performed on poly(ethylene glycol), poly(styrene) and the novel poly(isobutylene) samples previously investigated by MALDI using instruments fitted with curved-field and two-stage reflectrons. The type of information obtained using this method compared with tandem mass spectrometry techniques has been investigated. The effect of laser power and pressure has been studied. Ions formed by PSD processes were found to be the same as those formed by low energy CID processes. A range of standard peptide residues were also investigated as part of this work to highlight calibration difficulties associated with PSD analysis using a curved field reflectron.

Emitter activation and field desorption mass spectrometry experiments were attempted in order to study polymer materials with little success. Problems and difficulties associated with these experiments have briefly been described.

LIST OF FIGURES

Chapter One

Chapter Two

Chapter Three

Chapter Four

Chapter Five

Chapter Six

LIST OF ABBREVIATIONS

CID	**Collision-Induced Dissociation**
DE	**Delayed Extraction**
2,5 DHB	**2,5 Di-Hydroxy Benzoic Acid**
DOF	**Di-Olefinic**
DSC	**Differential Scanning Calorimetry**
EBEB	**Electric Magnetic Electric Magnetic**
EI	**Electron Impact**
ESI	**Electrospray Ionisation**
FAB	**Fast atom Bombardment**
FD	**Field Desorption**
FT-ICR	**Fourier-Transform Ion-Cyclotron Resonance**
HABA	**Hydroxyazophenyl Benzoic Acid**
IAA	**Indole Acrylic Acid**
IR	**Infra-Red**
LD	**Laser Desorption**
L-SIMS	**Liquid Secondary Ion Mass Spectrometry**
MALDI	**Matrix-Assisted Laser Desorption/Ionisation**
MIKES	**Mass Analysed Kinetic Energy**
MOF	**Mono-Olefinic**
MS/MS	**Mass Spectrometry/ Mass Spectrometry**
NMR	**Nuclear Magnetic Resonance**
PD	**Plasma Desorption**

PEG	**Poly(ethylene glycol)**
PIB	**Poly(isobutylene)**
PMMA	**Poly (methyl methacrylate)**
PS	**Poly(styrene)**
PSD	**Post-Source Decay**
Py-GC	**Pyrolysis- Gas Chromatography**
THF	**Tetrahydrofuran**
TIC	**Total Ion Current**
SEC	**Size Exclusion Chromatography**
TGA	**Thermal Gravimetric Analysis**
TOF	**Time-of-Flight**
UV	**Ultra-Violet**

TABLE OF CONTENTS

CHAPTER ONE

Introduction

1.1 General Background

Mass spectrometry has developed rapidly over the last few years and has become a powerful analytical tool, applicable in many new, exciting areas such as biological and polymer research. It is a highly sensitive technique which provides accurate information on molecular mass, and molecular structure by tandem techniques. This growth can be attributed to the development of new ionisation techniques coupled to advances made in instrumental capabilities.

Over one hundred years ago Goldstein observed luminous blue beams which radiated directly from the cathode towards the anode of an evacuated discharge tube [1]. It was later found that these rays were deflected by a magnetic field in the opposite direction to that of cathode rays and displayed various mass-to-charge ratios[2]. In fact, these beams were the first ion beams ever observed. Thompson continued to investigate these rays and built a positive ray analyser[3]. Thompson established that positively charged species were formed by the removal of electrons from neutral gas molecules in the discharge tube. This experiment used the same laws of motion that were discovered for the electron to interpret parabolic pathways followed by the ion beam as it passed through parallel electric and magnetic fields. Thompson later displayed the presence of isotopes using the same apparatus[4].

1.2 Ionisation Techniques

1.2.1 Overview

The growth of mass spectrometry and it ability to study new areas of chemical interest has closely followed the discovery of new ionisation methods. Discharge ionisation

was soon succeeded by the development of electron beam ionisation (EI), which was consistent in its ability to ionise gaseous atoms and small molecules. Electron impact involves the bombardment of gaseous or vapourised sample with a beam of high-energy electrons (70 eV). It is known as a 'hard' ionisation method since it tends to cause a large amount of fragmentation and, in many cases, the molecule ion cannot be detected. Yet despite these obvious disadvantages, electron ionisation continues to be used as a reliable fingerprinting technique. It may also provide information concerning the relative strengths of different chemical bonds.

The next important development was the introduction of chemical ionisation (CI) by Munson and Field in 1965[5,6]. This method involves the electron ionisation of a reagent gas. Sample molecules are then reacted with this gas resulting in ionisation of the sample. Chemical ionisation is generally regarded as a 'soft' ionisation technique, since abundant molecule ions are formed, allowing the determination of molecular mass.

Thermal decomposition of thermally fragile samples is a serious disadvantage in all the ionsation methods cited so far. A series of 'softer' ionsation techniques have been developed in order to overcome this problem and these include secondary ion mass spectrometry (SIMS)[7,8], fast atom bombardment (FAB)[9,10,11,12], plasma desorption (PD)[13,14], field desorption (FD)[15,16], electrospray (ESI)[17,18] and laser desorption (LD)[19,20] of which matrix-assisted laser desorption/ionisation (MALDI)[21] is the widely used variant. All of the ionisation methods except electrospray ionisation are desorption methods. A desorption ionisation process involved the rapid addition of energy into a condensed phase sample. This results in the formation and release of ions into the gas phase. A review of desorption ionisation has been published by Busch.[22]

1.2.2 Liquid-Secondary Ion Mass Spectrometry (L-SIMS)

SIMS was initially performed usually solid samples, however, the use of a liquid matrix was found to enhance sensitivity, reproducibility and stability of the method. L-SIMS closely resembles FAB ionisation in that both techniques make use of a liquid matrix, usually glycerol, for the reasons stated above. Both methods involve bombardment of the sample with particle beams. In L-SIMS, Cs+ are accelerated to potentials in the order of 10 keV or higher, and these are used as bombarding ions which are focused on the sample droplet. The continuous nature of the ion beam, which is formed from this process, makes it ideal for use with sector and quadrupole analysers. L-SIMS induces little or no fragmentation of high mass molecules and this has led to the application of L-SIMS to the study of fragile biological molecules upto 10 000 Da in molecular mass[23].

1.2.3 Field Desorption

Following the development of the electron emission microscope, Muller found that when a large positive potential was applied to a sharp metal tip, creating an electric field in the magnitude 10^8-10^{10} Vm^{-1}, molecules of the background gas were ionised[24]. Further, he demonstrated that ionisation of the gas was induced by the electric field. Inghram and Gomer used this effect and developed it by attaching a field ionisation microscope to a mass spectrometer[25]. The mass spectra obtained for various volatile compounds contained very little or no fragmentation in contrast to those obtained by 70 eV electron impact. Interest in field ionisation grew rapidly since these discoveries came at a time when a less harsh ionisation technique was needed. Beckey and his co-workers first reported the technique of field ionisation for the ionisation of substances of low volatiliy deposited onto the surface of an emitter [15] Robertson and co-workers[15b] noted that ion currents were increased after several hours of field ionisation of an organic gas. This increase in ion current was later attributed to the

growth of microneedles on the emitter wire during ionisation. The process of growing these micro-needles which enhanced the fields was developed further by Beckey and labelled' high temperature activation.' [26a] This method involves the formation of carbon micro-needles from organic vapours under high vacuum (0.1-1 Pa) in an intense electric field (6-15 kV potential difference between the emitters and the counter electrode.) A solid sample was loaded onto an activated emitter by dipping the emitter in a solution of the sample and evaporating the solvent. Later, a syringe technique for sample loading was developed by Beckey [26b] This ionisation technique of loading the solid sample directly onto the emitter and obtaining a mass spectrum under field ionisation condition is known as field desorption. Extensive research into emitter activation by Beckey *et al.* found that benzonitrile was one of the most efficient substances for the activation process[27,28]

1.2.3.1 Emitter Activation

Successful field desorption mass spectrometry (FD-MS) heavily relies upon a regular supply of activated emitter wires with reproducible parameters. The emitter growing process is particularly long process, the traditional methodology employed by Beckey taking up to 50 hours. This method typically involves spot welding tungsten wire either 10μm or 25μm in diameter onto two support posts, usually made of nichrome, on a ceramic base. Care has to be taken to ensure that emitter wires are welded with consistency in order to achieve batches of emitter wires with similar resistance values. Benzonitrile had classically been used as the activating agent.

A variety of different approaches have been tried and tested in order to develop faster and less complex methods including the development of different pre-activation treatments of the emitter wire, the use of alternative activating agents, the generation of silicon whiskers and the development of so-called 'high-rate' activation processes.

Rabrenovic and Ast tested a variety of different organic compounds including indane, indole and naphthalene as an alternative to benzonitrile[29], however, the microneedles which formed were thick and dense and, therefore, less effective at promoting desorption. Non-carbonaceous emitters have been investigated by many different research groups. Copper, lead and silver microneedles have been grown electrochemically on tungsten wire[30,31], and Matsuda and co-workers have developed the use of silicon emitters[32]. Linden modified Beckey's high temperature activation procedure to produce a 'high-rate' activation technique[33]. The efficiency of these emitters has been found to be sufficient for normal FD experiments, although, the adhesive strength of the needles to the wire has been observed somewhat inferior compared with those made using the classical technique[34]. More recently, Kosevich has described a new type of graphite emitter which was simply formed by fracturing a graphite rod[35]. It was observed , however, that the relative intensities of ions were approximately an order of magnitude lower than when standard carbon-activated emitters were employed.

Overall, emitters activated at high temperatures with benzonitrile as the activating agent still offer the best performance in terms of durability of the micro-needles when subjected to chemical attack, mechanical stress or high temperatures. Furthermore, this method is the most widely activation technique used today.

1.2.3.2 Mechanism of Field Desorption

Field desorption/ionisation is based upon the fact that atoms and molecules can be field ionised when they are subjected to high electric fields in the order of 10^8 Vcm^{-1}. The mechanisms of field desorption of involatile compounds have been discussed on the basis of field ionisation developed by Gomer[36]. The relative magnitudes of the work function (ϕ) of the emitter and the ionisation energy (IE) have been postulated to be the determining factors. If the ionisation energy of the emitter is of approximately the

same magnitude as the work function, the ion evaporation is said to be the dominant field desorption process. If the ionisation energy is much greater, then the pathway becomes dependent on the field strength and separation between ionic and neutral levels.

Figure 1.1 depicts the difference in sample supply between field ionisation and field desorption.

Figure 1.1

Schematic Diagram Illustrating the Definition of Field Ionisation and Field Desorption [16]

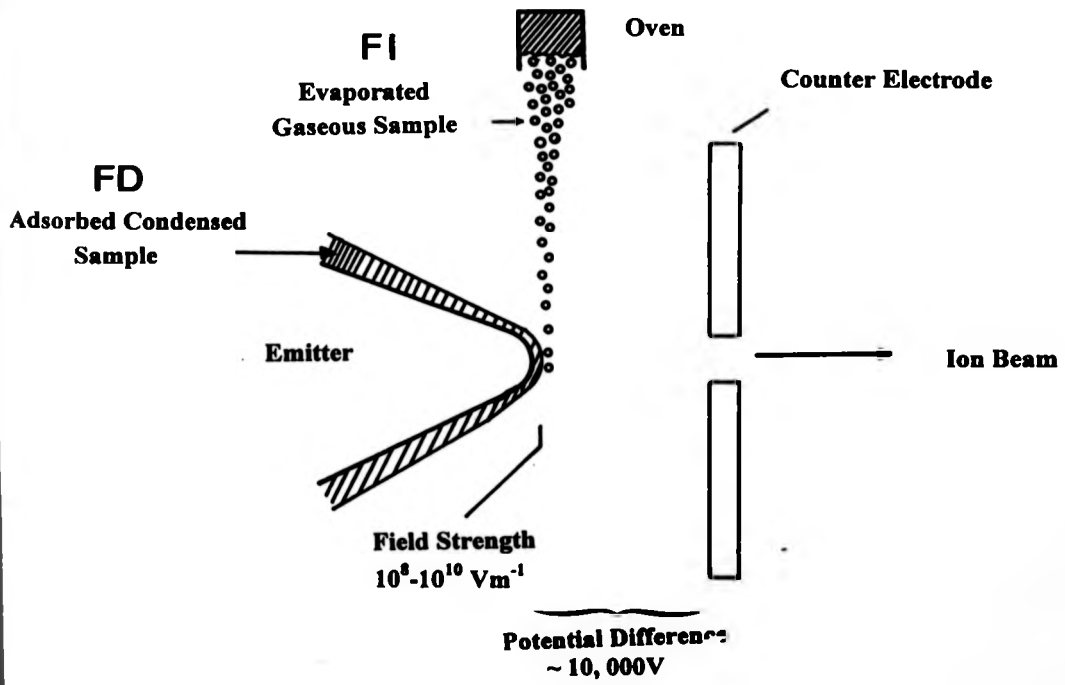

The many processes, which contribute to ion formation in field desorption mass spectrometry, may broadly be separated into low field (10^7-10^9 Vm^{-1}) and high field processes. (> 10^9 Vm^{-1}) Derrick proposed a 'field evaporation' mechanism at low field energies[37]. The essential feature in this mechanism for the formation of gaseous ions from involatile samples is the setting up of an electric charge at the interface between the sample and the vacuum. The next stage is the evaporation of the charged species from the condensed phase. According to Giessmann and Rollgen[38], in high field processes, the dominant mechanism is field-induced tunnelling of an electron (field ionisation) and mainly $M^{+\cdot}$, $[M+H]^+$ and $[2M]^{+\cdot}$ ions are formed.

Figure 1.2 ; Schematic Diagram of the Mechanism of Field Desorption/Ionisation[16]

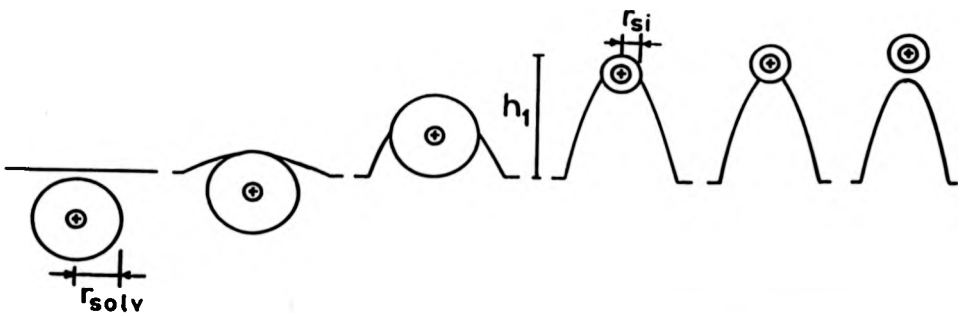

r_{solv} is the radius of the solvation sphere, r_{sl} is the radius of the separating species, and h_l is the height of the protuberance when the radius of its parabolic tip equals r_{sl}

1.2.4 Laser Desorption

Initial attempts to use laser ionisation for the analysis of organic compounds dates back to the 1970's. The desorption of intact molecule ions from large complex biomolecules

such as stachyose and digitonin may be regarded as important landmarks in the development of laser desorption/ionisation processes[19]. In order to reduce the thermal decomposition of labile organic molecules, lasers of a short-pulse duration were needed. This requirement coupled with ability of monochromatic laser beams to be focused very tightly on small spots has meant that laser desorption methods are particularly suitable for use with time-of-flight and Fourier transform ion cyclotron resonance analysers.

1.2.5 Matrix-Assisted Laser Desorption/Ionisation

The desorption methods described above involve direct laser desorption.. The main disadvantages with direct laser desorption are that 'soft ' desorption processes are limited to a small irradiance range and too high irradiance levels result in extensive fragmentation of the analyte. Furthermore, the upper mass limit for transferring intact biomolecules into the gas phase using this technique is about 1000 Da and for synthetic polymers the limit can only be extended upto a few thousand. Thus, the limitations of direct laser desorption methods promoted the search for small highly UV-absorbing organic compounds which might be used as matrices.

In the 1980's Tanaka and co-workers introduced the idea of mixing a matrix together with a biopolymer analyte in order to carry out desorption/ionisation process, without inducing fragmentation[39]. The method of sample preparation was novel and involved dissolving the analyte in glycerol and mixing this solution with a fine metal powder. A droplet of the resulting mixture was irradiated at 337nm using a nitrogen laser and the ions were analysed in a reflectron time-of-flight mass spectrometer. Glycerol is transparent and does not absorb at 337nm, however, the fine metallic particles present in this mixture would have absorbed the laser light highly effectively. The metal particles used were smaller in size than the wavelength of the incident light, thus, a current would have been created owing to the spatially coherent and rapidly varying

nature of the electromagnetic field of the laser light. The current would have had a heating effect and, owing to the low heat capacity of the metal particles, this heat would have been rapidly transferred to the glycerol matrix. The mechanism by which this energy is transferred to the analyte is not fully understood, however, the analyte molecules are consequently desorbed into the gas phase and detected as ions.

The development of matrix-assisted UV laser desorption/ionisation began in earnest when studies were carried out by Hillenkamp, Karas and colleagues in 1985 based on the desorption properties of smaller organic molecules, mainly amino-acids and di-peptides.[40,41] They hypothesised that large molecules could be desorbed intact into the gas phase with the use of a suitable organic matrix[42]. The mechanism of the MALDI process would involve the absorption of sufficient light by the matrix to result in its ablation and that this ablated matrix would be able to carry larger analyte molecules into the gas phase. Ion-molecule interactions in pulsed supersonic jet expansions would occur resulting in enough charge being transferred to analyte molecules. Such ions would be analysed and detected by time-of-flight mass spectrometry.

The breakthrough for MALDI came when Hillenkamp demonstrated this idea when polypeptide analytes were studied using nicotinic acid as a matrix material[43]. Analytes were dissolved in water and mixed in a ratio of 1:1000 with nicotinic acid. Nicotinic acid absorbs light strongly at 266 nm so a quadrupled Nd:YAG laser (base wavelength of 1064nm) was used to irradiate a crystal of the above mixture, formed by drying in air. Irradiance at just above the threshold resulted in high signal-to-noise ratios being observed in the time-of-flight mass spectrum.

The main advantage of this sample preparation method compared with that demonstrated by Tanaka and co-workers was increased sensitivity, picomoles and femtomoles of analyte yielding results of high quality. Sensitivity is a primary concern in the analysis of biomolecules where the sample is scarce. The consequence of this

perception is that the Hillenkamp-Karas method became the focus of international research while Tanaka's method did not receive as much attention. MALDI has maintained its roots bioanalysis in and the mass range of samples analysed by this method has been extended to 100 kDa using Fourier-transform ion cyclotron resonance (FT-ICR) mass spectrometry and in 1994, Solouki, Gillig and Russell detected a dimer of transferrin upto mass 157kDa using this technique, however, resolution was low[44, 45].

Analyte concentration for biomolecules is generally between 10^{-4} and 10^{-5}M, however, for polymers, the analyte solution is usually slightly higher at 10^{-3}M. In both cases, the matrix solution is 10^{-1}M.

The chemical conditions under which MALDI experiments are performed may in fact significantly alter the quality of the spectra obtained. High salt concentrations may lead to a loss of both mass resolution and accuracy and this may partly be attributed to adducts of analyte with matrix, mediated by salt cations. Both pH and solvent polarity effect the extent of ion formation, suggesting that these adducts may be formed prior to desorption[46, 47].

The most important parameters for the MALDI process are laser power and spot size. Yau and co-workers[48] discussed the problems of focusing laser beams onto the sample with standard optics and changing the laser fluence and more recently, Hillenkamp[49] and co-workers investigated these parameters further. Low laser power does not yield any ions initially, however, as the power is increased, matrix and analyte ions are detected. The point at which this occurs is defined to be the threshold laser energy. In general, MALDI experiments are carried out at a laser fluence just above this value where maximum signal-to-noise is achieved. Higher laser powers result in lower resolution and higher noise until, eventually, the analyte signal becomes suppressed.

Figure 1.3 depicts the behaviour of the analyte ion as a function of laser irradiance near ion production threshold.

MALDI usually yields singly-charged analyte molecule ions for both biomolecules and synthetic polymers, however, under specific conditions, cluster ions are detected. Biomolecules are ionised by proton attachment giving [M+H]+, however, other adduct species have been observed. Biomolecule adduct peaks are caused by salts, contaminants, fragments or intact matrix molecules. (Polymers are generally detected as cation-attached oligomer ions.)

1.2.5.1 Mechanism of MALDI

The fundamental mechanisms of MALDI are still not sufficiently understood to perform optimisation of instrumental parameters other than by trial and error, although a great deal of research has been devoted to investigating and improving various aspects of MALDI.

Two theories to describe the mechanism have been postulated by Hillenkamp *et al* [50,51,52] and Russell *et al* [53,54] respectively. Hillenkamp *et al* have described photo-ionisation as the common initial ionisation step which is followed by a series of ion-molecule reactions, whereas, Russell *et al* have postulated that proton transfer by an excited state neutral matrix species to a neutral analyte molecule occurs. In both cases, theories are largely based on experimental results obtained using peptides as analytes and aromatic acids, such as sinapinic acid, as the matrix.

Early work by Hillenkamp and colleagues have described the mechanisms of laser ion formation[55]. Primary reactions include energy transfers from the laser to the sample by linear or non-linear absorptions, and a series of secondary energy transfers such as collisions, heating, chemical reactions such as proton transfer or alkali-metal transfer,

Figure 1.3;

The Behaviour of Protein Ion Intensity as a Function of Laser Irradiance Near the Ion Product Threshold

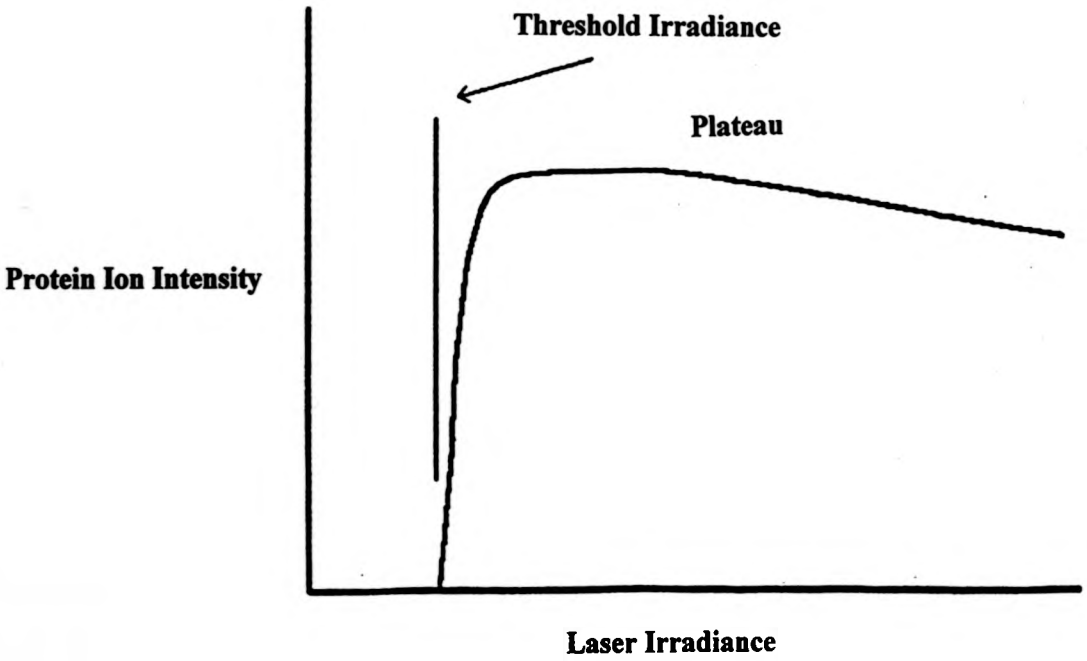

metastable decay or photofragmentation which strongly influence the type of spectra recorded.

Russell and colleagues have focused on proton-transfer mechanisms and have hypothesised that protonated peptides are formed by proton transfer reactions between an excited state of the matrix and the ground state of the neutral analyte. Further, guided by this theory they have experimentally demonstrated that conformations of peptides may be changed in order to probe secondary structures in peptides[56], and optical spectroscopic properties of MALDI matrices have been measured in order to probe relaxation pathways for excited state molecules[57]. Speculation about when exactly the protonation of an analyte occurs has arisen and Kinsel *et al* have attempted to investigate reactions occurring in the solid to gas transitional cluster phase[58].

A series of experiments by Amster *et al* [59] has shown that the source of protons in sinapinic and α-cyano-4-hydroxy cinnamic acids is the carboxylic acid function. Such studies of exchangeable protons are inconsistent with the model of excited-state species presented by Russell but rather support photoinduced chemical ionisation proposed by Hillenkamp. More evidence to support this model was presented by Dubois in his study on the effect of salt on the quality of MALDI spectra obtained[47]

Investigations of velocity and angular distributions of MALDI ions have led to the idea that after matrix excitation and sample deposition, analyte ions are entrained in a supersonic jet of matrix ions. Recent work by Kaufmann and Spengler has investigated the dynamical parameters of ion ejection and ion formation during the MALDI process[60]. A model of the analyte ionisation process in the gas phase which is driven by the kinetic parameters and the proton affinities of the matrix and analyte has been suggested.

1.2.5.2 Matrices in MALDI

The first condition which a material must satisfy to be successfully used as a matrix is solubility so that both the analyte and the matrix may be dissolved in the same solution. Sample preparation methods do exist which allow this condition to be overcome, and these involve depositing discrete layers of matrix followed by analyte, however, improved reproducibility is obtained using the homogeneous sample formed by mixing. The second requirement is absorption which allows energy to be deposited into the matrix, not the analyte. Most solids' absorption curves are red-shifted compared with their solution values and the extent of this shift varies from compound to compound. In general, solution absorptions are used as a guide. This condition is very restrictive and, in practice, the choice of matrix material is limited to compounds containing aromatic functions with electron-withdrawing groups on the ring. The wavelength of the laser light is less critical and many wavelengths have been tested out. Pulsed UV laser light has become the most commonly used partly because in most cases, the analyte remains transparent to the light and, therefore, unwanted photochemical reactions are avoided. The third requirement is reactivity. Matrices which covalently modify proteins or other analytes may not be used. Low sublimation rates , that is stability under vacuum is another important factor. High vapour pressures disturb the vacuum and result in significant changes during a single experiments matrix-to-analyte ratio and the short life-time of the sample. Even if a material satisfies all of the conditions stated above, there is no guarantee that it will work experimentally.

MALDI was developed primarily to investigate large biomolecules and some of the first matrices discovered reflect this fact. Apart form nicotinic acid, which was abandoned as a matrix owing to photochemical reactivity, some of the most commonly used matrices included ferulic acid, sinapinic acid and gentisic acid[61,62]. The structures of some of the early matrices used in MALDI are depicted in **Figure 1.4.** All the matrices described so far improved the sensitivity and were found to yield [M+H] +

Figure 1.4 ; Structures of matrices used in early MALDI experiments

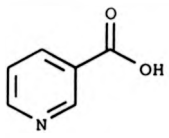

Nicotinic Acid

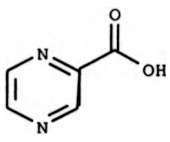

Pyrazinoic Acid

Gentisic Acid

(2,5 DHB)

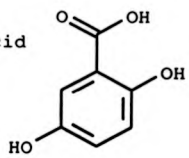

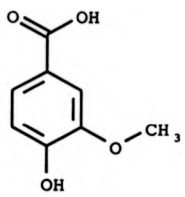

Vanillic acid

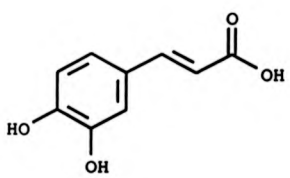

Caffeic acid

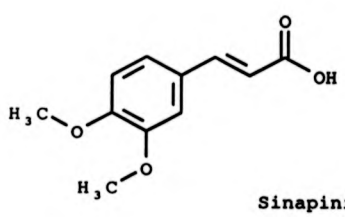

Sinapinic acid

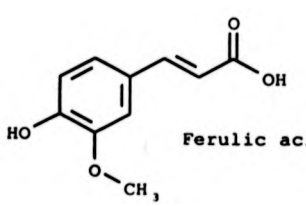

Ferulic acid

hydroxycinnamic acid, used in the analysis of peptides was discovered by Beavis and Chait[63]. This matrix has displayed increased ability to induce fragmentation of the analyte, a characteristic which has proved to useful in post-source decay experiments[64,65]

Some of the more recent developments in terms of the analysis of biological molecules have been the extensive investigations of substituted cinnamic acid derivatives to the analysis of a wide range of peptides and larger proteins with limited success[66] . 4-hydroxybenzylidene malonitrile (4-HBMN), which is also structurally similar to α-cyano-4-hydroxycinnamic acid, has been shown to be useful in the analysis of water insoluble analytes[67]. Furthermore, ice as been investigated as a suitable matrix for infra-red MALDI mass spectra of peptides[68a,68b,69].

In terms of the analysis of synthetic polymers by MALDI, a significant breakthrough came when 2,5 di-hydroxybenzoic acid was discovered as a suitable matrix material[70]. 2,5 Di-hydroxybenzoic acid was originally discovered and applied to the analysis of proteins and its use was extended by the same group to the analysis of a variety of different polymers which included poly(ethylene glycol), poly(propylene glycol) and poly (methyl methacrylate)[71]. Additives have used to enhance its performance in the analysis of proteins and oligosaccharides[72]. These are not generally used in the analysis of polymers. Poly(styrene) was investigated by MALDI using a liquid matrix, nitro-pheny octylether[71]. Since these initial experiments, extensive efforts have been devoted to searching for matrices which can efficiently volatise and ionise synthetic polymers. Danis and Karr reported the use of trans-3-indoleacrylic acid (IAA) for poly(hydroxystearic acid) and poly(methyl methacrylate)[73]. Costello and Juhasz studied oligometallocenes using 2-(4-hydroxyazo) benzoic acid (HABA), originally used in the analysis of biopolymers, and anthracene derivatives, such as dithranol as matrices[74]. Subsequently, Montaudo and co-workers substantially enhanced the detection of poly(styrene) and poly(buylenedipate) using HABA[75], a matrix which had previously been limited to the analysis of peptides and proteins .[76]

More recently, MALDI spectra of both poly(ethylene glycol) and poly(butadiene) were reported using azo-compounds as matrices[77]. The need to analyse a wide variety of different compounds by MALDI, which experimentally is a relatively simple mass spectrometry technique, has led to the search for new matrix materials in many different directions. Some of the more recent advances include the analysis of relatively hydrophobic compounds using glycerol mixed with potassium hexacyanoferrate[78] , and investigations into the possibilities of using electron transfer reagents such as carbon sixty[79] and polycyclic aromatic compounds as matrix materials[80]. It is hoped that the use of these matrices will lead to the analysis of inorganic complexes and more non-polar species.

Following the success of MALDI in the ultra-violet (UV) range, studies were carried out by Hillenkamp and co-workers on the application of the infra-red (IR) to this ionisation method.[81a,81b]. Short pulse IR lasers such as Er-YAG (Erbium-yttrium aluminium garnet, λ = 294 nm). It was found that all compunds suitable for use in the UV region were suitable for use in the IR range. Furthermore, a large range of aliphatic carboxylic or hydroxy containing compunds may also be used in the IR range. Sensitivities were comparable to UV-MALDI. IR-MALDI generally produces more highly charged macromolecule ions and larger amounts of sample ions are ablated per single laser shot. It is hoped that IR-MALDI will eventually complement UV-MALDI. The larger variety of usable matrices will certainly prove to be advantageous.

1.3 Detection and Separation Methods

There are several techniques commonly used for the mass analysis of ions according to their mass-to-charge ratios. These are sector analysers, quadrupole mass filters, time-of-flight analysers, ion trap analysers and ion cyclotron analysers. Detailed discussions of these methods can found elsewhere[82,83] and a description of those most relevant to this research will be presented.

1.3.1 Overview

Growth in the application of mass spectrometry mirrors advances made in instrumental capabilities and the development of new ionisation techniques. Time-of-flight mass spectrometry has regained popularity since its initial introduction in 1955 by Wiley and co-workers[84] with the development of matrix-assisted laser desorption as a reliable ionisation for both polymers and biomolecules. Ion cyclotron resonance analysers coupled with electrospray ionisation also displays enormous potential in solving complex biological issues [85,86].

1.3.2 Sector Analysers

The original and most obvious way of analysing charged species of different masses is to use a magnetic field in the form of a magnetic sector analyser which is essentially a momentum analyser. An ion of mass-to charge ration m_i / z_i will be brought to a focus at the focal point of the magnetic field where:

$$m_i / z_i = B^2 r_i^2 / 2V$$

It can be seen that the radius r_i of the ion's path is directly proportional to the square root of its mass. Higher mass ranges are, therefore achieved either by detecting the paths of large radii, using higher strength magnetic fields or by reducing the

acceleration potential. Extension of the mass range to higher masses by lowering the ion acceleration potential often leads to reduced sensitivity. Furthermore, the mass resolving power of an instrument using only a magnetic sector analyser is limited by an energy dispersion value. A major improvement is observed when an electric sector is coupled with a magnetic sector in either a so-called reverse geometry or normal geometry configuration.

An ion of mass-to charge ration m_i / z_i passing through an electric field of strength E will follow a circular path whose radius r_i is dependent on the energy-to-charge ratio:

$$m_i v_i^2 / r_i = E z_i$$

which gives

$$m_i v_i 2 / z_i = E r_i$$

Herzog found a general solution for the paths of charged species in the presence of magnetic and electric fields[87]. Mattauch and Herzog matched complementary sectors in order to focus a diverging non-monoenergetic beam based on Herzog's previous work. This design proved to be very popular and was used in the 100" Argonne isotope analyser built in the 1960's.[88,89]. Johnson and Nier went on to improve previous designs to develop a 'Nier-Johnson' geometry instrument which is presently the most widely used sector instrument[90]

1.3.3 Time-of-Flight Analysers

Time-of-flight (TOF) mass spectrometry was prominent in the field early on during the 1960's, however, it was soon replaced as research focused on the application of magnetic and quadrupole analysers to mainstream mass spectrometry with their higher

mass resolving powers and improved sensitivities. One of the main reasons for the apparent lack of growth in TOF has been technological drawbacks, most recorders and processors being incapable of coping with microsecond time-frames. Technological advances have now been made in order to deal with this requirement and TOF is now beginning to re-appear as a sound candidate for the analysis of large molecules and for mixture separation.

A brief overview of TOF is presented in the proceeding section. A more detailed description of the principles and instrumentation in TOF has recently been published by Guilhaus[91].

1.3.3.1 Linear Time-of-Flight Mass Analysers

A linear time-of-flight analyser is a simple method of separating species according to their mass. Consider two ionised species created at specific time in a homogeneous electrostatic field. In the ideal case, after leaving the acceleration region, their kinetic energies will be the same, their velocities being unambiguously related to their mass-to-charge ratios. For a particular charge state, the times of arrival at the detector are proportional to the square roots of their masses.

In a time-of-flight analyser ions are formed in a short source region (s) in the presence of an electrical field, (E) which accelerates the ions into a longer, field-free region (D). Ideally, all ions enter this region with the same kinetic energy (KE) :

$$KE = zeEs$$

e is the charge on an electron, z is the number of charges on the ion and the velocity v of an ion of mass, m is given by:

$$v = (2zes / m)^{1/2}$$

This equation gives the mass resolution for the time-of-flight mass spectrometer as:

$$\Delta m / m = 2\Delta t / t$$

Δt is the peak width.

A schematic representation of a linear time-of-flight mass spectrometer is depicted overleaf in **Figure 1.5**

In reality when ions of different masses are accelerated through the source region their kinetic energies will be spread out over some range of energies

1.3.3.2 Historical Overview

The principle of time-of-flight mass spectrometry was demonstrated for the first time by Stephens in 1946[92] Time-of-flight instruments have been particularly successful in the analysis of high mass ions (m/z >10 000)[93,94]. In principle, the mass range is unlimited since the mass-to charge ratio is determined through the direct measurement of the time-of-flight of the ions although in practise, it is not as easy to detect and ionise large fragile molecules without inducing fragmentation processes. Calibration is generally a straightforward procedure, and time-of-flight mass spectrometers are easy to set up and tuning is generally a simple procedure. This type of analyser is particularly suited to pulsed ionisation techniques where the sensitivity is enhanced as all ions are collected together, offering an obvious advantage over sector and quadrupole instruments. This property is known as the 'Fellgett Principle.' The major disadvantage with time-of-flight experiments is poor resolution although this may be significantly improved with the use of delayed extraction in the ion source combined with the use of an ion reflectron. Both of these are discussed later.

In reality, there are a number of time-widening parameters in addition to the initial energy spread For example, the spread in position of ion formation which will cause a

Figure 1.5

Schematic Diagram of a Time-of-Flight Analyser

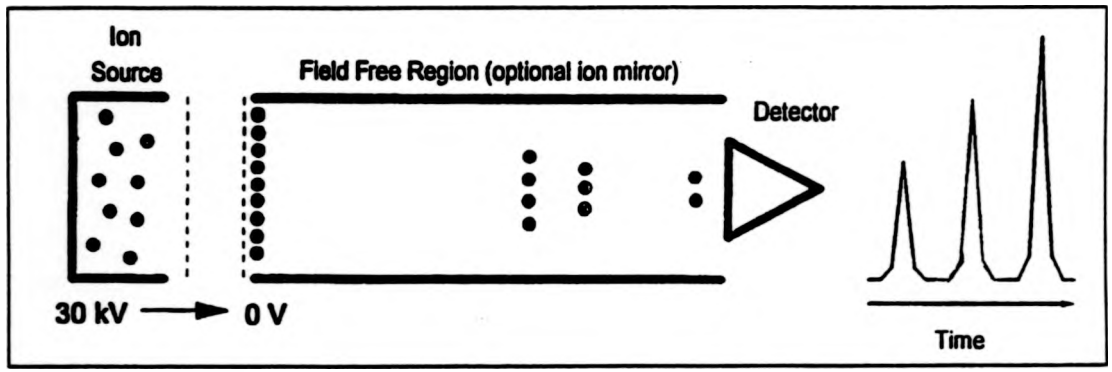

high energy ion, which has started its flight further away from the exit electrode, to pass a low energy ion at a point in the field -free region known as the space focus point. The nearer this point is to the source region, the greater the spread of the ions. By addition of a second acceleration region and the proper choice of the electric fields, the location of the space focus point can be shifted to positions further away from the ion source and, therefore, to longer flight times resulting in an improvement in resolution. Other parameters which may result in a decrease in resolution are metastable ion formation and ion optical aberrations.

1.3.3.3 Ion Reflectron Time-of-Flight Mass Analysers

In 1973, Mamyrin[95] and co-workers suggested a compensation for the flight time differences of ions with different kinetic energies by stopping them in a decelerating electric field and by reversing their flight direction before detecting them. The idea was that high energy ions penetrate deeper into the reflectron field and thus spend longer in the device than ions of a low energy. If the retarding field of the reflectron is adjusted properly, then this effect can be used to compensate for the different times of the ions in the field-free regions.

There are currently three main types of ion mirror: single-stage, double-stage and quadratic (curved) field. Single-stage reflectrons are the simplest type and consist of two-flat grids used to create a homogeneous electric field. The first grid is positioned at the entrance of the ion mirror and the second is located at the end. Homogeneity of the field can be improved by using a series of equally-spaced ring electrodes placed between two end electrodes which are connected with a chain of equal-value resistors. The flight-time in a single-stage reflectron is proportional to $(m / ze)^{1/2}$ and the disadvantage of these reflectrons is that a velocity spread still persists. Mamyrin[96,97] showed that it was possible to remove this velocity spread using a double-stage ion

mirror, where a second grid is positioned within the ion reflectron in order to define two homogeneous field regions possessing different electrostatic field values. Finally, ion beams with large energy spreads can be resolved effectively with the use of a quadratic or a curved field reflectron. Unlike conventional linear time-of-flight reflectrons which focus product ions according to their mass dependent kinetic energies, quadratic field reflectrons focus ions independent of their energy spreads.

It was postulated that if an electric field with an infinite number of potential gradients could be introduced all aberrations would vanish resulting in a high resolution for ion beams with large energy spreads. The physical analogue of such a reflectron is a pendulum. Time-of-flight is completely dependent upon the mass-to-charge ratio of an ion, not their initial velocities. The electrostatic field is described by the following potential distribution :

$$U(x) = 1/2\ k\ (x-a)^2 + C$$

k and C are all constants, U is the electric field potential and a defines the co-ordinates of the minimum potential field strength as shown in **Figure 1.6.**

In summary, the introduction of the ion mirror and its subsequent development to date has led to the re-birth of time-of-flight mass spectrometry as an efficient and commercially viable means of analysing high-mass ions with medium to high resolutions .

1.3.3.4 Delayed Extraction

One of the main drawbacks of MALDI coupled with TOF is the high energy spread of the analyte beam which can be attributed to the spread of initial velocities of the analyte ions. One of the most widely used solutions has been to increase the acceleration potential which, at first glance, is a particularly good solution since larger molecule ions formed in the MALDI process need to be accelerated to high energies to

Figure 1.6

Electric Field Potential in a Quadratic Field Reflectron[112]

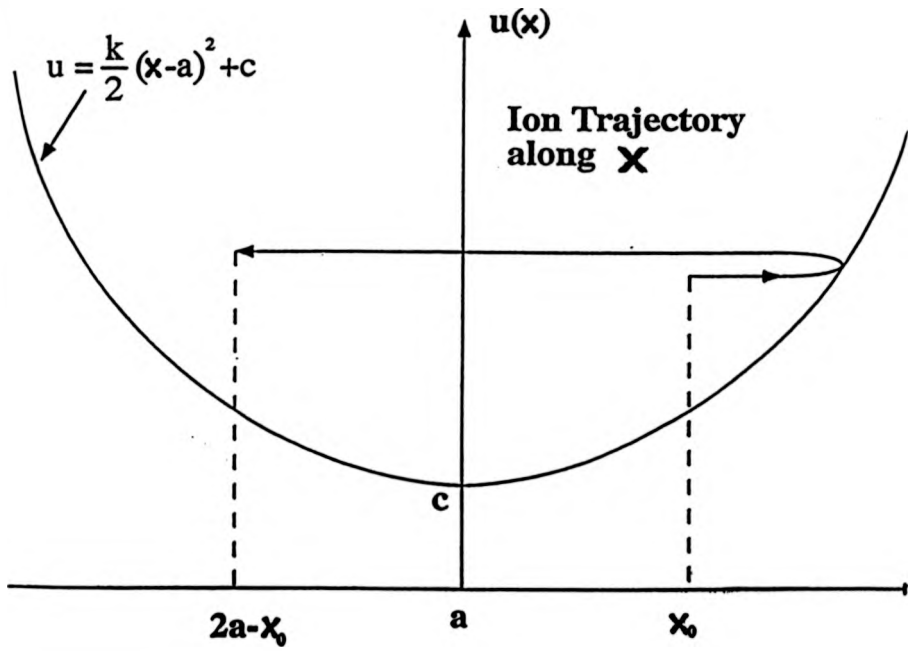

be detected. However, increasing the acceleration potential does create further difficulties and, in fact, results in a further increase in the energy spread of the analyte ions. As the analyte ions are ionised they become aware of the high electric field and acquire extra velocity. Random collisions occur with neutral gas molecules in a dense plume and can either be stopped or deflected off in random directions.

The chaotic nature of the whole process results in a small amount of fragmentation along with an increased energy spread of ions.

Delayed extraction or time-lag focusing was a method,originally devised by Wiley and McClaren[84], and used to improve the resolutions of early TOF mass spectrometers to acceptable levels of a few hundreds. Suitable pulse were applied to the ion source so that initial energy spreads of the ion packet were partially compensated for. In this early instrument, the ion source consisted of two parts. Ions were created in the extraction region by a timed electron beam, of typical time-width of 1μs and, as they drifted apart, a 'pusher-pulse' was applied to one of the sides of the extraction region at a certain time delay. This meant that ions at the rear end of the ion packet eventually acquired more energy than those in front and were able to catch up with them further down the ion trajectory.

Wiley and McClaren focusing with gas sources cannot achieve resolutions better than a few hundreds, since this technique compresses random ion packets. This, in effect, means that initial positions of ions are in no way related in their initial energies prior to the extraction pulse, thus ions at the front may still have higher or lower energies than those at the rear.

Delayed extraction has recently been employed as a new method for improving mass resolution in MALDI-TOF analysis and has been reported to obtain resolutions upto 10, 000[98]. The reason why the modern-day version works so much better than the Wiley and McClaren version is that as ions drift in the field-free MALDI source, those with higher velocities are in positions related to their velocities. The ions at the front

end of the extraction region acquire less energy than those at the back when the extraction pulse is switched on and correct choice of the extraction pulse's parameters can lead to practical elimination of energy spread effects on resolution. Furthermore, since the ion plume becomes less dense during its expansion, unwanted fragmentations by CID processes are reduced.

Examples of the application of MALDI-TOF coupled with delayed extraction methods are detailed later.

1.3.4 Fourier Transform Ion Cyclotron Resonance Analysers

Fourier transform ion-cyclotron resonance (FT-ICR) is based on the cyclotron motion of ions trapped within a uniform magnetic field and was initially introduced by Comisarow and Marshall in 1974[99]. This type of mass spectrometer operates on the principle of induction of a current by a charge in a conductor. The principle of cyclotron resonance in a Fourier-Transform mass spectrometer is shown in **Figure 1.7.**

Figure 1.7

Principle of ion cyclotron resonance

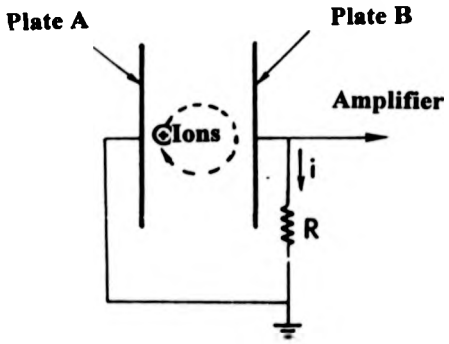

When a group of positively charged ions move between two-plates A and B, an electron flux is induced as electrons accumulate on these plates. This flux is determined by the interaction of electrostatic forces. In FT-ICR, ions are made to follow a circular

path between these two plates by the application of a magnetic field resulting in an alternating current between the two plates. The amplitude of the alternating current is dependent on the number of ions and the frequency f is related to m/z in the following way :

$$f = 2\beta / 2\pi m$$

β is the strength of the magnetic field.

Ions do not reach the detector but are detected by means of this alternating current image.

If several ion species are present then the alternating signal is complex, consisting of various frequencies which are superimposed. The frequency spectrum obtained corresponds to the mass spectrum and is deconvuluted by the FT analysis.

In theory ion cyclotron resonance has an extremely high resolution and should also be highly sensitive. In addition, to their use as conventional mass spectrometers, FT-ICR's are very versatile instruments and can be used to study comformation changes of proteins in the gas phase by hydrogen/deuterium exchange reactions[100], collision-induced decomposition reactions[101] and photodissociations of gaseous molecular or fragment ions[102].

1.4 Tandem Mass Spectrometry

Tandem mass spectrometry or mass spectrometry/ mass spectrometry (MS/MS) is a technique which employs two stages of analysis. The utility of MS/MS as a method for structural determination rests on the following relationship :

M $\Rightarrow$ molecule-ion $\Rightarrow$ fragment ions

A neutral molecule is ionised to form a molecule-ion. In the case of positive ions, this may take the form of the molecular ion, M+, a protonated molecule [M+H]+ or a

cationised species such as [M+K]+, depending on the ionisation method used. MS/MS was initially designed and used for fundamental studies in gas-phase ion chemistry and it is now extensively used for the structural elucidation of organic ions and for the analysis of organic mixtures. In general, MS/MS methods are used in conjunction with 'soft' ionisation methods which produce high intensities of the parent ion. Discussion here will be limited to the two main ionisation techniques used during the course of this work and their application to synthetic polymers.

1.4.1 Sector Tandem Mass Spectrometry

Experiments were initially intended to be performed on a large-scale four sector instrument of forward geometry (EBEB) as described in chapter 2, using field desorption/ionisation mass spectrometry.

There are three important parameters in all sector experiments and these are acceleration potential, V, the magnetic field strength, B and the electric field strength, E. Normal mass spectra can be obtained by scanning the magnetic sector, while the acceleration potential values and the electric field strength remain constant.

The ionisation of a sample often results in the formation of molecule ions possessing a range of internal energies. Such species may be sufficiently energetic to undergo one or more dissociation processes. Ions which react with rate constants 10^4-10^6 s^{-1}may decay whilst moving between the ion source and the detector and are known as metastable ions Special scanning methods are used with double-focusing instruments in order to assign metastable peaks. The type of scan employed depends on the geometry of the instrument. In forward geometry (EB) sector instruments linked scans are used, whereas in reverse geometry instruments the mass analysed kinetic energy (MIKE) scan is applied.[83]

Decompositions of metastable ions between the field-free region of the mass spectrometer are studied using the mass-analysed kinetic (MIKE) technique where a

particular ion (parent) is selected using the first magnetic sector and its daughter ions can be studied by scanning the electric sector. The energy, e_2 with which daughter ions are transmitted is given by the following equation :

$$e_2 = m_f e_1 / m_1$$

m_f is the mass of a fragment ion, e_1 is the translational energy of a parent and m_1 is the mass of a parent ion.

The disadvantage of the MIKES technique is that instruments are not able to provide high resolution data, and decomposition reactions within the acceleration region result in interference and artefact peaks. However, MIKES does allow investigation of all parent-to-daughter ratios. All reactions may be investigated at constant currents and the characterisation of the parent ion may utilise either unimolecular decay or collision-induced decompositions (CID) or various high-energy charge exchange reactions.

Decompositions of mass-selected ions are enhanced using collisions normally with an inert gas and the overall process is known as collisionally-activated decomposition (CAD) or collision-induced decomposition (CID). CID processes were first recognised by Aston[103]. He interpreted a series of broad peaks described by Thompson as originating from CID of hydrogen ions with residual or background gas molecules. Early work carried out by Mattauch and Lichtblau[104] presented a unified formula for secondary reactions which may occur in the analyser of the mass spectrometer.

The apparent mass of the product m*, of any reaction could be related to the masses of the reactant ion,$(m_1)^+$ and the analysed product $(m_2)^+$ in the following way :

$$m^* = m_2^2 / m_1$$

The peak positions were observed to be displaced to lower masses during the course of this experiment and this was interpreted as evidence for the loss of a small amount of

kinetic energy during the collision. Hipple and co-workers[105] later suggested that characteristic peak widths could in part be attributed to a release in kinetic energy which occurred during collisions.

Extensive research has been carried out on peptides using both MIKES and CID experiments by Derrick and colleagues. Shiel[106] studied peptides using He as the collision gas and at a collision energy of 8 keV and revealed a boundary at ~ m/z = 1500 below which CID spectra of peptides contained useful information. Bradley[107] extensively investigated CID reactions of peptides and MIKES with a view to improving theoretical models used to understand energetics involved. More recent work by Cooper[108] and Moseley[109] have used CID experiments to induce the formation of fullerene complexes with inert gases and to study the decomposition reactions of these species.

1.4.2 Post-Source Decay

MALDI is generally used to produce molecule ions and, as a consequence of the lack of prompt fragmentation processes, structural information is not usually achieved using this method. Metastable decay of matrix-desorbed peptide ions in the field-free region of a time-of-flight mass spectrometer was first detected using a two-stage reflectron instrument. The combination of unimolecular and bimolecular reactions has been labelled as 'post-source decay' processes by Spengler and Kaufmann[110,111] and these reactions have been exploited in such a way so as to obtain useful structural information.

One of the main disadvantages with MALDI-TOF mass spectrometry had been its inability to obtain medium to high resolution data in the high mass ranges above 100,000 Da and it was suspected that this could be attributed to detection mechanisms at these masses, where the spread in the flight-times of secondary ions caused substantial peak broadening. Spengler and co-workers[110,111] reported that the metastable decay of proteins and peptides led to peak broadening by two mechanisms:

time-of-flight differences between neutrals, parent ions and fragment ions resulting from their passage through electric fields and kinetic energy release.

Post-source decay processes have been shown to depend on the residual gas pressure and vacuum conditions inside the instrument and this is an important factor if data obtained by different research groups and with different instrument designs are to be compared. A schematic diagram of post-source decay is shown in **Figure 1.8.**

The key to the detection of fragment ions formed by post-source decay processes is the use of an ion mirror. Suitable reflectrons are capable of separating metastable ions possessing approximately the same velocity as their parent ions but widely different kinetic energies depending on their masses. Such ions will penetrate the ion mirror to different extents and will become separated in time. Single and two-stage reflectrons have been used for metastable ion separation although a deceleration region may be used as an alternative in which ions are separated according to their kinetic energy This latter design of ion mirror suffers from the problem that it discriminates against low-mass fragments.

Uniform reflectrons are not capable of successfully time-focusing all ions in the beam due to the large energy spread. Two-stage reflectrons have widely been used where the voltage is stepped down in order to achieve acceptable resolution throughout the mass spectrum. The process of stepping down the reflectron voltage in segments typically from 20.0 kV to ~0.1 kV and collecting a spectrum at each voltage is laborious and time-consuming.

Figure 1.8

Metastable Ion Formation

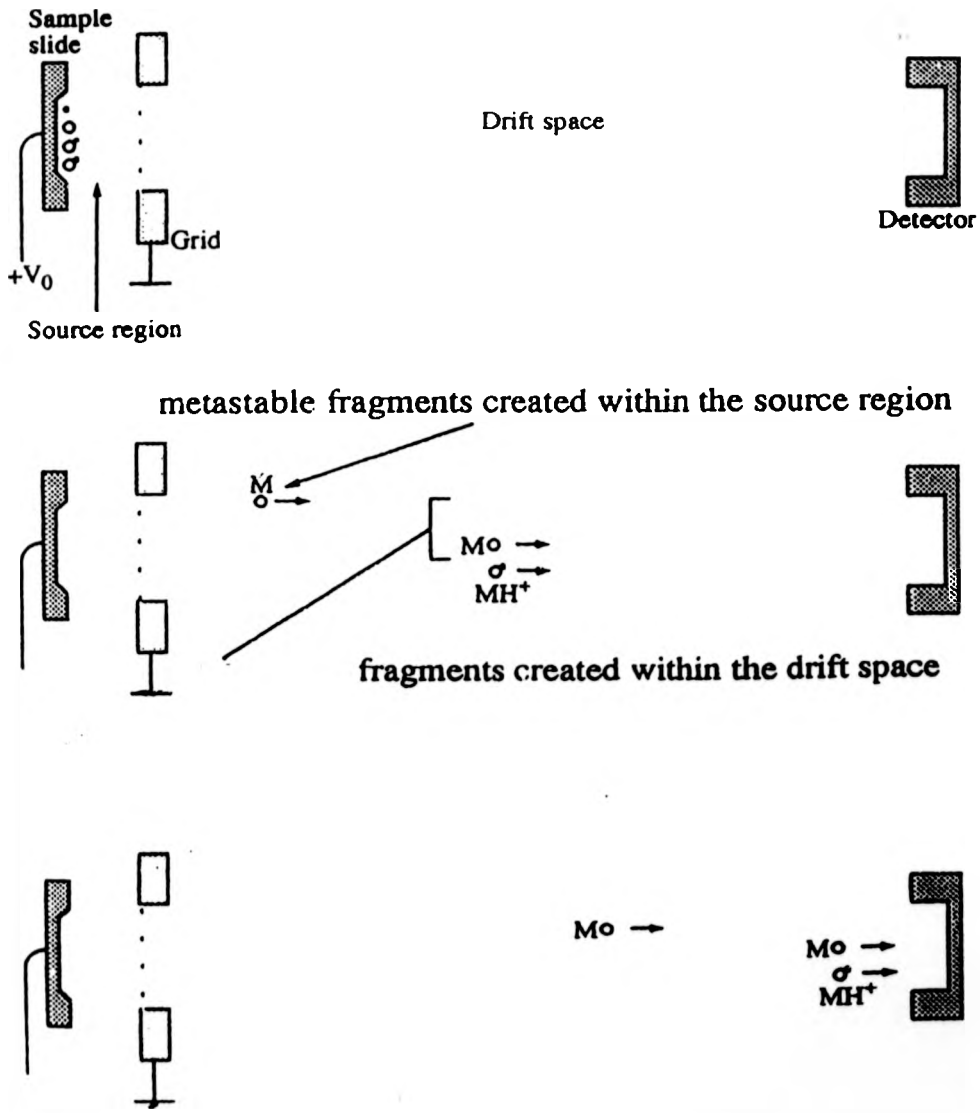

This disadvantage may be overcome with the use of a quadratic (curved field) ion mirror as demonstrated by Raptakis[112] and built by Cotter and co-workers[113,114] Such reflectrons enable the acquisition of focused product-ion spectra at a single reflectron voltage.

Metastable decay following MALDI is optimised by increasing the laser fluence to a value higher than that used for normal MALDI experiments and at which the resolution is maximised. Fragment ion formation is believed to arise from excess internal energy deposited in the ions during desorption and ion-neutral collisions in the dense plume over the sample surface. The application of post-source decay as a method for structural elucidation started with peptides and proteins, and commercial instruments featuring post-source decay are marketed by most time-of-flight instrument manufacturers for this purpose. The main advantage of post-source decay is increased sensitivity. 10 Femtomoles of protein have been successfully used to obtain a complete amino-acid sequence[113] and fragmentation efficiency has been reported to increase with higher masses (upto 12360 Da in the case of cytochrome C)[110]. Peptide sequencing data as been compared with traditional tandem mass spectrometry methods for a variety of different standards including substance P, angiotensins I and II, bradykynin and renin substrate[115,116]. It is generally accepted that the internal energy deposited in ions formed by MALDI is approximately equal to values quoted for low-energy collision-induced dissociation (CID) experiments. Spectra obtained by MALDI-PSD experiments tend to show more resemblance to low-energy CID spectra than high-energy CID spectra. Furthermore, cation and anion PSD experiments have been shown to yield complementary information on primary structures. Peptide cations produced predominantly fragments from the N-terminus whereas, anion dissociation gave primarily C-terminus fragment ions and, in both cases, side-chain cleavages were absent[116,117].

MALDI -PSD experiments have been largely devoted to the analysis of peptides and proteins although more recent work has investigated the possibility of structural

elucidation of carbohydrates and oligonucleotides by this method. The presence of sialic acid functions in the oligonucleotide's structure has been unambiguously determined and the sequence of a natural carbohydrate has been partially determined using sub-picomole amounts[118]. Modified cyclodextrins have been investigated and a correlation between chemical structures and relative intensities in post-source decay fragment ions has been found.[119] Some of the most recent research published has used PSD to sequence a branched peptide and peptide anions have been investigated by PSD in order to differentiate between hydroxy and amino terminal groups[120,121]. Following Spengler's pressure dependency investigations[111], Bowdler and colleagues have demonstrated how PSD processes may be enhanced with the use of collision gases.[122]

Despite rapid growth in applications of MALDI coupled with PSD analysis[123,124,125], no reports on its application to the analysis of synthetic polymers, as presented in this thesis, have been made in the open literature. The correlation between laser fluence and the nature of the post-source decay data obtained has also been investigated.

1.4.3 Hybrid Tandem Mass Spectrometry

More unusual combinations of analysers have been designed and constructed in order to take advantage of the many advantages offered by MALDI as an ionisation method. MALDI is essentially a pulsed ionisation technique hence its compatibility with time-of-flight mass spectrometry. The need to obtain structural detailed information concerning a broader range of substrates has led to the use of so-called ' hybrid' mass spectrometers which permit tandem mass spectrometry experiments to be performed on such compounds.

Makarov, Raptkakis *et al* [112] have successfully designed and built a hybrid mass spectrometer which consisted of a MALDI source coupled with a double-focusing

sector analyser, a collision cell and a time-of-flight analyser followed by an array detector. The advantages of such an instrument are that ions formed by MALDI may be focused and selected at higher resolutions in the first half of the instrument and collisionally activated in the collision cell using an inert gas at high collision energies. Fragment ions which are formed during this process may be subsequently separated using the time-of-flight analyser with increased sensitivity. An account of the performance and construction of this instrument has been described elsewhere.

Instruments of this kind are now commercially available and have been used extensively for peptide sequencing experiments.[126] Polymers and their additives have also been studied using MALDI-CID methodology on these types of instruments[127].

1.5 The Analysis and Characterisation of Polymers

1.5.1 Overview

The complete characterisation of polymers and their properties, which includes molecular mass distributions, end-group information and monomer identity, is crucial in being able to correlate chemical properties with physical and morphological behaviour. As well as completing identification, characterisation of a polymer can aid with material design at molecular level, processing control and failure analysis. A range of techniques are often required in order to obtain such detailed information. Historically, polymer technology has primarily been concerned with the bulk properties. Typically, the thermal and photo degradation of polymers has been of interest in order to prevent deterioration of performance and appearance.

Differential scanning calorimetry (DSC) has been used to measure glass transition temperatures and melt temperatures within a sample by probing first and second order

phase transitions and thermogravimetric analysis (TGA) has been used to identify thermal degradation parameters. The degree of crystallinity of polymers is usually studied using powder X-ray diffraction. As other analytical methods have developed, they too have been applied to the characterisation of polymers, notably size exclusion chromatography (SEC) used extensively in quantifying molecular mass,[128,129] and nuclear magnetic resonance (NMR) which is highly effective in quantitatively investigating tacticity, copolymer statistics and stereochemical configurations in solution.[128,129] Many specialised techniques have been used to investigate the relationship between polymer structure and properties including electron spin resonance, infra-red and raman spectroscopies, electron microscopy and electron diffraction. The development of softer ionisation techniques, in particular, field desorption (FD) and more recently, matrix-assisted laser desorption/ionisation (MALDI) and, to a lesser extent electrospray ionisation (ESI), has lead to the wider application of mass spectrometry to polymers. Analysis by mass spectrometry had previously been limited to pyrolysis gas chromatography (PyGC-MS)[130].

Molecular mass information is one of the main properties of interest to polymer chemists. Techniques for measuring molecular mass divide into two main groups, those which are relative and those which are absolute. Routine mass analysis of polymers is still carried out using relative techniques, such as viscosity measurement on melts or dilute solutions. These methods involve the comparison of measured masses to those of standard materials. Absolute methods give average molecular mass information directly. The most important parameters of interest to the polymer chemist are weight average molecular mass (M_w), number average molecular mass (M_n) and polydispersity index (M_w/M_n) which are defined as :

$$M_n = \Sigma N_i M_i / \Sigma N_i$$

$$M_w = \Sigma N_i M_i^{\,2} / \Sigma N_i M_i$$

Polydispersity index is a parameter which defines the width of a polymer's mass distribution. A mono-dispersed polymer or a polymer of a single mass has a

polydispersity index value of unity. A broad polymer distribution results in a polydispersity index of greater than unity. The majority of polymers in everyday use have high polydispersity indices.

1.5.2 Mass Spectrometry of Polymers

1.5.2.1 Field desorption mass spectrometry of organic polymers

The application of mass spectrometry of polymeric materials has been inhibited by the fact that such compounds possess high molecular mass and are inherently thermally labile and involatile. The development of soft ionisation techniques such as FD and more, recently, MALDI has led to renewed interest in the study of synthetic polymers by mass spectrometry. The oldest method applied to polymers is field desorption.

The first field desorption mass spectrum of a synthetic polymer was reported by Wiley and Cook[131]. Interest in this area grew and a significant number of papers were published. Matsuo et al demonstrated the potential of field desorption in studying oligomers upto m/z 11,000[132]. Craig and Derrick observed ions of masses up to 13 600 in the field desorption mass spectrum of poly(styrene) average molecular mass 9,000[133,134] The fact that field desorption experiments result in the production of a high abundance of molecular ions makes the method ideal for the determination of the statistical averages which are of interest to polymer chemists. Experiments carried out by Lattimer[136,137] and colleagues and Derrick[134,137] and co-workers compared data obtained by conventional techniques, such as size exclusion chromatography and viscosity values, with those obtained by field desorption mass spectrometry and showed that this technique compared favourably.

1.5.2.2 Tandem Mass Spectrometry of Polymers

Field desorption/ionisation has been used in order to generate molecule-ions of relatively high intensities which may undergo fragmentations either by unimolecular decay decomposition reactions or by collision-induced decompositions. A range of polymers have been investigated and these have included poly(ethylene glycol), poly(propylene glycol), poly(methyl methacrylate), poly(styrene) and poly(butadiene). One of the main driving forces has been the need for medium-high resolution data concerning the chemical composition of such polymers, such as end-group information and monomer-mass separation.

Some of the earliest research into the fragmentation mechanisms has been carried out by Derrick and colleagues using field desorption/ionsation mass spectrometry. Thermal degradation reactions of poly (1-butene sulfone) and poly (propene sulfone) was studied and the FD spectra revealed ionisation degradation products in the first step of a two-stage degradation process[138]. Shifts were observed in the mass spectrum which resulted from rupturing of weak links in the polymer chain via a proposed β-hydrogen shift mechanism. Craig performed a series of experiments on poly(styrene) chains using both CID and MIKES mass spectrometry[134,139,140]. CID spectra revealed that the mechanism of the decomposition reaction involved random initial cleavage of the polymer chain followed by a series of consecutive depolymerisation reactions. From the MIKES data it was inferred that at low energies cationic poly(styrene) chains fragmented near the ends of the poly(styrene) chain and that this effect was most pronounced with longer poly(styrene) chains. Investigations carried out on poly(butadiene) upto m/z 11,000 has shown that the little fragmentation, which was evident, was structurally diagnostic of the polymer chain[137].

The role of the field in the field desorption fragmentation patterns of poly(ethylene glycol) has been attributed to a field dissociation mechanism. The field was observed to

lower the critical energy for the dissociation of molecules to such a level that the rate of dissociation was relatively insensitive to temperature[141].

Agma performed a comprehensive investigation of poly(ethylene glycol) and poly(propylene glycol) by field desorption mass spectrometry[142]. Both unimolecular and collision-induced decompositions of protonated and alkali-metal cationised poly (glycol) ions were studied. Unimolecular decomposition spectra of [M+H]+ showed a series of four fragment peaks and three mechanisms were proposed by Craig involving C-O and C-C cleavages along the back-bone of the polymer followed by hydrogen transfers were proposed. Alkali-cationised molecules of poly(propylene glycols) unimolecularly decomposed to form only high-mass fragmentations and the reproducibility of the fragment ions were observed to be within 3 amu. All unimolecular decay processes were found to occur more readily with increasing mass. Evidence obtained from CID experiments showed that both unimolecular decompositions and CID reactions occurred when the beam of poly(glycol) ions collided with an inert gas such as argon, however, as the pressure increased the intensity of the low mass fragment ions originating from CID increased. In contrast to unimolecular decay, the intensities of fragment ions produced by CID decreased with increasing mass of incident ion. Hope performed a set of parallel experiments on poly(methyl methacrylate) [143] More recent work used FAB ionisation as a means of generating molecular ions over a longer period of time for the MS/MS analysis of 3,3,3-tri-fluoro-1-phenypropline oligomers by unimolecular and CID processes[144].

1.5.2.3 Matrix-Assisted Laser Desorption/Ionisation of Polymers

Ever since the introduction of matrix-assisted laser/desorption ionisation and its initial application to biomolecules, there has been a considerable amount of interest shown by the polymer community in applying this technique to polymeric material. No other analytical method allows the rapid, accurate determination of the complete mass distribution, so the need for its development was great. The discovery of 2,5-di-

hydroxybenzoic acid by Karas and Hillenkamp as an effective matrix may be considered to be one of the early breakthroughs in this area[71] This allowed the first definitive application of the method to synthetic polymers in the range 100 to 70 000 Da by Karas and Hillenkamp in 1992. 2,5 Di-hydroxybenzoic acid was used to analyse poly(ethylene glycol) samples with masses as large as 40 000 Da. The calculated average masses showed good agreement with the manufacturer's data and values obtained by size exclusion chromatography and vapour pressure osmometry although deviations were observed. Poly(methyl methacrylate) was also investigated using 2,5-di-hydroxybenzoic acid as the matrix[72]. The spectrum featured a distribution of singly charged cation-attached molecule ions, differing by the expected monomer mass of 100, with no evidence of fragmentation. The mass averages calculated from the observed distributions were in good agreement with those found by other methods. The polydispersities of these sample were all close to unity.

The first hint that polymer analysis using matrix-assisted laser desorption/ionisation was dependent on the chemical and physical nature of the matrix, came when Karas and Hillenkamp discovered that the analysis of poly(styrene) was not possible using 2,5 di-hydroxybenzoic acid as the matrix material since the analyte phase separated upon deposition[72]. Nitro-phenyl octyl ether, a liquid matrix was used in conjunction with the addition of silver tri-fluoroacetate which increased the production of positive ions. The spectrum of the silver cationised poly(styrene) with a mass of 20 000 Da showed strong signals representing the singly-charged distribution. A mass spectrum of poly(styrene) of molecular mass 70 000 Da was also shown and, although, the signal-to-noise ratio was low, it was sufficient to evaluate the polymer's mass distribution. At about the same time, Danis and Karr investigated a water soluble poly(styrene sulfonic acid) sample with an average molecular mass of 200 000 Da[73]. Sinapinic acid was used to obtain a negative ion spectrum and clearly show a singly charged molecular mass distribution centred around 171 800 Da[73]. Multiply-charged ion distributions were also seen at lower mass values. The polydispersity value calculated from the spectrum was

found to be close to unity which is in agreement with the value quoted by the manufacturers.

MALDI has been successfully used to analyse a range of synthetic polymers and has become increasingly popular with synthetic polymer chemists as a means of obtaining data concerning end-groups and probing synthetic pathways. Some of the most noteworthy research has been carried out by Haddleton and colleagues who have applied MALDI to a variety of polymers including methyl methacrylate and butyl methacrylate co-polymers[145], poly(styrene)[146] and poly(methyl methacrylate)[147,148] analysis. Research in this area has also been carried out by Montaudo *et al* who has studied ester exchange reactions with cyclic oligomer formation in the ring opening polymerisation of lactide with aluminium complex initiators[149] and the end-group characterisation of poly(methy phenyl silanes)[150]. Pasch and co-workers have studied condensation polymer products of co-polymer reactions by MALDI-TOF[151] and Spickerman has investigated characterisation of oligo styrene macromonomers with methacryloyl end-functions[152].

Growth in the application of MALDI to polymer analysis has been coupled with an acknowledgement for the need for more fundamental studies, particularly concerning the role of the cation during the ionisation of polymers. Polymer ions formed by the MALDI process are generally cationised. The effect of cationisation on the average molecular mass and average molecular number obtained from MALDI data is a subject of present debate.

Initial research on cation-attachment to polymer used laser desorption as the ionisation technique. O'Malley and Llenes[153] studied cation attachment in the analysis of poly(styrene) and poly(ethylene glycol) by this method. Al+, Cr+, Fe+ and Cu+ were found to attach efficiently to both types of polymer although poly(styrene) was found to have a higher affinity for attachment to Al+, Cr+ and Cu+ and PEG had a higher affinity for K+. These observations were explained in terms of hard and soft acids and

bases principle. Metal ion attachment was also studied by Mowat and Donovan who showed that attachment of Cr+, Cu+ and Ag+ to non-polar polymers such as poly(butadiene) and poly(styrene) could readily be achieved using 337nm laser desorption/ionisation[154].

Trends in the cationisation of polymers in matrix-assisted laser/desorption/ionisation were investigated by Fong[155] who studied the interaction of PEG's upto m/z = 4000 with a range of alkali-metal cations and concluded that the formation of the polymer-solvated cation was influenced by the alkali metal and so-called 'cavity size' of the polymer. Research carried out by Scrivener[156] and co-workers has studied the effect of cation size on the molecular mass statistics on a range of poly (alkyl methacrylates) of a broad mass distribution (polydispersity value quoted from size exclusion chromatography as > 1.2). Shifts of upto 35 % were seen depending on the cation combination. This effect has also been studied using a narrow mass poly (ethylene glycol) (PEG) (polydispersity index quoted from size exclusion chromatography approx. 1.1). The source of this effect has been attributed to the various cations' abilities to attach and detach to polymers during the desorption phase and such observations fit in with the work of von Helden[157,158] and co-workers on gas phase conformations. This suggests that MALDI is indeed a gas phase process and that both polymer size and cation size will influence the stability of the cation-polymer complex.

Cations attached to oligomers have always been detected as singly-charged species and work by Chan and Wong[159] has used divalent and trivalent metal ions as cationisation reagents. Singly-charged molecule ions were generated in all cases.

Similar work by Deery *et al* [160] has used electrospray as the ionisation method to study cation attachment to poly(styrene) although results presented have high-lighted potential difficulties in using electrospray as the ionisation method for such studies.

1.5.2.4 High Mass Polymer Analysis by MALDI

Several factors still need to be addressed in order to analyse successfully high mass polymers using this ionisation technique. One of the main problems is the fact that matrices which are successful in biomolecule analysis are not necessarily suitable for use with polymers which tend to be more non polar. It is also impossible to predict the effectiveness of a matrix candidate even if it fulfils the crucial properties earlier. It may, therefore, be concluded that the desorption and cationisation processes must be optimised for each class of polymer analysed by MALDI.

Low resolution at high mass is one of the many difficulties presented in the analysis of such polymers. Delayed extraction methods have improved the situation significantly. In fact, many commercially available instruments now employ delayed extraction. Humphrey *et al* has analysed poly(styrene) and poly(methyl methacrylate) polymers upto 100 kDa in mass[161] and Jackson and co-workers have utilised delayed-extraction to obtain higher resolution data concerning end-groups of polymers upto 12 kDa[162]. Mowat and Donovan have successfully applied delayed extraction techniques to enhance the cationisation reactions of polymers[163].

Detector performance may also be crucial factor in the analysis of high-mass polymers by MALDI-TOF-MS. Work by Axellson[164,165,166a] and co-workers has highlighted this problem. Micro-channel plates which are the most commonly used type of detector readily saturate when bombarded with a large number of low-mass ions.[82,83] If the detector does not sufficiently recover, then the high-mass ions may be detected at a lower signal strength resulting in a mass distribution which is biased towards the low mass end[166b].

Many of the difficulties associated with the analysis of high-mass polymers are inherently connected to the problems observed in investigating more poly(disperse) samples. Some of the instrumental effects have been described by McEwen[167] who has

in part attributed these problems to instrumental limitations rather than ionisation limitations.

The problems associated with the analysis of broad molecular mass distributions have widely been acknowledged. Much of the work has focused on comparisons between data derived from SEC and those derived from MALDI for a range of compounds[168,169]. Mullen and co-workers have studied a range of polymer mixtures and have developed a quantitative method for the successful analysis of broad molecular mass polymers[170,171]. Montaudo et al have also exposed the polydispersity problem[172] and has presented a similar novel procedure for the measurement of molecular mass of polydisperse polymers directly from MALDI measurements[173].
The ability of MALDI to analyse successfully high-mass polymers possessing high poly(dispersity) values still remains an important question since most polymers of commercial interest have these characteristics. The majority of work performed on polymers by mass spectrometry is still limited to relatively low-mass species dominated by samples of low poly(dispersity) values.

1.5.2.5 FT-ICR of Polymers

Many polymers have been analysed by time-of-flight methods because of the extended mass ranges afforded by these mass spectrometers, however, researchers are currently developing techniques base on the high-resolving power and reasonable mass ranges obtainable by Fourier-transform ion cyclotron resonance (FT-ICR).

One of the first difficulties encountered with the application of FT-ICR to polymer analysis is mass discrimination which can occur as ions are brought into the analyser and trapped for further analysis. In 1992, Hogan and Laude found that the number average molecular mass value, M_n increased as the desorption site was displaced a specific distance form the cell for a series of low-mass cationised-PEG samples[174]. The

variation appeared to indicate that higher-mass oligomers were having difficulty in penetrating the static trapping voltages. However, Wilkins and co-worker[175] used a gate-trapping procedure to overcome this problem and a series of polymers with wide molecular-mass distributions were measured by this method without mass discrimination. The end-groups of synthetic polymers have been studied by taking advantage of the high resolution capabilities of FT-ICR. Several derivatised PEG polymers of average molecular mass 1000 and 4000 Da were investigated using graphical methods to determine end-group functions and precise repeat units[176] Van Rooj *et al* used a 7 Teslas instrument to characterise end-groups from synthetic polymers upto 5000 Da with a mass accuracy within 20 amu[177].

Laser desorption coupled with FT-ICR analysis has also continued to be useful in the analysis of synthetic polymers. A wide variety of natural polymers have been investigated and these have included humic acids and lignins[178]. Polymer films, such as perfluorinated poly(ether) on metal substrates have also been studied[179]. Wilkins and Karr used silver nitrate chemical ionisation for the analysis of another class of difficult compounds, hydrocarbon polymers. Poly(styrene), poly(isoprene), poly(butadiene) and poly(ethylene) polymers produced spectra containing spectra containing signals from oligomers with masses upto 6000 Da, mass accuracy being quoted as 3-12 ppm for the full distribution[180]. An overview of polymer analysis by FT-ICR has been published by Campana and co-workers.[181]

1.6 Aims of this Work

The aim of this research is to investigate the ion chemistry of synthetic polymers formed by both matrix-assisted laser desorption/ionisation (MALDI) and, the oldest soft ionisation method, field desorption.

The development of matrix-assisted laser desorption as a soft ionisation technique and its initial application to the analysis of biological samples by mass spectrometry has

renewed the interest of polymer chemists in the application of mass spectrometry to the analysis of synthetic polymers. Non-polar polymers are one of the most difficult class of compounds to investigate by mass spectrometry and classically, such studies have been limited to the use of field desorption/ionisation. One component of this work has been to develop a suitable sample preparation for the analysis of a set of poly(isobutylene) samples by MALDI. A rapid and accurate method for the calculation of absolute molecular mass statistics of polymers has yet to be developed and such values will be calculated from MALDI and compared with traditional techniques, such as size exclusion chromatography. This work is presented in Chapter Four.

The chemistry of ions formed by MALDI is investigated in Chapter Five. Research focuses upon the application of post-source decay experiments to the analysis of synthetic polymers and focuses on the effect of laser power and pressure on the types of ions formed.

Finally, a major component of this work was the application of field desorption/ionisation mass spectrometry to the analysis of synthetic polymers. This work involved the successful growth of suitably robust emitter wires and work carried out in this area is presented in Chapter Six.

CHAPTER TWO

Instrumentation and Experimental Methods

2.1 Instrumentation

The experiments carried out in this work were performed on a variety of different instruments, and these included a Kratos Kompact III MALDI-TOF Mass Spectrometer, a Kratos Kompact IV MALDI-TOF Mass Spectrometer, a Bruker Biflex I MALDI TOF Mass Spectrometer and a Kratos Concept II HH Four-Sector Mass Spectrometer. All of the above are essentially commercially available instruments, although some modifications have been made to the Kompact IV instrument which are described here. Initial intentions were to use the four-sector instrument to study polymer ions by tandem field desorption mass spectrometry. A brief description of the instrument used for this purpose follows. The four-sector was also modified by Raptakis and co-workers[112] in order to carry out MALDI experiments on the second half of the instrument, and these modifications are briefly described here.

2.1.1 Kratos Kompact Instruments

Kratos Kompact III and Kratos Kompact IV MALDI -TOF Mass Spectrometers have been use in this work. The basic components common to both instruments are described along with additional features present on the Kompact IV.

Laser System

Both instruments were fitted with a standard nitrogen laser (337nm) which had a 3 ns pulse width. The area of the laser spot size was measured to be approximately (60 x 500) μm^2. The optical density values d, for the Kompact III and Kompact IV Mass Spectrometers were related to the computer controlled software value through the

following equations where d_{IV} and d_{III} are the optical density values for the Kompact IV and III respectively and L is a software value in the range 0-180 ;

i) $d_{IV} = 2.5 - (2.4*L/180)$

ii) $d_{III} = 2.0 - (1.9*L/180)$

The optical density value on the Kompact IV instrument ranged from 0.1 to 2.5 whereas on the Kompact III instrument this value ranged from 0.1 to a maximum value of 2.0. The full transmission for each pulse was 300μJ and the percentage of laser energy transmitted , *T%* was calculated using the equation below ;

$$T\% = 100 / 10^{d}$$

Figure 2.1 shows how the laser energy varied with software values for the Kompact IV MALDI-TOF mass spectrometer.

It must be noted that over time, the laser performance of these lasers will deteriorate, hence higher software values will be needed to reach the same laser power densities.

Ion Source

The MALDI ion source consisted of a positively or negatively charged metal electrode and a grounded accelerating grid at a distance of 1.6cm. The ion source design in both instruments was identical.[182] Neither source was modified in any way. Accelerating potentials were either set at 5kV in 'low' mass mode or at 20kV in 'high' mass mode.

Detection

The Kompact III was fitted with two standard electron multiplier detectors one for reflectron and the other for linear mode.[182] The Kompact IV was also fitted with standard electron multiplier detectors in both reflectron and linear modes, although, originally, multi-channel plates had been fitted for detection for use with the reflectron.

Figure 2.1

Plot to Show How the Laser Power of the Kompact IV Varied With Software Values

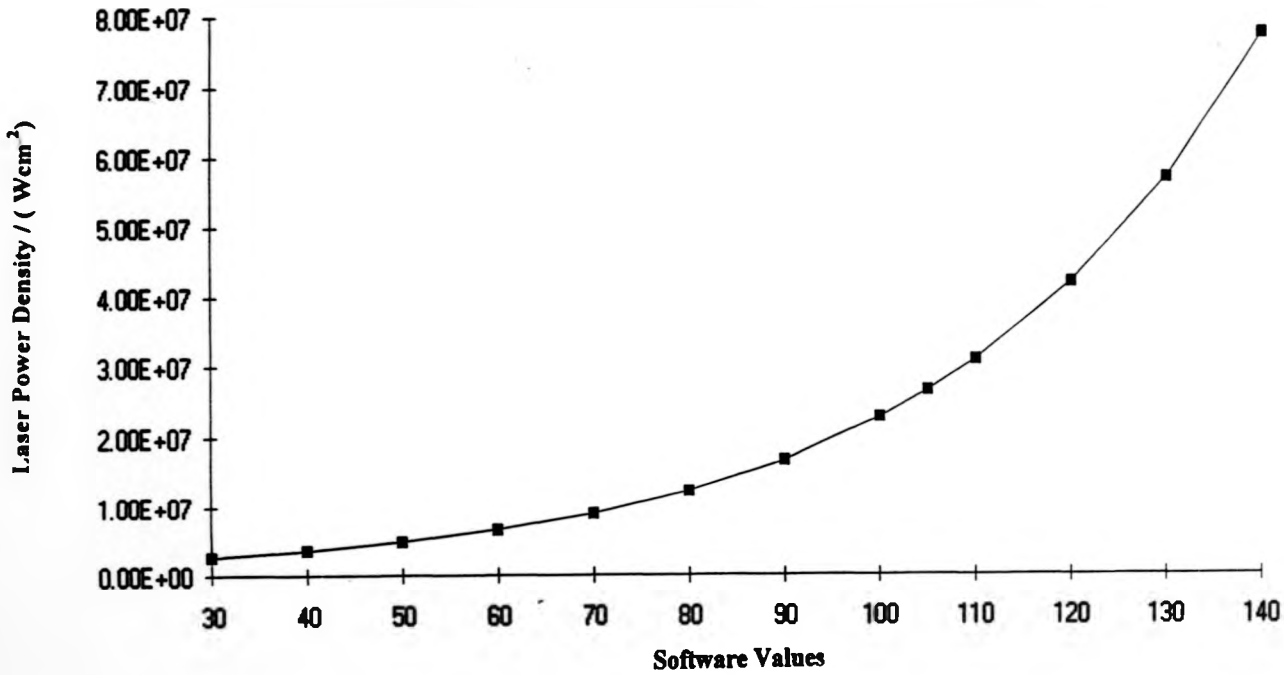

Figure 2.2 depicts the dimensions of the Kompact IV MALDI-TOF Mass Spectrometer which was used for the majority of experiments carried out.

Ion Gate

The Kompact IV mass spectrometer was fitted with an ion gate which consisted of two electrodes which are were able to generate an electrical field orthogonal to the ion beam. An electric pulse of equal and opposite polarity was applied to either plate when ions of interest entered between the plates. These ions were transmitted, undeflected through the blanking aperture. The duration of the pulse was software controlled.

Reflectron

The Kompact III was fitted with a reflectron which had a dual linear-slope electric field whereas the Kompact IV was fitted with a quadratic (curved) field reflectron which was specifically designed to allow the a complete fragment spectrum to be collected in one normal length experiment.

Data Acquisition and Instrument Control

The signal from both detectors was in analog form and was converted to a digital signal using a 300MHz analog to digital converter. The converted signal was sent to a SUN work station where all operations such as calibration, averaging, data processing took place using the software provided by Kratos.

The Vacuum System and Source Chamber

A pressure of $< 1.0 \times 10^{-6}$ Torr was maintained by a single turbomolecular pump backed by a rotary pump. Pressure inside these instruments could not

Figure 2.2
Schematic Diagram Depicting the Dimensions of the Kompact IV Mass Spectrometer

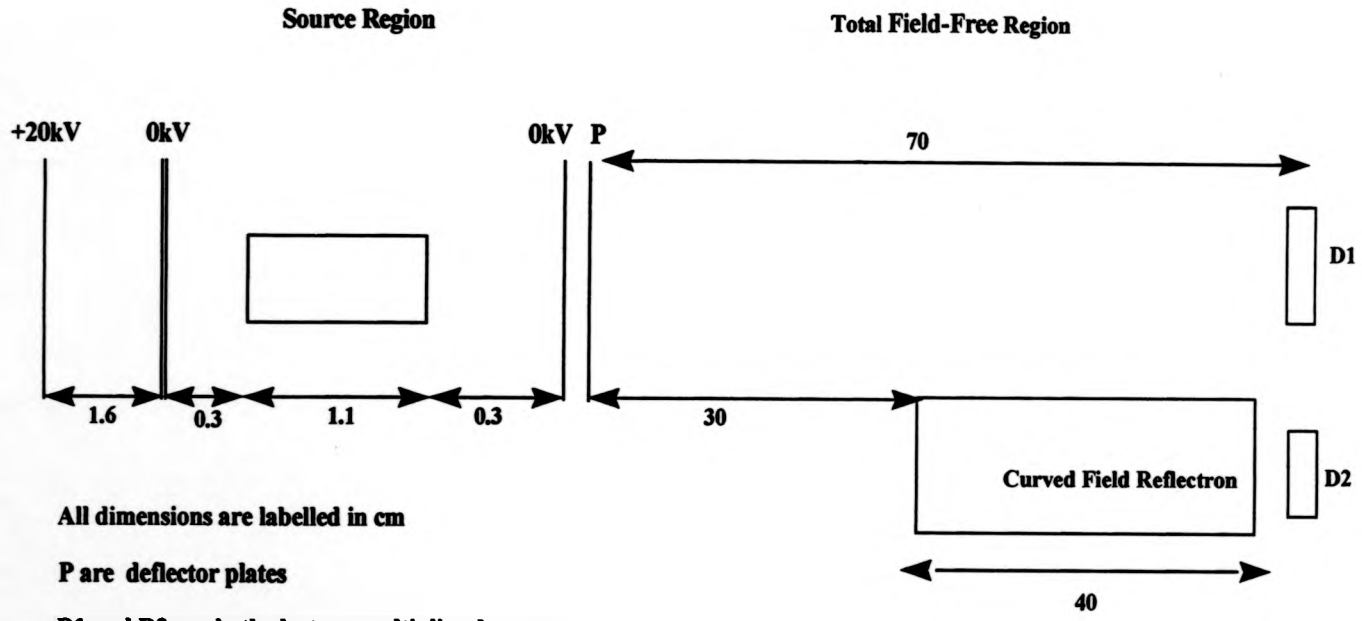

All dimensions are labelled in cm

P are deflector plates

D1 and D2 are both electron multiplier detectors

be measured directly during an experiment, although the high voltage supply could not be turned on unless backing pressure was sufficiently below ~3.5 x 10^{-4} Torr. A direct measurement of the pressure in the source region is described later.

Samples for investigation by MALDI were inserted on a stainless steel sample slide directly into the source. Sufficient backing pressure of less than 5 x 10^{-6} Torr in the source region allowed a series of electronically controlled valves to be opened and the rest of the source region to be pumped down.

A schematic diagram of the Kompact III MALDI-TOF Mass Spectrometer is shown in **Figure 2.3**

2.1.2 Kratos Concept 2 HH Four Sector Mass Spectrometer

This instrument consisted of two-double-focusing forward geometry (EBEB) mass spectrometers linked by a collision cell and associated electrostatic lenses (flexi-cell). Tandem mass spectrometry on a four-sector instrument involved mass selection of the ions of interest into the collision region by a suitable combination of the first two electric and magnetic sectors (MS1). The use of MS1 to mass-select parent ions removes artefacts formed by metastable decay of other ions formed in the source. Such artefacts are dependent on resolution. Theoretically, all parent ions may be mass selected with high resolution although in practice, sensitivity was far more important and a resolution of 1500-2000 was much more commonly used. A schematic diagram of the Concept II HH mass spectrometer is shown in **Figure 2.4** and depicts ion beam trajectories exemplifying the double-focusing properties of this instrument.

The Vacuum System and Source Chamber

A pressure of 10^{-7} Torr was maintained by 7 turbomolecular pumps which were backed in turn by 4 rotary pumps. Pressures inside this instrument were monitored by

Figure 2.3

Schematic Diagram of the Kratos Kompact IIIMALDI-TOF Mass Spectrometer

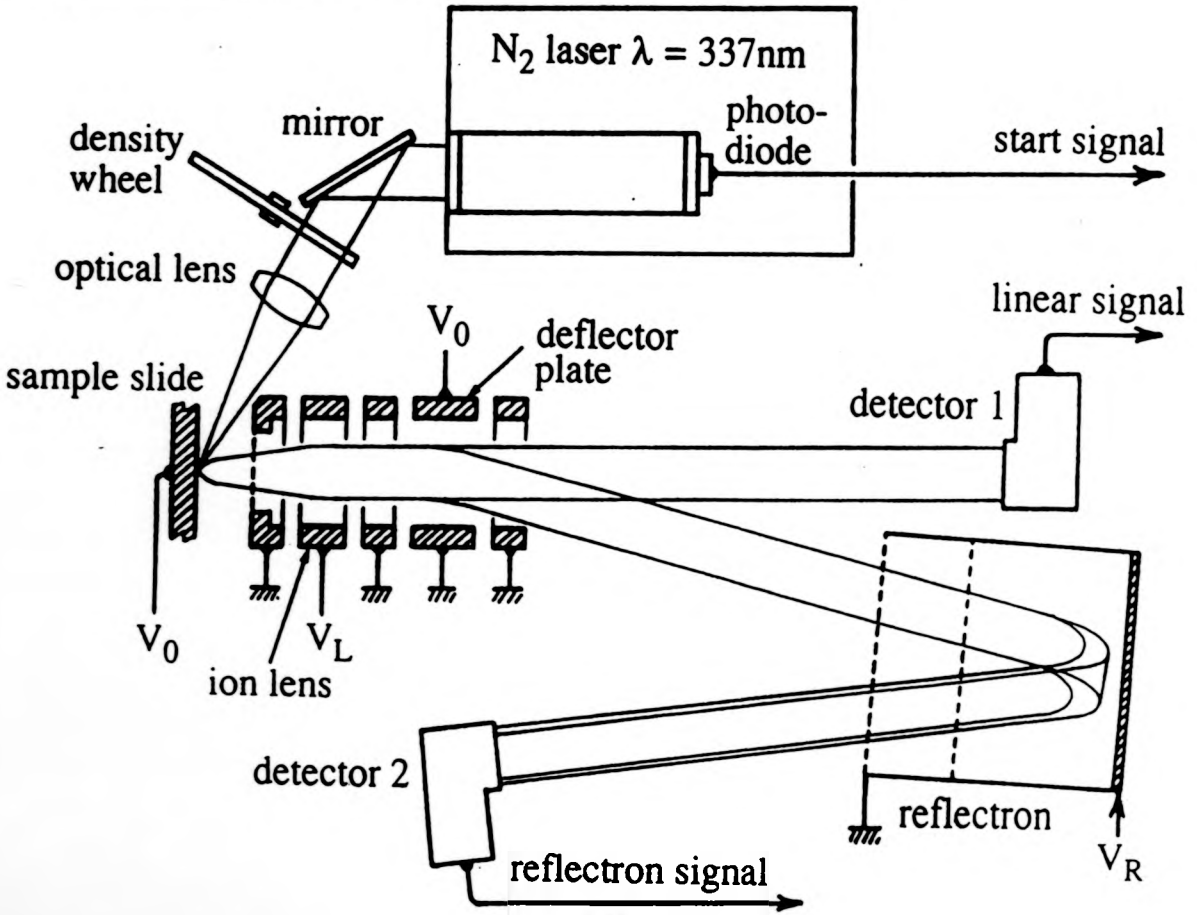

Figure 2.4

Schematic diagram of the Kratos Concept II HH Four-Sector Mass Spectrometer

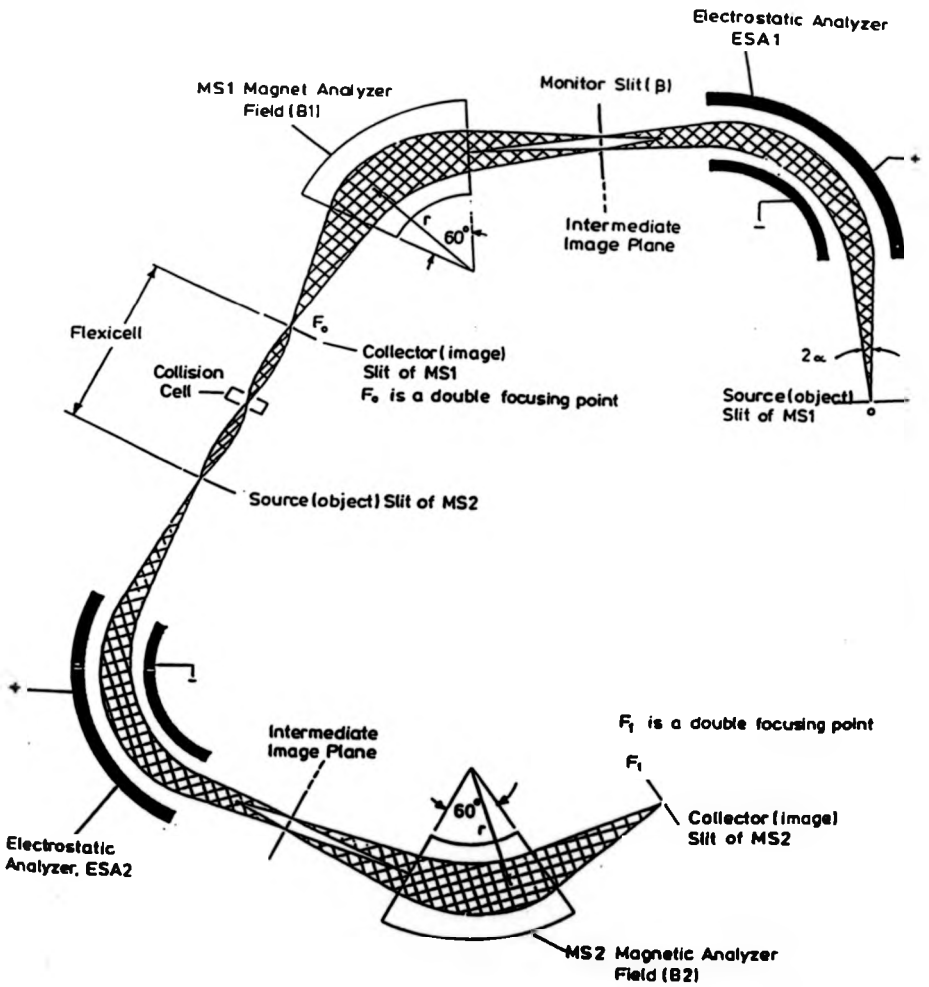

flange-mounted ion gauges and backing pressures by thermocouple gauges and in the event of too high an increase in pressure, overheating or electrical power failure, the turbo pumps and high voltages were shut down.

Samples for investigation by L-SIMS or FD were introduced into the source via a direct insertion lock. The first section of the air lock was evacuated after the probe was inserted prior to further insertion further into the air lock. A ball valve isolated the air lock from the source and the source chamber was isolated from the rest of the instrument by an electronically controlled valve.

Ion Sources and Ion Lenses

i) L-SIMS Source and Ion Lens

The L-SIMS ion source was of standard Kratos design.[182]

The accelerating potential was applied to the probe tip by a contact block similar to the one described for the field desorption lens. 8kV caesium ions were used to bombard the L-SIMS target.

ii) Field Desorption Source and Ion Lens

The lens stack used for the field desorption experiments on the four-sector had been constructed 'in house' based on the original manufacturer's design[182] and modifications had previously been made by Curtis and co-workers[107] in order to improve the performance.

A z-lens had been added in place of a cylindrical earthed barrel which had previously been part of the mounting block and an earthed a plate had also been added in front of the mounting block, in order to define the beam at that point by the reduction of stray electric fields. Ion beam trajectories calculated by Davis[183,184] had shown the effect of a shield electrode in enhancing focusing of the ions through the counter electrode slit and such a shield electrode had been added to this source. This was to be held the same potential as the field desorption emitter which was positioned 1.5mm from the

counter electrode. In the case of the four-sector field desorption lens stack, the shield electrode consisted of two separate plates with the emitter being positioned parallel to them. A schematic diagram of the field desorption source as modified by Curtis and successfully used by Bradley[107] is shown in **Figure 2.5.**

Before any field desorption experiments were carried out, the dimensions of the source were measured so that the performance of its theoretical ion optics could be assessed. A schematic diagram of the source as determined by myself and Mr. P. Lloyd is shown in **Figure 2.6.**

Ion optical modelling of the standard field desorption ion source by Makarov using the SIMION program revealed a series of problems. Two main areas of interest were modelled; the filament region and the ion source optics. The main conclusions suggested[9] that only the central part of the filament was working (which constituted only 17-22 % of the filament area) and that aberrations occurred in beam width and angular divergence for ions with entrance angles over 6-7^{o} and that these ions could not be effectively focused onto the y-slit.

MALDI Source on the Concept II HH Four-Sector Mass Spectrometer

Raptakis[1] modified the collision cell exit on this instrument to incorporate a MALDI source which used a nitrogen laser with a 3ns pulse width to generate the ions of interest. The ion optics of this exit had the ability to prepare a divergent ion beam, such as that formed in the MALDI process, for ejection into a double-focusing mass analyser. Ions were then focused using an electric sector followed by a magnetic sector and detected using an array detector. Under normal operation of the instrument, external calibration experiments were performed using $(CsI)_n$ Cs+ clusters on the second half of the instrument.

Figure 2.5

Modified Field Desorption Ion Source

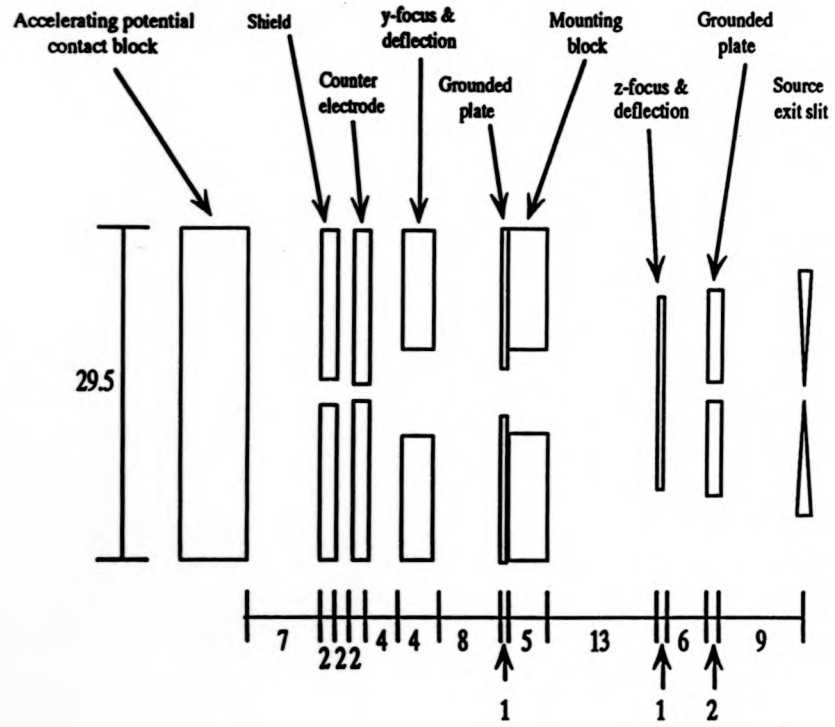

Slit Widths

Shield 3 mm
Counter Electrode 2 mm
y-focus 10mm
First Grounded Plate 5 mm
z-deflector 5 mm
Second Grounded Plate 2 mm

All measurements are shown in mm.

Figure 2.6

Non-aligned Field Desorption Ion Source Dimensions

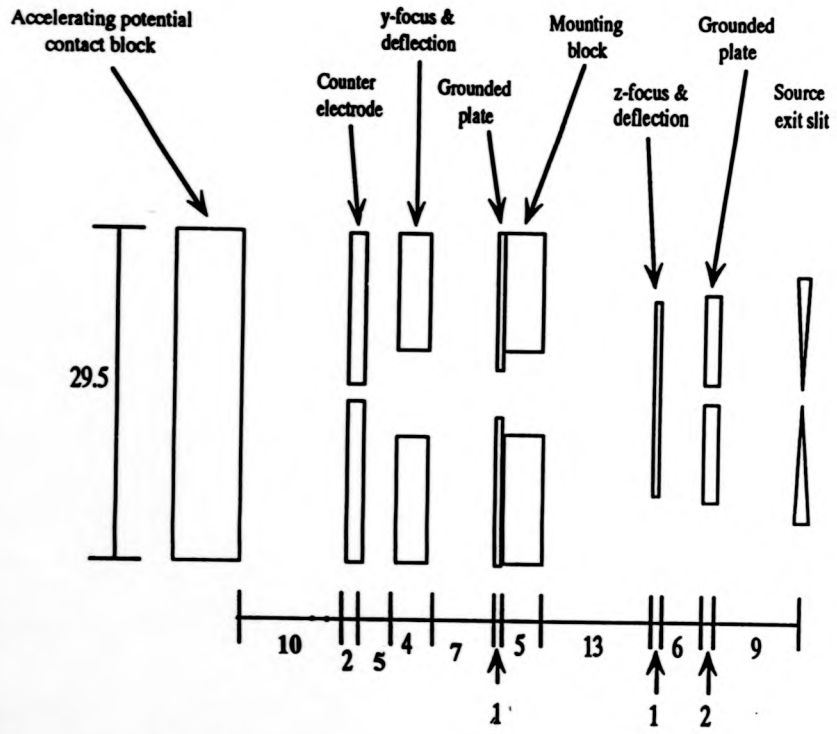

Slit Widths

Counter Electrode 2 mm
y-focus 10mm
First Grounded Plate 5 mm
z-deflector 5.1 mm
Second Grounded Plate 2 mm

All measurements are shown in mm.

The main differences between this source and the one shown in Figure 2.5 are the lack of the shield and the positions of the y-focus and z-focus deflection plates.

This set-up had the advantage of providing higher resolution data than that obtained by MALDI time-of-flight experiments on the Kompact instruments and was used to investigate the attachment of silver cations to poly(styrene) during the desorption/ionisation process.

2.1.3 Bruker Biflex I MALDI-TOF Mass Spectrometer

This instrument was used at the Central Research Institute for Chemistry in Budapest, Hungary. All experiments carried out on this instrument were part of a collaboration between the British and Hungarian Research Councils, between two research groups lead by Prof. P. J. Derrick at the University of Warwick and Dr. K. Vekey of the above Institute. A description of the basic components of this instrument follows.

Laser System

The instrument was fitted with a standard nitrogen laser (337nm) which had a 3 ns pulse width, an attenuator which allowed fine adjustment of the laser fluence, beam splitters to direct a fraction of the laser light to a photodiode starting the time-of-flight measurement, a lens to focus the laser beam and a mirror system to direct the beam onto the ion source on the target. In all of the experiments performed the aperture was half-closed and the area of the laser beam was calculated to be 1.5×10^{-4} cm ^{2}. The laser power was software controlled. For a range of software values, the laser energy was measured thus allowing direct calculation of the laser power used for each experiment. A plot of laser energy against software attenuation values for this instrument is shown in **Figure 2.7**

Ion source

The ion source is of commercial design[10] and consists of a positively or negatively charged metal electrode, that is the sample probe, and a grounded accelerating grid at a distance of 1cm. Accelerating potentials are possible for this instrument in the range

Figure 2.7

Plot to Show How Laser Energy Increased with Software Attenuation Values

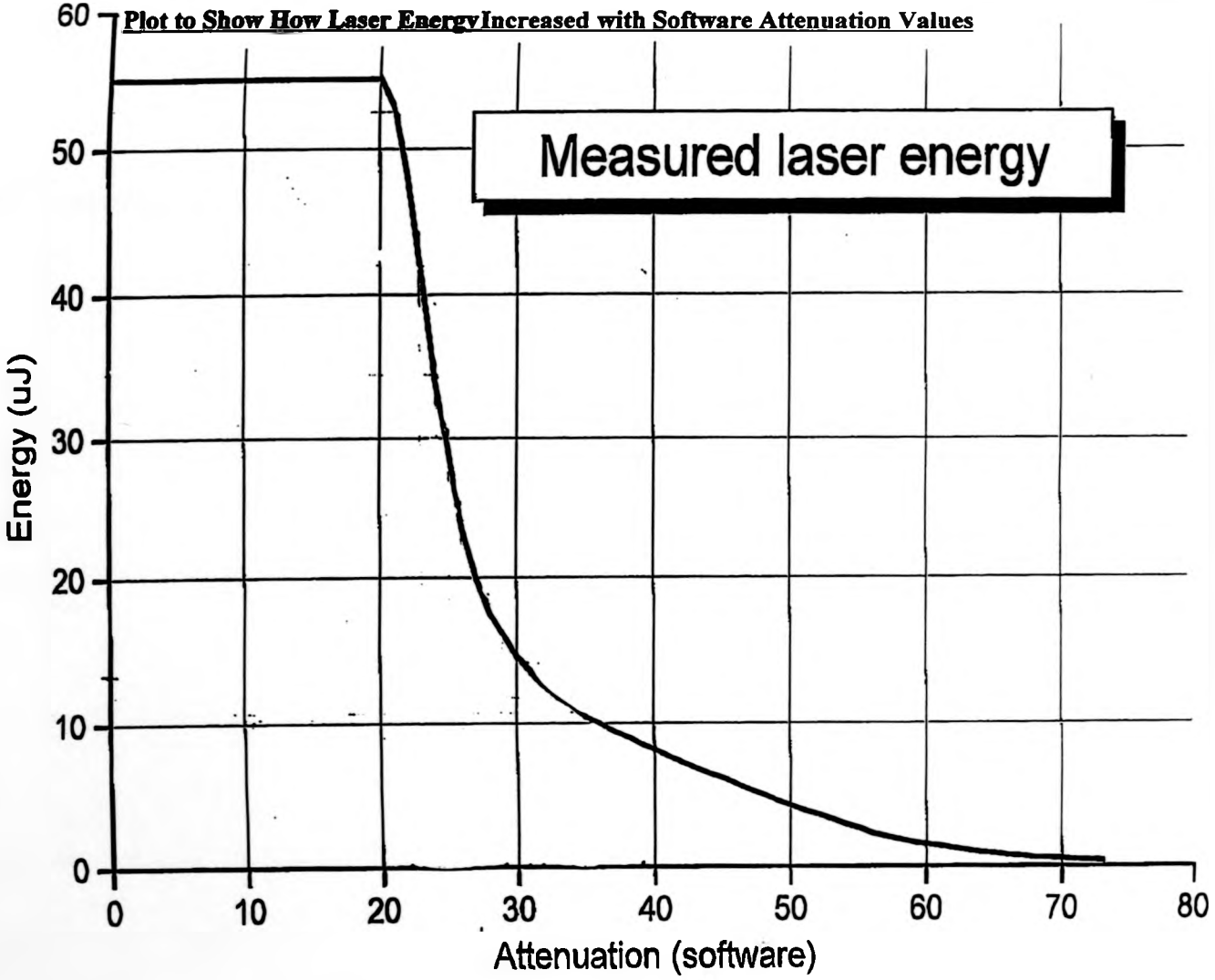

+30 to - 25 kV. This instrument is fitted with a manually operated sample loading facility. Sample selection is completely computer controlled and is performed on a circular area which may be rotated about its own axis as shown in **Figure 2.8.**

Figure 2.8

Sample Selection Using the Bruker Biflex MALDI-TOF Mass Spectrometer

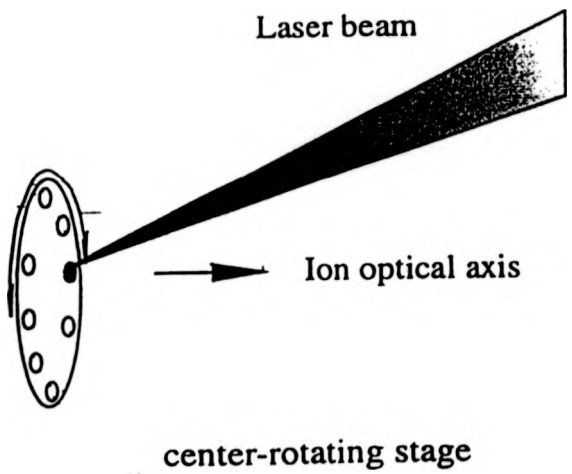

Ion Gate

This was mounted approximately 10cm behind the ion source and consists of two electrodes 10 mm part which were able to generate and electrical field of 2kV per cm orthogonal to the ion beam for short periods of time. By using this orthogonal electrical field, ions were deflected off the optical axis so that they did not reach the detector. The ion gate was 'closed' for a specific time in order to deflect ions of a certain mass range. The starting time and duration of this deflection was specified by the software in nano-seconds and the minimum duration of the pulse was set at 100ns.

Detection

The Biflex I instrument was fitted with an electron multiplier detector for use in linear mode, whereas in reflectron mode, dual micro-channel plates were fitted.

Reflectron

A two-stage gridless reflectron was used in order to increase the number of ions transmitted by focusing the divergent ion beam. The reflectron was tilted with respect to the beam to ensure off-axis detection.

The reflectron voltage was set at 20 kV in order to collect normal reflectron spectra. For post-source decay spectra, a maximum number of twenty time-of-flight segment spectra were acquired by reducing the reflectron voltage stepwise from 20.0kV to 0.68kV.

Data Acquisition and Instrument Control

The basic components of the system incorporated a SUN work station and a VME bus computer. After the vacuum control had reached its set points, the VME bus computer controlled all high voltages, the target position and the laser attenuation value. These operations were all carried out via the SUN work station. Detector signals were amplified in two stages, digitised and transferred to the SUN work station where they were displayed, saved and processed using software provided by Bruker. A schematic diagram of the instrument is shown in **Figure 2.9**.

Vacuum System and Source Chamber

A pressure of $< 1.0 \times 10^{-6}$ Torr was maintained by a turbomolecular pump backed by a rotary pump. Pressures inside this instrument was monitored by a thermocouple gauge which was linked up the VME bus computer system. The high voltage supply was electronically controlled and could not be switched at the computer until a minimum pressure of 3.5×10^{-6} Torr was reached.

Figure 2.9

Schematic diagram of the Bruker Biflex I MALDI-TOF Mass Spectrometer

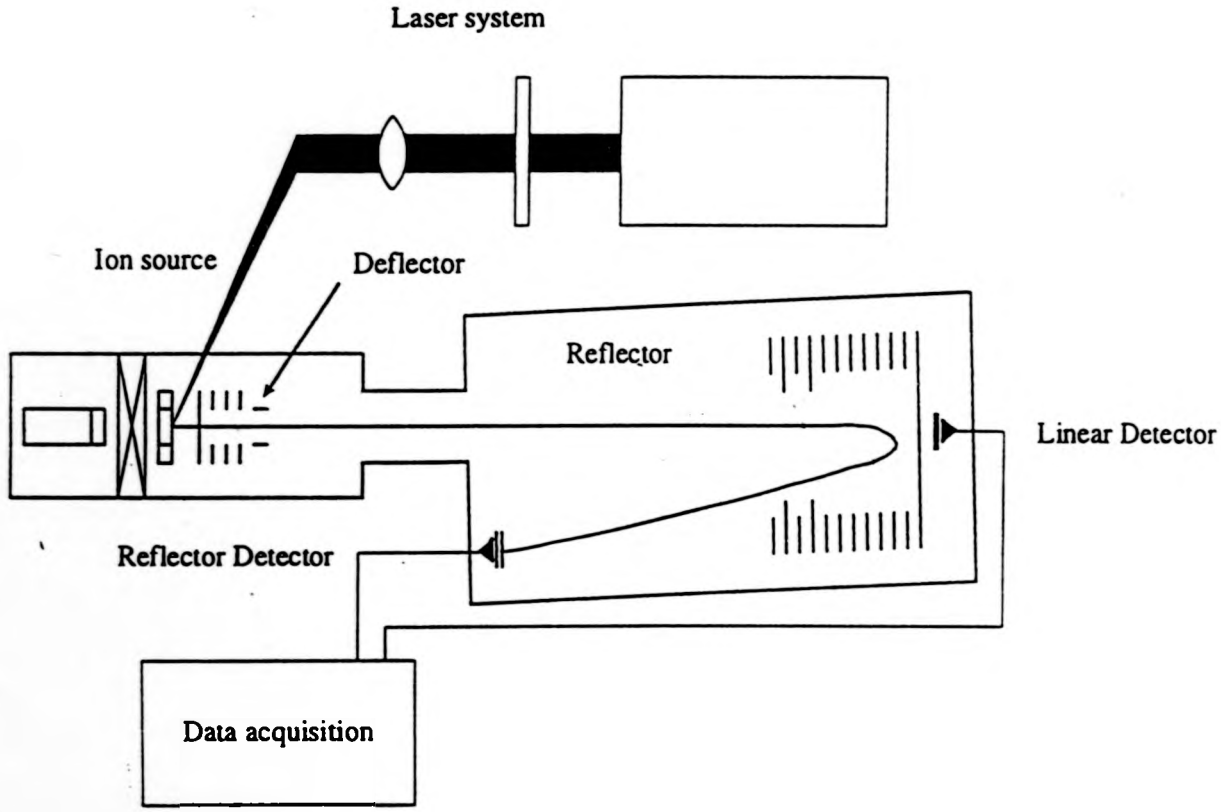

Samples for investigation by MALDI were introduced in to the source via a direct insertion lock. The first section of the air lock was evacuated after the sample slide was inserted. The source was isolated from the air lock by a ball valve and the source chamber is isolated form the rest of the instrument by an electronically controlled valve.

2.2 Experimental Methods.

2.2.1 Sample Preparation Methods for MALDI Experiments

Successful analysis of compounds by matrix-assisted laser desorption/ionisation depends on a number of different factors. In particular, the choice of matrix material and sample preparation method are of great importance. The matrix must have a strong absorption coefficient in the wavelength of the incident laser beam and, in most cases, this is in the ultra-violet region of the spectrum at ~ 337nm. A homogeneous sample preparation aids the efficiency of the MALDI process, so the ability of the analyte to mix effectively with a suitable matrix material in solution is also important. Matrix materials also have to fulfill the criteria of being stable under vacuum conditions. Many of the matrices used for the analysis of biomolecules are aromatic acids which have labile protons, and initial criteria for the choice of a suitable matrix material included the need for acidic protons. Growth in this area of research has been rapid and many materials which do not contain such a function have been reported to act succesfully as matrices. Materials which are either liquid or solid under standard temperature and pressure have been used as matrices.

Biomolecules such as peptides, carbohydrates and oligosaccharides readily form $[M+H]+$ ions by the MALDI process, however, synthetic polymers are usually detected as cation-attached oligomer ions in the form $[M+X]^+$, where X is usually an

alkali metal in the case of such polymers as poly(ethylene glycol) and poly(methyl methacrylate) or a transition metal cation in the case of poly(styrene).

General sample preparation procedures for the analysis of both polymers and biomolecules are outlined in this section.

2.2.1.1 Traditional MALDI Sample Preparation

i) Biomolecules

Compounds such as insulin and bradykynin were used as calibration materials. A solution of the analyte (~10^{-4}M in acetone or acetonitrile / water solution) was mixed 1:1 with suitable matrix, usually sinapinic acid or alpha-cyano hydroxy cinnamic acid. A 1 µl spot of the sample mixture was spotted onto the stainless steel sample slide and dried off in a stream of warm air.

ii) Polymers

A solution of polymer (~10^{-3}M, 3-5 mg per ml in THF) was doped with a solution of cation salt (0.1M, 1-100µl in THF). Equal quantities if this mixture and the matrix solution (0.1M in THF) were mixed and 1µl of this mixture was deposited onto a stainless steel sample slide and the solvent was evaporated off under a stream of warm air.

There are many other techniques which can be used to affect the results obtained by MALDI. For instance, air drying the solution gives different results form stirring during air drying.[185] Other methods such as two-layered deposition[186], spin-coated drying[187] or crushing the crystals[188,189] after drying have been proposed to improve sample homogeneity. Electrospray (ES) as a sample prepration method was also investigated as part of this research.[190]

2.1.1.2 Electrospray Sample Preparation

The electrospray set-up consisted of a 100μl sample-container feeding the analyte solution through a needle placed at at high potential relative to an adjustable grounded sample-table. The potential applied to the needle was ~ 8kV and the distance from the needle to the sample table was between 2 and 4 cm. A wire which was adjusted upwards and downwards was inserted into the needle to regulate the flow through the needle. The flow rate of the analyte solution was determined by measuring the time taken to empty the 100μl container. A positive electric field was used to drag the solution out from the needle into a cone, the apex of which was enhanced with positive charge. An equal flow of solution was emitted from the apex of the cone in the form of micrometer-sized positively-charged species.

The experimental procedure was concerned with optimising both the distance between the needle and the sample table and the needle potential , such that a single spray was emitted from the apex of the liquid cone. These sprayed droplets had to evaporate before they hit the MALDI sample slide located on the sample table.

A single spray ensured spot-to-spot reproducibility, however, the needle potential could be increased so that multi-sprays were emitted from the vertex of the cone and this function was used to decrease spraying time. Single sprays produced a circular spot which was ~ 1 cm in diameter whereas multi-sprays covered an area of 3cm in diameter with many domains. Work carried out with this apparatus used only the single-spray function.

A strong light positioned between the operator and the electrospray apparatus was used to observe the spray-cone to optimise the conditions. The needle potential was gradually increased until a single-cone was observed, and, if the sample slide was viewed at an angle, it was possible to see the formation of a thin layer within a few seconds. A schematic diagram of the electrospray apparatus is shown in **Figure 2.10**

Figure 2.10

Apparatus for Electrospray Sample Preparation of MALDI Slides

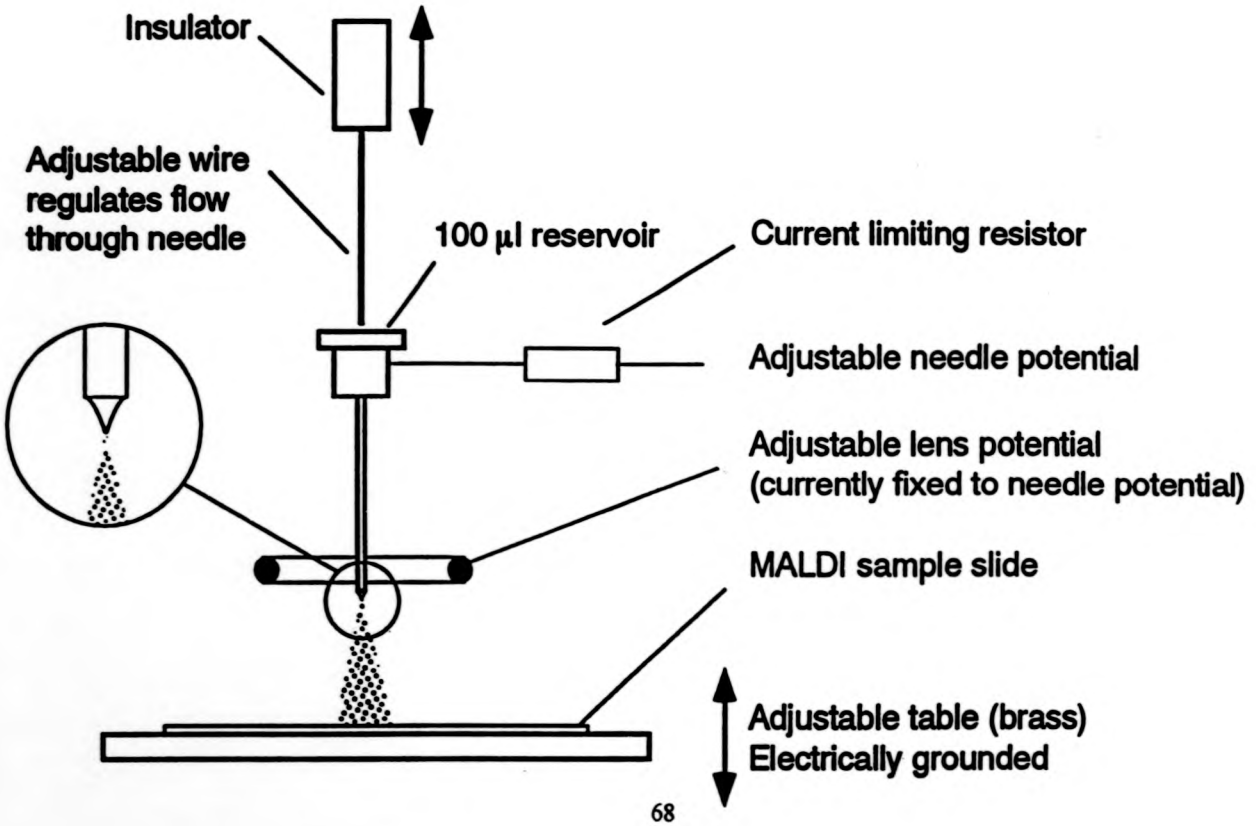

The conditions under which the samples were electrosprayed were carefully monitored. A typical polymer sample spot would take between 2 and 3 minutes to spray at a needle potential of ~ 6kV.

2.2.2 Emitter Activation Rig

The emitter activation apparatus can be divided into four main components: a vacuum system, a high voltage supply, a constant current supply and a BBC micro-computer. A schematic diagram of the apparatus used is shown in **Figure 2.11**

Vacuum Unit

The cylindrical activation chamber was made of stainless steel. The chamber was evacuated by a small oil diffusion pump (Edwards 63/105M) backed by a dual-stage rotary pump (Edwards ED 100). There were two separable plates attached to the chamber one of which was fitted with 19 brass emitter holders for the installation of emitters. The other plate was used to hold the removable stainless steel electrode. The activation chamber was furnished with two glass observation windows through which the emitters in the chamber could be observed. A brass baffle disc with a 3 mm diameter aperture in it was located between the activation chamber and the diffusion pump to reduce the pump speed of the diffusion pump. The gas pressure in the chamber was controlled by a precision variable leak (Granville-Phillips No. 203) located between the sample inlet and the vacuum chamber. Pirani gauges (Edwards PR-25K and PR-10) were used to measure the chamber pressure and the backing pressure respectively.

Heating Current Supply

The heating supply was floated at the emitter potential (upto 14kV) and was designed to produce a maximum current of 2.55 Amps. Insulation between the floated parts of the supply and the unfloated regions was provided by four 100 mm teflon supports.

Figure 2.11

Emitter Activation Rig

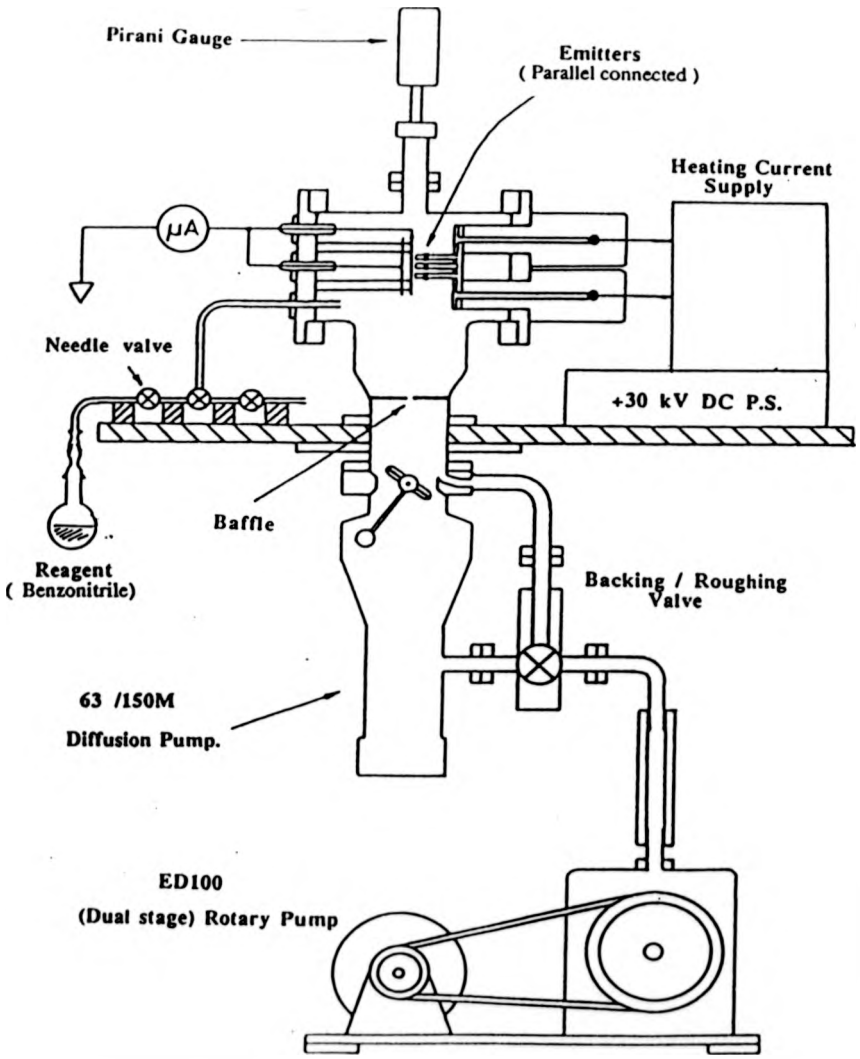

High-Voltage Supply

The emitters and the current supply were floated up to 15kV using a regualted 30 kV DC power supply (Brandenburg 2807R) which provided the high potential needed between emitters and cathode to field ionise the reagent gas, benzonitrile. The cathode plate was grounded via micro-ampere meter which was used to monitor the total ion current between the emitters and the cathode.

Micro-Computer Unit

An emitter-activation program had been written and installed by Chan[191] on a BBC micro-computer fitted with 32K of memory with an additional 32k Ram card. The 1 MHz bus was used to transmit output data from the central processing unit to an external four channel digital-to-analogue unit.

Accidental leakage of the high potential from the transducers to the computers was prevented by joining data lines to optical fibres. Voltage-to-frequency and frequency to-voltage converters were used at the junctions.

CHAPTER THREE

Matrix-Assisted Laser Desorption/Ionisation of Non-Polar Polymers

3.1 Introduction

One of the many challenges faced by modern mass spectrometry is the successful analysis of polymers of high molecular masses and broad molecular mass distributions. Even more important than the development of the technique to confront the difficulties surrounding this challenge, is perhaps the commercial need to analyse non-polar polymers such as poly(propylene), poly(butylene) and poly(ethylene). These polymers are of great importance owing to their many and varied applications, yet their rapid and accurate analysis still remains difficult.

No experiments concerning direct analysis of high-mass non-polar polymers by mass spectrometry have been reported in the open literature, although field desorption mass spectrometry continues to play an important role in the characterisation of high-boiling point petroleum mixtures. Early work by Derrick and co-workers demonstrated the application of field desorption mass spectrometry to a range of polymers including poly(styrene)[134,139,140] and poly(butadiene)[137]. In all cases, the major peaks in the spectra corresponded to (M+H)+ ions and fragmentation patterns provided information concerning the polymers' end-groups. More recent work by Evans and co-workers has evaluated the application of field desorption mass spectrometry to the analysis of poly(ethylene)[192].

The key to obtaining matrix-assisted laser desorption/ionisation (MALDI) spectra with high signal-to-noise ratios of unusual systems lies in developing and optimising preparations of suitable matrix materials. MALDI experiments had previously been devoted to synthetic polymers such as poly(methyl methacrylate) and poly(ethylene

glycol) which both can be readily analysed using 2,5 di-hydroxybenzoic acid as the matrix in combination with alkali metal cation attachment[62,70]. Before this work was started, in terms of MALDI, the most non-polar polymer investigated had been limited to poly(styrene)[70]. Here a series of experiments is described where conditions have been developed in order to study poly(isobutylene) by matrix-assisted laser desorption time-of-flight mass spectrometry.

3.2 Optimisation of Poly(styrene) Sample Preparation for Analysis by MALDI

Research initially focused on optimising the conditions under which a series of poly(styrene) Size Exclusion Chromatography (SEC) Standards could be analysed on a Kratos Kompact III MALDI-TOF mass spectrometer. The main problem with many of the matrices used in the analysis of biological samples such as sinapinic acid and alpha-cyano cinnamic acid is their polarity and consequently their inability to from homogeneous sample preparations. A series of experiments were carried out on a range of different matrices. These included dithranol, quinizarin, 9-nitroanthracene and hydroxy-azophenylbenzoic acid (HABA) and were chosen because of their previous successful application to oligometallocenes or to poly(styrene) itself[74]. All except HABA are anthracene derivatives and it was hoped that, owing to their mainly non-polar core, these compounds would readily mix with analytes of a similar nature. The structures of the matrices tested are depicted below.

9-Nitroanthracene

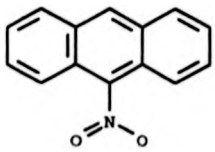

Dithranol

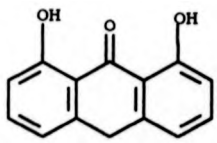

Quinzarin

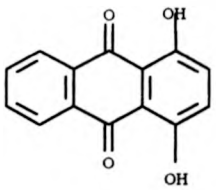

Hydroxy-Azo Phenylbenzoic Acid

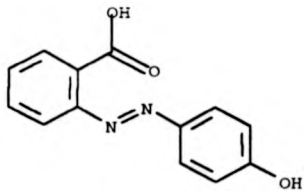

Cationisation of polymer species is generally acknowledged as a method of enhancing the number of polymer ions formed in the gas phase. Silver was chosen as a suitable cation and its addition took the form of silver tri-fluoroacaetate.

All experiments were carried out on a Kratos Kompact III MALDI-TOF Mass Spectrometer, a full description of which is found in the experimental chapter. The spectrometer was operated in the positive reflectron mode at an accelerating potential of 20 kV. Each spectra was collected over 200 laser shots and at a constant laser power just above the threshold of the sample. Analysis of the data was carried out using software installed on the Kompact III.

3.2.1 General Sample Preparation Method

In each case a poly(styrene) SEC standard was diluted in tetrahydrofuran (THF) such that the solution contained 3-5 mg of sample per ml of solvent (~ 10^{-3} M). Various volumes of silver tri-fluoroacetate (1-100µl) in THF were used to dope the analyte solution (0.5ml). Equal quantities of this solution and the matrix solution being tested were mixed. 1µl of the solution was deposited on the sample slide and the solvent was evaporated off in a stream of warm air.

i) Dithranol

A distribution of singly-charged silver-cationised polymer species was observed. This assigment is not unambiguous since the resolution of the instrument does not allow direct observation of the silver isotope distribution. It is, therefore, not possible to differentiate between ^{109}Ag and ^{107}Ag cations attached to an oligomer and it cannot be stated whether the main species ionised and detected is [M+Ag] + or [(M-H)+Ag] +. Further experiments carried out under similar conditions using 9-nitroanthracene as the matrix material and a higher-resolution instrument led to the conclusion that the dominant ion formed during the MALDI process was indeed [M+Ag]+. The signal-to-noise ratio observed using this sample preparation was mediocre.

ii)Quinizarin

A distribution of singly-charged silver-cationised polymer species was again observed and assignments could be made in a similar way to the dithranol case, however, quinizarin worked less effectively as a matrix material than dithranol since the total ion current was typically decreased by a factor of ten. The mass range which could be invetsigated using this matrix was limited to the same extent as dithranol; poly(styrene) oligomers of up to 4000 Da could be detected using this sample preparation on the Kompact instruments. Characteristic matrix peaks were observed in the mass range upto 400Da.

iii) 9-Nitroanthracene

9-Nitroanthracene proved to be the most effective matrix for the analysis of poly(styrene)s on the Kompact III. The total ion current values increased dramatically and the mass range which could be investigated was noticeably higher (up to 11000Da). A typical MALDI spectrum using this matrix contained a distribution of singly-charged silver cation attached poly(styrene) oligomers. No multiply-charged species were observed. Peak assignment was not unambiguous owing to the limited

resolution of this technique, however, further experiments are described later in this chapter which confirmed the attachment of one silver cation to a poly(styrene) oligomer. Characteristic matrix peaks were observed upto 500 Da.

The optimised sample preparation used 50μl of a solution of silver tri-fluroacetate in THF to dope the analyte solution (0.5ml). Equal quantities of this solution and the matrix solution (0.1M 9-nitroanthracene in THF) were mixed. 1 μl of this mixture was deposited on the stainless steel sample slide and the solvent evaporated off.

Figures 3.1, 3.2 and 3.3 show the spectra obtained for a poly(styrene) standard (M_n value of 2950 Da polydispersity index of 1.1, quoted by Polymer Laboratories) using dithranol, quinizarin and 9-nitroanthracene as the matrix materials. These are characteristic of poly(styrene) spectra obtained by MALDI. Each peak represents an oligomer which has a silver cation attached. In general, only one silver cation attached to a polymer oligomer and no multiply-charged polymer species were observed. Polymer analysis using the software available on the Kompact III yielded the tabulated data shown below for the spectra depicted overleaf. It can be seen that there is good agreement among the data obtained using different matrices.

Matrix	Calculated monomer mass (Da)	Total ion current (mV)	M_n	M_w	Polydispersity
Dithranol	104	50	2864	2933	1.02
Quinizarin	104	5	2762	2836	1.03
9-Nitroanthracene	104	137	2839	2917	1.03

The maximum error in both M_n and M_w is ≤1.5% and the maximum error in the poly(dispersity) index value is ≤3%.

Figure 3.1a

MALDI Spectrum of a Poly(styrene) Standard (Molecular Mass~ 2950 Da)Using Dithranol as the Matrix

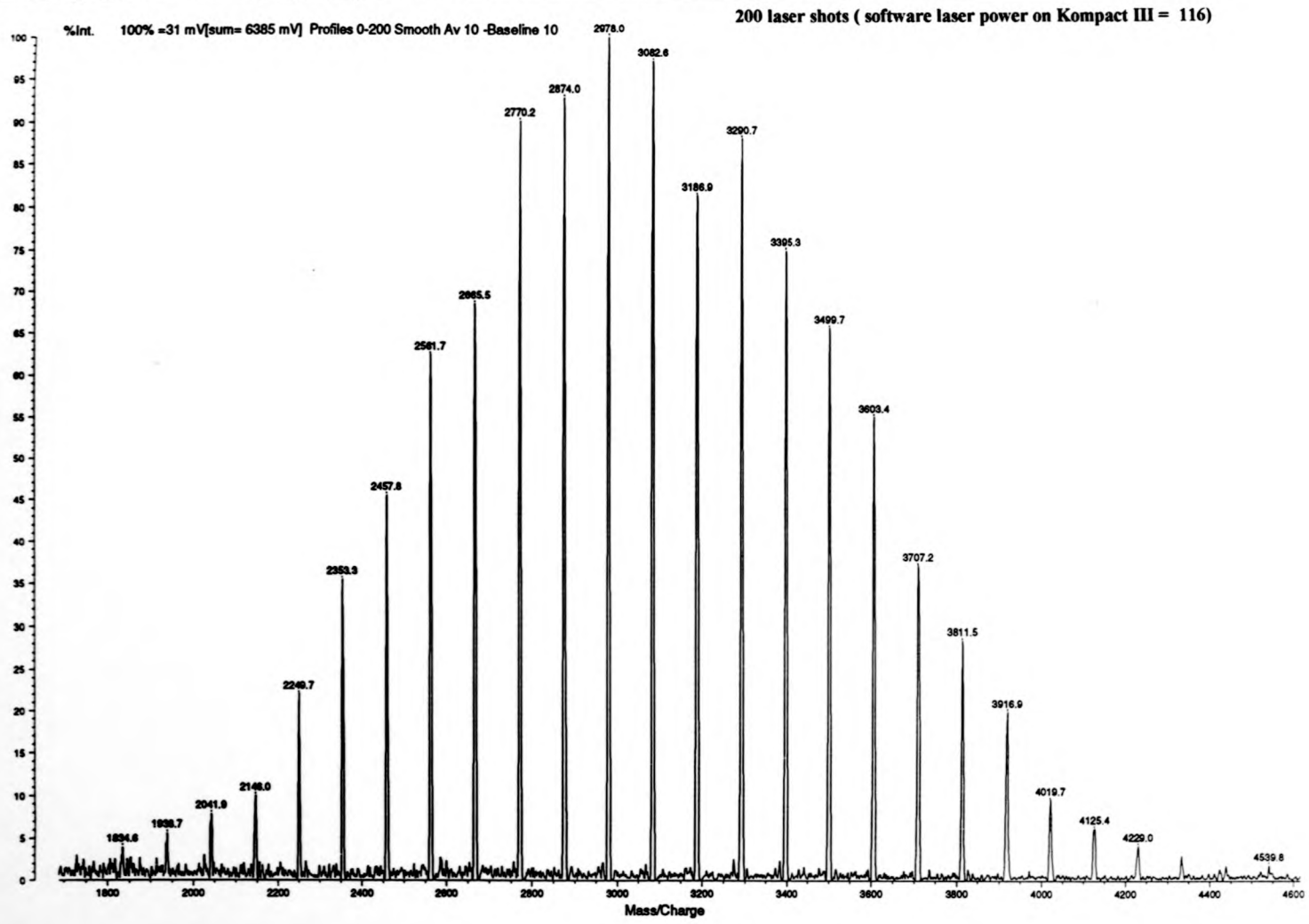

Figure 3.1.b

Part of the Poly(styrene) Spectrum Showing 104 Monomer Mass Separation

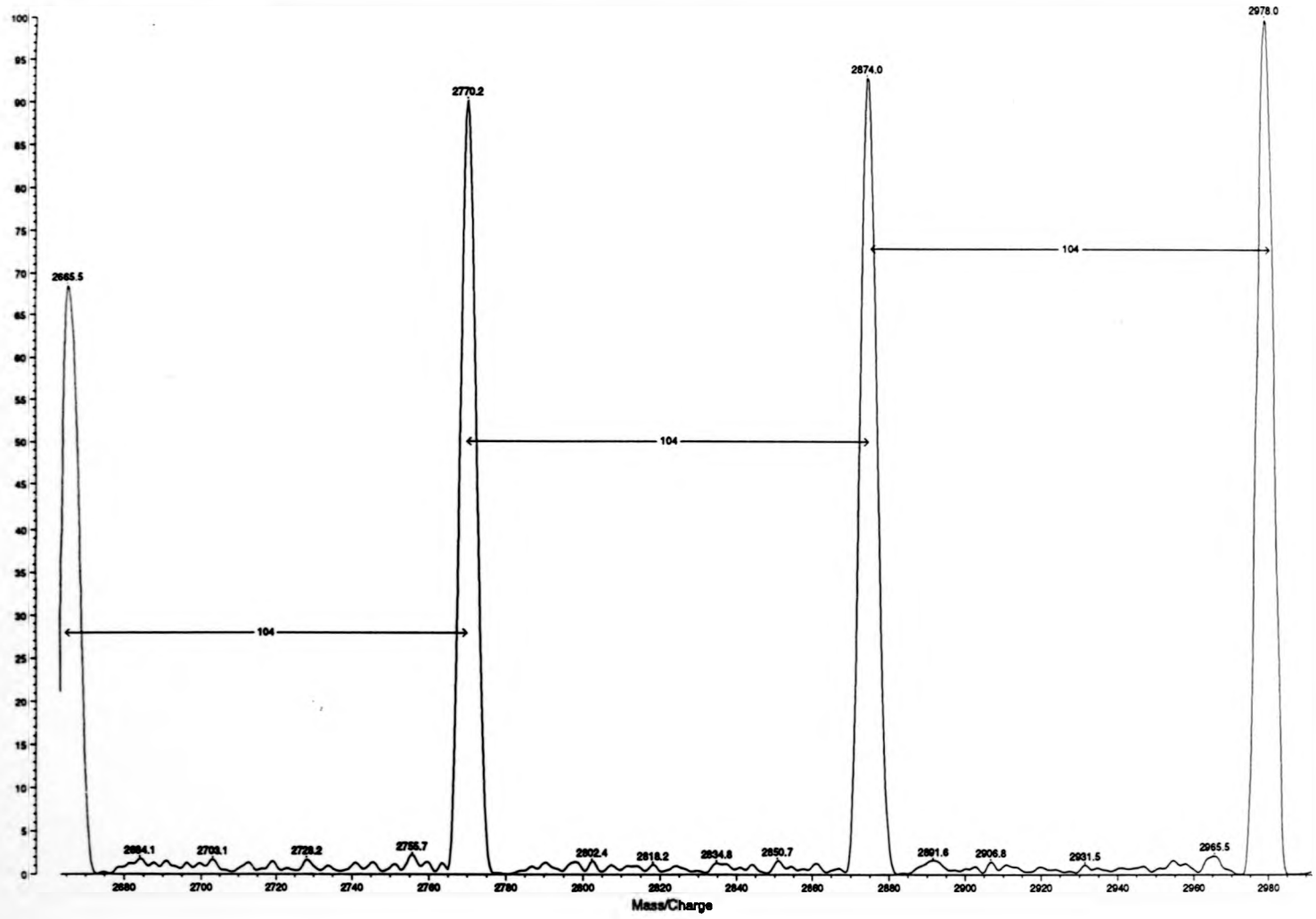

Figure 3.2a

MALDI Spectrum of a Poly(styrene) Standard (Molecular Mass ~2950 Da) Using Quinizarin as the Matrix

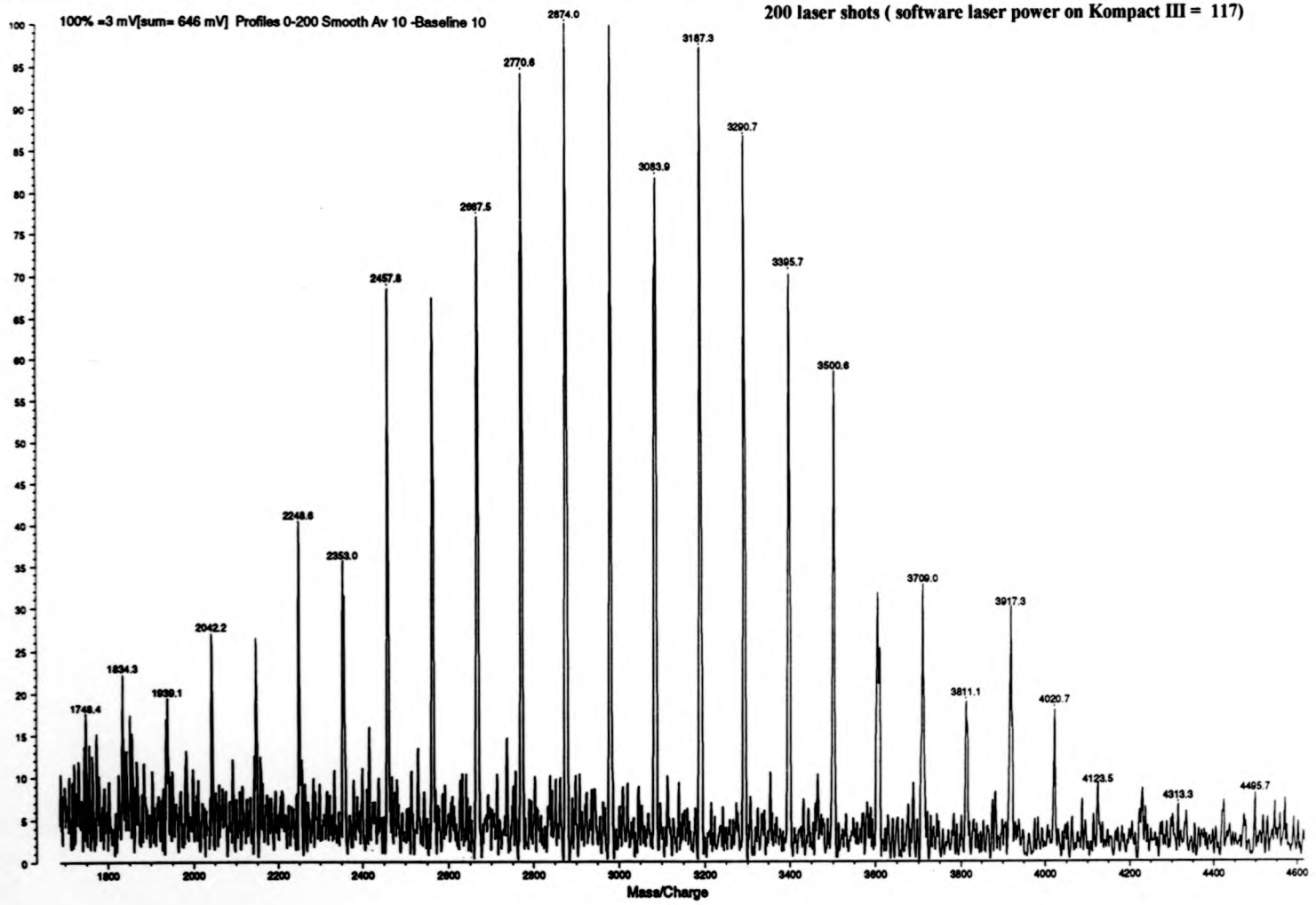

Figure 3.2.b

Part of the Poly(styrene) Spectrum Showing 104 Monomer Mass Separation

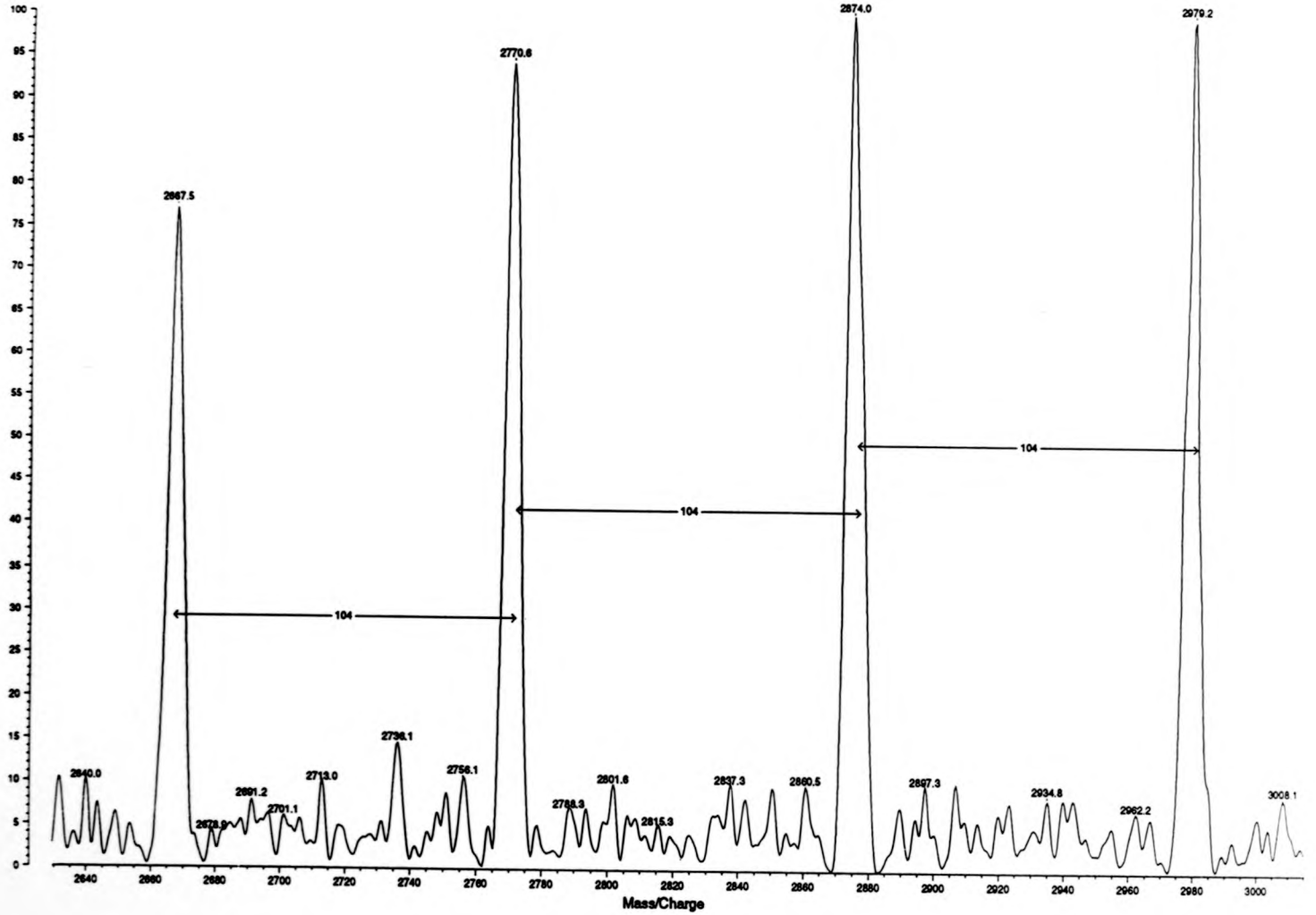

Figure 3.3a

MALDI Spectrum of a Poly(styrene) Standard (Molecular Mass ~2950 Da) Using 9-Nitroanthracene

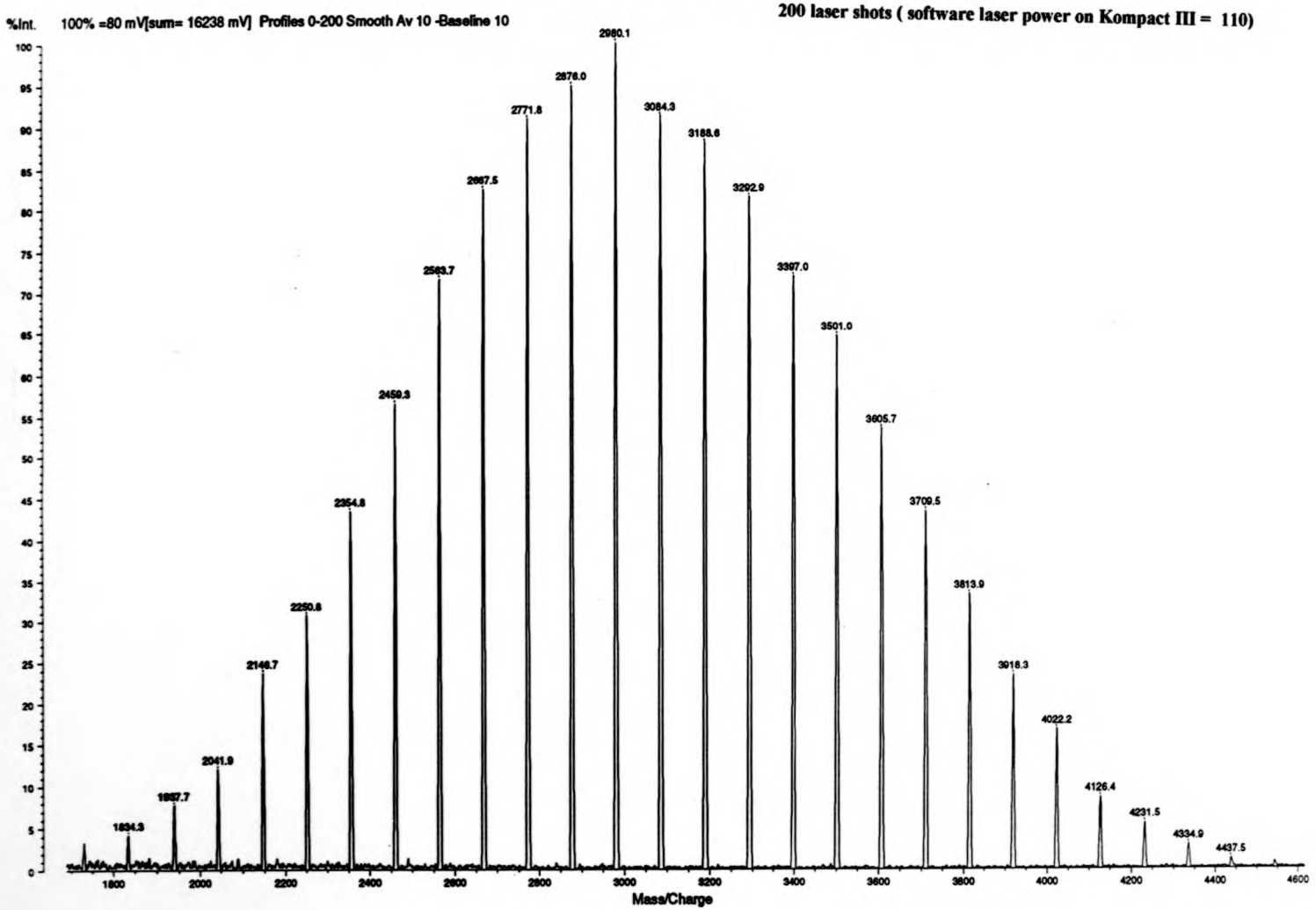

Figure 3.3b

Part of the Poly(styrene) Spectrum Showing 104 Monomer Mass Separation

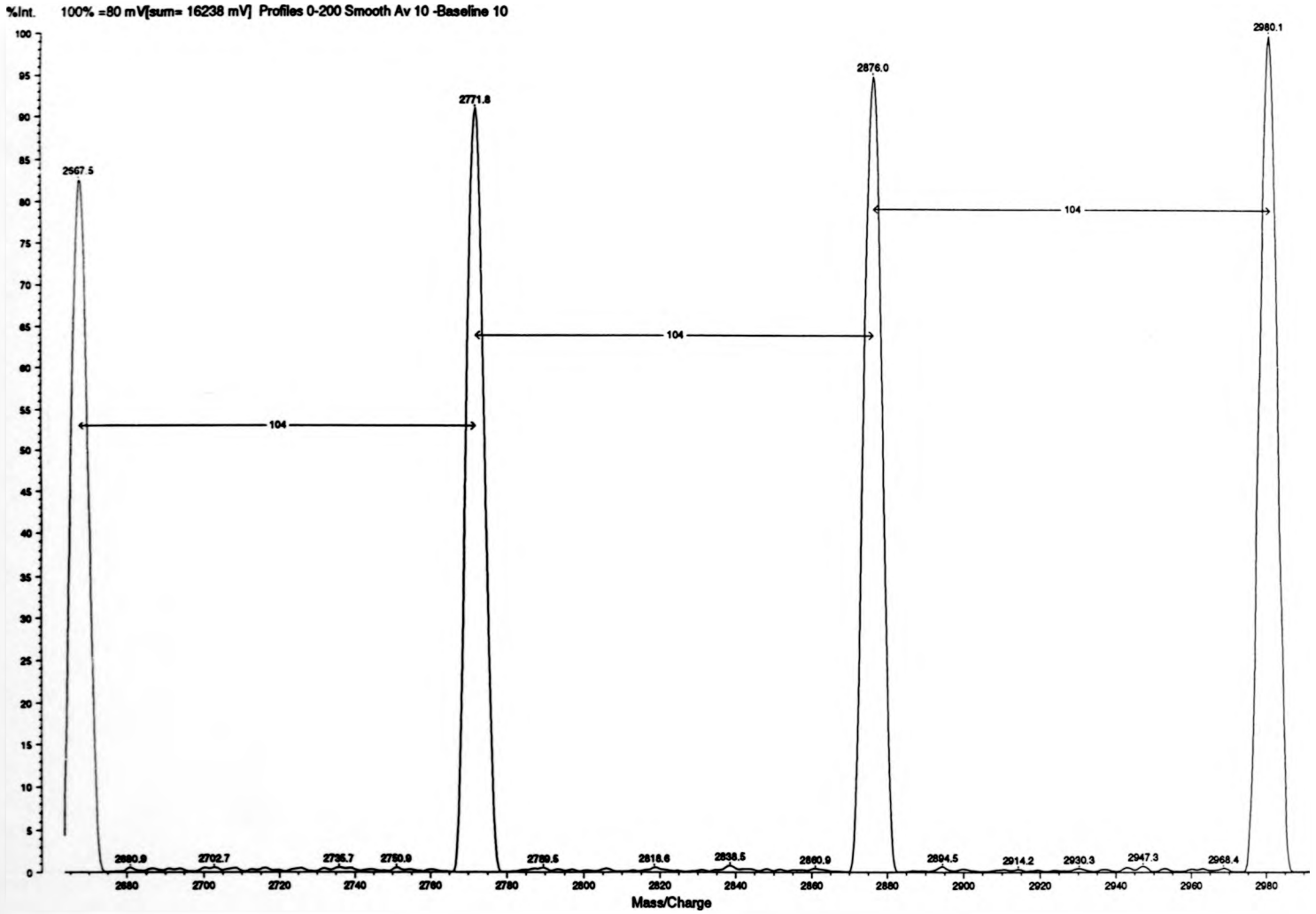

The increase in total ion current and signal-to-noise values did not extend to all substrates analysed with 9-nitroanthracene. **Figure 3.4a** shows a poly(methyl methacrylate) SEC standard (Polymer Laboratories, M_n = 3400Da, poly(dispersity) index = 1.09) under the same conditions. **Figure 3.4b** clearly depicts the 100 Da mass separation of each monomer unit. The total ion current and signal-to-noise values were considerably less than those obtained when 2,5- dihydroxybenzoic acid was used as the matrix material.

3.2.2 Confirmation of Silver Cation Attachment Poly(styrene)

Experiments were carried out on a Four Sector Kratos Concept Instrument. A brief description of and the modifications made to this instrument are located in the experimental chapter. For a more detailed account the reader is referred to the full description by Raptakis.

An external calibration of the double-focusing mass spectrometer was initially carried out by L-SIMS using caesium iodide clusters. The laser spot in the MALDI source was aligned to the centre of the sample probe using a beam steering device. Thermal paper was attached to the surface of the sample and the laser beam was irradiated at full power on this paper in order to centralise the position of the burn mark. A poly(styrene) standard (Mn=1680, polydispersity index value <1.1, Polymer Laboratories, UK) was prepared using the optimum conditions described in section 3.2.1. 1μl of the sample mixture was loaded onto the probe and the sample dried off in air. The sample probe was manually manipulated in order to expose a fresh sample area to the laser beam spot and the laser was operated at a repetition rate between 10 and 20 Hz. The laser power was adjusted using an attenuator. Snapshots of the mass spectrum were obtained with a 1 second integration time. A number of scans, typically between 5 and 8, were required in order to obtain good quality spectra Data of a moderate resolution was obtained for this sample and **Figure 3.5** shows part of the polymer distribution for the poly(styrene) sample investigated.

Figure 3.4a

MALDI Spectrum of a Poly(methylmethacrylate) Standard Using 9-Nitroanthracene as the Matrix with Silver Cationisation

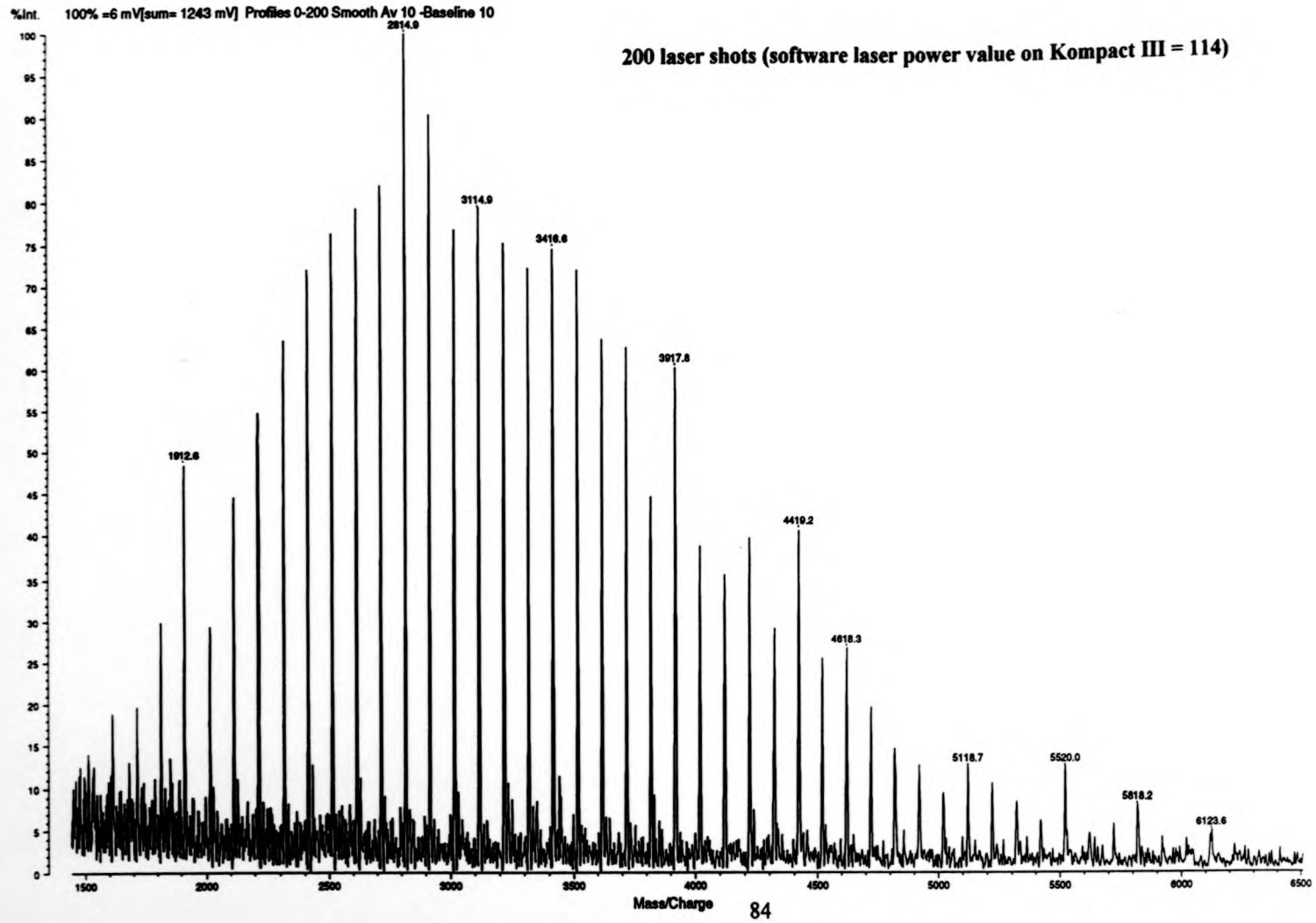

Figure 3.4b

Part of the PMMA Spectrum showing 100 Monomer Mass Separation

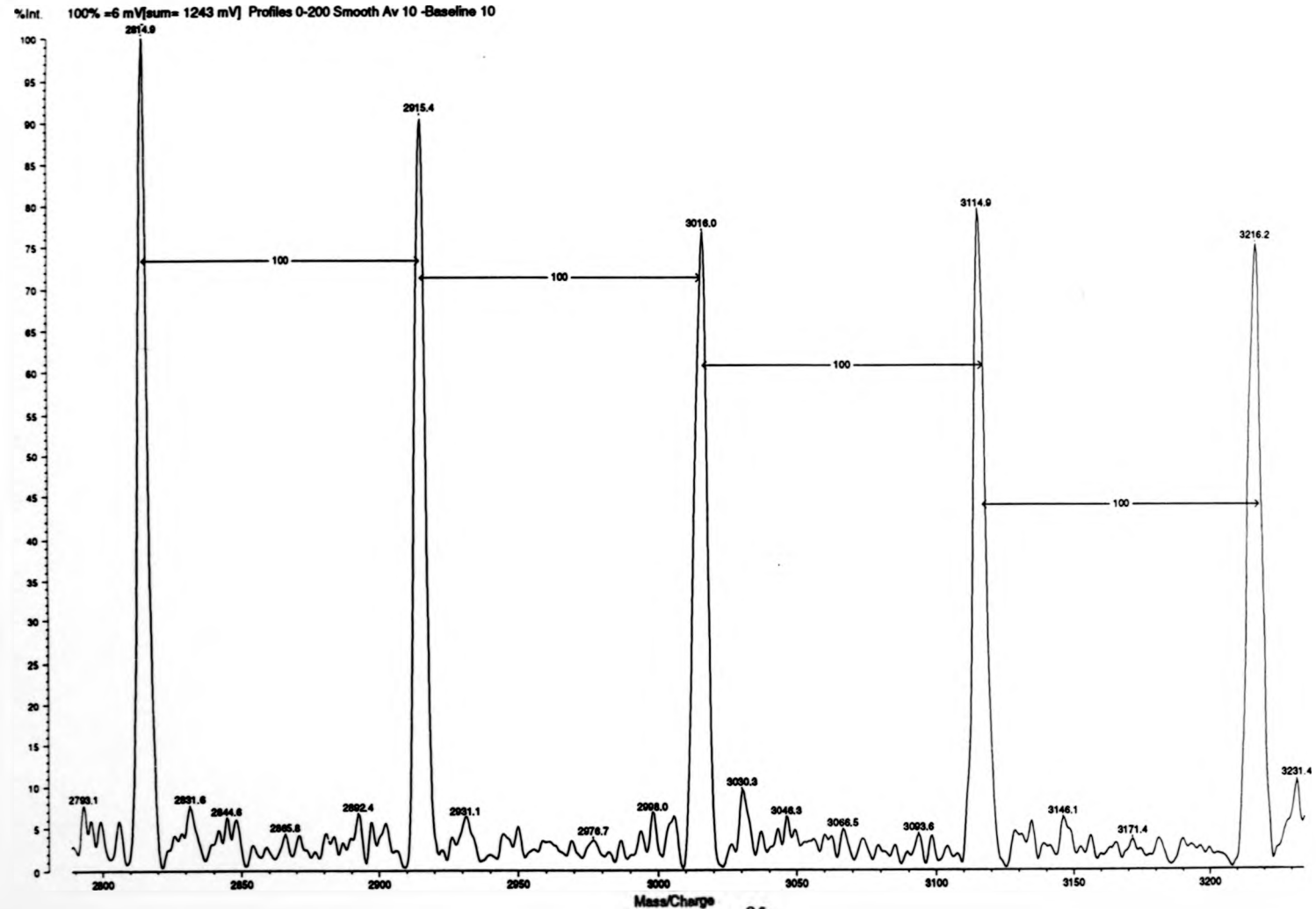

Figure 3.5

Part of the Poly(styrene) Distribution as Detected on the Four Sector Instrument

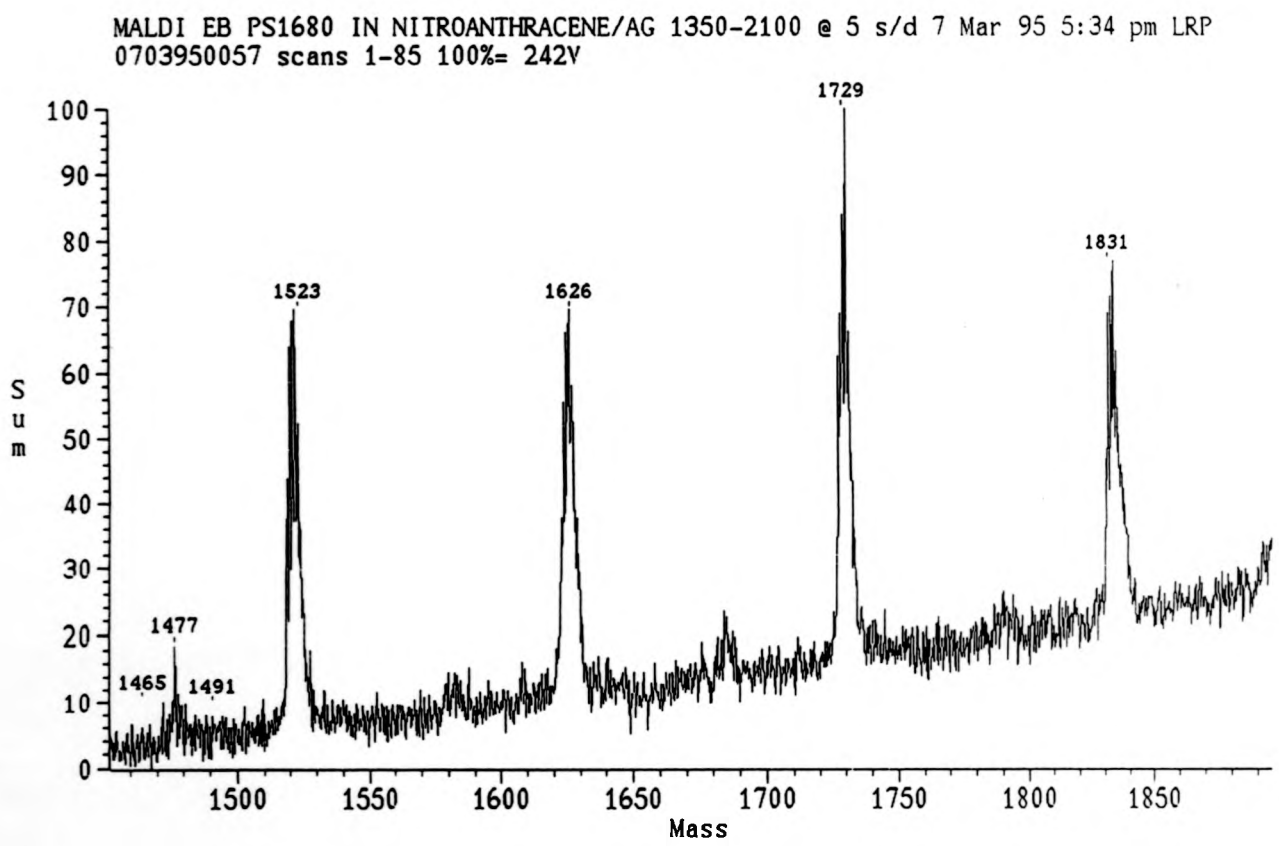

This distribution was compared with a calculated isotope pattern assuming that each oligomer ion is detected as [M+Ag] + and **Figure 3.6** shows a comparison between experimental and theoretical isotope patterns. It can be seen that good agreement was achieved between the two sets of data. The peak at 1625 Da corresponds to an intact poly(styrene) oligomer consisting of 14 styrene units with a singly-charged silver cation attached. Further experiments were carried out on the poly(isobutylene) samples containing an aromatic ring function using this instrument. The general sample preparation described in section 3.2.1 was used to attempt to obtain higher resolution spectra of these samples and to confirm the attachment of a singly-charged silver cation to each oligomer ion, however, no interpretable data could be obtained by adding between 1 and 100μl of silver salt to the sample preparation.

It is likely that no spectra were obtained for these samples owing to the reduced sensitivity of this method compared with time-of-flight analysis. Decreased sensitivity on sector instruments is one of their main disadvantages. This difference was highly noticeable even when analysing a poly(styrene) standard. The use of a time-of-flight analyser led to rapid and reproducible results being obtained with high sensitivity but with relatively low resolution. The use of a double-focusing mass analyser meant that results were much harder to obtain and generally took much longer.

Thus, the addition of the silver salt in the analysis of poly(styrene) by MALDI was crucial in obtaining a spectrum. and only one cation attached itself to a polymer oligomer. No multiply-charged species were seen. The interaction between the poly(styrene) oligomers and poly(isobutylene) oligomers is likely to involve the aromatic ring function present since silver ions are renown for their strong interaction with aromatic rings. [208]

Figure 3.6

Comparison Between Experimental and Theoretical Isotope Distributions for Poly(styrene)-Silver Adducts

i) Experimental

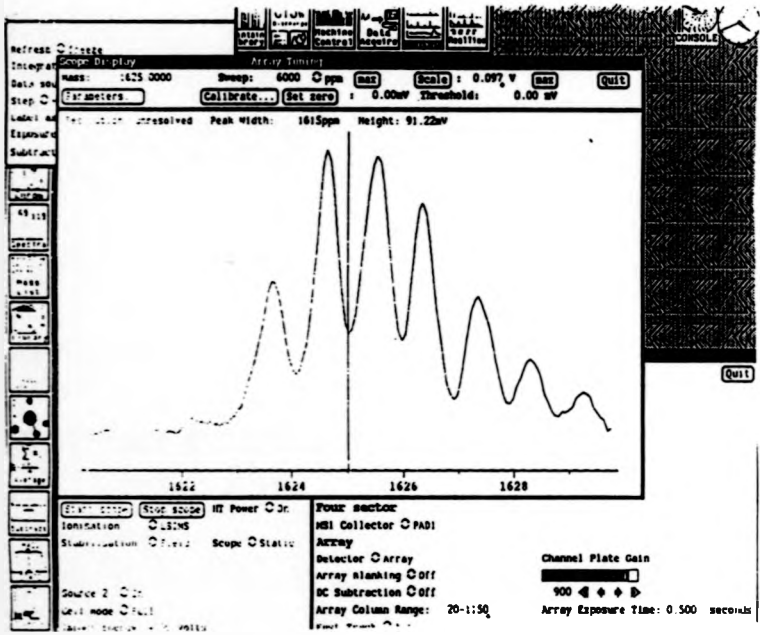

ii) Theoretical

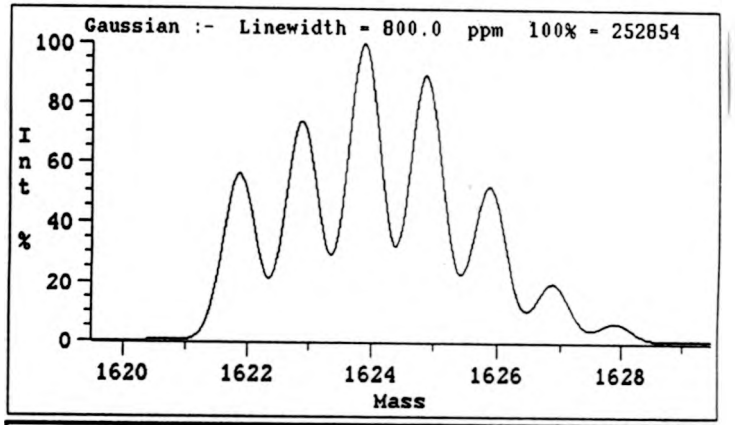

Mass	Abundance	12 C	13 C	1 H	2 H	107 Ag
1621.85974	14.8021	116	0	122	0	1
1622.86310	19.2731	115	1	122	0	1
1623.85935	13.7623	116	0	122	0	0
1623.86645	12.4391	114	2	122	0	1
1624.86271	17.9193	115	1	122	0	0
1624.86981	5.3057	113	3	122	0	1
1625.86606	11.5654	114	2	122	0	0
1626.86942	4.9330	113	3	122	0	0

3.2.3 Calculations on the Molecular Mass Distributions

The successful analysis of a range of polystyrene standards by MALDI-TOF mass spectrometry lead to comparisons being made between molecular mass statistics obtained by MALDI and those obtained by size exclusion chromatography (SEC). This work was carried out in response to a paper published by Lehrle and Sarson who claimed poor agreement between the two methods. Calculations on the mass distributions of polymer samples analyse by MALDI-TOF are presented and discussed in chapter 4.

3.3 The Analysis of Poly(isobutylene) Samples by MALDI-TOF Mass Spectrometry

The optimisation of conditions under which poly(styrene) could be analysed led to the application of 9-nitroanthracene in conjunction with silver tri-fluoroacetate to the analysis of poly(isobutylene) samples containing an aromatic ring function.
Three main poly(isobutylene) samples have been studied, of average molecular mass approximately equal to 1000 Da and a poly(dispersity) index value close to unity. The structures of these samples are shown in **Figure 3.7.**

3.3.1 Effect of Silver Salt Concentration on the MALDI Spectra of Poly(isobutylene)

The amount of silver tri-fluoroacetate salt added to the sample and the ratio of aromatic ring to chain length both proved to be determining factors in obtaining reproducible spectra. A range of silver tri-fluoroacetate volumes (1-100μl, 0.1M in THF) were added to a solution of each poly(isobutylene) sample. (0.5ml, 10^{-3}M in THF).

Figure 3.7

Structures of Poly(isobutylene) Samples Investigated by MALDI

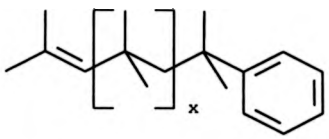

Mono-olefinic Poly(isobutylene)

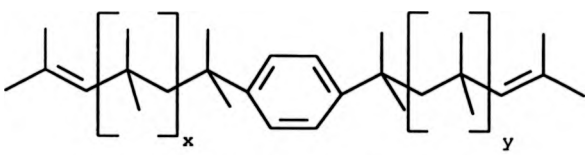

Di-Olefinic Poly(isobutylene)

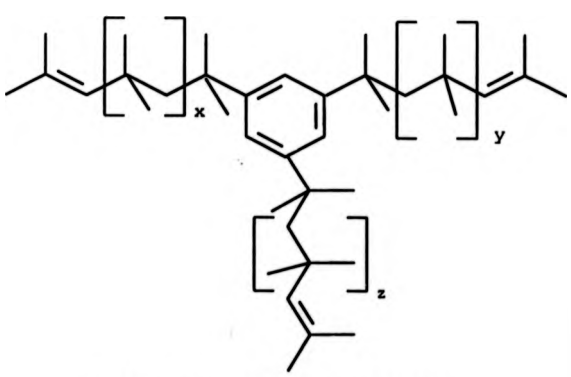

Tri-Olefinic Poly(isobutylene)

The minimum amount of silver tri-fluroacetate salt which could be added to obtain a spectrum of the tri-olefinic sample was found to be 10µl, however, the spectrum with the best signal-to-noise values was obtained when 50µl of salt was added. Addition of excess silver salt led to the detection of a second distribution which also had a monomer mass value of 56Da.

For all silver salt volumes, the spectrum observed consisted of a distribution of singly-charged silver cation-attached PIB oligomer ions, [M+Ag]+, the mass difference between each peak being the monomer mass value of 56 Da.
In the case of the di-olefinic sample, ions of the type described could be detected when 20-50µl of silver salt was added to the sample solution. Excess silver salt resulted in no interpretable data being obtained, furthermore, spectra were often dominated by silver clusters of the type Ag_n^+.

The mono-olefinic sample proved to be the most difficult to analyse under these conditions. A mass spectrum of this sample could be obtained by adding 50µl of the silver salt solution to 0.5 ml of the sample solution. Ultra-sonification at room temperature for 2-3 minutes was necessary in this instance to ensure complete mixing and the formation of the most homogeneous sample preparation.

Figures 3.8a, 3.9a and 3.10a depict spectra of the mono-olefinic, di-olefinic and tri-olefinic samples respectively. The monomer repeat unit of 56 Da can be seen in **figures 3.8b, 3.9b,** and **3.10b** indicating the presence of poly(isobutylene) units with possible silver attachment. All spectra were obtained with the addition of 50µl of silver tri-fluoroacetate (0.1M in THF).
Figure 3.11 shows a spectrum of the tri-olefinic sample when excess salt had been added. A second distribution is clearly observed and the mass separation between these peaks also corresponds to 56 Da.

Figure 3.8a

MALDI-TOF Mass Spectrum of Mono-Olefinic Poly(isobutylene) **200 laser shots (software laser power on Kompact III = 158)**

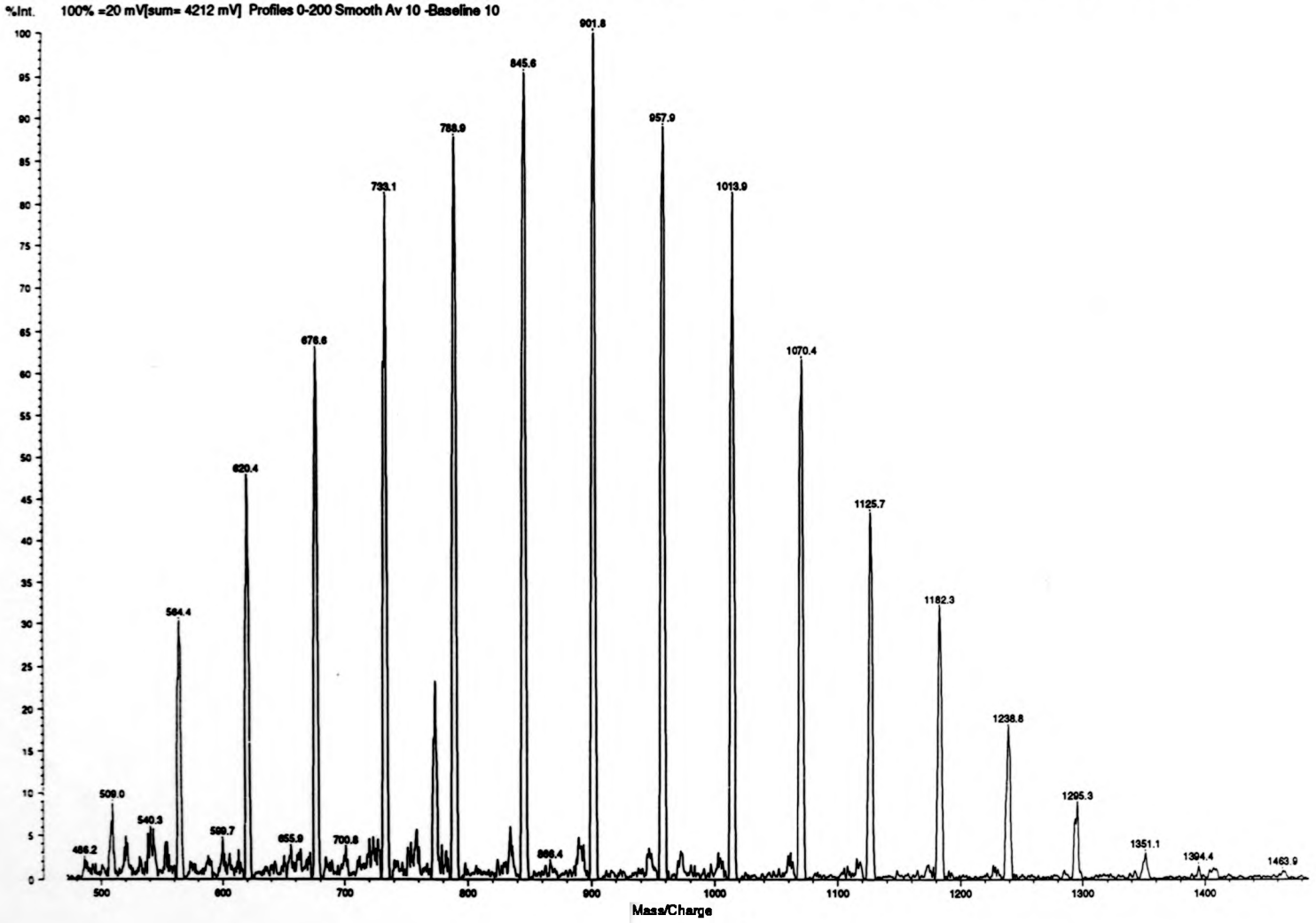

Figure 3.8b

Part of the Mono-olefinic PIB Sample Showing 56 Monomer Mass Separation

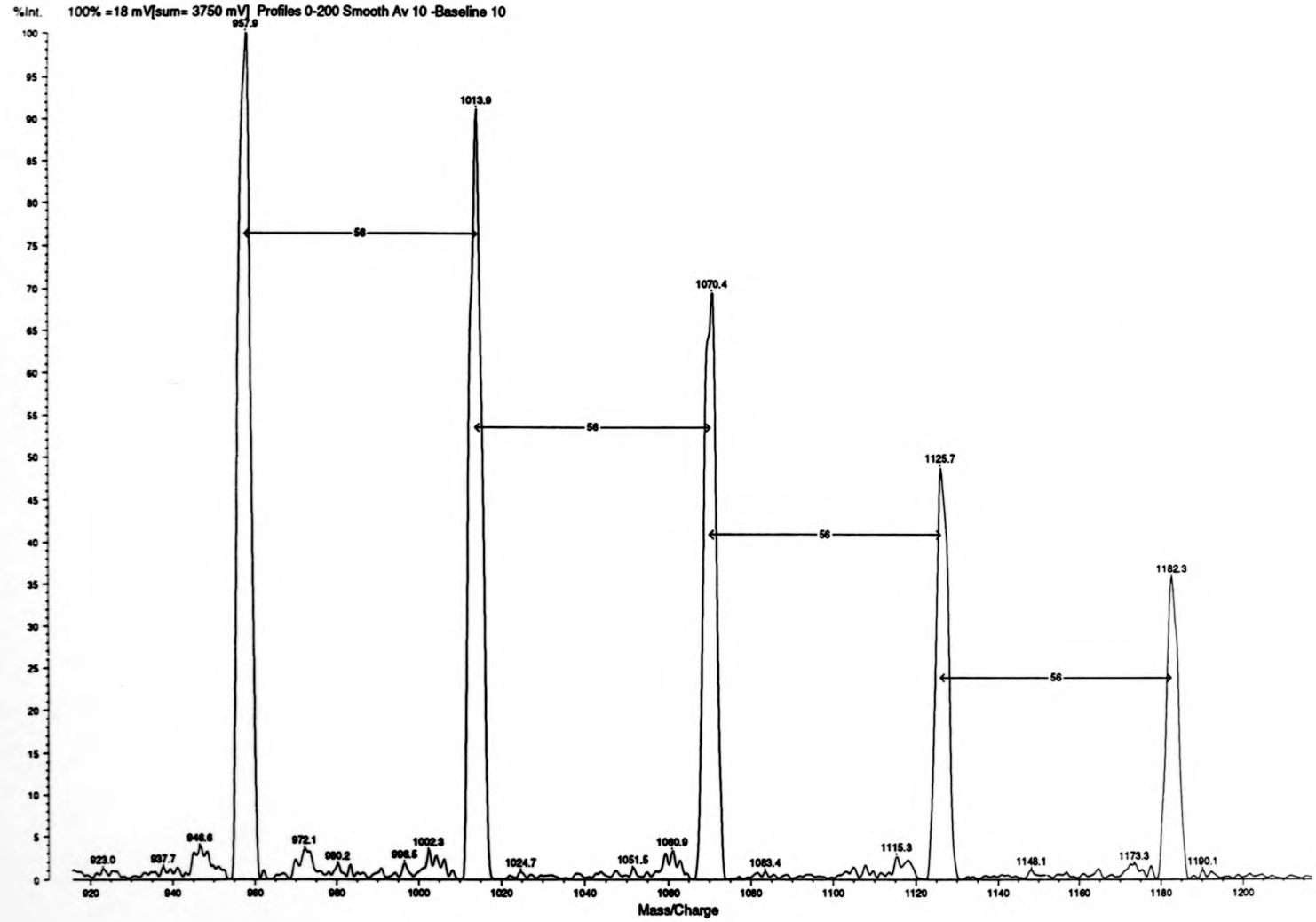

Figure 3.9a

MALDI-TOF Mass Spectrum of Di-Olefinic Poly(isobutylene) **200 laser shots (software laser power on Kompact III = 143)**

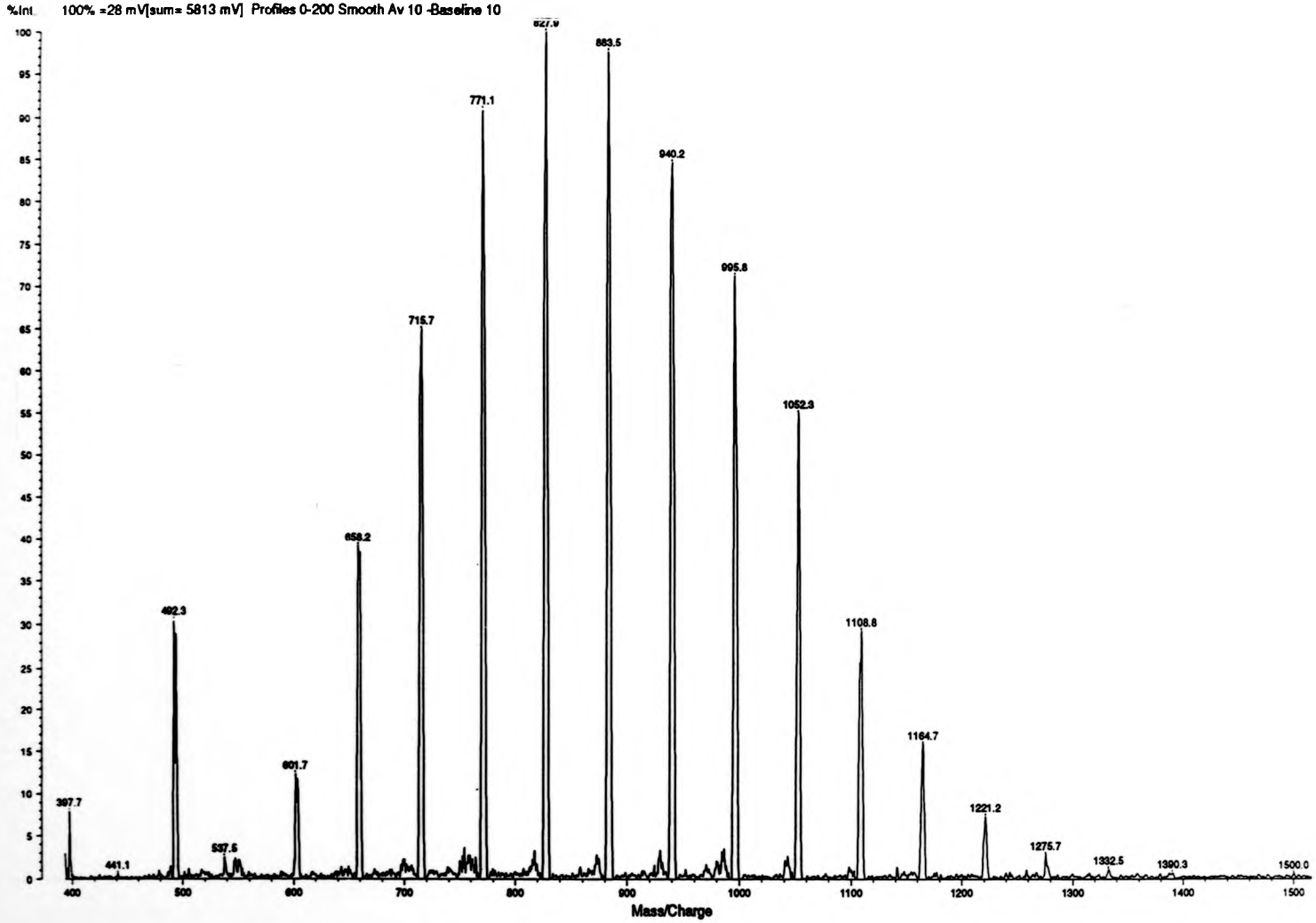

Figure 3.5b

Part of the Di-olefinic PIB Sample Showing 56 Monomer Mass Separation

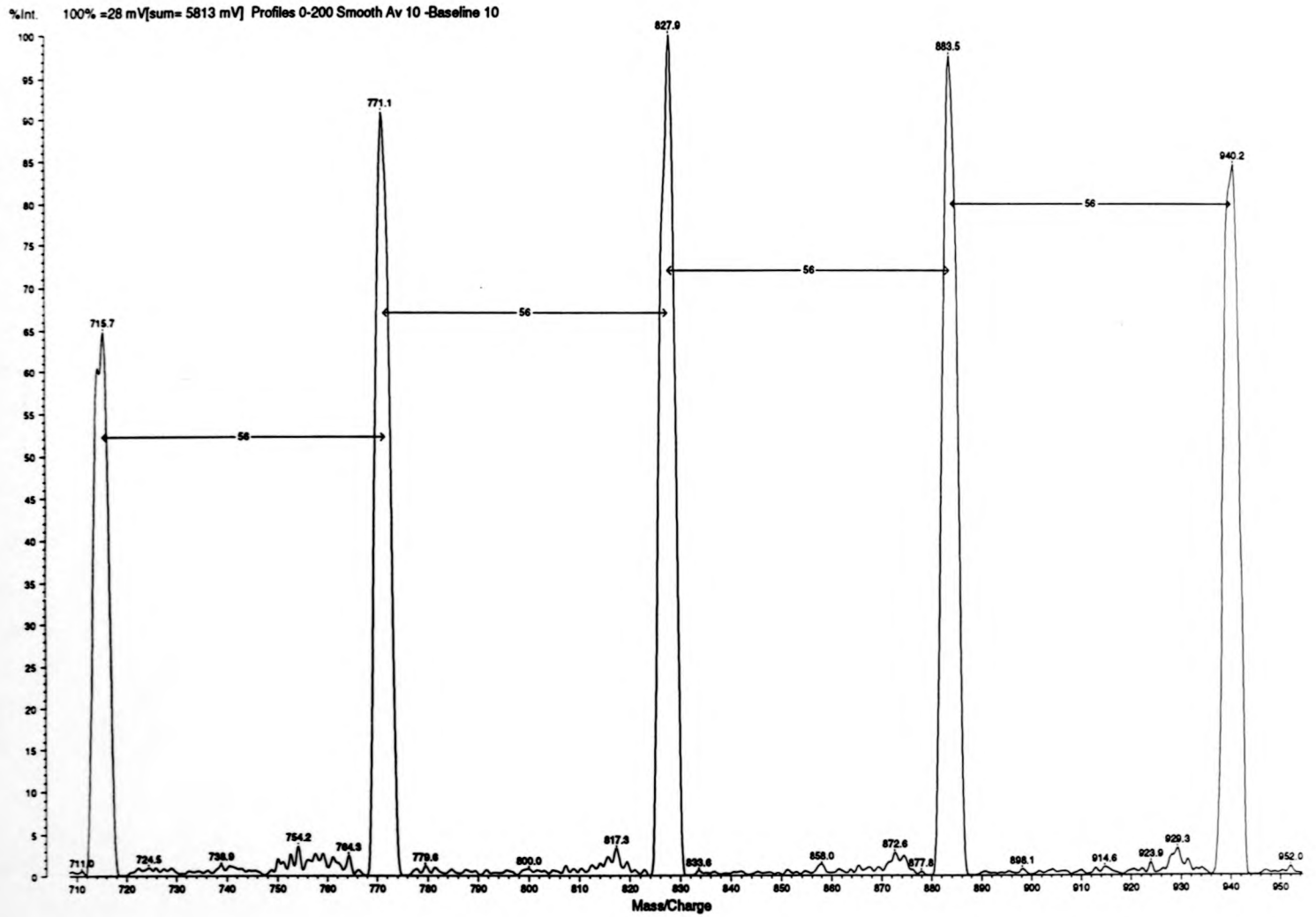

Figure 3.10a

MALDI-TOF Mass Spectrum of Tri-Olefinic Poly(isobutylene) **200 laser shots (software laser power on Kompact III = 150)**

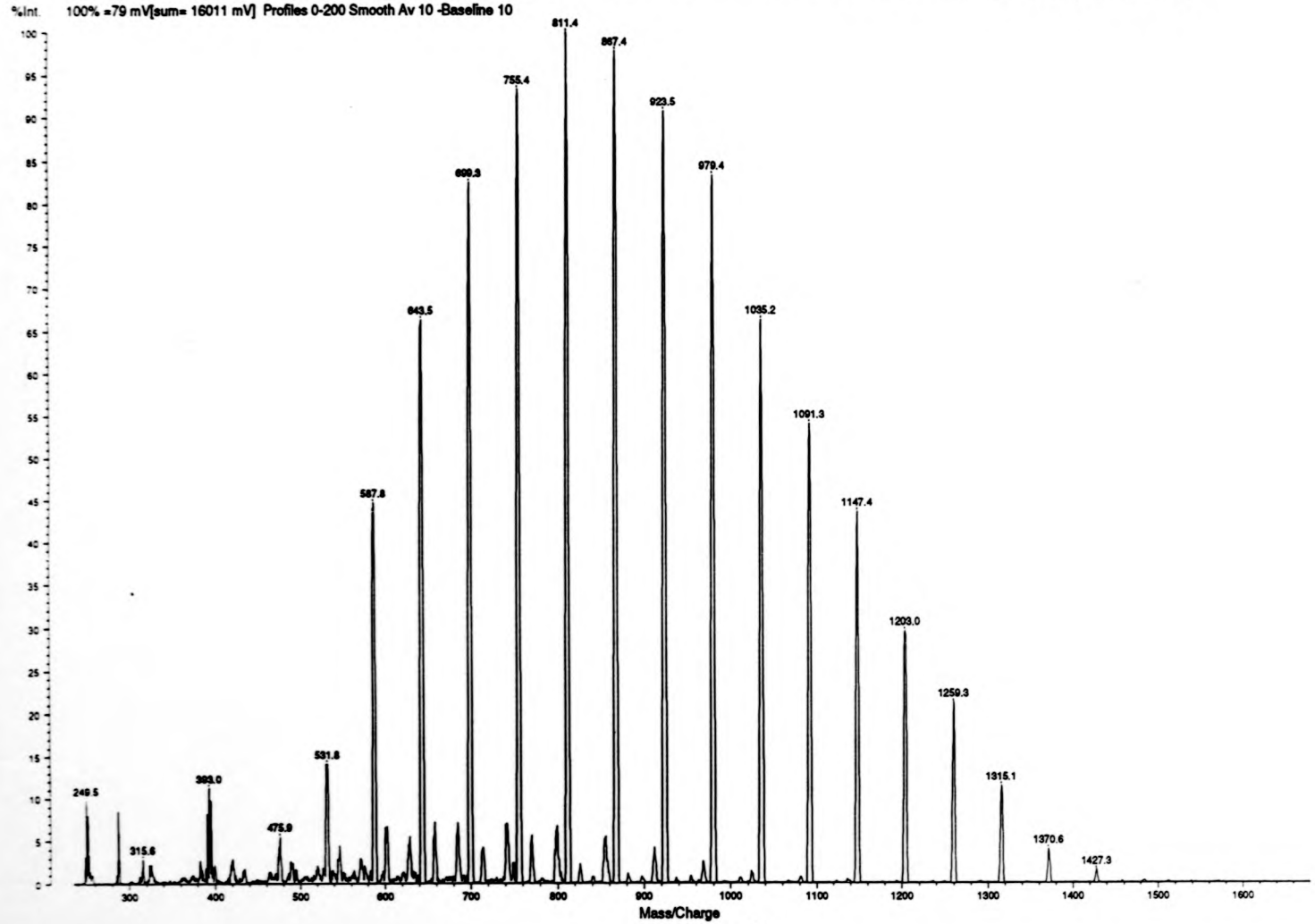

Figure 3.10b

Part of the Tri-olefinic PIB Sample Showing 56 Monomer Mass Separation

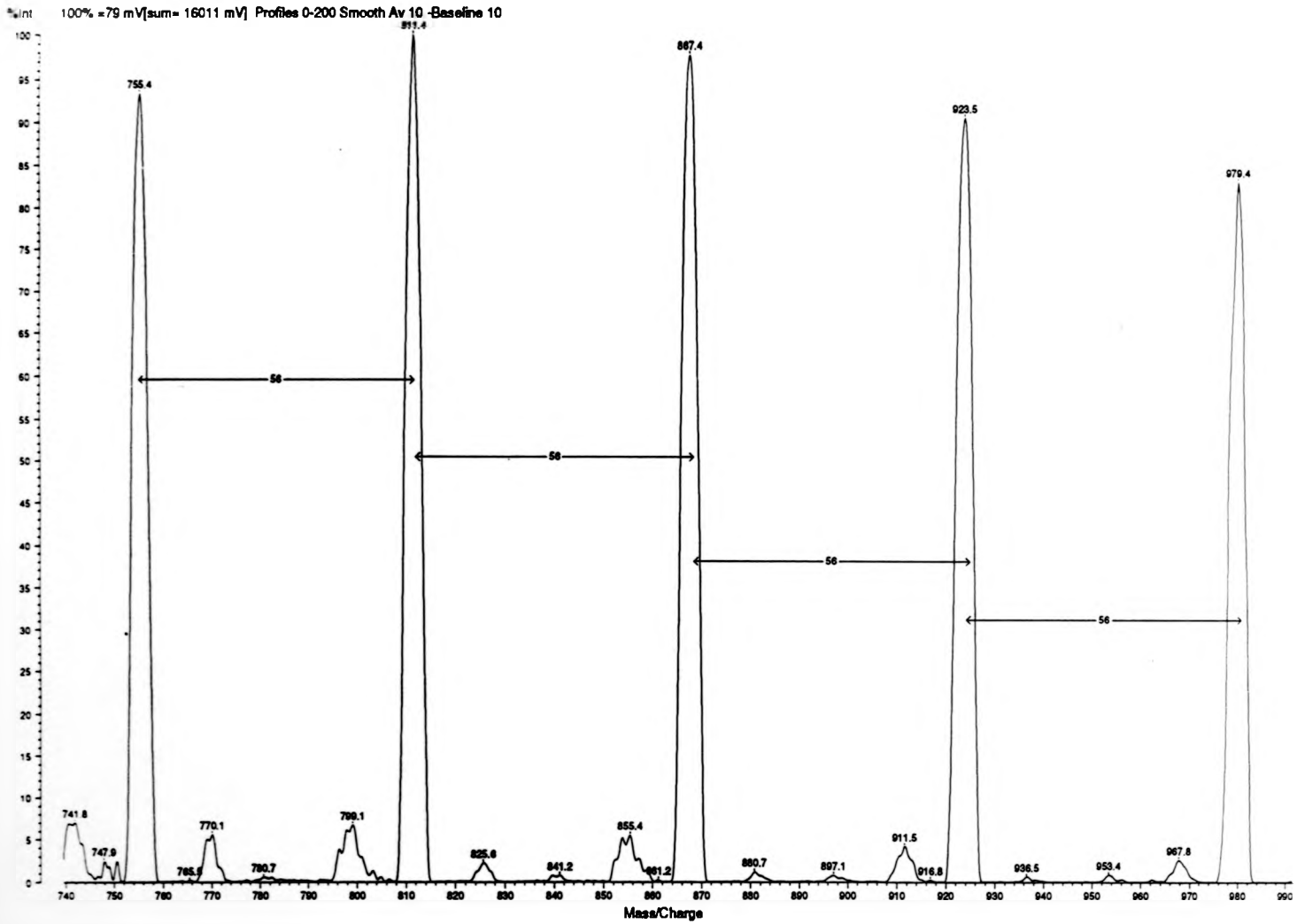

Figure 3.11

MALDI -TOF Mass Spectrum of Tri-Olefinic Poly(isobutylene) Obtained Using Excess Silver Salt on the Kompact III Instrument

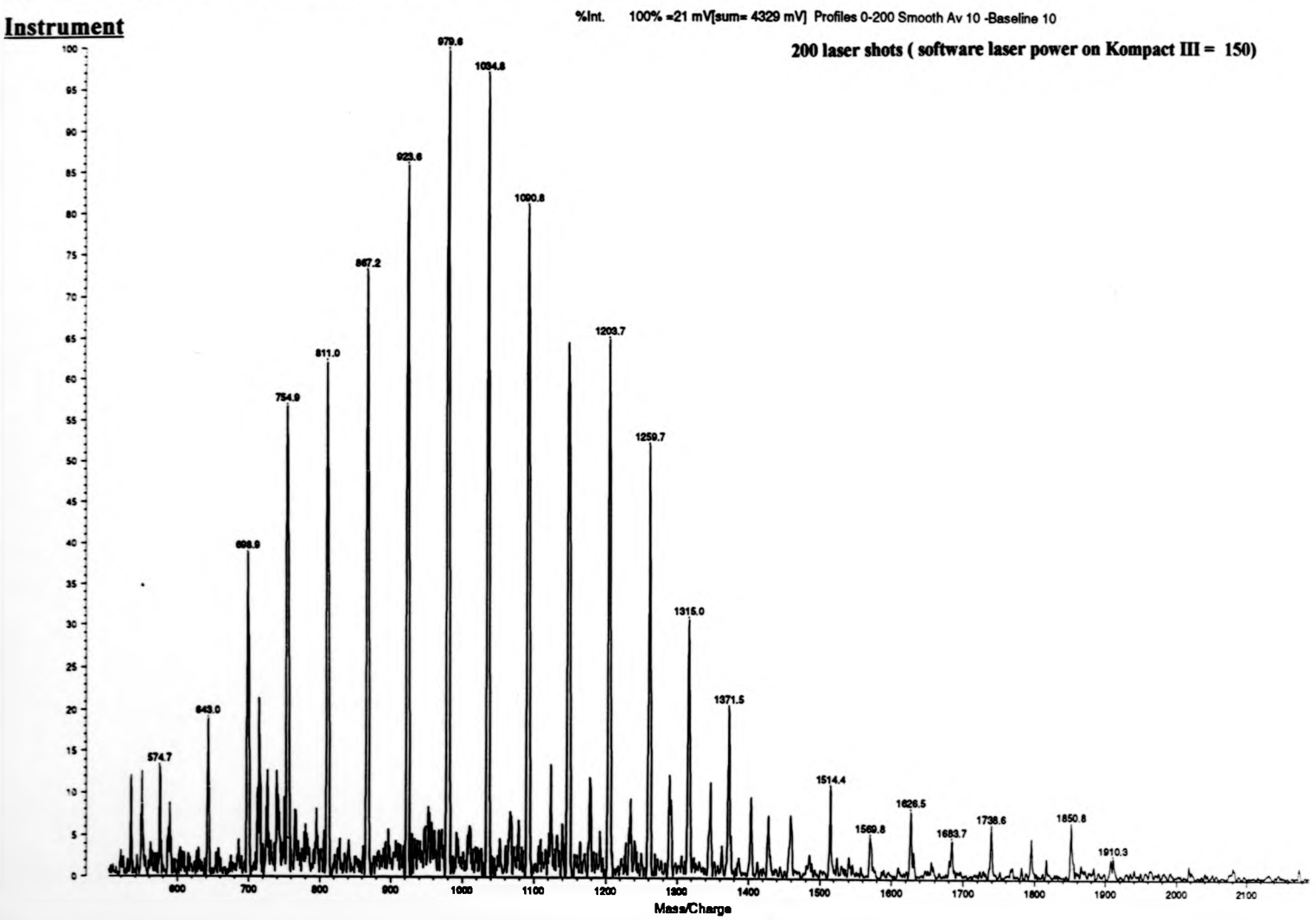

The total ion current and signal-to-noise values for the mono-olefinic sample were consistently lower than those obtained for the di-olefinic and tri-olefinic samples. Even at higher silver concentrations (upto a factor of ten times as much), a spectrum of the mono-olefinic sample was particularly difficult to obtain, although, higher silver concentrations led to a second distribution being observed in the spectrum of the tri-olefinic sample.

3.4 The Analysis of Poly(sulfide) Samples by MALDI-TOF Mass Spectrometry

In this section preliminary results are presented for the use of 9-nitroanthracene as a matrix material in combination with silver cationisation in the analysis of poly(sulfide) polymers by matrix-assisted laser/desorption ionisation time-of-flight mass spectrometry. No results of this kind have been published in the open literature. Indeed, Ludicky of Morton Thiokol has reported that his group have been unsuccessful in obtaining MALDI spectra of such polymers.

The structure of the polysulfide samples investigated in this section are depicted below. Work primarily focused on the analysis of two standard compounds labelled Model A and ZL-2264 whose poly(dispersity) index values are all much greater than unity. A non-model compound, LP-2C (poly(dispersity) index value >> 2.00), whose major component's structure resembled that of Model A was also investigated.

Model A

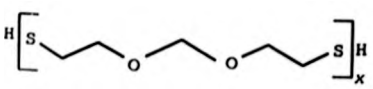

ZL-2264

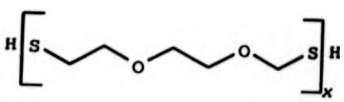

3.4.1 Sample Preparation Investigations

Initial experiments using 2,5, di-hydroxybenzoic acid as the matrix material in combination with sodium or potassium salts produced spectra containing no interpretable peaks. Dithranol incombination with silver tri-fluoroacetate had successfully been shown to produce silver attached oligomers during the MALDI process and was chosen a suitable candidate to apply to the analysis of linear poly(sulfide)s by MALDI no interpretable data was however, obtained.

Previous work described in sections 3.2 and 3.3 of this chapter had shown that 9-nitroanthracene in combination with silver tri-fluoroacetate was a suitable matrix mixture with which to analyse poly(styrene) and more interestingly, poly(isobutylenes). Two main approaches were tested out. The first involved mixing a poly(styrene) standard of a slightly higher molecular mass distribution with the poly(sulfide) standard of interest. The approach was that the poly(styrene) sample would encourage the poly(sulfide) sample to ionise in the MALDI process. The second approach involved using 9-nitoanthracene (0.1M in THF) mixed with various volumes of silver tri-fluoroacetate solution (0.1 M in THF) in order to optimise sample preparation conditions. The latter method yielded positive results more readily and consequently, this methodology was investigated further.

Each poly(sulfide) sample was diluted in tetrahydrofuran (THF) such that the solution contained 3-5 mg of sample per ml of solvent (~ 10^{-3} M). Various volumes of silver tri-fluoroacetate (1-100µl) in THF were used to dope the analyte solution (0.5ml). Equal quantities of this solution and 9-nitroanthracene were mixed. 1µl of the mixture was deposited on the sample slide and the solvent was evaporated off in a stream of warm air.

3.4.2 Effect of Silver Concentration on the MALDI Spectra of Poly(sulfides)

The best signal-to-noise ratios and most even distributions were observed with addition of the minimum amount of silver trifluoroacetate and by preparing the sample mixture well in advance, leaving to stand for up to 24 hours. High-mass insensitivity was observed but this effect was also seen in electrospray results obtained by Mahon and co-workers compared with titration and size exclusion chromatography results.[197,198]

The MALDI spectrum of Model A with 10µl of silver tri-fluoroacetate (0.1M) added in the way described in the general sample prepration method is described below. This polymer produced a very clear MALDI spectrum consisting of three main linear poly(sulfide) series, A, B and C. Series A , the main distribution corresponded to ions of the type [M+Ag] + where M is the poly(sulfide) molecule. The monomer mass repeat unit of 166 Da was clearly observed. Series B was a minor distribution which showed the presence of an extra sulfur function on the polymer chain. Likewise, series C corresponded to the presenece of an additional sulfur function. ZL-2264 was investigated under the same conditions and a sinple spectrum was detected. Higher resolution data was obtained for this sample which allowed an unambiguous assignment of the main polymer distribution as [M+Ag]+ since two peaks corresponding to $[M+Ag^{107}]+$ and $[M+Ag^{109}]+$ were observed. Hydrogen atoms were confirmed as end-groups at both ends of the polymer chain.

Figures 3.12 and 3.13 show MALDI spectra of Model A and Zl-2264 respectively.

A non-model compound, LP-2C was investigated under these conditions and a spectrum was obtained at low resolution. The molecular mass distribution obtained was somewhat lower than that expected. Assignment of the main polymer series was not completely unambiguous, however, results from the ZL-2264 standard compound suggests that ions detected are of the type, [M+Ag]+ where M is the molecular ion with end-groups intact.

Figure 3.12a

Typical MALDI-TOF Mass Spectrum of Model A **200 laser shots (software laser power on Kompact III = 140)**

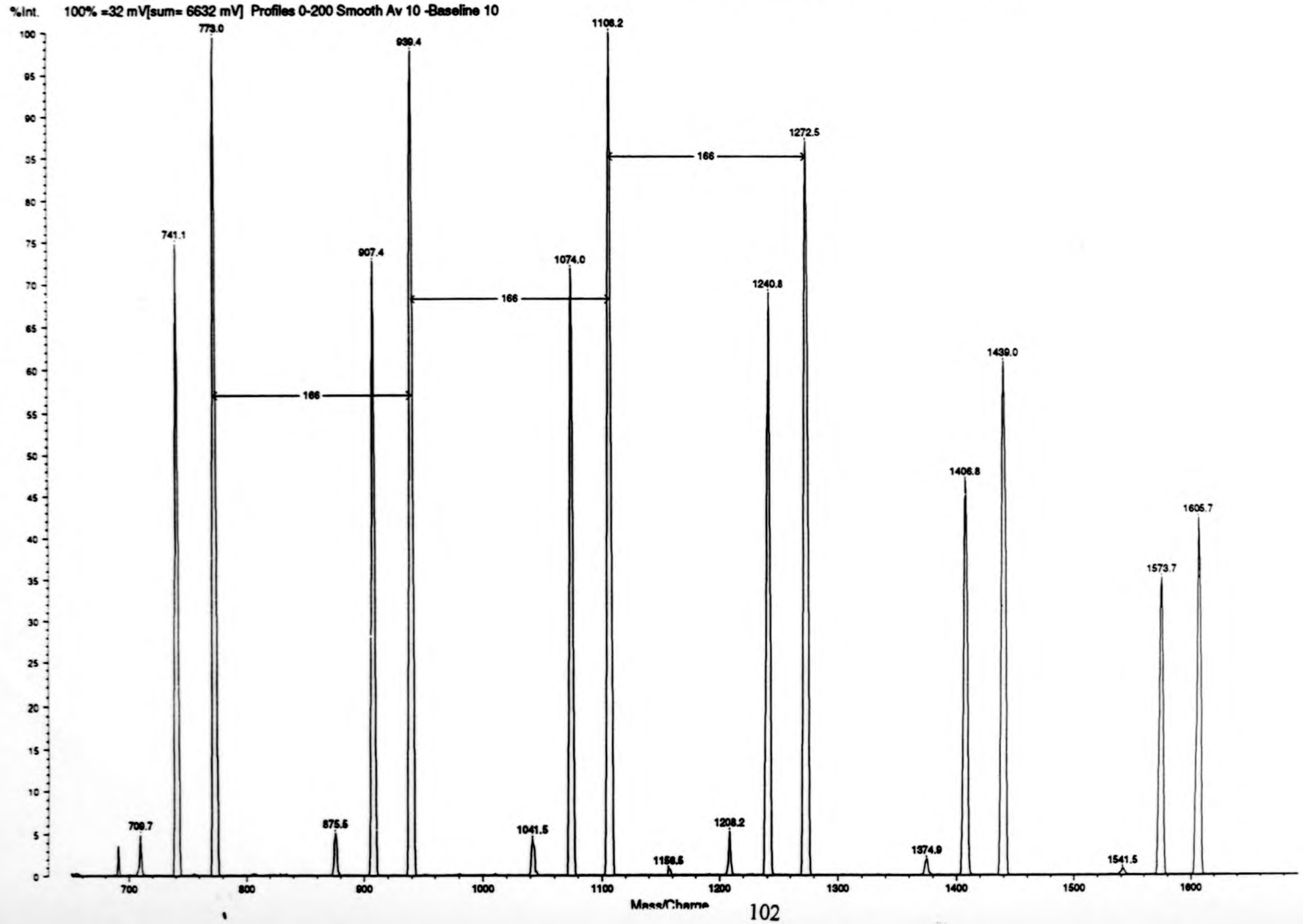

Figure 3.21b

Part of the Model A Spectrum Showing Three Different Polymer Series

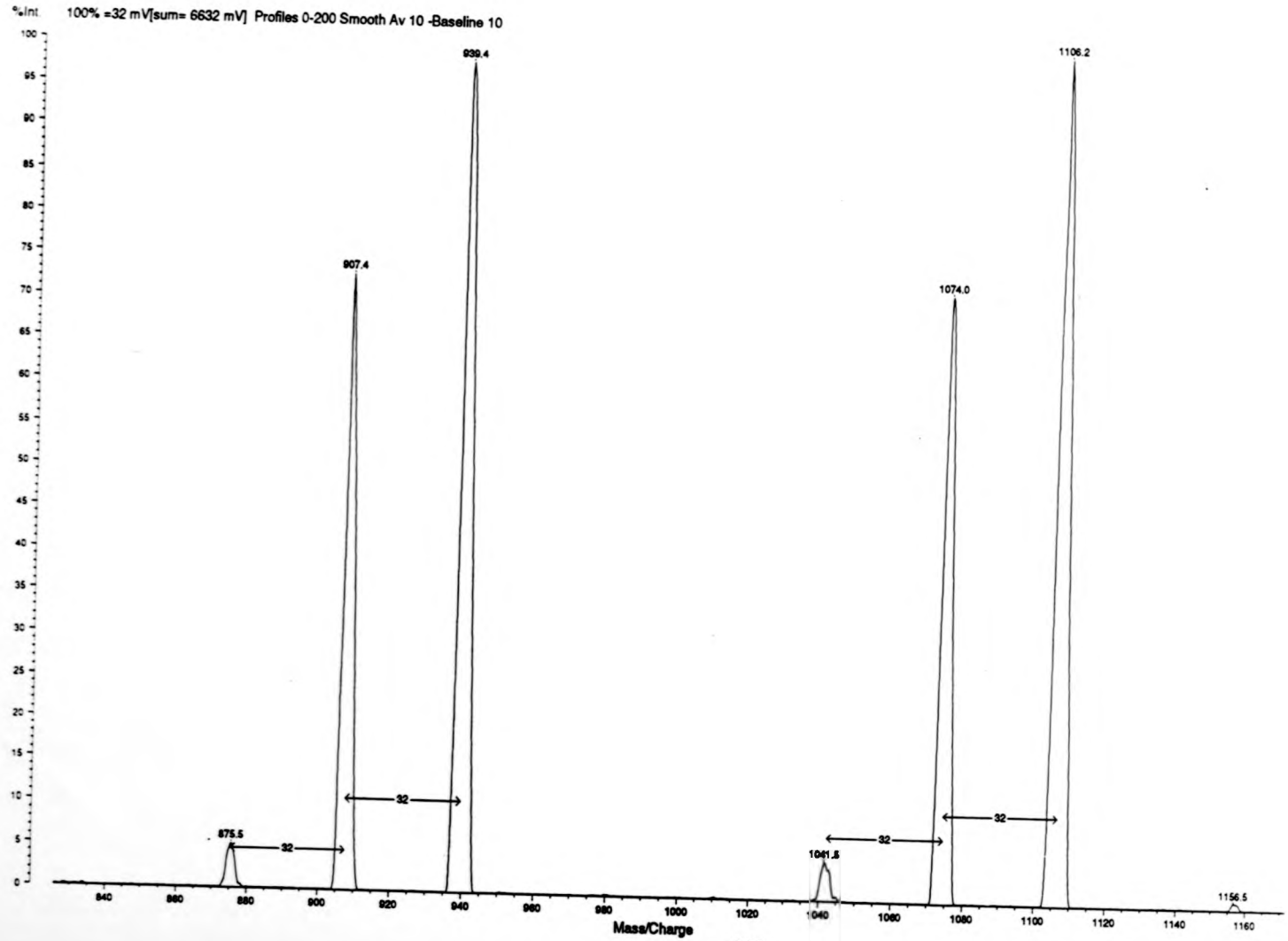

Figure 3.13a

Typical MALDI-TOF Mass Spectrum of ZL-2264 200 laser shots (software laser power on Kompact III = 135)

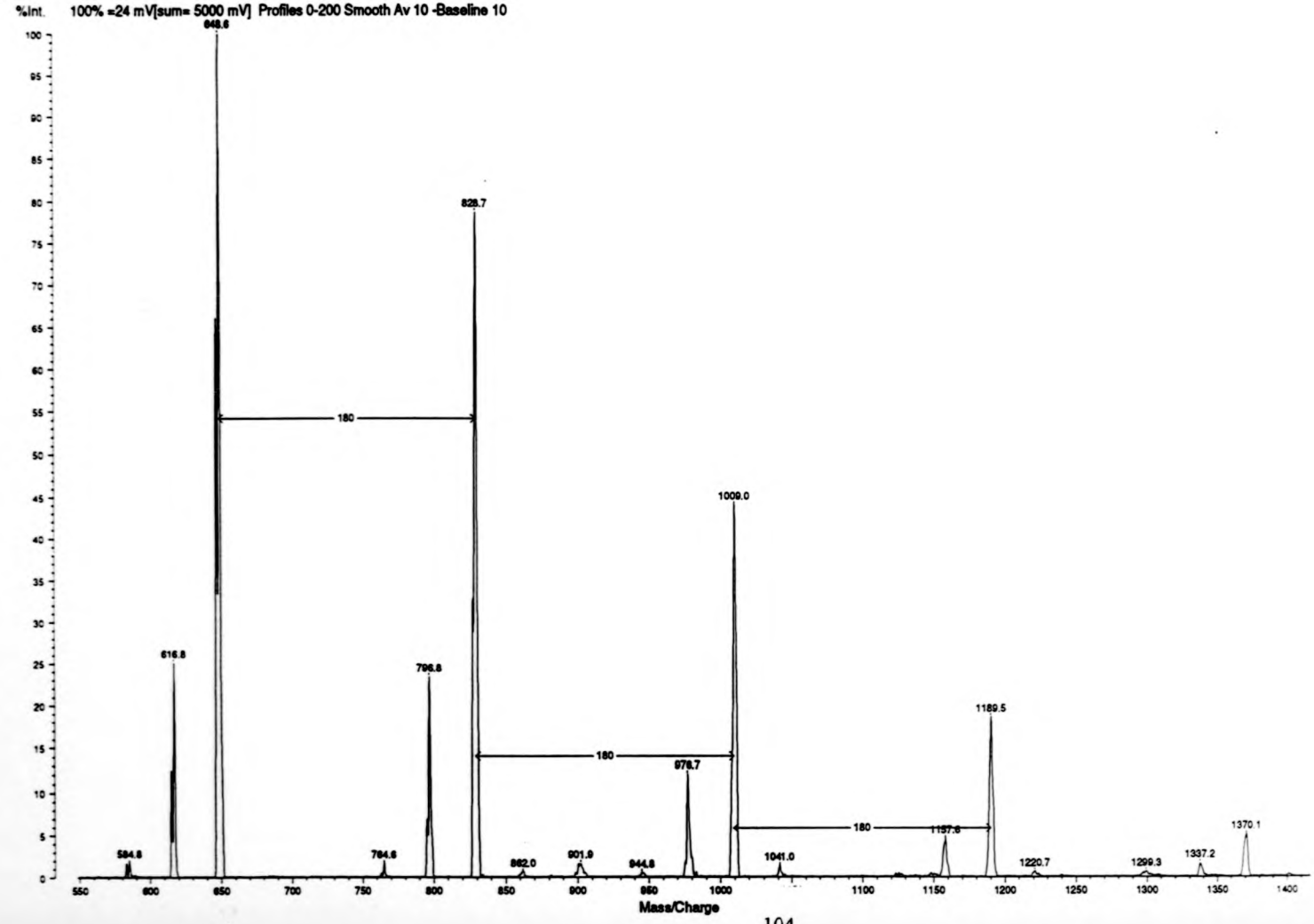

Figure 3.13b

Part of the ZL-2264 Spectrum Showing Three Different Polymer Series and Sulfur Isotopes

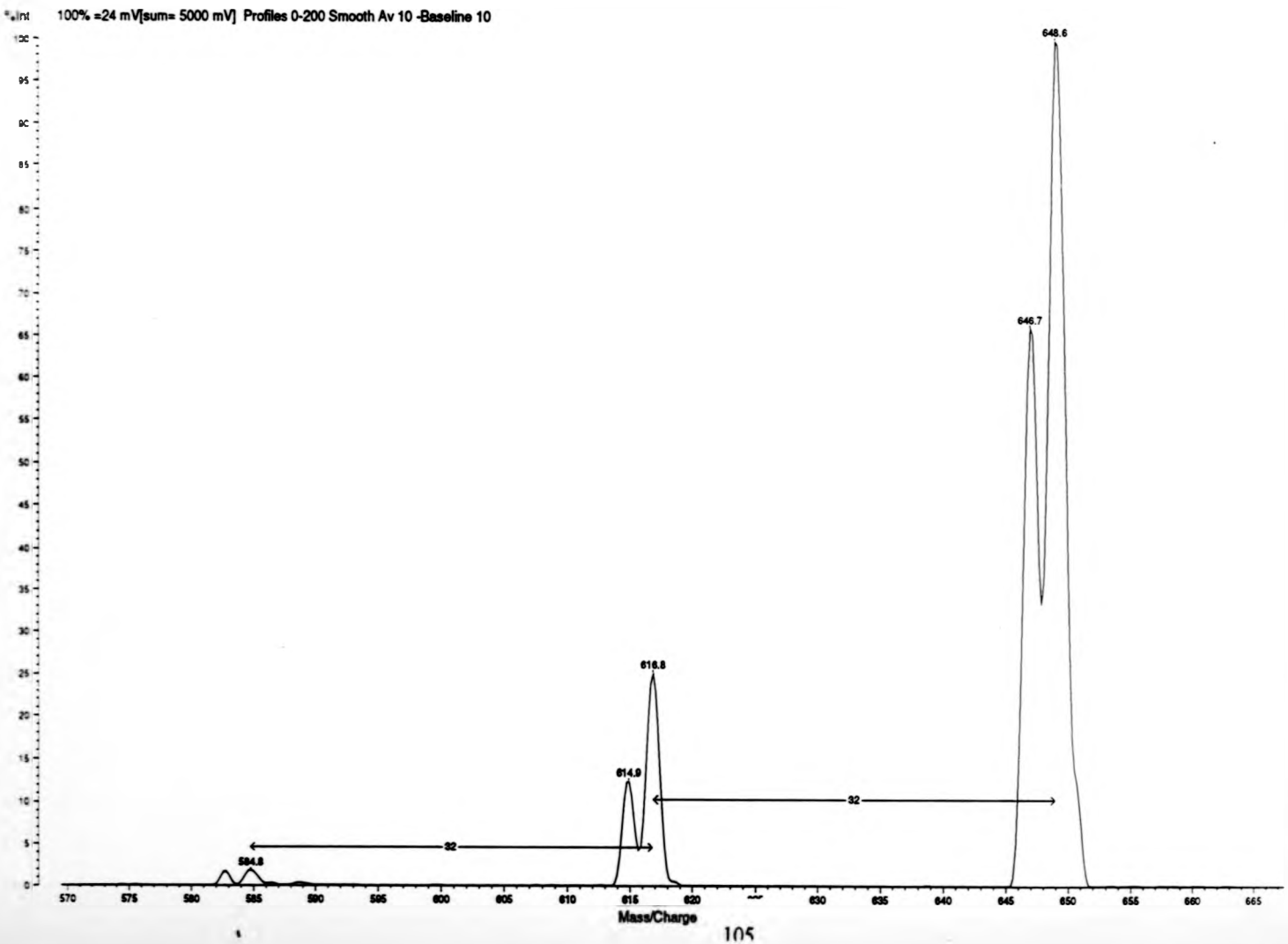

Under specific experimental conditions, the MALDI spectra of the poly(sulfide) samples studied changed completely from those originally presented. The conditions under which these anomalies were observed included excess silver salt addition, high laser powers and when silver/analyte solutions were mixed together and left for a relatively long time prior to laser irradiation.

Figure 3.14 shows a typical spectrum of ZL-2264 at high laser power obtained when 200 µl of silver trifluoroacetate has been added to the sample preparation.

The set of peaks observed in the mass spectrum are separated by 248 amu compared with the usual 166 amu associated with a linear polysufide of this kind. This phenomenon can be attributed to the formation of Ag_2S clusters, formed either during sample prepration or during laser irradiance of the matrix/sample prepration. The series observed is of the general formula, $(Ag_2S)_nAg^+$. The analysis of poly(sulfide) compounds under these sample preparation conditions is a good exmple of how experimental conditions must be carefully selected in order to ensure that clusters of this type are not fromed which may easily lead to the false analysis of such samples.

3.5 Electrospray Sample Preparation

Investigations were carried out using an electrospray sample preparation with a view to increasing sample homogeneity. A series of poly(styrene) standards were initially investigated using 9-nitroanthracene as the matrix and silver cation addition in the form of silver tri-fluoroacetate. This sample preparation was particularly suited to the use of electrospray since THF solutions are readily ionised.

A full description of the experimental procedure is described in section 2.2.2. It was hoped that an increase in sample homogeneity would lead to increased reproducibility

Figure 3.14a

Typical MALDI Mass Spectrum of ZL-2264 Obtained at Higher Laser Power with Excess Silver Salt

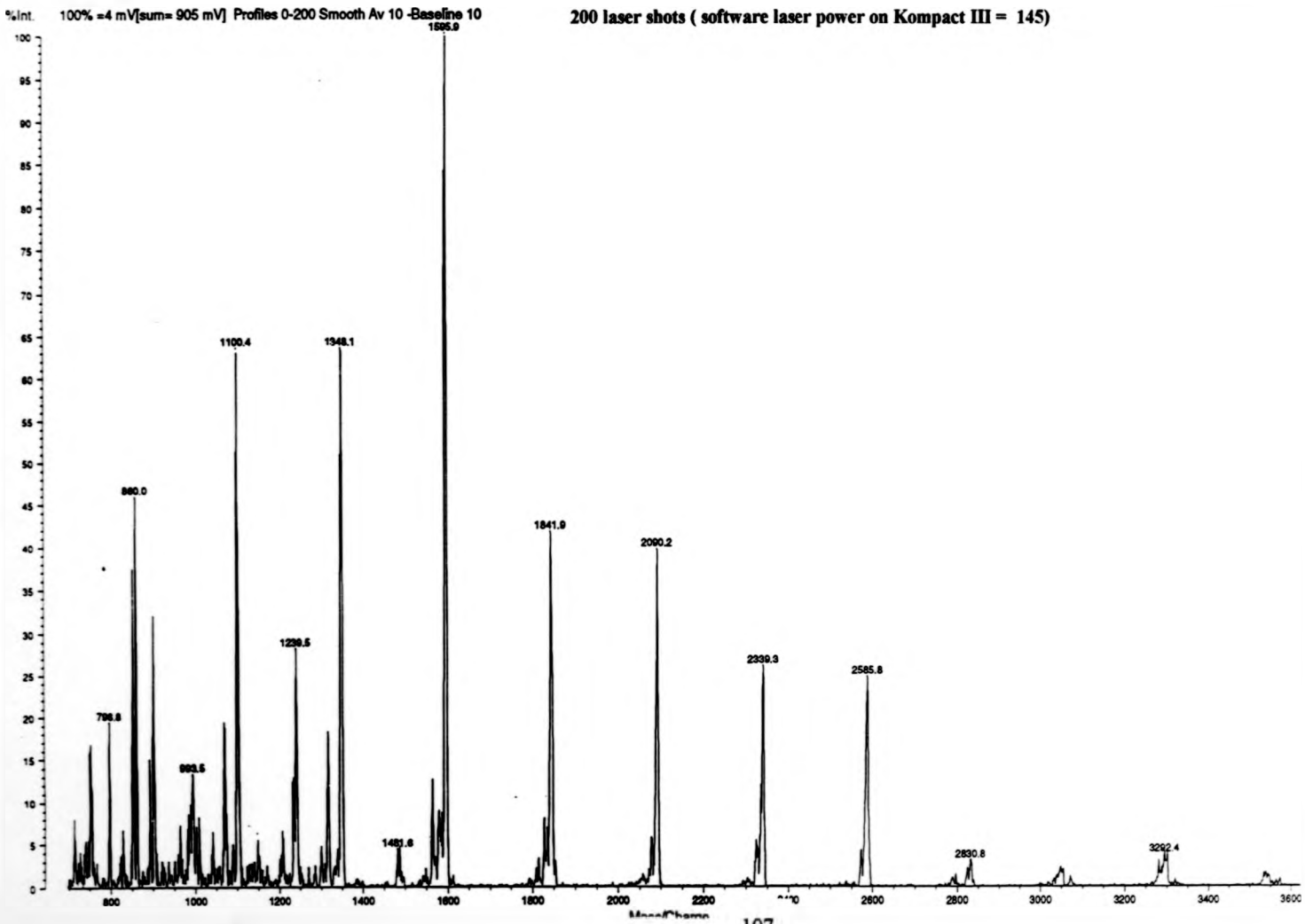

Figure 3.14b

Part of the ZL-2264 Spectrum Showing Silver Cluster Formation

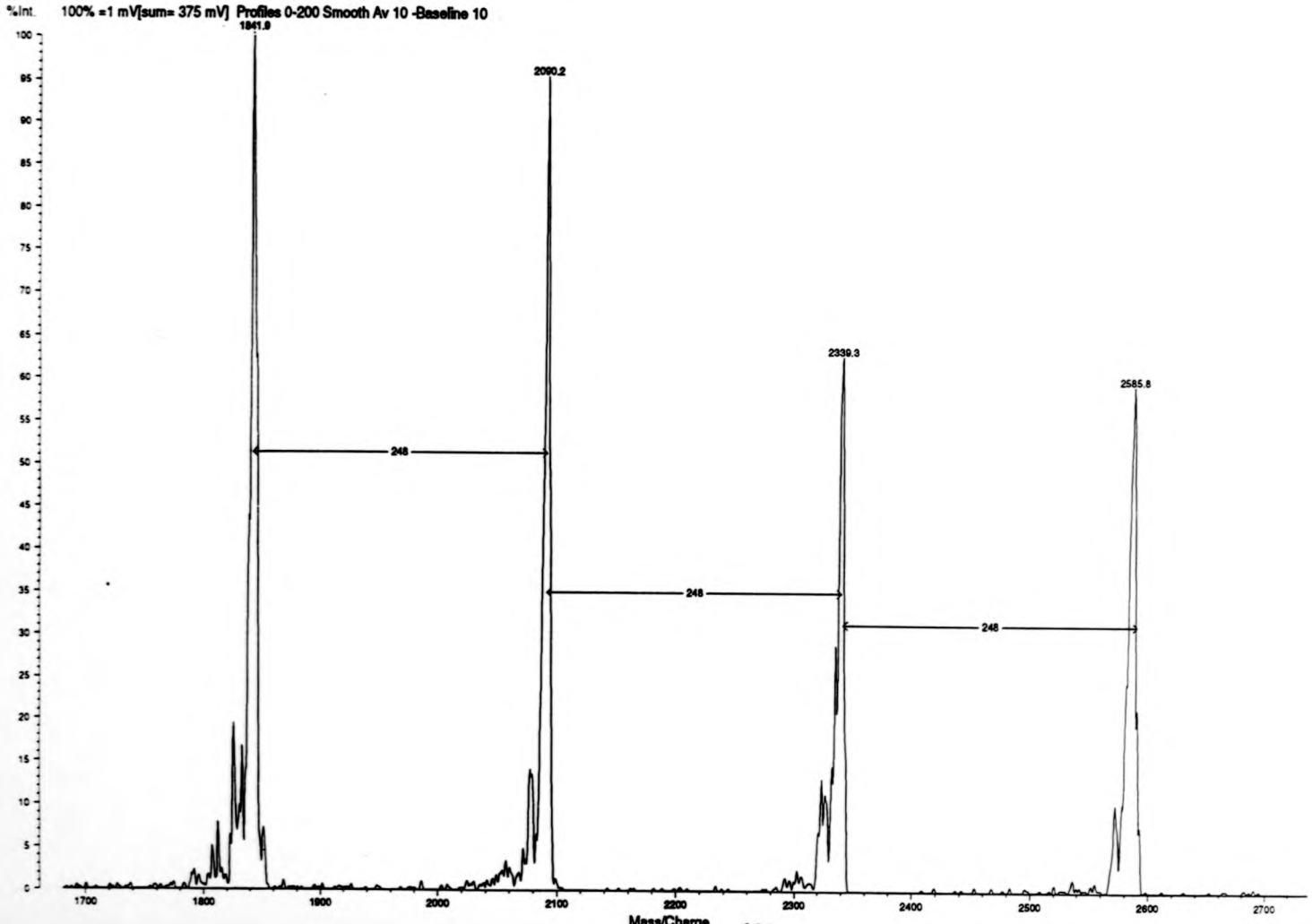

and might extend the mass range of sample capable of being analysed by MALDI-TOF on the Kratos Kompact Instruments. Conditions under which the sample was sprayed were optimised. In general the apparatus was operated in single-spray mode at a potential of 6-8kV for 2 minutes to obtain an even coverage on the sample slide. The spotting method involved allowing a 1μl droplet of the same sample solution to dry in air. Total ion current plots were compared between the traditional spotting method and data obtained by electrospraying the sample solution.

Figure 3.15a and figure 3.15c shows a typical poly(styrene) mass spectrum obtained by i) by electrospraying and ii) by spotting respectively. The corresponding total ion current plots are shown in **figure 3.15b and figure 3.15d respectively.**

The shot-to-shot reproducibility of the data obtained was comparable to that obtained using a normal spotting method and, although the total ion current was more reproducible, the total ion current recorded was often less than a good spotted sample preparation. Furthermore, masses of > 5000 Da were generally more difficult or simply impossible to obtain using the electrospray sample preparation method.

The possibility that electrospraying may be useful in the analysis of polydisperse polymers (polydispersity index > 1.1) was investigated using mixtures of poly(styrene) standards.

Sample Preparation

A series of poly(styrene) samples were made up such that the ratio of monomer units to silver cation and matrix was 2: 1: 100. Mixtures A, B and C consisted of a standard of average molecular mass 2450 Da (Polymer Laboratories, Manchester, UK) mixed with three standards of average molecular mass 3050, 5050 and 7000 respectively (Polymer Laboratories, Manchester, UK). Each mixture was prepared by mixing solutions of poly(styrene) ($\sim 10^{-3}$M in THF) such that each component was equal in mass to the other one. This meant that each standard contributed effectively the same number of poly(styrene) monomer mass units.

Figure 3.15a

Typical Poly(styrene) Mass Spectra and Total Ion Current Plots Obtained by

i) Spotting

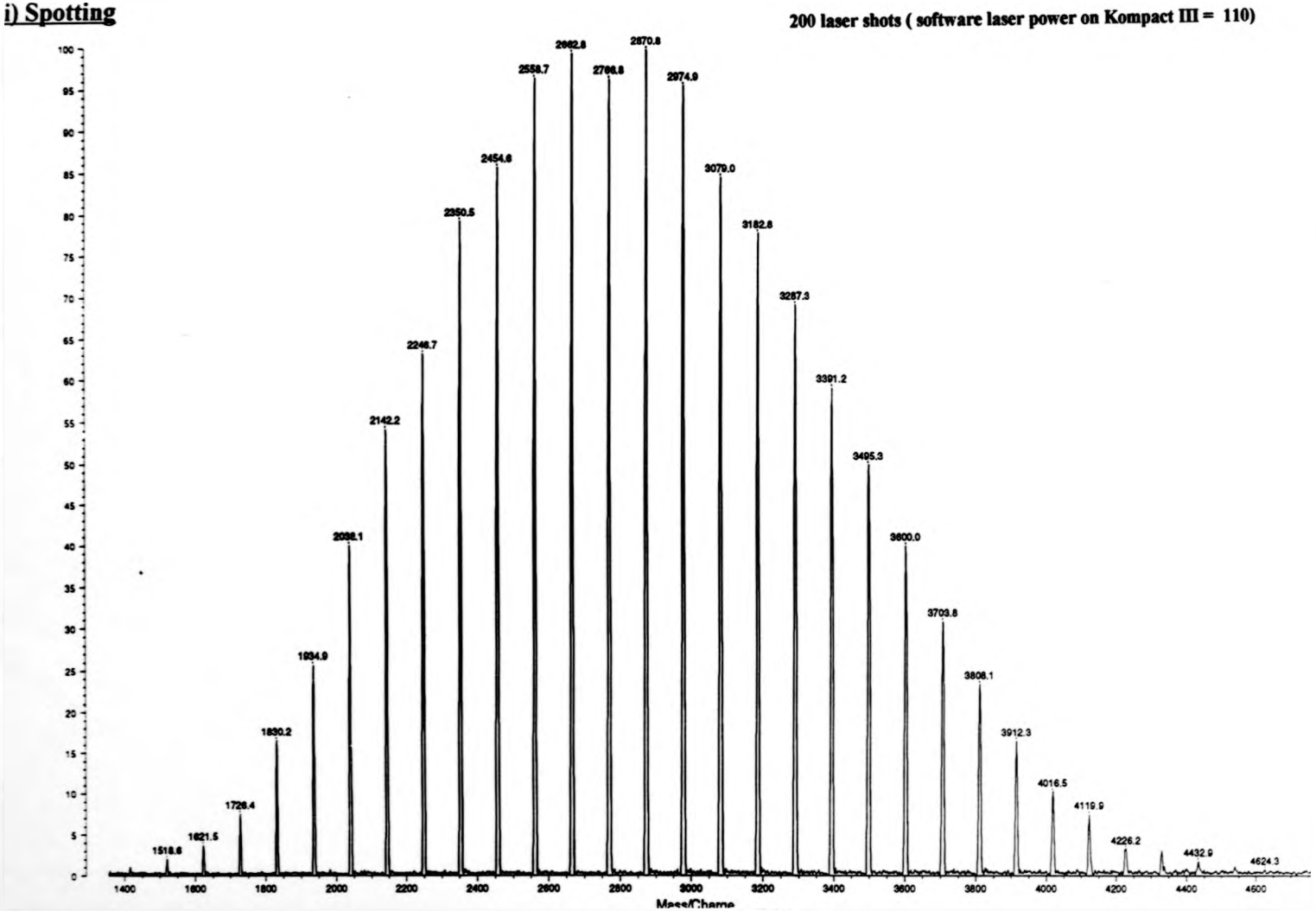

Figure 3.15b

Total Ion Current Plot Obtained by Spotting

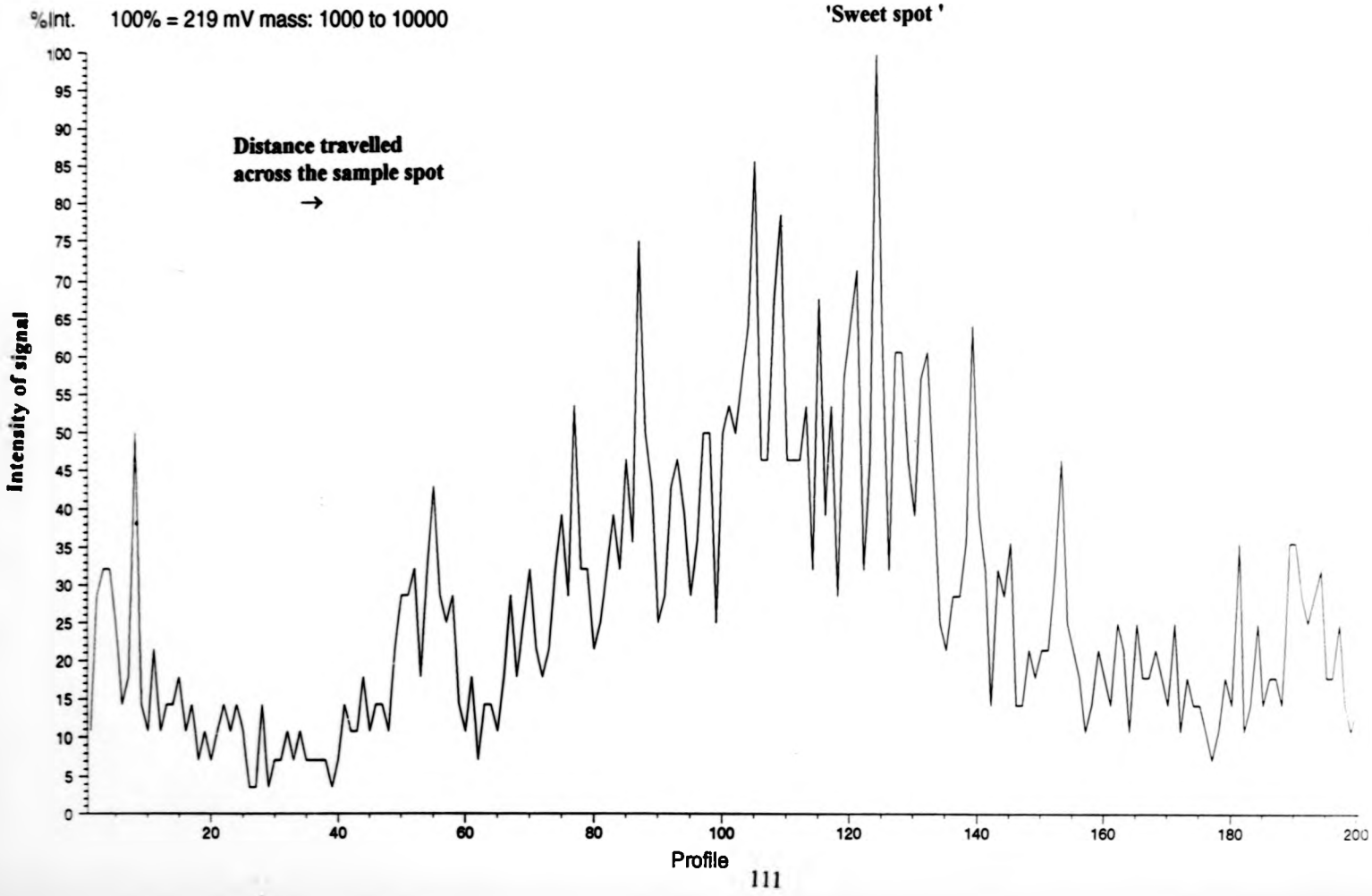

Figure 3.15c

Typical Poly(styrene) Mass Spectra Obtained by ii)Electrospraying

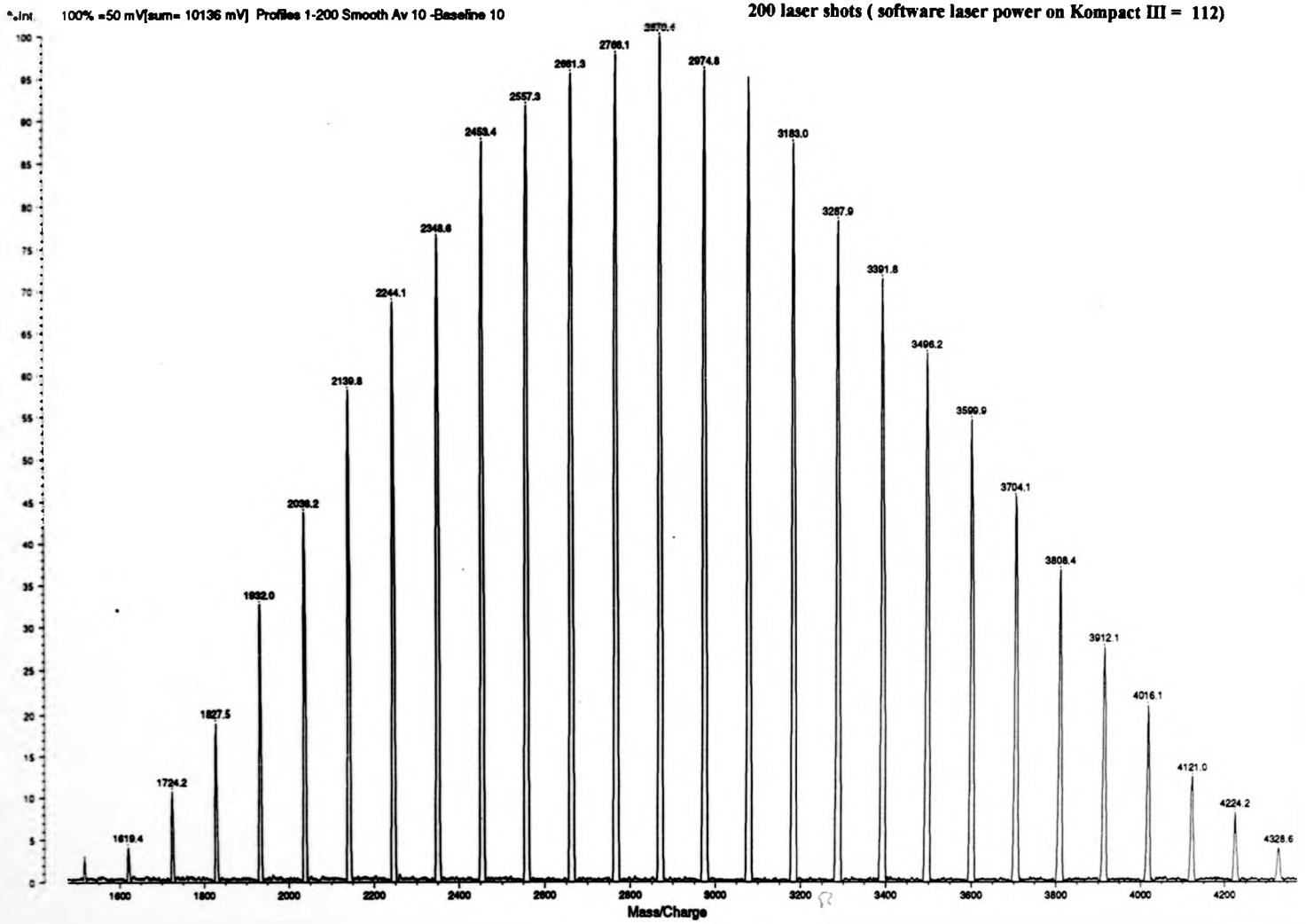

Figure 3.15d

Total Ion Current Plot Obtained by ii) Electrospraying the Sample

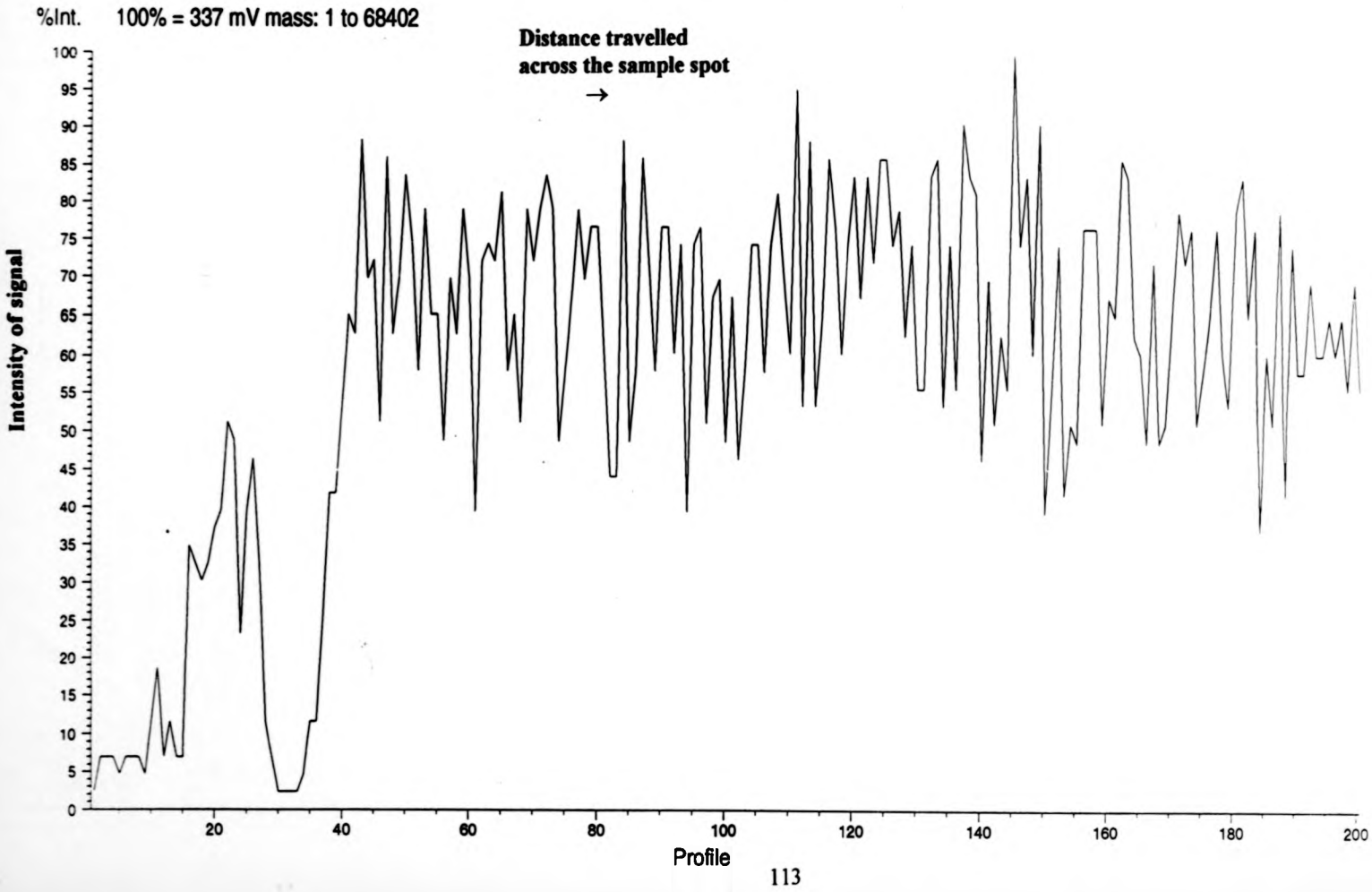

In all cases, the MALDI spectra detected consisted of a singly-charged mass distribution of silver-attached poly(styrene) oligomer. The same mass distribution was obtained by spotting and spraying mixture A and total ion currents (TIC) values did increase significantly (upto 100%) when electrospray sample preparation was employed. Mixture B was detected as two distinct mass distributions using the spotting sample preparation method, however, electrospraying the same mixture resulted in the detection of only a low mass distribution originating from the low mass standard. Mixture C, which consisted of the lowest and highest mass poly(styrene) components, was investigated using both sample preparation methods. Neither preparation technique resulted in the detection of the higher mass distribution. Furthermore, spotting proved to be the only sample prepration by which this heavier mass sample could be analysed by MALDI on the Kompact instruments.

Figure 3.16 depicts a MALDI spectrum of mixture B obtained using the electrospray sample preparation method.

From these experiments it is concluded that electrospray sample preparation of polymers may result in a low-mass bias in MALDI spectra. This bias may be due to a number of factors, which include the decomposition of the polymer sample during the spraying process itself or perhaps the formation of a crystal structure which favours low mass oligomers being preferentially ionised over those of higher masses.

To concude, the traditional method of spotting the sample solution onto the slide or probe, provided that due care is taken, is by far the most effective way of producing rapid and reproducible results. Furthermore, this technique does not suffer from the disadvantage of potentially changing the sample in any way.

Figure 3.16

MALDI Spectrum of Mixture B Obtained Using the Electrospray Sample Preparation Method.

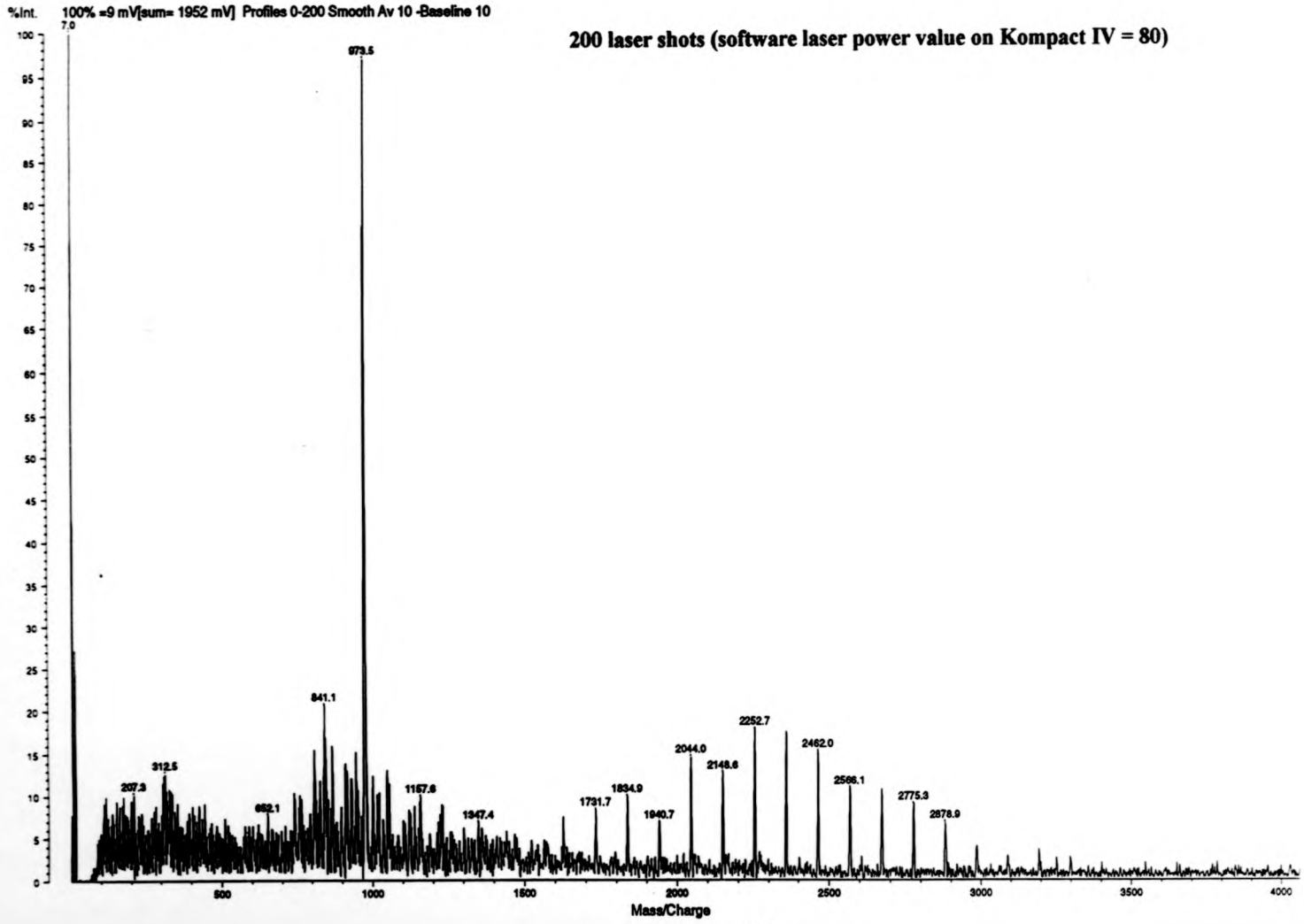

3.6 Discussion

The work described in this chapter has clearly demonstrated the use of 9-nitroanthracene as an efficient matrix for the analysis of poly(styrenes) (upto mass 12000 Da), poly(isobutylenes) (upto mass 1000Da) and poly(sulfides) (upto mass 2500Da). All of these samples investigated usiing this matrix have a polydispersity index which is close to unity. Research carried out by Lloyd has also shown that this sample preparation is applicable to the analysis of poly(ketones) and epoxyresins of a limited mass range (upto 3000Da)[193].

The potential limitations of this matrix material used in conjunction with silver trifluroacetate have been outlined. One of the main problems is the fact that only samples of a mass > 500 Da may be analysed using this system owing to the abundance of matrix and silver cluster peaks detected within this mass range. Judicial amounts of silver salt must be used to obtain good quality data. Excess silver cations combined with the use of too high laser power results in silver cluster formation which may easily lead to the false analysis of a sample.

In the case of poly(styrene) optimum conditions are obtained if the cation to monomer unit ratio is limited to < 2:1. For a poly(styrene) of average molecular mass 3000Da this equates to approximately 10 cations per discrete polymer chain. Despite the high abundance of silver cations compared with poly(styrene) units only one silver cation attaches itself to the polymer chain. This in itself is somewhat surprising if the driving force behind the cationisation process is the interaction of a silver cation with an aromatic ring function as there are many such functionalities in a poly(styrene) polymer chain. Similar results have been obtained using field desorption as the ionisation method. From the statistics presented it is, therefore, more likely that the interaction between a silver cation and a poly(styrene) chain occurs in the gas phase and is consequently dominated by such kinetics.

The limited mass range for poly(styrene) analysis by MALDI using this sample preparation may be attributed to instrumental constraints. These include detector saturation, accelerating potential differences and the lack of delayed extraction. All samples studied have been standard compounds with polydisperity values close to unity. There are difficulties with analysing samples with higher polydispersity values and many of the problems are not only instrumental in origin but may be inherently tied up in the MALDI ionisation process itself which is far from completely understood. Some important factors which may influence the ability of an instrument to analyse a specied by MALDI include sample homogeneity, gas-phase kinetics, detector saturation and fragmentation of fragile high -mass polymers in the field-free region of the time-of-flight analyser.

The MALDI spectra of the novel poly(isobutylene) samples are, to date, the most non-polar polymers analysed by this technique. It is, however, disappointing that the mass range is very limited. Repeated attempts to analyse analogues of molecular mass upto 2000 Da failed. Poly(isobutylene) samples containing hydoxy end-groups or amino end-groups of upto ~1000Da were also investigated and the spectral data obtained did not contain any useful structural information. Results, therefore, suggests that the aromatic ring function present in the oligomers is essential in obtaining MALDI data. The observation that the ease of analysis increase with the ratio of phenyl functions to chain length adds weight to this argument. The amount of silver tri-fluoroacetate added to the sample is crucial in determining the quality of data obtained and the optimum ratio silver cation to polymer chain is approximately the same as poly(styrene). This suggests that the interaction between the polymer chain and the cation does indeed occur in the gas phase. The apparent anomaly that ease of analysis increases with the ratio of phenyl functions to hydrocarbon chain length may be explained by the physical properties of the polymer. MALDI relies heavily on the ability to prepare a homogeneous sample. All poly(isobutylene) samples which have

been analysed were viscous liquids and this made the preparation of homogeneous sample preparations particularly difficult.

The analysis of poly(sulfide)s using the same sample preparation method has clearly shown how the chemistry of a particular system may dominate the type of results obtained. The strength of the silver-sulfur bond is obviously a determining factor here and this is clearly demonstrated by the formation of clusters under specific conditions.

Electrospray sample prepration has been investigated as a method of producing a homogeneous MALDI sample prepration. A low-mass bias results under specific conditions and in general, the traditional method of spotting the sample solution onto the sample slide is the msot effective and reproducible method for the analysis of polymers by MALDI.[190]

To conclude, several different approaches for the analysis of polymers by MALDI have been investigated. The type of information obtained using MALDI-TOF mass spectrometry has been outlined and the difficulties and problems which may occur have been briefly described. The analysis of the polymers studied by MALDI are presented and discussed in chapter 4.

CHAPTER FOUR

Molecular Mass Calculations on Polymers Analysed by Matrix-Assisted Laser/Desorption Ionisation Time-of-Flight Mass Spectrometry

4.1 Introduction

Since the initial discovery of matrix-assisted laser desorption/ionisation (MALDI) [39,43] and its subsequent application to the analysis of large biomolecules[21,41,42,43,61,62] interest has rapidly grown in the development of this technique to the analysis of synthetic polymers.[71,72,146,147,148] The drive for a rapid and accurate method for the absolute mass determination of synthetic polymers, coupled with the fact that there are already many relatively inexpensive bench-top instruments commercially available, has meant that the great potential of MALDI as a routine method for the measurement of molecular mass statistics has been appreciated. The most widely used method for polymer analysis is size exclusion chromatography (SEC)[128,129] and, in principle, MALDI has a considerable number of advantages over this technique. MALDI is generally able to resolve individual species and provide molecular-mass information which makes MALDI useful for the compositional analysis of individual species, allowing end-group information to be obtained. Such data provides an invaluable insight into polymerisation mechanisms. In MALDI, oligomer ions are separated according to their mass-to-charge ratios and, in most cases, only singly-charged species are observed. In SEC, molecules are separated according to their hydrodynamic size, a function which is particularly sensitive to a polymer's architectural features such as branching. A further disadvantage of SEC is that a calibration must be carried out using standards of a similar nature to the analyte. For many polymers such compounds are not available.

Recent work has questioned whether MALDI-TOF mass spectrometry can give representative data for a sample of poly(methyl methacrylate) (PMMA, M_n = 3150) with a narrow molecular mass distribution on the basis of a comparison with data obtained by size exclusion chromatography.[194] This paper induced a quick response within the MALDI mass spectrometry community and it is generally accepted that for polymers of narrow molecular-mass distributions (polydispersity index < 1.2) MALDI gives good agreement with data obtained by SEC. In this chapter we present molecular mass statistics obtained for poly(styrene)s, poly(methyl methacrylate)[195] poly(sulfide)s and poly(isobutylene)s using MALDI and software available provided by Kratos on their Kompact MALDI-TOF Mass Spectrometers. The data are compared with SEC data and statistics quoted by the manufacturers.

4.1.2 Molecular Mass Calculations

In this chapter, MALDI-TOF gave resolution of the individual species that made up each sample. The following equation was used to calculate molecular mass averages :

$$M_{avg} = \Sigma N_i M_i^{x} / \Sigma N_i M_i^{x-1}$$

The most important parameters of interest to the polymer chemist are weight average molecular mass (M_w), number average molecular mass (M_n) and polydispersity index (M_w/M_n) which are defined as :

$$M_n = \Sigma N_i M_i / \Sigma N_i$$

$$M_w = \Sigma N_i M_i^{2} / \Sigma N_i M_i$$

Polymer analysis software installed by Kratos on the MALDI-TOF mass spectrometer uses the areas of the polymer species to calculate the number fracrion of each species. once the user has defined two peaks within the polymer distribution, the software, using the separation between those peaks, systematically searches for more peaks in the polymer series within the tolerance value set (in general this was set to 5 mass units unless otherwise stated) either side of this separation.

Figure 4.1

Definition of Peak Area Using Software Installed on the Kompact Instruments.

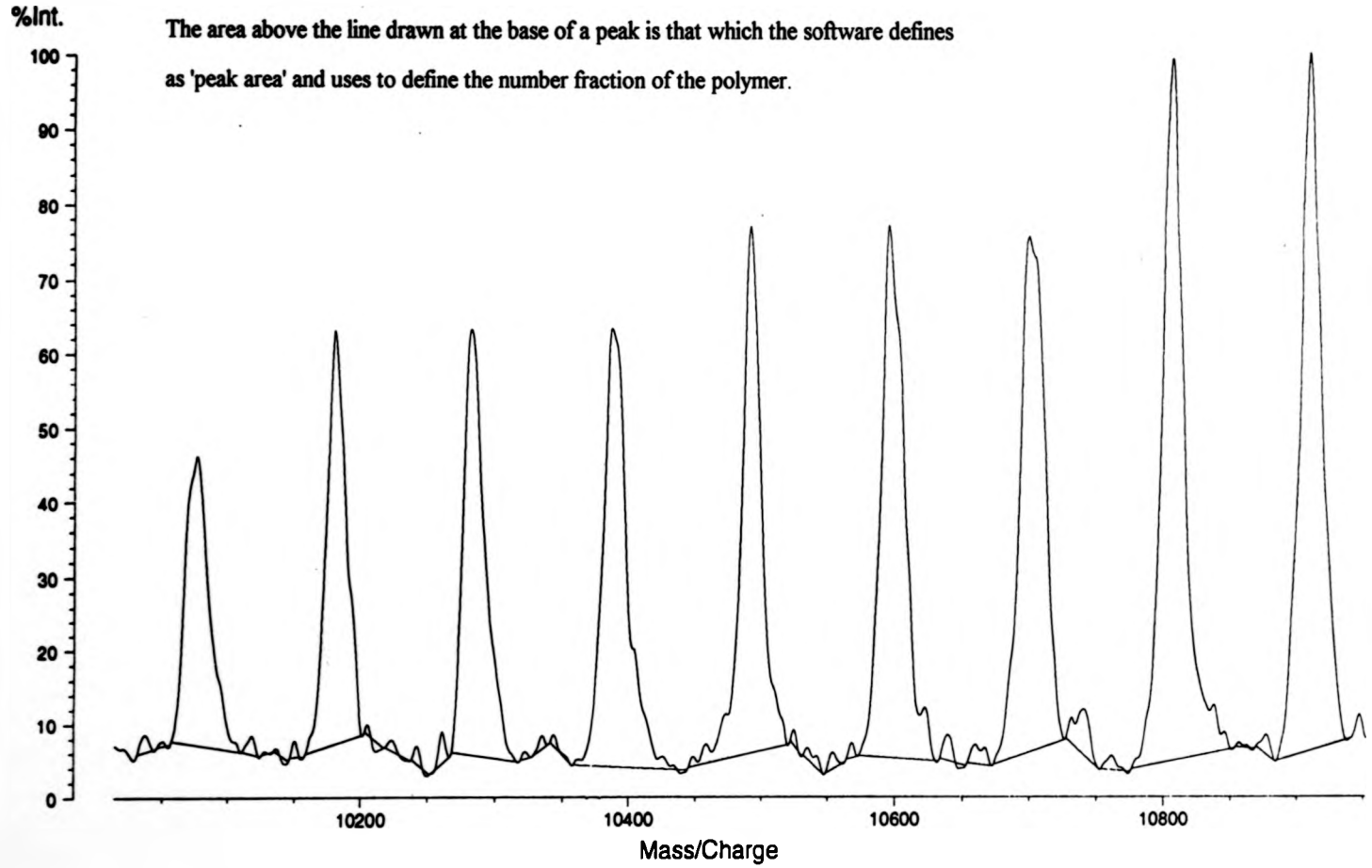

The software considers only the peak closest to the separation value for calculating the number fraction and how the software defines peak area is shown in **figure 4.1** any adducts that are attached to the polymer species is specified by the user and the mass of the adduct is removed from each polymer series by the software, when the number fraction is calculated.

4.2 Experimental Conditions

All experiments were carried out on a Kratos Kompact III or Kompact IV MALDI-TOF-MS (Kratos, Manchester, UK) incorporating a 337nm pulse duration and an electron multiplier detector. The instrument was operated in positive ion reflectron mode with an accelerating potential of +20kV. The mass scale can be assumed to have been calibrated, unless otherwise stated, using bovine insulin with a combination of matrix and cation peaks.

4.3 Poly(styrene) Analysis

4.3.1 Sample Preparation

All samples were supplied by Polymer Laboratories and had a polydispersity value close to unity as shown in figure 4.3. Six poly(styrene) standards were analysed in the mass range, 1000-12000 Da. Each sample was prepared using the optimised sample preparation method described in chapter 3 and the same solutions were used for both MALDI-TOF experiments and SEC analysis.

50µl of a solution of silver tri-fluoroacetate in THF (0.1M) was used to dope the analyte solution (0.5ml). Equal quantities of this solution and the matrix solution (0.1M 9-Nitroanthracene in THF) were mixed. 1µl of this mixture was deposited on a stainless steel sample slide and the solvent was evaporated off in a stream of warm air.

The same solutions of poly(styrene) were used for both SEC and MALDI-TOF experiments.

Figures 4.2a, 4.2b, and 4.2c all depict spectra, typical of those obtained by MALDI. The styrene repeat unit (104Da) was clearly identified in all of the samples analysed. In all cases, 9-nitroanthracene was used as the matrix material in combination with silver cation addition. All spectra were averaged over 200 laser shots and were collected at 100 on the laser power scale on the Kompact III instrument.

4.3.2 Molecular Mass Calculations

The silver adduct, which was attached to each poly(styrene) oligomer was specified by the user and the mass of this adduct was removed from each member of the polymer series by the software when the number fraction was calculated. In all calculations, the tolerance value was set at 3 mass units either side of the monomer mass separation and the cut-off parameter was set at 5 %.

Figure 4.3 shows the molecular mass statistics obtained by MALDI compared with those quoted by the manufacturer* and calculated by SEC**.

Figure 4.3

Manufacturer		**MALDI**				**SEC**			
Mn	Mn/Mw	Mn	Mw	Mz	Mw/Mn	Mn	Mw	Mz	Mw/Mn
1680	1.05	1636	1725	1815	1.055	1573	1666	1759	1.059
2050	1.05	1985	2072	2158	1.044	1908	2008	2108	1.052
2950	1.04	2898	2985	3068	1.030	2802	2922	3043	1.043
5050	1.04	4850	4929	5005	1.016	4767	4956	5150	1.040
7000	1.04	6738	6798	6856	1.007	6891	7096	7314	1.029
11500	1.03	11202	11209	11217	1.007	11523	11786	12075	1.023

* Polymer Laboratories, UK

** All SEC data provided by K. Suddaby.

Figure 4.2a

Typical Spectra of Poly(styrene) of Molecular Mass ~ 3000 Da Using 9-Nitroanthracene as the Matrix in Combination with Silver Trifluoroacetate

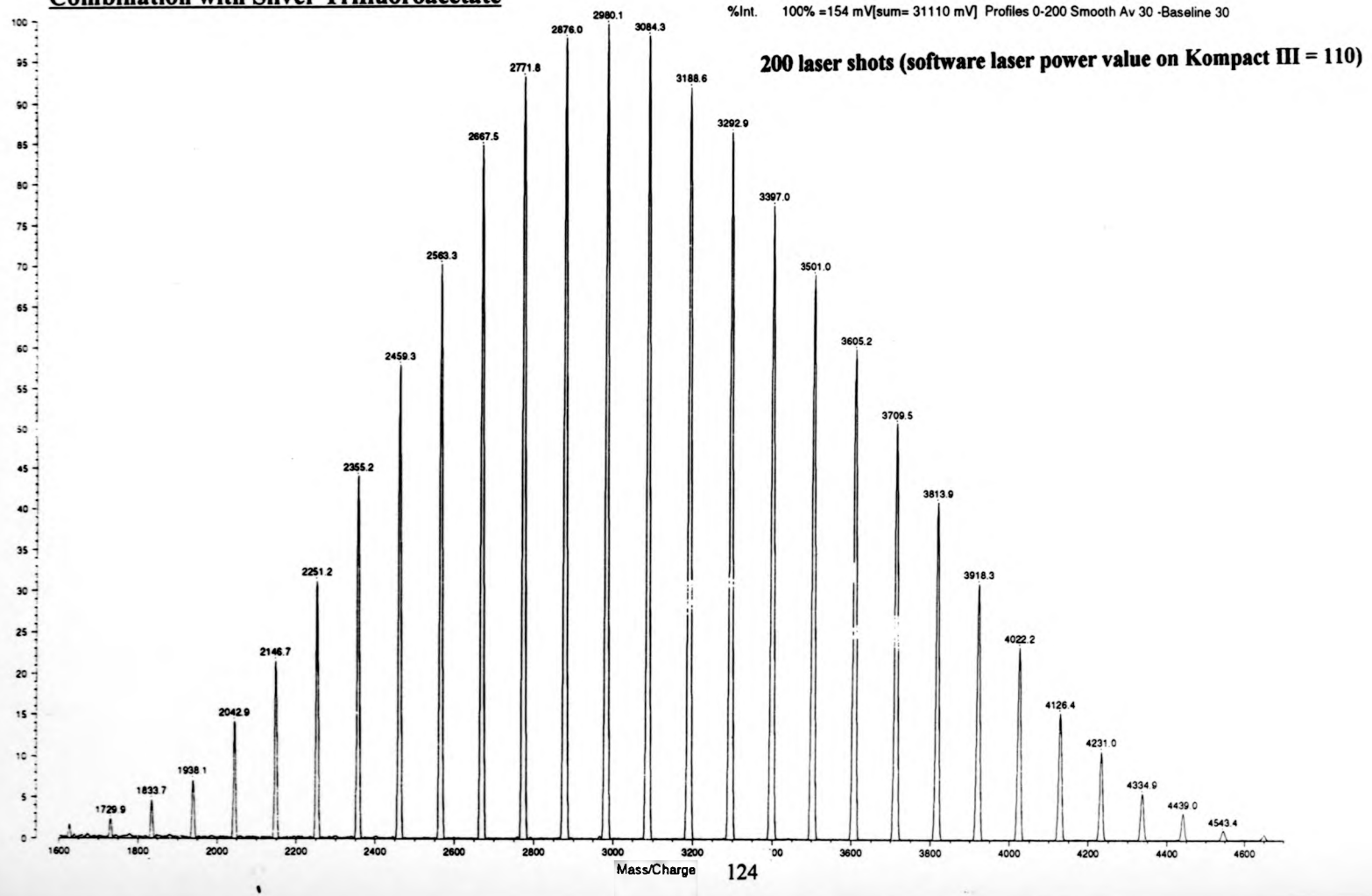

Figure 4.2a (Close-up)

Part of the Poly(styrene) Spectrum Showing 104 Monomer Mass Separation

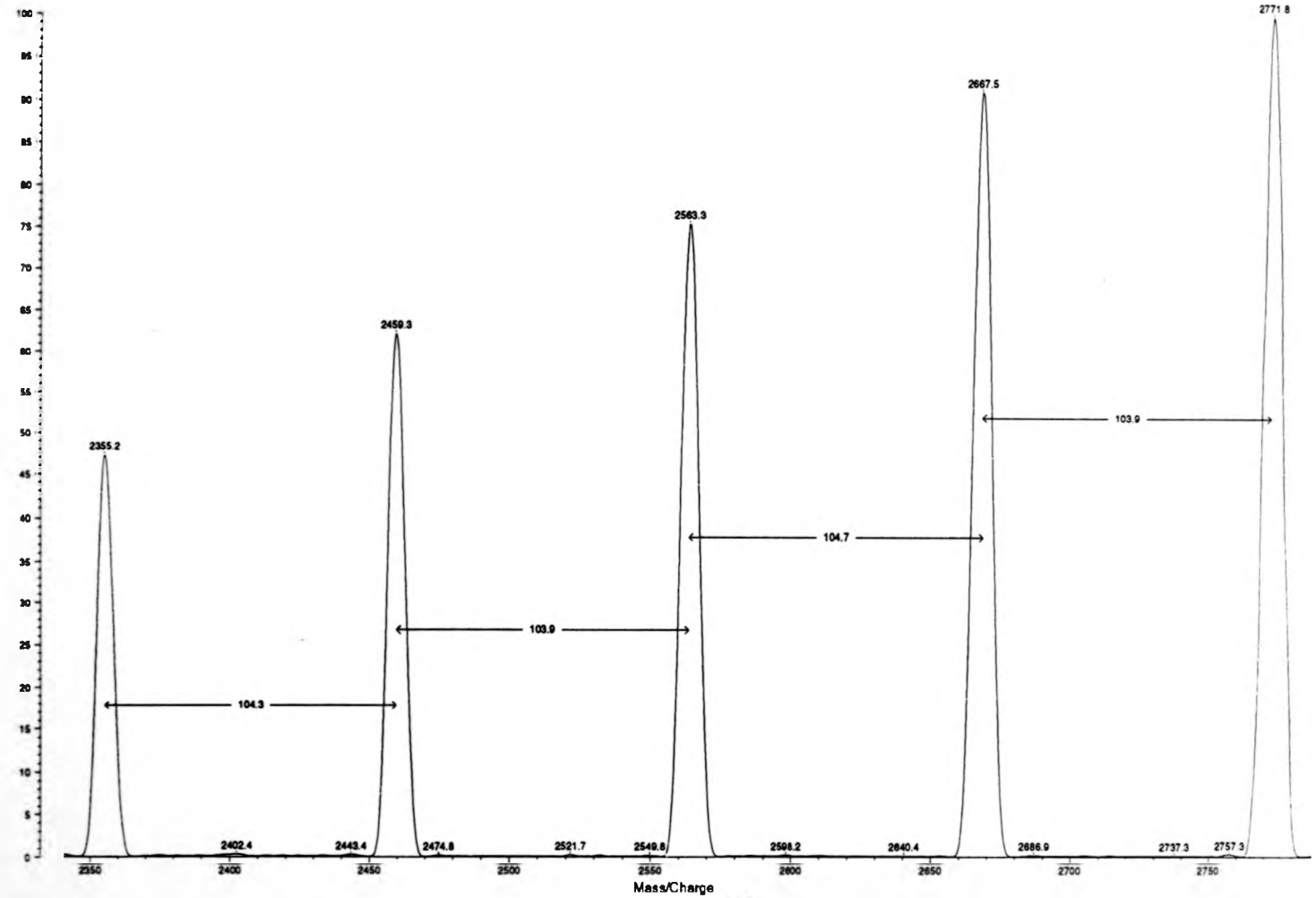

Figure 4.2b

Typical Spectra Poly(styrene) of Molecular Mass ~ 7000 Da Using 9-Nitroanthracene as the Matrix in Combination with Silver Trifluoroacetate

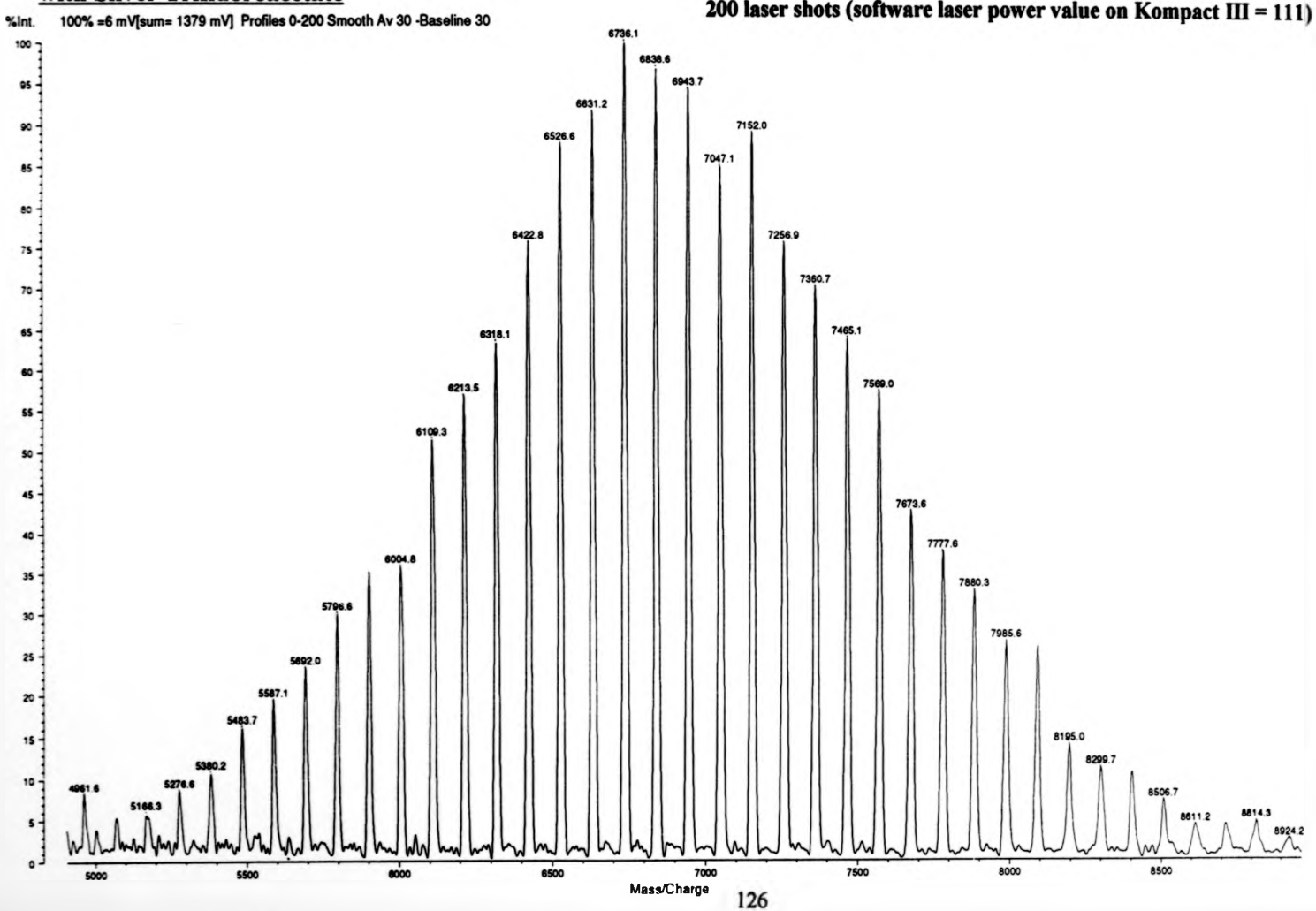

Figure 4.2b (Close up)

Part of the Poly(styrene) Spectrum Showing 104 Monomer Mass Separation

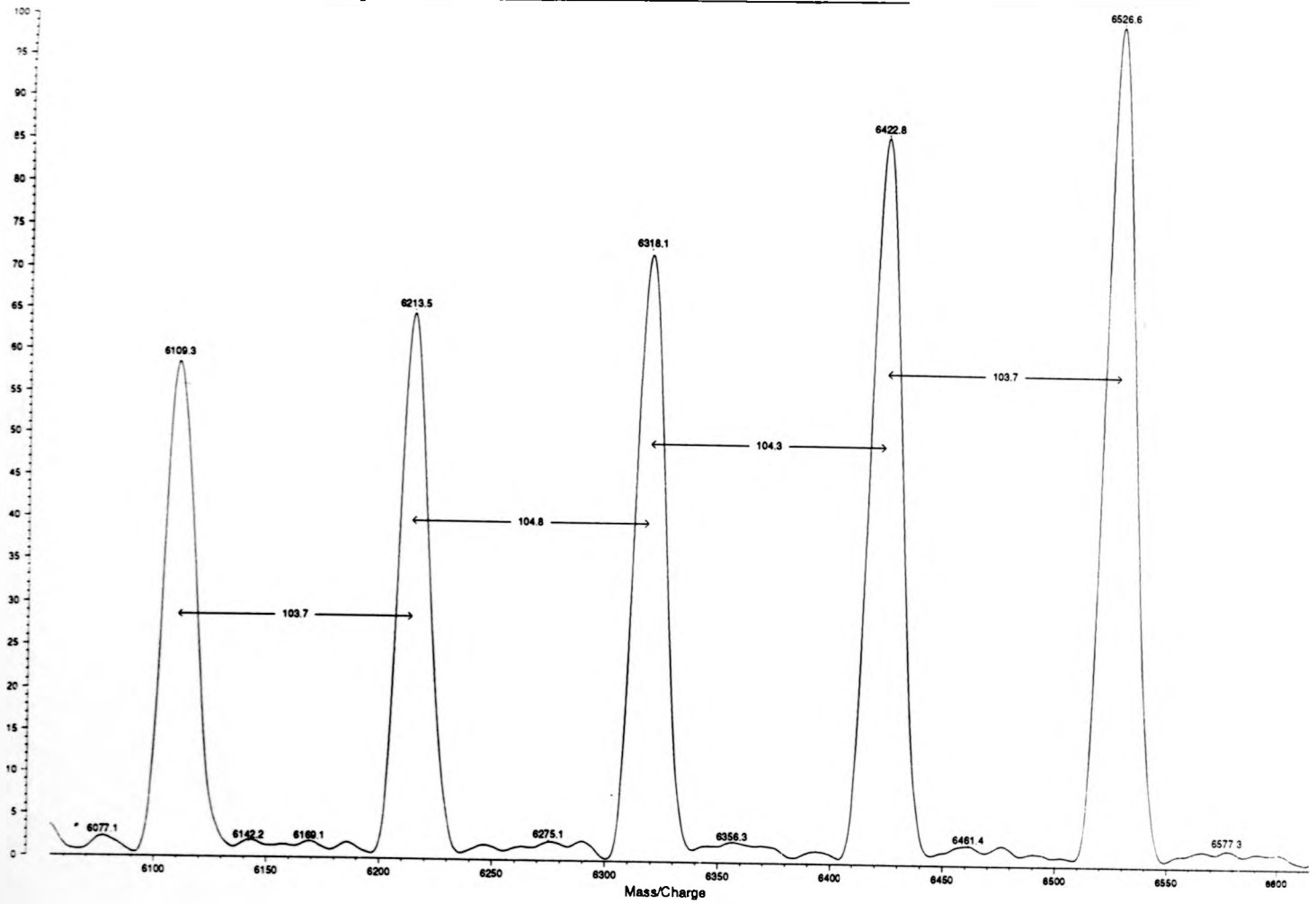

Figure 4.2c

Typical Spectra of Poly(styrene) of Molecular Mass ~ 12 000 Da Using 9-Nitroanthracene as the Matrix in Combination with Silver Trifluoroacetate

200 laser shots (software laser power value on Kompact III = 112)

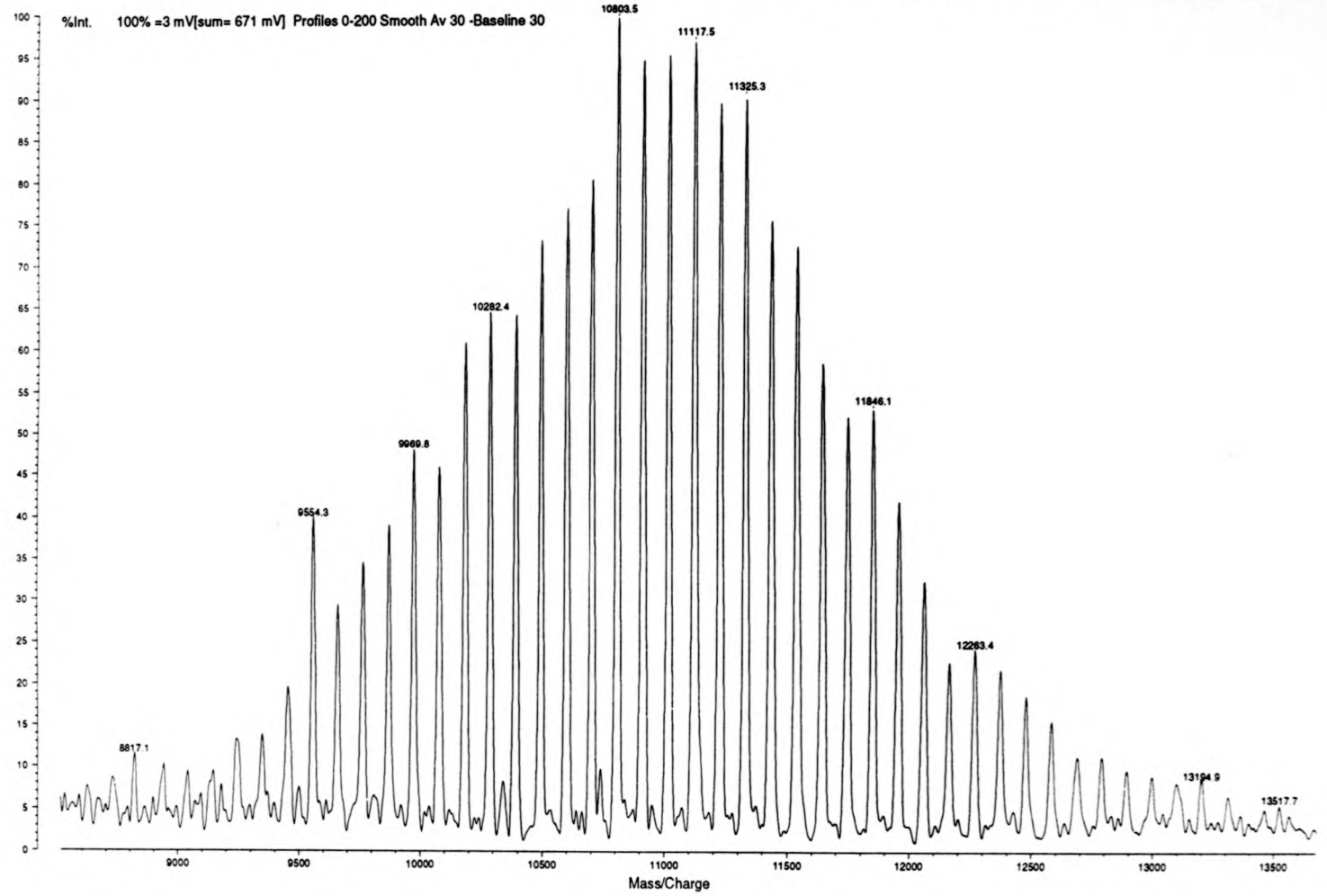

Figure 4.2 c (Close-up)

Part of the Poly(styrene) Spectrum Showing 104 Monomer Mass Separation

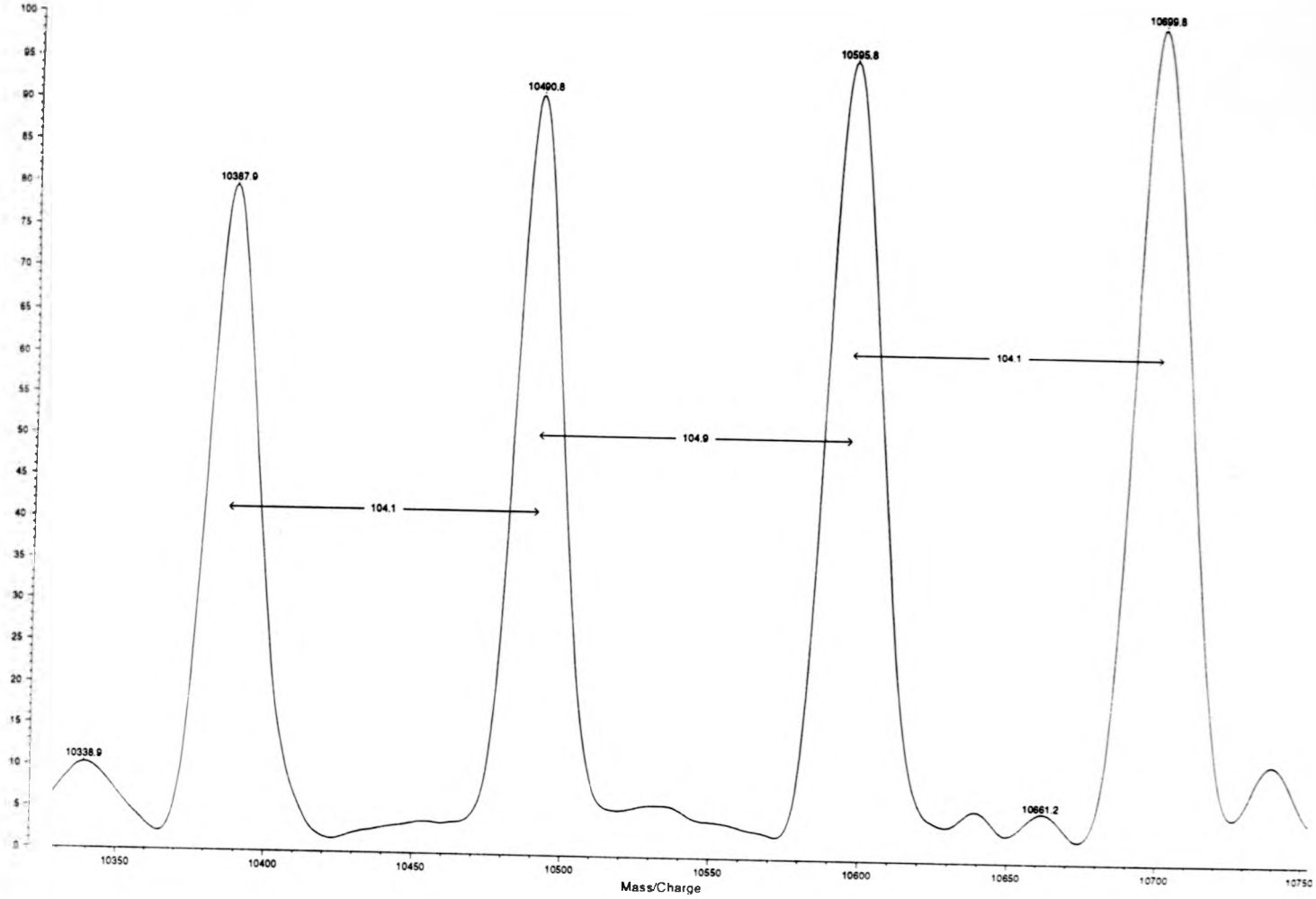

The experimental error in M_n and M_w was ≤ 1.5 % and the maximum error in the poly(dispersity) value was ≤ 3 %.

The results in **Figure 4.3** show the molecular mass statistics obtained from the MALDI-TOF data compared with those quoted by the manufacturer and those calculated by SEC. It can be seen that there is good agreement between weight average molecular mass distributions M_w, and number average molecular mass distributions M_n, calculated from MALDI and SEC. The correct distribution for the purposes of comparison between MALDI and SEC is the number average molecular mass distribution M_n, which shows reasonable agreement.

Analysis of the results presented indicates that there are subtle but systematic trends in the data which reveals differences which exist between MALDI-TOF and SEC. There is a correlation between the relative values of the number-average molecular masses from MALDI-TOF and SEC and the number average molecular mass which is shown in **Figure 4.4.** Similar trends can be seen in the relative values of the weight average molecular mass and *z*-average molecular masses. **Figure 4.5** shows other trends found in the relative values of the different types of molecular-masses of a sample where there is an approximately monatonic decrease in the number average molecular-mass average obtained from MALDI-TOF relative to that derived from SEC.

4.4 Poly(methyl methacrylate)

4.4.1 Sample Preparation

All samples were supplied by Polymer Laboratories and had a polydispersity value close to unity. Four poly(methyl methacrylate) (PMMA) standards were analysed in the mass range, 1000-10,000 Da. Each sample was analysed using 2,5 di-

hydroxybenzoic (DHB) acid as the matrix material and each solution used for MALDI investigations had been previously used for analysis by SEC.

50µl of the matrix solution (0.1M, 2,5 DHB in THF) was deposited on the stainless steel sample slide and the solvent evaporated off under a cool stream of nitrogen. Each PMMA standard was diluted such that each solution contained approximately 1.5 mg per ml and 0.5µl of this diluted analye solution was then deposited on top of the matrix and the solvent was evaporated off under a stream of warm air.

No salt was added to these samples, however, the [M+H]+ species was not detected. Molecule ions detected were all either [M+Na]+ or [M+K]+ or both. The source of these cations was not known, however, alkali metal cations are common impurities originating from glassware. human contact, matrix salts and solvents are not readily removed.

Figure 4.6 depicts four PMMA spectra typical of those obtained by MALDI.

Spectrum 4.6.a shows two distributions and these can be assisgned to sodium attached and potassium attached oligomers. The most intense distribution was not clear since approximately half-way into the polymer distribution, the most intense peak switches from the sodium adduct to the potassium adduct. **Spectrum 4.6.b** shows two similar distributions, however, the sodium-attached polymer distribution remains the most intense throughout the mass range of the polymer. **Spectrum 4.6.c** depicts the heaviest PMMA sample analysed by MALDI. The resolution and signal-to-noise values were both low in this spectrum, furthermore, it was noted that the only PMMA series observed was potassium-attached.

Figure 4.4

Graph to Show Percentage Difference Between Number Average Molecular Mass for Poly(styrene) for Samples derived from SEC and MALDI

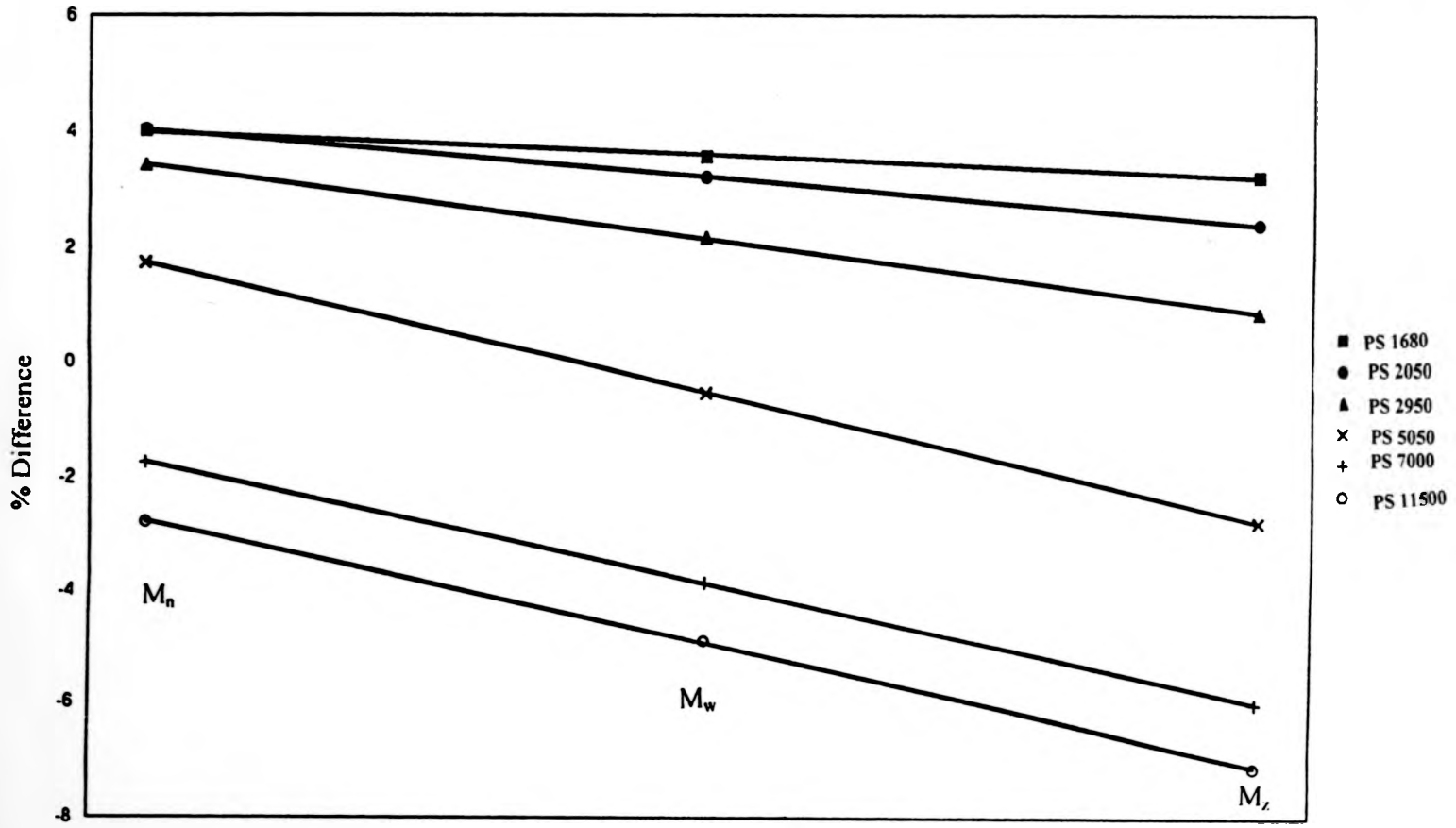

Figure 4.5

Chart Depicting Discrepancy Trends in Data Obtained by MALDI and SEC

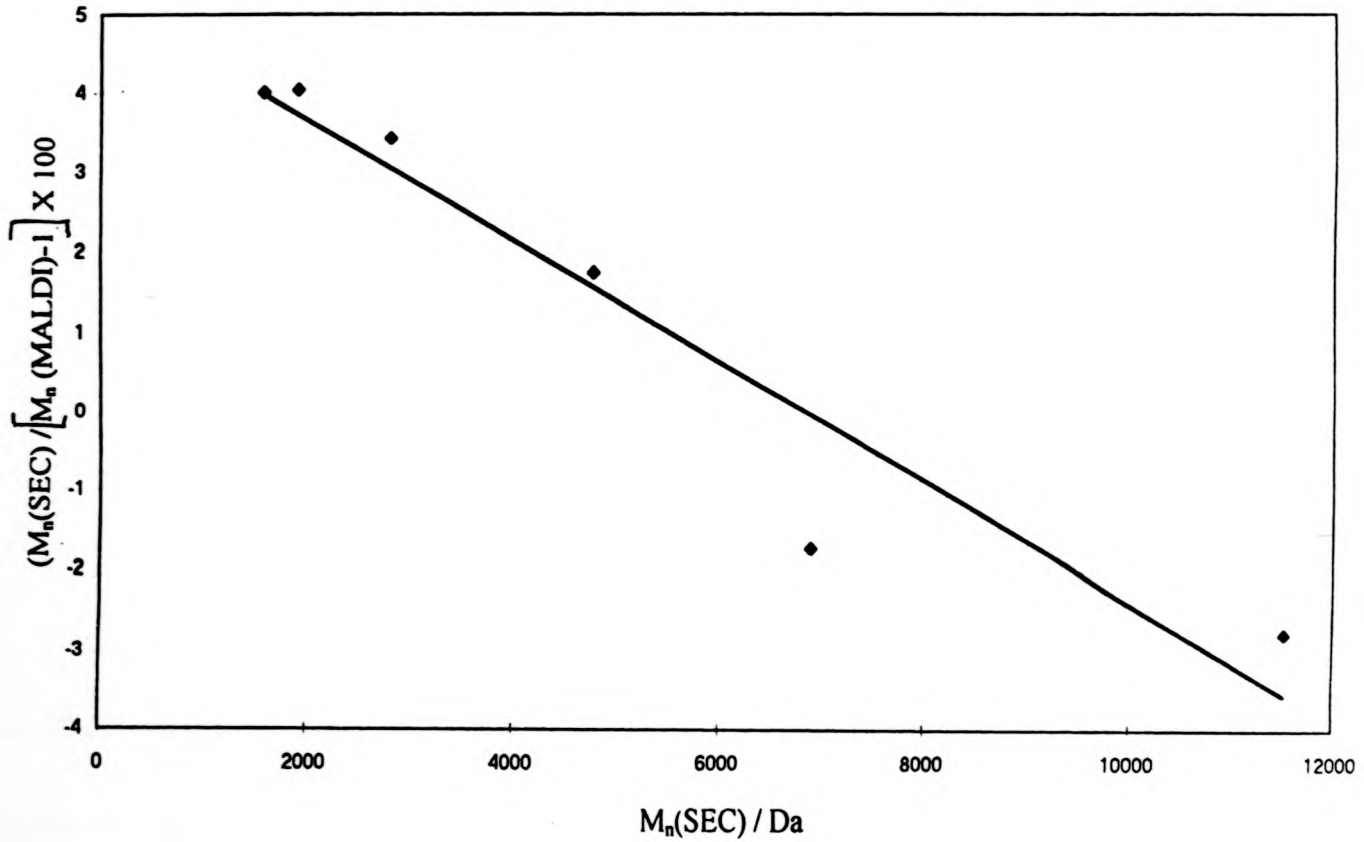

Figure 4.6.a i

Typical Spectra Poly(methyl methacrylate) of Molecular Mass ~ 1200 Da Using 2,5 DHB as the Matrix

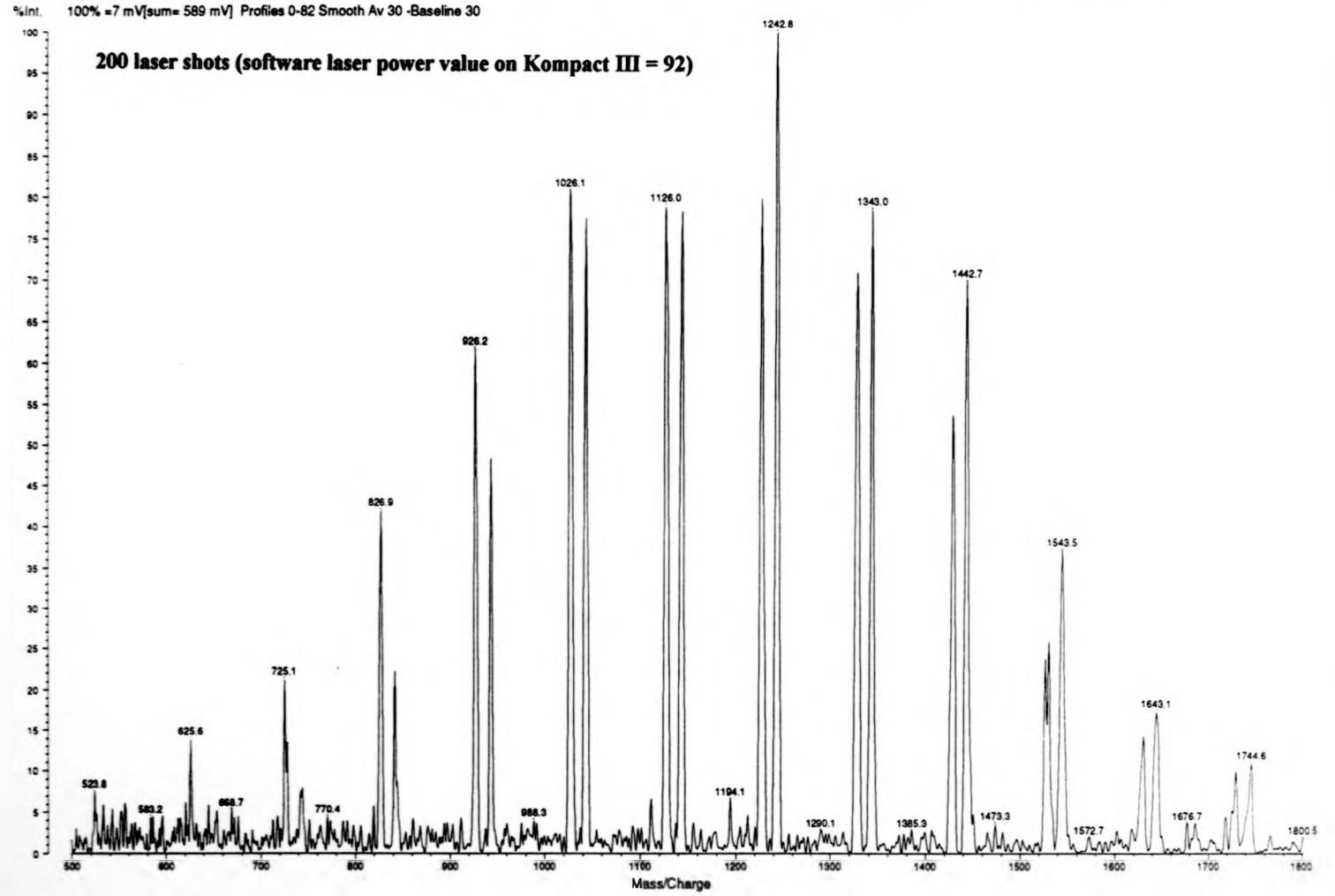

Part of Spectrum Showing Sodium and Potassium Adducts

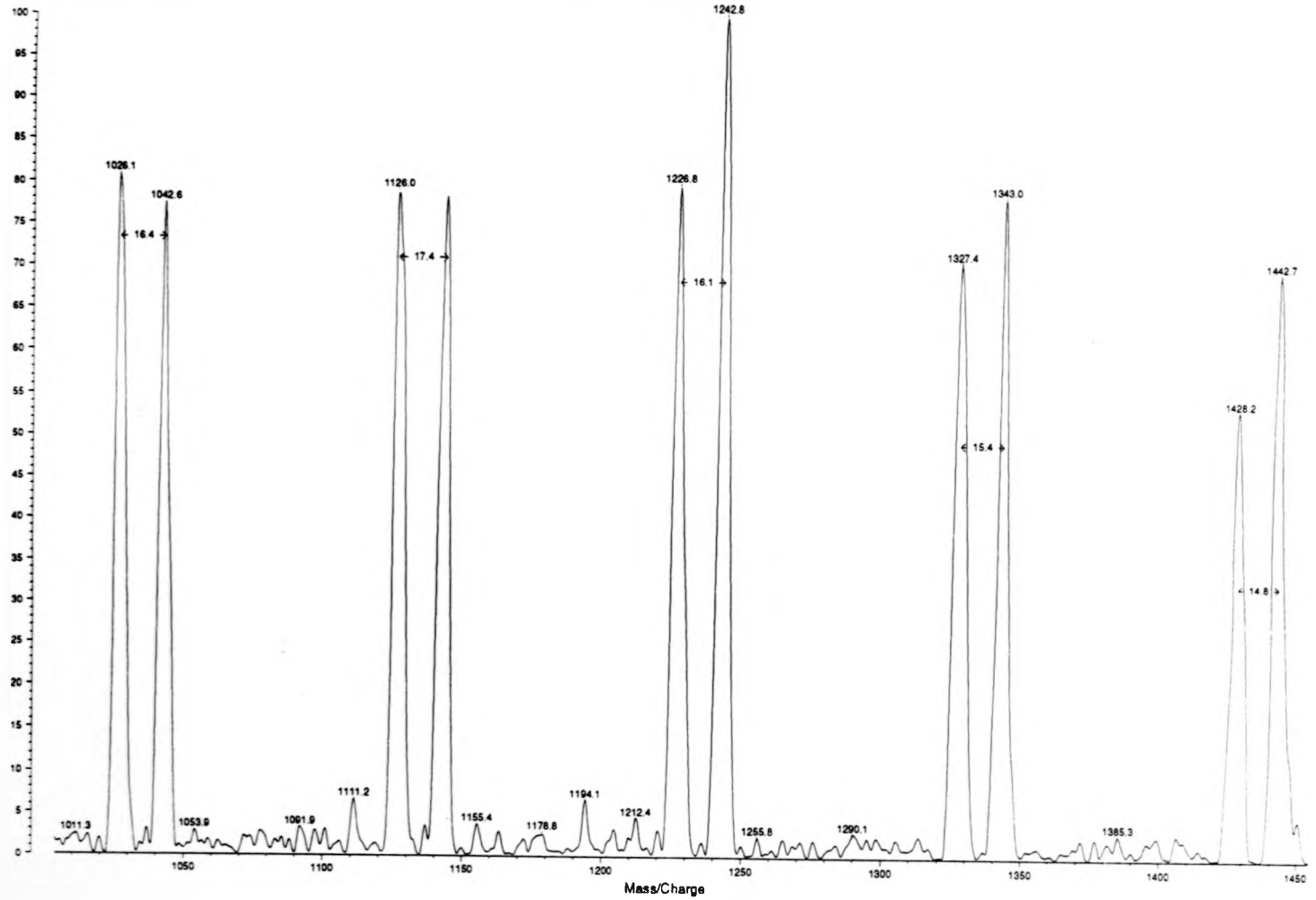

Figure 4.6.b.i

Typical Spectra Poly(methyl methacrylate) of Molecular Mass ~ 5000 Da Using 2,5 DHB as the Matrix

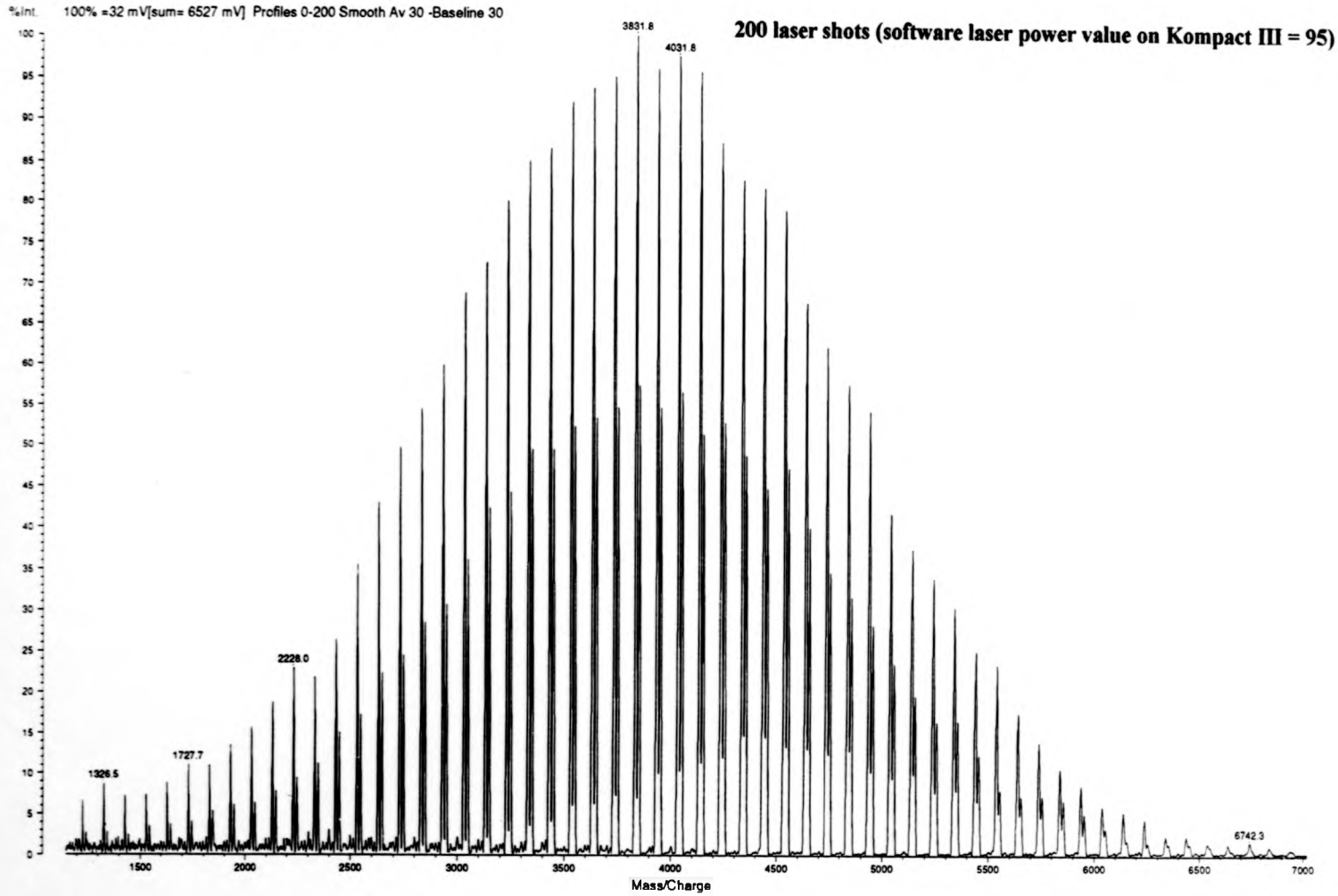

Part of Spectrum Showing Sodium and Potassium Adducts

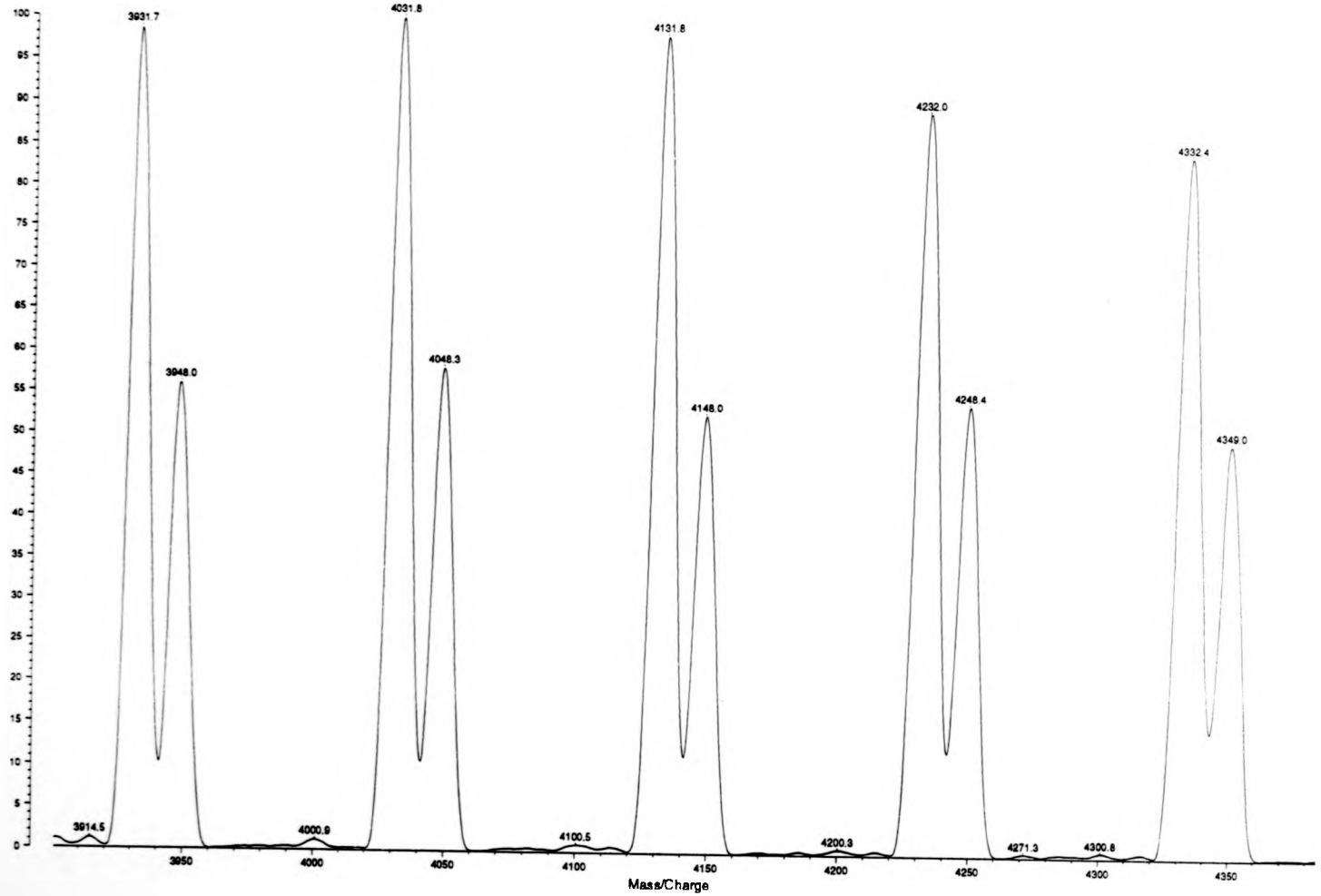

Figure 4.6.c

Typical Spectra Poly(methyl methacrylate) of Molecular Mass ~ 10 000 Da Using 2,5 DHB as the Matrix

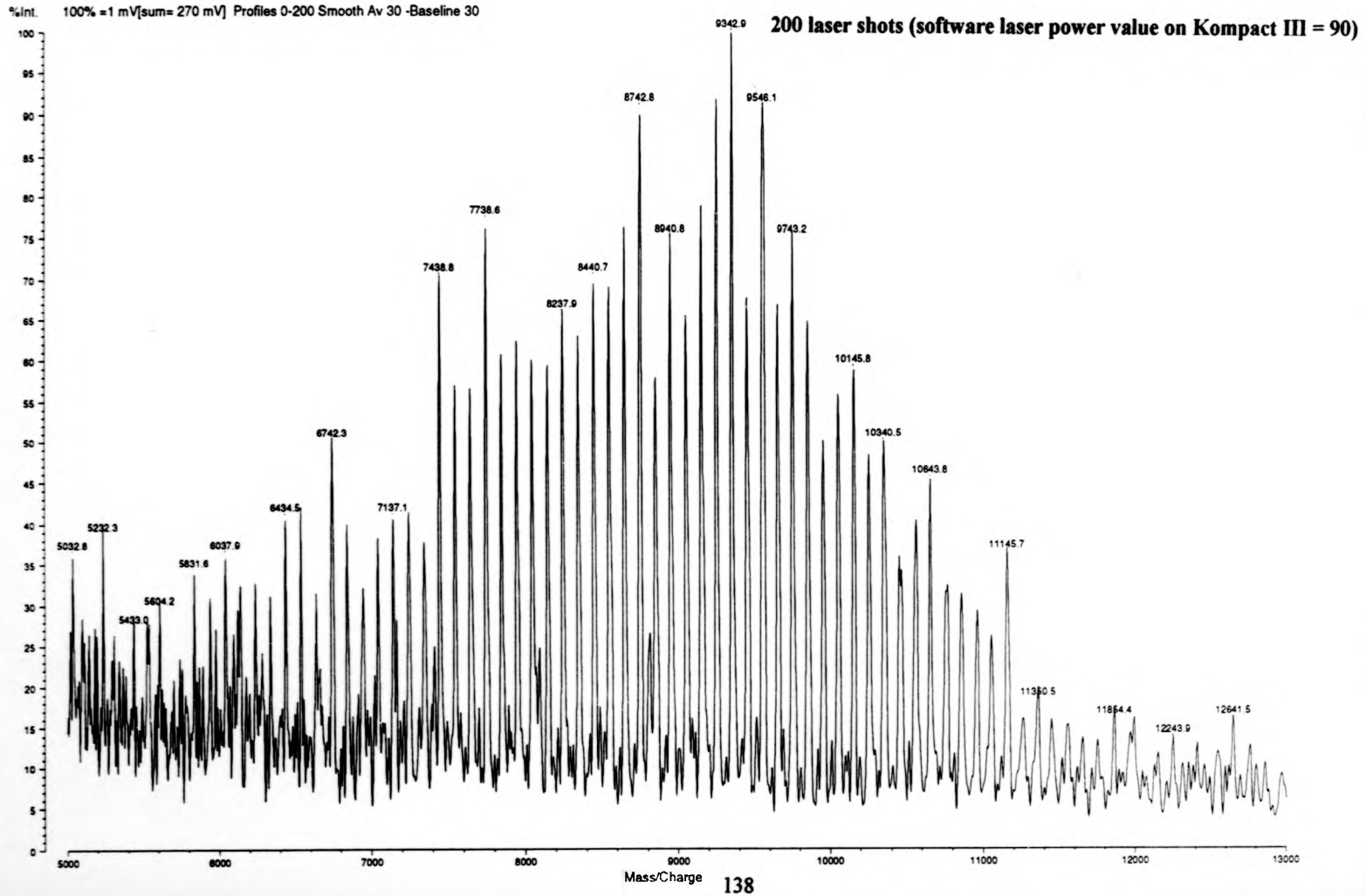

4.4.2 Molecular Mass Calculations

Two series of peaks were detected resulting from the formation of potassium or sodium adducts either in solution or in the gas phase. The nature of the adduct was specified by the user and the mass of this adduct was excluded from all calculations carried out. For lower-mass PMMA standards, the most intense distribution detected was the sodium adduct series. The tolerance value and the cut-off parameter were set at 3 mass units and 5% respectively and these values ensured that any other adducts present were exempt from all calculations performed.

Figure 4.7 shows the molecular mass statistics obtained by MALDI compared with those quoted by the manufacturer* and calculated by SEC**. Molecular-mass data derived from both Na+ and K+ are presented where available.

Figure 4.7

Na+ Series				**K+ Series**				**SEC**			
Mn	Mw	Mz	Mw/Mn	Mn	Mw	Mz	Mw/Mn	Mn	Mw	Mz	Mw/Mn
1157	1225	1290	1.06	1125	1267	1311	1.04	984	1117	1231	1.14
1755	1876	1979	1.07	1653	1880	1990	1.13	1721	1917	2116	1.11
4128	4309	4460	1.04	3753	4018	4206	1.07	4022	4373	4706	1.09
N/A	N/A	N/A	N/A	9553	9612	9674	1.01	10,100	10,654	11,209	1.06

* Polymer Laboratories, UK

** All SEC data provided by K. Suddaby.

The experimental error in M_n and M_w was ≤ 1.5 % and the maximum error in the poly(dispersity) value was ≤ 3 %.

The results in **Figure 4.7** show the molecular mass statistics obtained from the MALDI-TOF data compared with those quoted by the manufacturer and those calculated by SEC. It can be seen that there is good agreement between weight

average molecular-masses M_w, and number average molecualr masses M_n, calculated from MALDI and SEC, however, both sets of data are lower than figures quoted by the manufacturer. The correct distribution for comparison between MALDI and SEC is the number average molecular mass M_n, which shows reasonable agreement. There are some discrepancies between molecular-mass data calculated from Na+ adducts and K+ adducts, although, generally the differences were found to lie within acceptable experimental errors.

4.5 Poly(isobutylene)

4.5.1 SEC Measurements

SEC experiments were performed at Warwick in order to obtain an approximate value of the molecular mass values.

The SEC equipment used in these experiments consisted of a dual piston HPLC pump (ICI Instruments LC1110), an injection valve with a 20µl sample loop (Rheodyne 1725) and a differential refractive index detector (ICI instruments LC1240). Data was analysed using Polymer Laboratories Calibre SEC software.

Each polymer solution (100mg/ml in THF) was analysed using THF as the effluent and toluene (≈0.2 %wt) was used an internal standard and flow marker for each sample. The column used was a Polymer Laboratories (PL) Mixed E-type (300 x 7.5 mm) which was connected to a Polymer Laboratories 5 µm bead size guard column (50 x 7.5 mm). The column was calibrated between 200 and 30,000 mass units using a suitable set of standards polymers of a narrow polydispersity. Two sets of standards were used in the case of the poly(isobutylene) polymers ; poly(styrene) and poly(methyl methacrylate). A further set of molecular mass statistics were supplied by the manufacturer. (Steve Harley, BP Chemicals, Grangemouth, UK).

Figure 4.8 shows SEC data obtained using two calibration standards and data provided by the manufacturer.

Figure 4.8

	Poly(styrene)				PMMA				Manufacturer		
	Mn	Mw	Mz	Mw/Mn	Mn	Mw	Mz	Mw/Mn	Mn	Mp	Mw/Mn
MOF	993	1083	1161	1.09	1203	1313	1410	1.09	898	1074	1.12
DOF	891	952	1012	1.07	1079	1154	1228	1.07	798	893	1.09
TOF	933	1020	1102	1.09	1131	1237	1338	1.09	836	988	1.12

The experimental error in M_n and M_w was $\leq$ 1.5 % and the maximum error in the poly(dispersity) value were $\leq$ 3 %

Figure 4.9 a, Figure 4.9b and Figure 4.9 c depict typical SEC data for MOF, DOF and TOF respectively.

4.5.2 MALDI Sample Preparation

All samples were supplied by BP Chemicals (Steve Harley, Grangemouth). Three samples analysed by MALDI-TOF (MOF931, DOF9411 and TOF 9416) have been mass analysed. Each sample was prepared using the optimised sample preparation method described previously. The optimum amount of silver salt was used so that maximum signal-to-noise values were obtained and the occurrence of silver clusters in the mass spectrum was reduced.

4.5.3 Molecular Mass Calculations

The silver adduct which was attached to each poly(isobutylene) oligomer ion was specified by the user and the mass of this adduct was removed from each polymer series by the software when the number fraction was calculated. In all calculations, the tolerance value was set at 3 mass units either side of the monomer mass separation and the cut-off parameter was set at 3 %.

Figure 4.9a

Mono-olefinic Poly(isobutylene) Size Exclusion Chromatography Data

Calibration Using	Narrow Standards			Curve Used	3rd Order Polynomial
Calibration Limits	5.62	to 10.08	Mins	Last Calibrated	Wed May 21 07:52:58 1997
Flow Rate Marker		found at 11.05		in Standards at	11.07 Mins
Broad Peak Start	7.60	End 9.83	Mins		

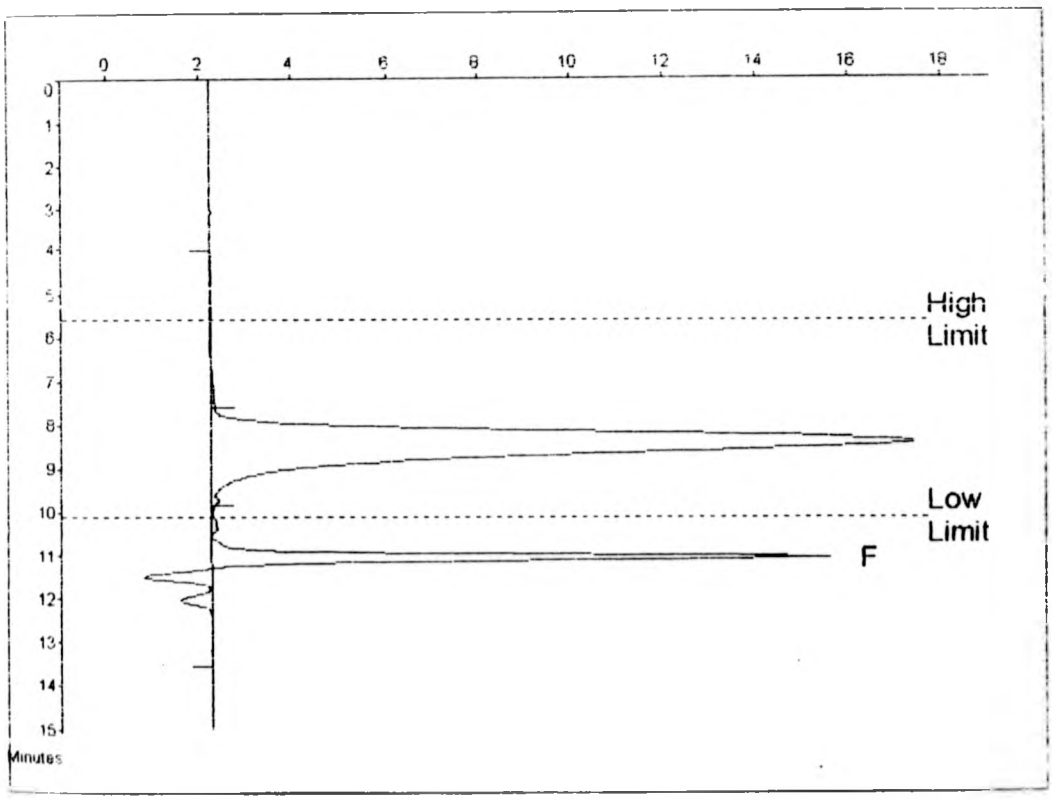

Figure 4.9b

Di-olefinic Poly(isobutylene) Size Exclusion Chromatography Data

Calibration Using	Narrow Standards			Curve Used	3rd Order Polynomial
Calibration Limits	5.63	to 10.10	Mins	Last Calibrated	Wed May 21 07:53:56 1997
Flow Rate Marker		found at 11.08		in Standards at	11.07 Mins
Broad Peak Start	7.63	End 9.83	Mins		

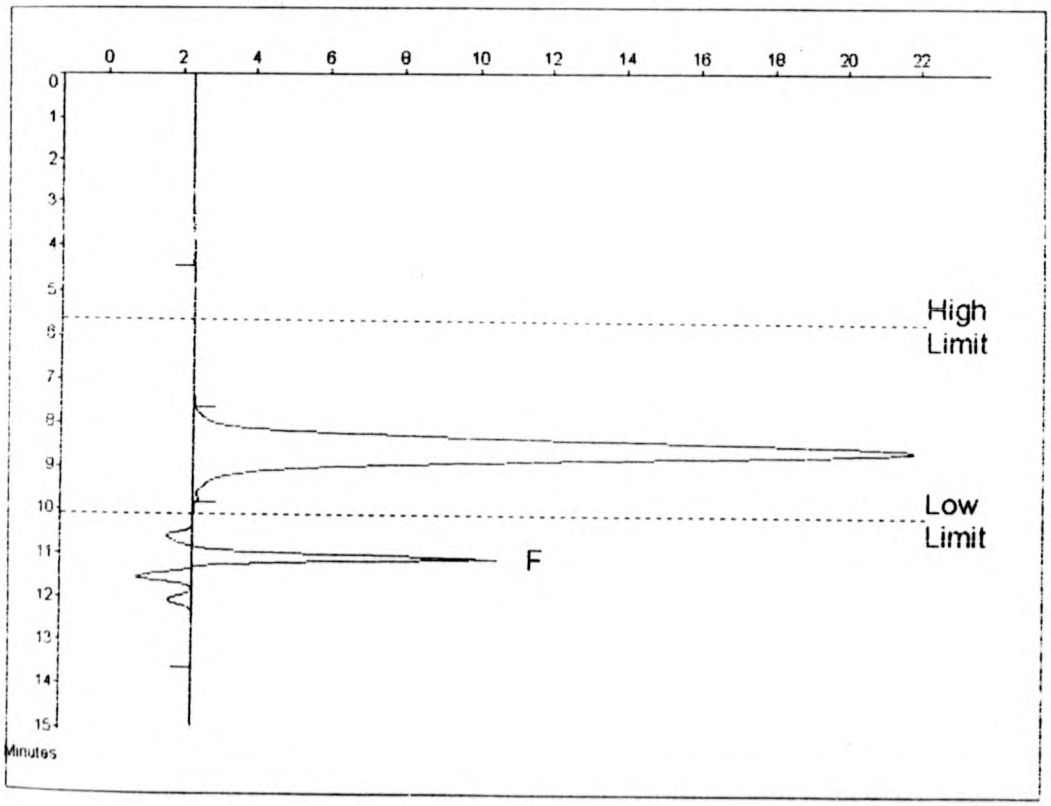

Figure 4.9.c

Tri-olefinic Poly(isobutylene) Size Exclusion Chromatography Data

Calibration Using	Narrow Standards			Curve Used	3rd Order Polynomial
Calibration Limits	5.86	to 10.12	Mins	Last Calibrated	Wed May 21 07:53:56 1997
Flow Rate Marker		found at 11.10		in Standards at	11.07 Mins
Broad Peak Start	7.58	End 9.85	Mins		

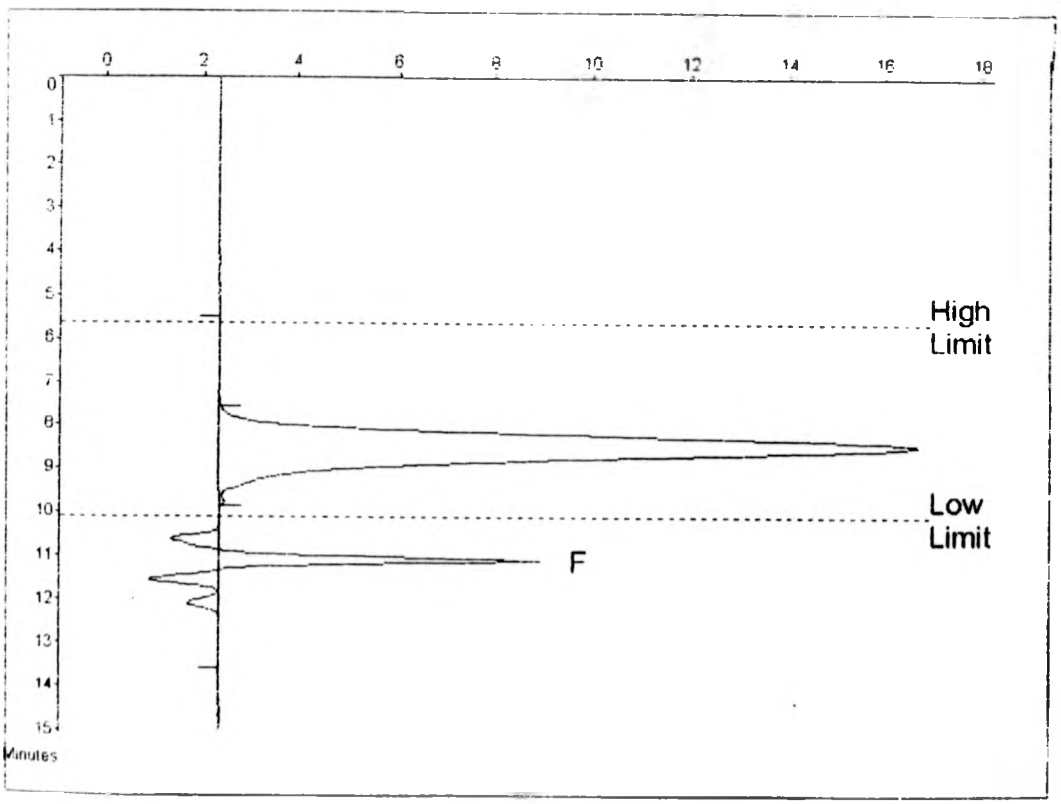

Results labelled MOF, DOF and TOF were obtained for the mono-olefinic, di-olefinic and tri-olefinic samples respectively under the same conditions. In the case of the tri-olefinic sample, two polymer distributions were observed when excess silver salt was added to the sample preparation. The molecular mass data calculated from these two distributions are included in the results presented and and the different distributions are labelled TOF1 and TOF2. TOF1 can be assigned the same molecular structure as the TOF distribution, however, the chemical nature of TOF2 is not known.

Both mono-olefinic and di-olefinic samples were investigated using excess salt in the sample preparation. The di-olefinic sample was detected as the same detected as the same distribution, however, the mono-olefinic sample was much more sensitive to changes in silver salt concentrations and could not be analysed under such conditions .

Figure 4.10

Molecular Mass Statistics Obtained by MALDI for Poly(isobutylene).

	Mn	Mw	Mz	Mw/Mn
MOF	716	782	827	1.09
DOF	747	774	799	1.03
TOF	733	775	816	1.06
TOF1	867	908	945	1.05
TOF2	1228	1281	1335	1.05

The experimental error in M_n and M_w was $\leq$ 1.5 % and the maximum error in the poly(dispersity) value was $\leq$ 3 %

Figure 4.11 shows tri-olefinic polymer distributions under normal prepration conditions and in the presence of excess silver salt.

SEC data obtained at Warwick was in reasonable agreement with data quoted by the manufacturer. Discrepancies within the SEC data set might be attributated to the fact the neither poly(styrene) or PMMA are suitable calibration standards for the analysis of

Figure 4.11a

Typical MALDI Spectrum of the Tri-Olefinic Poly(isobutylene) Obtained on the Kompact III Instrument

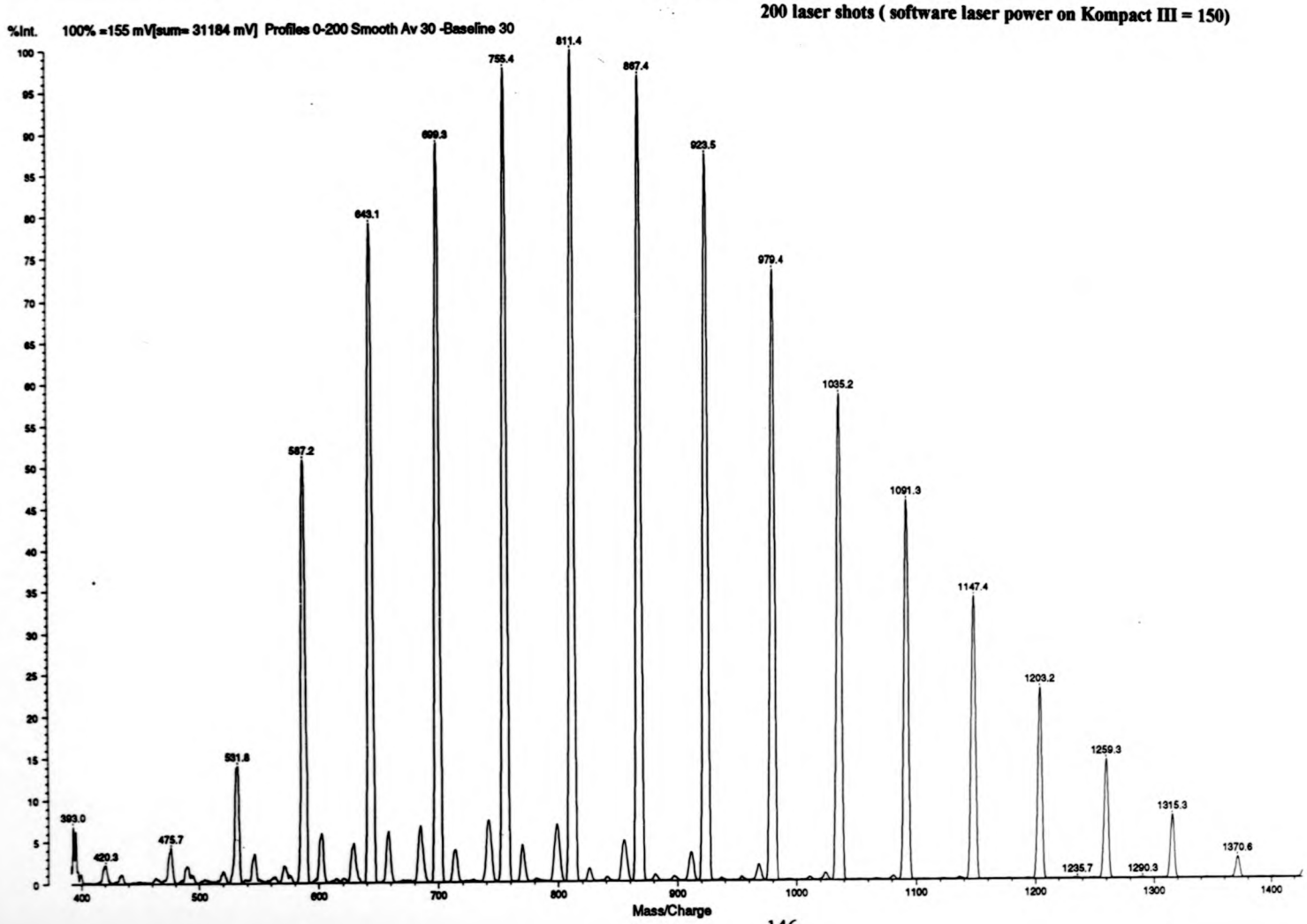

Figure 4.11b

Typical MALDI Spectrum of the Tri-Olefinic Poly(isobutylene) SampleObtained on the Kompact IV Instrument

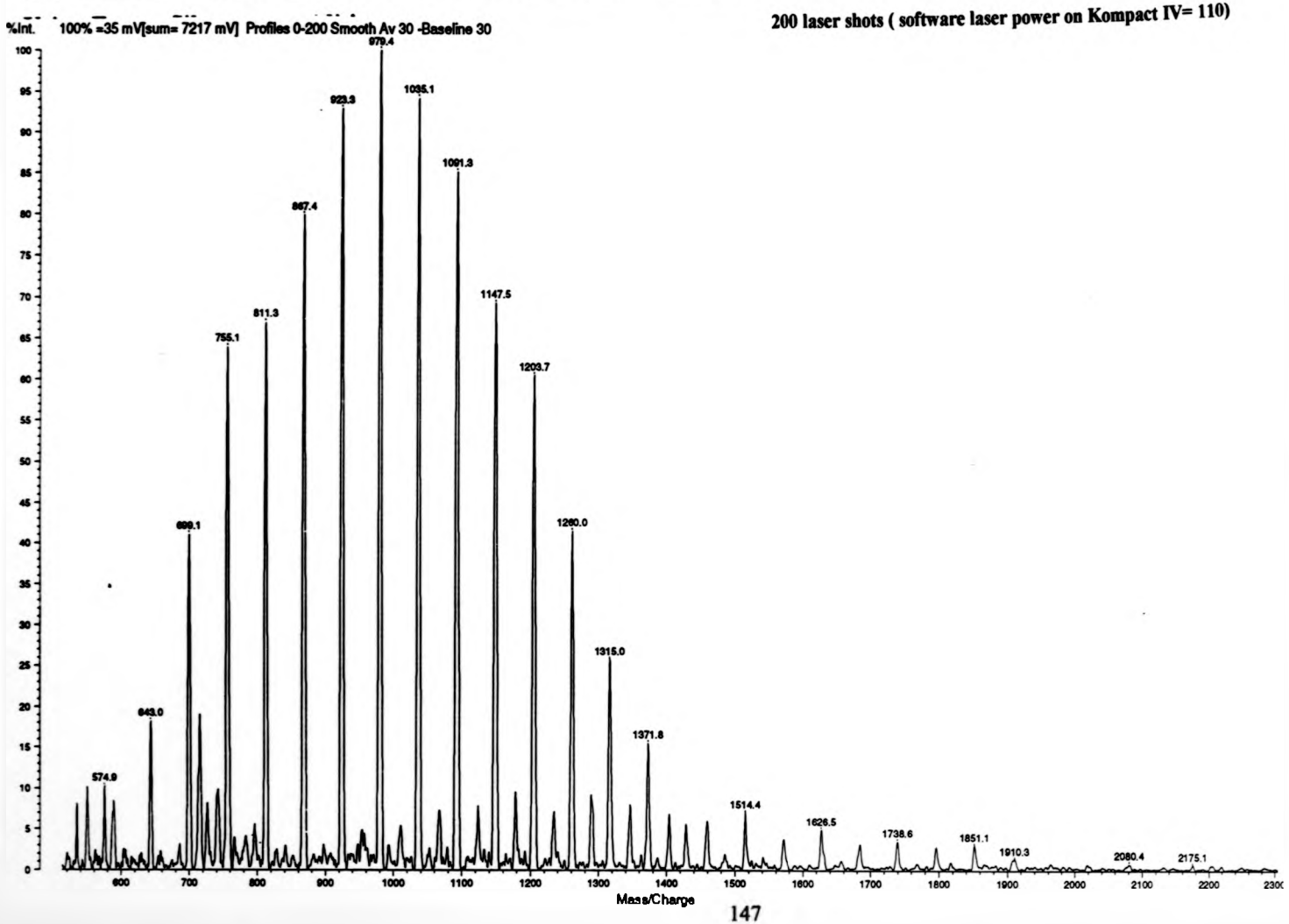

Figure 4.11b.i

Inset of Second Distribution

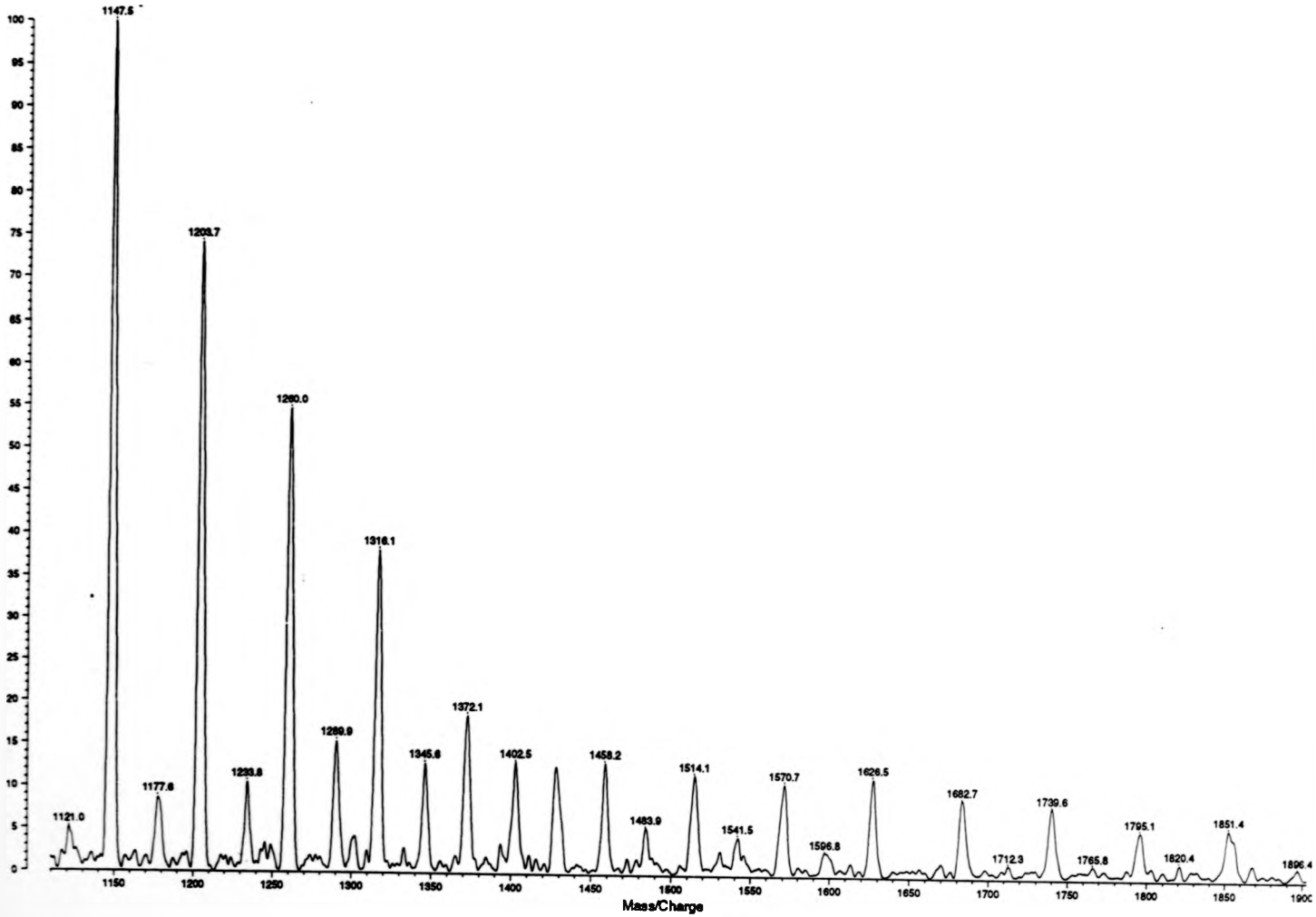

these poly(isobutylene) compounds by SEC. The data provided by the manufacturer (Steve Harley, BP Chemicals) can be regarded as being the most accurate as far as SEC goes, however, the values quoted for the tri-olefinic sample are still regarded as 'dubious' owing to a different size-molecular mass relationship for highly branched polymers. The discrepancies between these data sets clearly highlight some of the problems associated with SEC molecular-mass measurements.

Despite the fact that these polymers have a quoted polydispersity value <1.2, molecular-mass statistics obtained by MALDI are not in good agreement with those obtained by SEC. In general, the figures obtained by MALDI are slightly lower than those obtained by SEC. Furthermore, when more silver salt was added to the sample mixture, the tri-olefinic sample was detected at a slightly higher mass and a secondary polymer distribution which also has a monomer mass unit of 56 Da was observed. Neither of the two analogues displayed this behaviour under the same conditions.

4.6 Poly(sulfide) Analysis

4.6.1 Sample Preparation

All samples were supplied by Dr. A Mahon (Morton Thiokol). Two samples which had a poly(dispersity) index value close to unity were analysed (Model A and Zl-2264). A non-model compound (LP-2) whose poly(dispersity) index ≥1.1 was investigated Each sample was prepared using the optimised sample preparation method described in chapter 3, ensuring that silver cluster formation did not occur.

20μl of a solution of silver tri-fluoroacetate in THF (0.1M) was used to dope the analyte solution (0.5ml, 10^{-3}M in THF). Equal quantities of this solution and the matrix solution (0.1M 9-Nitroanthracene in THF) were mixed. 1μl of this mixture was deposited on a stainless steel sample slide and the solvent was evaporated off in a stream of warm air.

Figure 4.12 shows a MALDI spectrum of LP-2 under the conditions stated.

Figure 4.12

MALDI-TOF Spectrum of Polysulfide LP-2

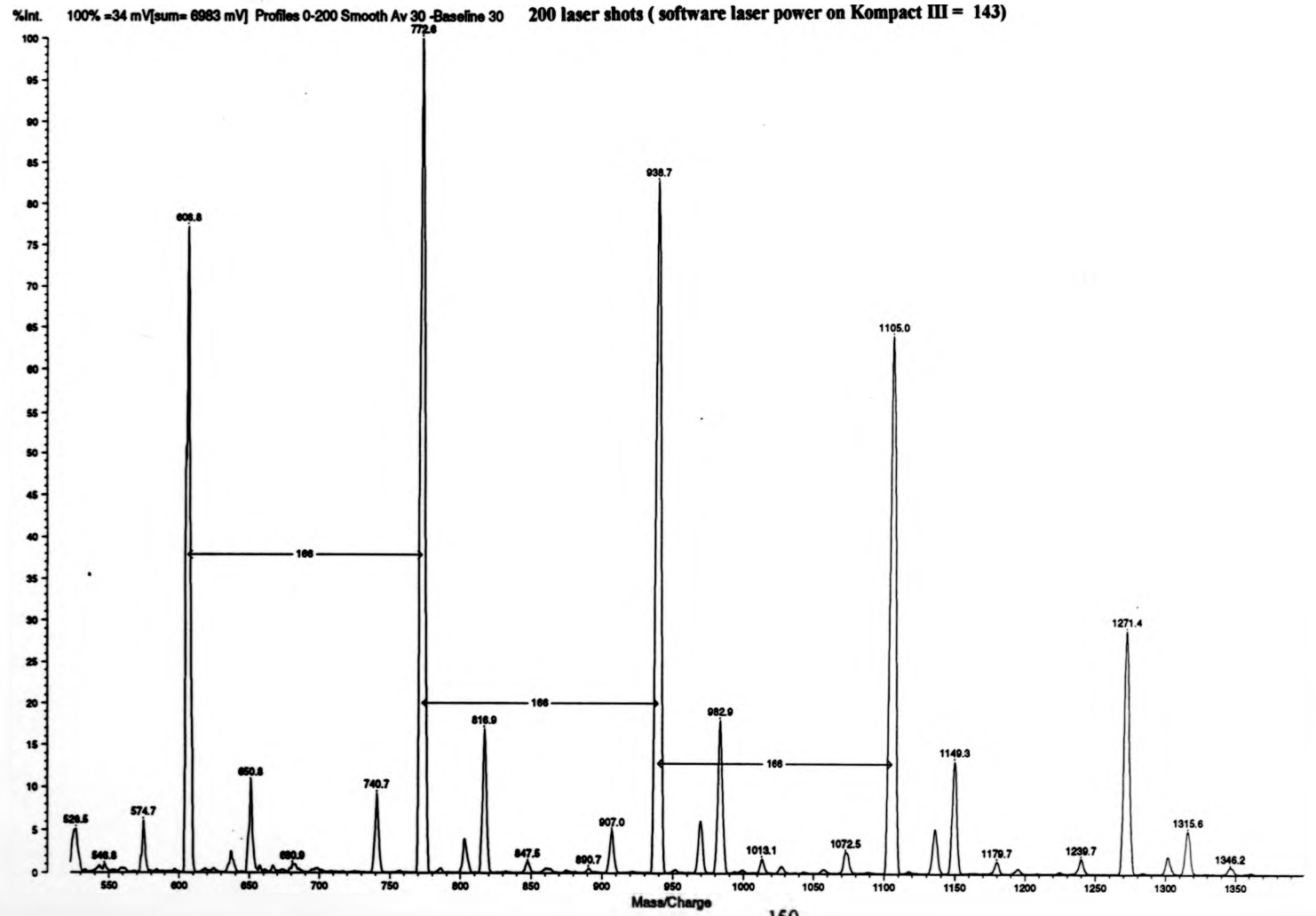

4.6.2 Molecular Mass Calculations

A minimum of two peaks were observed in the MALDI spectrum of each of the poly(sulfide) samples studied. These were not a consequence of the attachment of different types of cations but resulted from the presence of an additional functionality, such as a sulfur atom, in the long polymer chain as discussed in chapter 3. The most intense series was used in molecular-mass calculations and this series was silver attached. The silver adduct was specified by the user and the average mass of the adduct was excluded from all calculations performed. The tolerance value and cut-off parameter were set at 4 mass units and 4 % respectively. These values ensured that any secondary polymer series were exempt from all calculations.

Figure 4.13 shows molecular mass statistics obtained by MALDI.

Figure 4.13

	Mn	Mw	Mz	Mw/Mn
Model A	967	1060	1149	1.09
ZL-2264	607	683	753	1.13
LP-2	770	832	891	1.08

The experimental error in M_n and M_w was $\leq$ 1.5 % and the maximum error in the poly(dispersity) value was $\leq$ 3 %

All of the molecular-mass statistics calculated by MALDI are much lower than those expected. All three compounds analysed have a high poly(dispersity) index, approaching two. M_n values for Model A and ZL-2264 are approximately equal to 2500 whereas for LP-2 this value is nearer 4000.

4.7 Discussion

The mass range of all of the compounds analysed by MALDI-TOF mass spectrometry has been restricted by instrumental constraints. One of the main disadvantages of polymer analysis on the instrument used to obtain results described here is potential detector saturation. This has been documented elsewhere.[165,166,167] Experimentally, the limit of detection for polymers using the reflectron to resolve oligomer ions approaches 12,000Da for samples with a narrow poly(dispersity) index. The mass limit of studying more poly(disperse) polymers depended heavily on dispersity values and was observed to be generally much lower with more poly(disperse) samples. Lower resolutions which are typical of time-of-flight mass spectrometry may be improved significantly with the use of delayed-extraction and longer flight times [163,196] The time-of-flight tube length in this instrument was relatively short (~70cm)[182] and this instrument was not fitted with delayed extraction. Furthermore, the ion source potential was limited to either 5 kV(low mass detection mode) or 20 kV(high mass detection mode). The ability to increase this value upto 25 kV may have improved the mass range available for polymer analysis.

The experimental limit of polymers analysed by MALDI-TOF on this instrument has been achieved using two sets of standards, poly(styrene) and poly(methyl methacrylate), whose polydispersity values all lay close unity. Molecular mass statistics obtained by MALDI compared favourably with those obtained by SEC, agreeing typically within 3%. Subtle trends were observed within the poly(styrene) data which are more likely to reflect instrumental constraints rather than the potential problems of using MALDI as a technique for polymer analysis.

Poly(methyl methacrylate) was not detected as [M+H]+ species despite the fact that no salt was added to the sample preparation. This is in contrast to many biomolecules which are commonly detected as [M+H]+. Two main adducts were detected, Na+ and

K+. The most noticeable observation was that heavier mass poly(methyl methacrylate) standards tended to form K+ adducts . Slightly different molecular mass statistics were calculated using the two distributions, however, these data were in agreement within experimental error. Work by Scrivener and co-workers has shown that molecular mass distributions of poly(methyl methacrylate) and poly(ethylene glycol) can be shifted using different alkali metal cations, higher mass oligomers favouring attachment to heavier mass metal cations[155,156] This effect was particularly noticeable in more polydisperse samples, thus results presented in this chapter are not in disagreement with this work. Furthermore, the fact that heavier PMMA samples have only been detected as potassium adducts when no salt is added substantiates these findings.

Molecular-mass data derived from MALDI for three poly(isobutylene) polymers were slightly lower than statistics quoted by the manufacturer. The effect of a silver cation on the true molecular mass distribution has not been quantified although good agreement between SEC and MALDI has been obtained for poly(styrene) samples using silver cation attachment.[195] Heavier mass analogues ≥ 2000 Da could not be analysed under the same conditions. These observations are more likely to be due to the increased aliphatic nature of the polymers and the difficulties associated with sample preparation than detector saturation or any other instrumental constraint. The discrepancies which arise within SEC data sets for these compounds are typical of types of problems which arise in SEC analysis, in particular, the lack of suitable standards with which to calibrate data obtained.

All of the molecular mass statistics derived by MALDI for the poly(sulfide) samples were much lower than those quoted by the manufacturer. This can be attributed to the fact that these samples have a broad molecular mass distribution and the problems associated with the analysis of such samples by MALDI have been extensively documented and have continued to be a growing area of research.[171,172,173] Despite these problems, the spectra of poly(sulfide) presented in this chapter are still of interest

since no polymers of this kind have previously been analysed by MALDI, preceding work having focused on the application of electrospray ionisation to these samples.[197,198]

CHAPTER FIVE

Investigations of Polymer Fragments Formed by Post-Source Decay Processes in Matrix-Assisted Laser Desorption/Ionisation

5.1 Introduction

Metastable decay of matrix-desorbed peptide ions in the field-free region of a time-of-flight mass spectrometer was reported by Kaufmann and co-workers[110,111] as an explanation for peak broadening observed in MALDI-TOF spectra of biomolecules. These processes were exploited as a method of detailed structural elucidation of peptides and subsequently used to obtain amino-acid sequencing information. [110,111,112,113]

MALDI-post-source decay (PSD) experiments have mainly focused on the application of this technique to the analysis of biomolecules, in particular, peptides[115,116] Oligonucleotides[118], oligosaccharides[118] and modified cyclodextrin[119] have been investigated with limited success. In all PSD experiments, the use of an ion mirror is the key in detecting fragment ions formed[112,113,114]. In this chapter post-source decay data obtained for a range of polymers including poly(ethylene glycol), poly(styrene) and poly(isobutylene), using two different instruments of contrasting reflectron design, are presented. The type of structural information which may be obtained relating to polymers is discussed. In particular, the effect of laser fluence and pressure[111] on the quality of data have been investigated.

5.2 Post-Source Decay Using a Two-Stage Reflectron

5.2.1 General Post-Source Decay Analysis

All experiments were carried out on a Bruker Biflex I MALDI-TOF Mass Spectrometer (Bruker Analytik, GMBH Bremen, Germany) equipped with a nitrogen

laser (337nm). This instrument was fitted with a manual probe assembly, a single-stage acceleration source and a two-stage 'gridless' reflectron. The accelerating voltage was set at 19.5kV for all experiments. For normal MALDI experiments, the reflectron voltage was set at 20.0kV. Ions were detected at the end of the field-free region using dual-micro channel plate detectors and the pressure in the source chamber was≤ 3.5 x 10^{-6} Torr. MALDI spectra were generally collected prior to all post-source decay experiments in order to confirm that the mass of the parent ion was as expected.

Calibration of MALDI spectra was carried out using a PEG standard (Mn value 1470, polydispersity ≤1.1, Polymer Laboratories, UK.) The most abundant isotope of several sodium adducts were used over a suitable mass range (700-1600), similar to that of the samples under investigation. This calibration procedure ensured that the uncertainty in m/z measurements of all of the parent ions was ≤0.5 Da.

Sample Preparation for PEG Standard

The sample was diluted in an acetone/water mix (1:4) such that the solution contained 3-5mg of polymer per ml of solvent (~10-3M). An aqueous solution of sodium chloride(10µl, 0.1M) was used to dope the polymer solution (0.5ml) and this solution was mixed 1:1 with the matrix solution (2,5 DHB, 0.1M in acetone/water, 1:4). 2µl of the resulting mixture was spotted onto the sample slide and dried off slowly in a stream of warm air.

5.2.1.1 Parent Ion Selection

PSD analysis on this instrument involved selecting a parent ion of interest using an ion gate of variable time-width and optimising the transmission of the parent. In the case of polymer experiments, the difficulty was in selecting a suitable time-width which gave optimum transmission without the selection of neighbouring oligomer ions.

The time at which the ion gate pulse was switched on had to be calculated. The mass of the parent ion was converted in to time units using the software available, and the approximate time of the ion gate pulse was calculated using the following formula .

$$t_i = C * t_m$$

C is a constant defined by instrumental parameters (0.28), t_i is the start time of the pulse and t_m is the flight time of the parent ion.

The duration of the ion gate pulse was controlled by the user but was defined by the software to have a minimum value of 100 ns.

Each PSD spectrum was collected over 20 reflectron voltages in the range 0.68-20.0kV. A segment of the spectrum was collected at each voltage which covered a specific mass range, depending on the mass of the parent ion, M_{parent}.

$$M^i_{min} = U^i_{ref} / U^o_{ref} * PSD_{low} * M_{parent} * 100$$
$$M^i_{max} = U^i_{ref} / U^o_{ref} * PSD_{hi} * M_{parent} * 100$$

M^i_{min} / M^i_{max} is the mass range of the *i th* segment

U^i_{ref} is the reflectron voltage of the *ith* segment

U^o_{ref} is the reflectron voltage of the first segment

PSD_{low} and PSD_{hi} are constants with values 0.7 and 1.05 respectively

5.2.1.2 Calibration of Post-Source Decay Data

Calibration of each post-source decay segment was carried out using standard compounds whose fragmentation patterns have been characterised. In this case, Angiotensin II was chosen since it formed many intense fragments within the mass range of the samples of interest.

Calibrant Preparation

An aqueous solution of Angiotensin II (10-4M) was mixed in a 1:1 ratio with a solution of alpha-cyano hydroxycinnamic acid (10-1M in 25% acetonitrile/ 75 %water). 2µl of this mixture was spotted on the sample slide and the solvent was slowly evaporated off in a stream of warm air.

Figure 5.1 shows how the reflectron voltage varied with segment number.

Figure 5.1

Plot to Show How Reflectron Voltage Varied with Segment Number

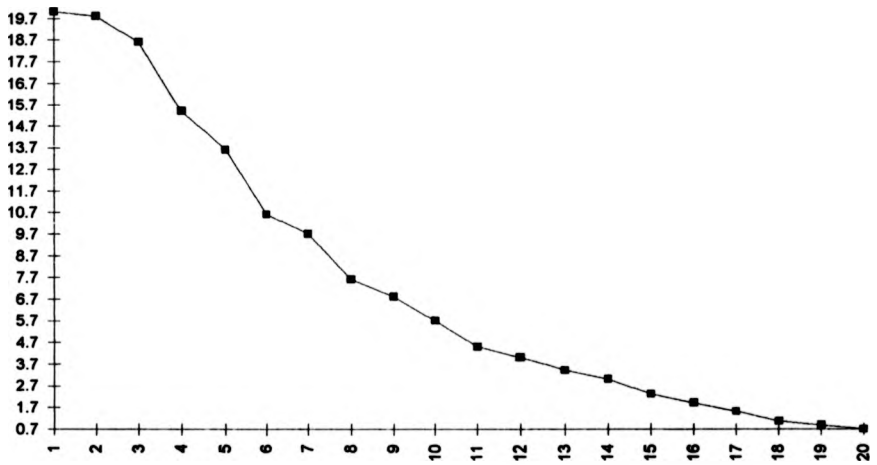

The accelerating voltage was kept constant at 19.5 kV and the laser power was optimised so that the intensity of fragment ions was maximised. This typically corresponded to an increase of upto 50% above the threshold value.

Figure 5.2 shows a calibration spectrum of Angiotensin II collected over the maximum range of voltages.

Figure 5.2

Typical PSD Spectrum of Angiotensin II Collected Over Twenty Reflectron Voltages

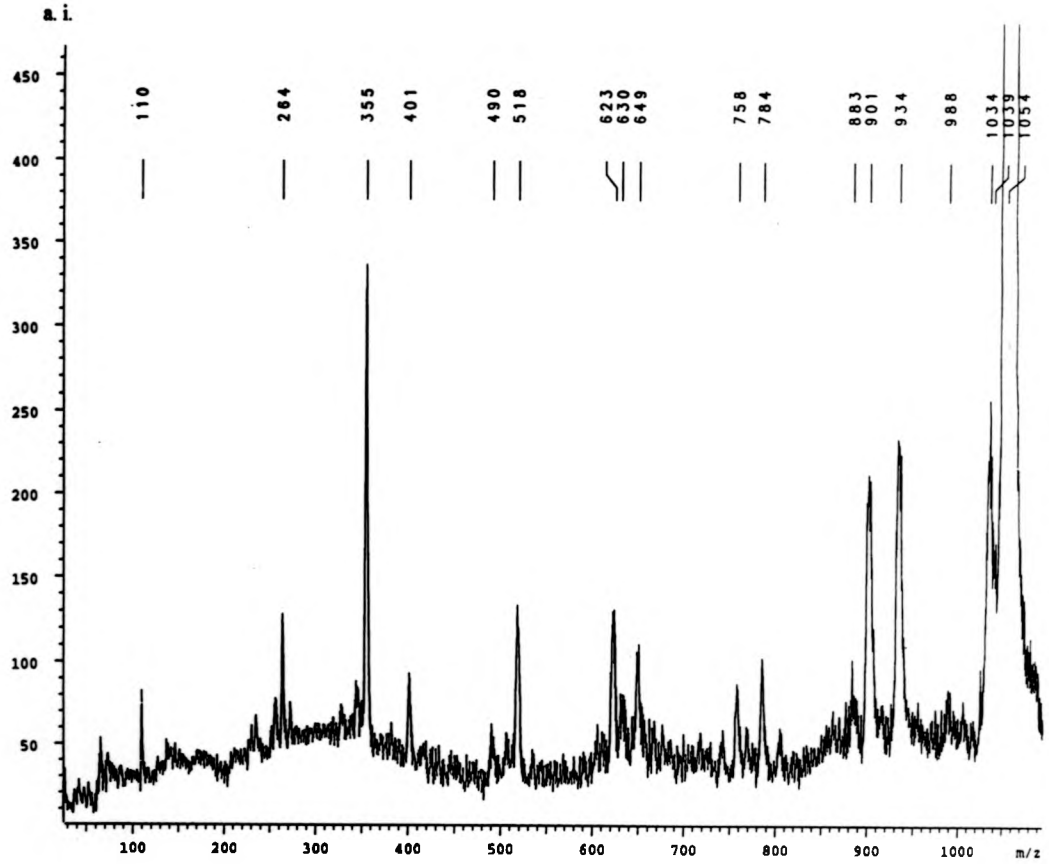

The amino-acid sequence of Angiotensin II is Asp-Arg-Val-Ile-His-Pro-Phe The majority of fragments formed by post-source decay processes are a and b type fragment ions.[117]

5.2.2 Post-Source Decay Experiments on Polymers

5.2.2.1 Optimisation of PSD Conditions using PEG

PEG was adopted as a standard to optimise post-source decay conditions since it formed a reproducible series of intense peaks separated by 44 amu, a value which was suitably close to the poly(isobutylene) monomer mass separation of 56 amu.

The sample was prepared in the way described for standard calibration of the instrument.

Figure 5.3 depicts a normal MALDI-TOF mass spectrum of a PEG SEC standard (Mn = 1470, polydispersity index ≤ 1.1, Polymer Laboratories, UK). The peaks represented the sodium adducts. The molecule ion at m/z = 1450 (32 monomers, Na+ adduct) was chosen as the most suitable to study since it was the most intense peak in the distribution.

Ion Gate Tuning

In the case of PEG, the maximum signal for the parent ion was obtained using a 300 ns pulse width and the pulse start time was set at 11300 ns for m/z = 1450. It was observed that smaller pulse widths resulted in decreased signals, whereas, increased pulse widths resulted in unwanted neighbouring oligomer ions passing through the ion gate.

Laser Energies

It was observed that the best intensities and signal-to-noise values were obtained, when the laser power was increased as the reflectron voltage was stepped down. All data for any given segment were collected at a constant laser energy.

Figure 5.3

Typical MALDI Spectrum of a Polymer (PEG) Obtained Using a Bruker Biflex Instrument

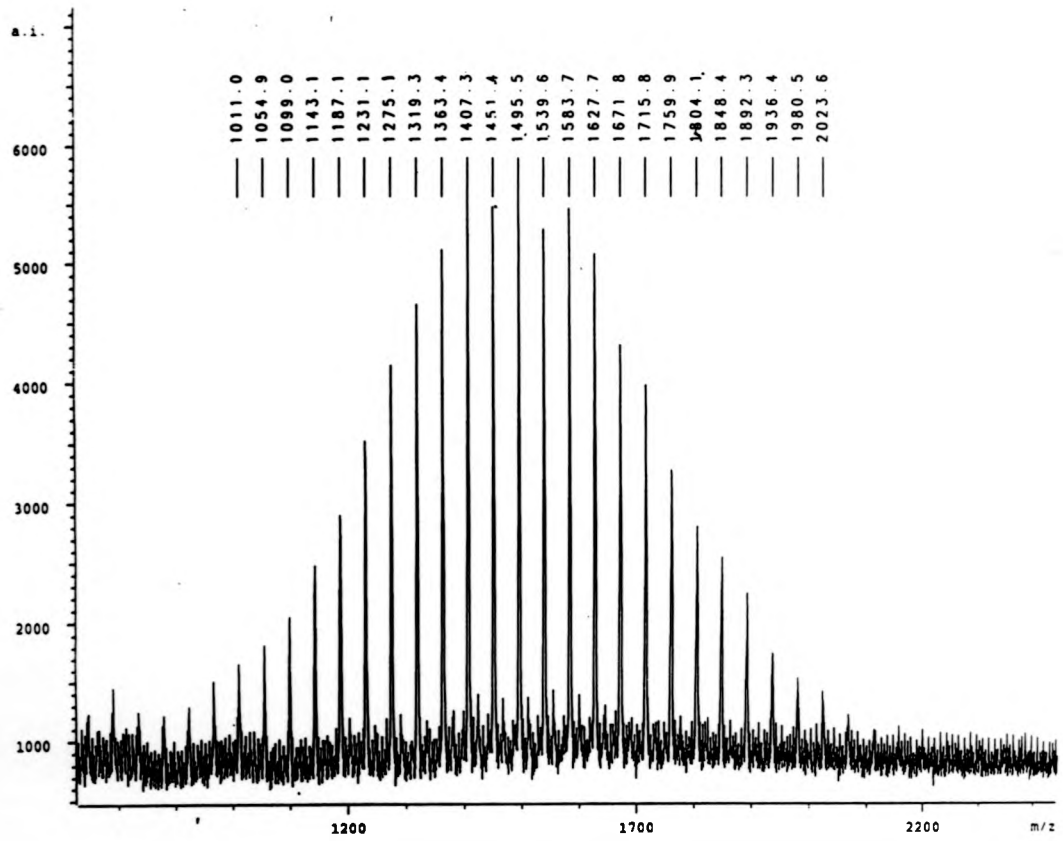

10 laser shots were fired before the position of the laser was moved a specific distance across the sample spot. 50 laser shots of data were collected at each reflectron voltage.

Figure 5.4 shows how the laser energy was increased as the reflectron voltages were decreased for the PEG PSD spectra collected. At each reflectron voltage, the laser power density has an associated error value which represents ≤ 5 % of the total laser power density. A linear regression has been carried out on this data set and the red line plotted represents the best fit of this function. Its gradient gives an approximate measure of the change in laser power required to form and detect ions formed by PSD processes. This value has been calculated for all samples studied by PSD to enable comparisons to be made.

Figure 5.5 shows a typical PSD spectrum of PEG.

Figure 5.6 summarises PSD data obtained for the PEG 1451 oligomer ion.

Fragment Ion Assignment

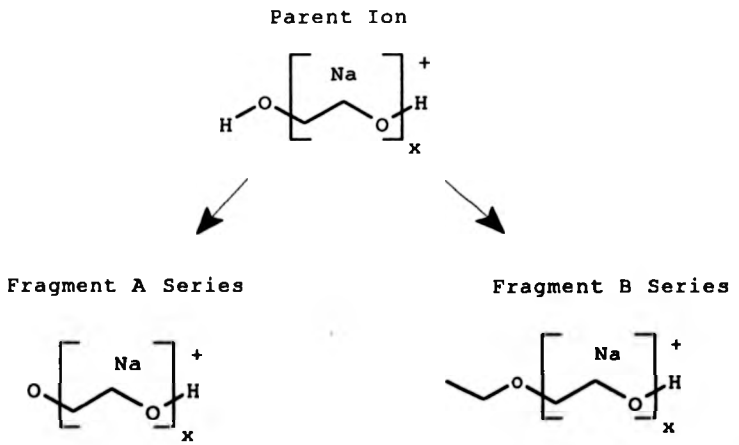

Fragment Series A corresponds to the loss of a hydrogen end-group, whereas, Fragment Series B corresponds to the loss of a hydroxyl function. The difference in mass between the two fragment ion series is 16 mass units.

Figure 5.4

Plot to Show How the Average Laser Power Density Increased as Reflectron Voltages Decreased for PEG Post-Source Decay Investigations

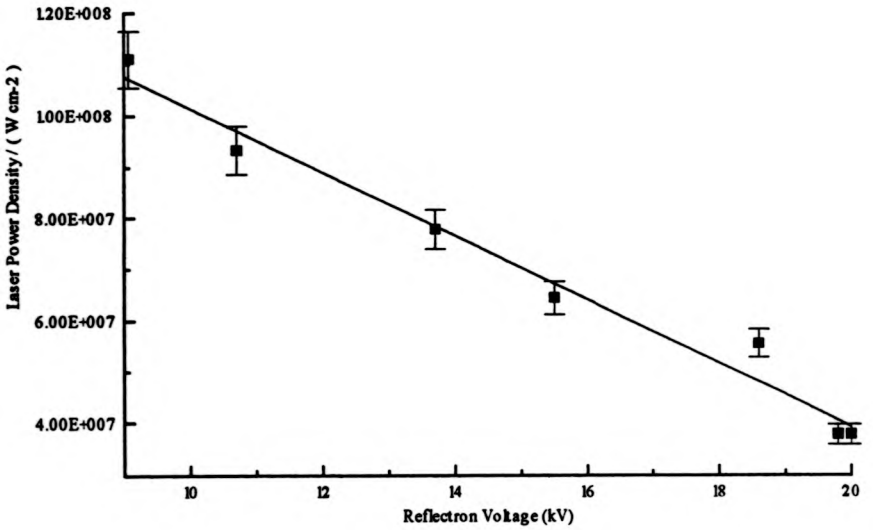

Linear Regression Statistics

$Y = A + B * X$

$A = 1.63E+08 W/cm^2$ $B = 6.21 \times 10^6 W/cm^2 kV^{-1}$

Figure 5.5

Typical PSD Spectrum of PEG (collected over 7 segments only)

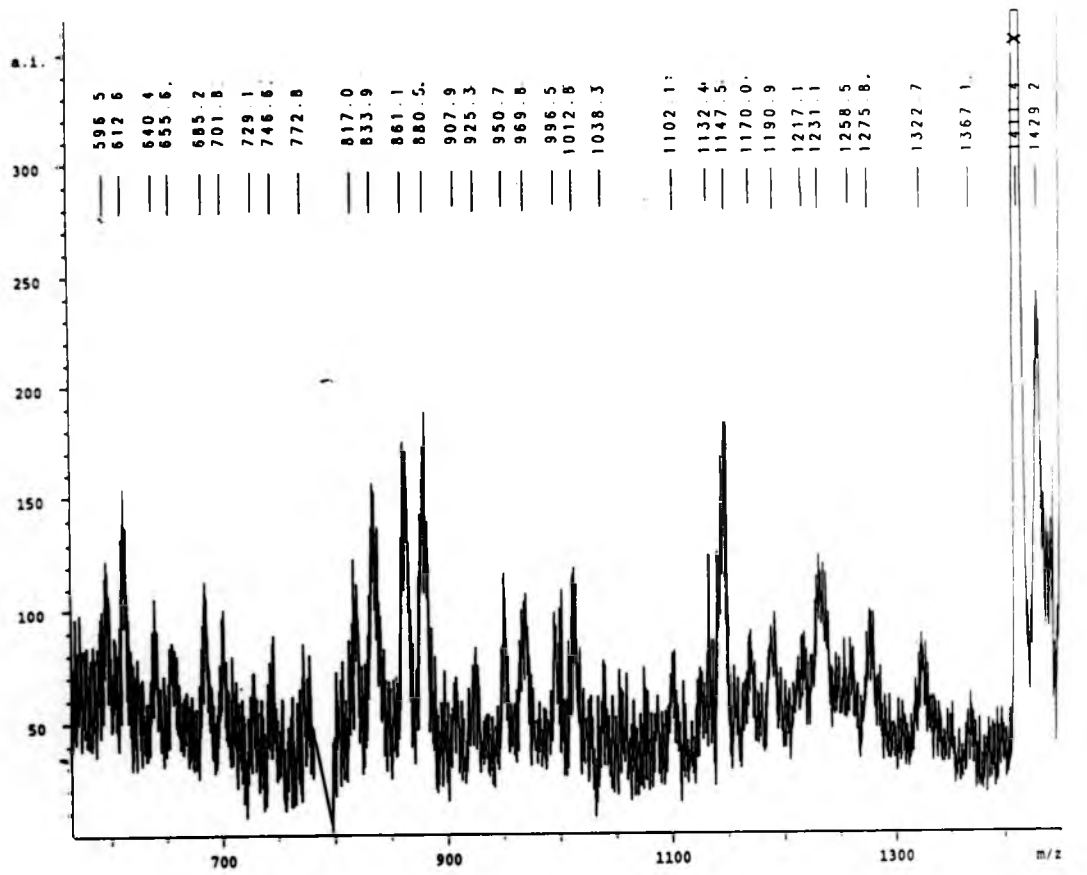

Figure 5.6
Summary of Fragment Ion Masses Observed for a Series of Repeat Experiments Performed on PEG m/z =1450 Parent Ion

Fragment Ion Mass				*Neutral Loss*				*Average Loss*	*Error*	*Assignment*
m1	*m2*	*m3*	*m4*	*l1*	*l2*	*l3*	*l4*	*l (av)*	*std dev*	
1411.7	1408.8	1411.4	1410.5	39.7	42.6	40.0	40.9	40.8	1.3	A
1367.9	1367.5	1367.1		83.5	83.9	84.3		83.9	0.4	A
1322.6		1322.7	1322.7	128.8		128.7	128.7	128.7	0.1	A
1277.6	1278.2	1275.8	1277.6	173.8	173.2	175.6	173.8	174.1	1.0	A
1143.7	1143.7	1147.5	1143.1	307.7	307.7	303.9	308.3	306.9	2.0	A
1039.9	1039.9	1038.3	1038.5	411.5	411.5	413.1	412.9	412.3	0.9	B
1011.3	1011.3	1012.8	1011.0	440.1	440.1	438.6	440.4	439.8	0.8	A
995.6	995.6	996.5	995.1	455.8	455.8	454.9	456.3	455.7	0.6	B
964.9	964.9	969.8	966.3	486.5	486.5	481.6	485.1	484.9	2.3	A
950.5	950.5	950.7		500.9	500.9	500.7		500.8	0.1	B
922.3	922.3	925.3	922.0	529.1	529.1	526.1	529.4	528.4	1.6	A
906.1	906.1	907.9	905.7	545.3	545.3	543.5	545.7	545.0	1.0	B
878.1	878.1	880.5	879.4	573.3	573.3	570.9	572.0	572.4	1.2	A
862.0	862.0	861.1	863.3	589.4	589.4	590.3	588.1	589.3	0.9	B

At low mass losses, mass assignments were difficult to make with any degree of accuracy. Series A, should, in fact, have low mass losses of 44, 88, 132 Da etc. The masses quoted are lower than those expected although high mass losses can be assigned with a higher degree of confidence to the structures depicted earlier. The justification of the assignments made lies in the structure of the PSD spectra collected. In all cases, pairs of ions separated by 16 +/-2 Da were observed throughout each spectrum.

Constant Laser Energy PSD Spectra

A series of experiments were performed to assess whether it was possible to collect data using the same laser power for all of the reflectron voltages. These spectra were found to be of poor quality containing many broad peaks. No structural information was derived from these spectra.

5.2.2.2 Poly(styrene)

Further experiments were performed using a poly(styrene) SEC standard (Mn = 1320 Da, polydispersity index ≤1.1, Polymer Laboratories, UK).

Sample Preparation

The standard was diluted in THF such that the solution contained 3-5 mg sample per ml. A solution of silver tri-fluoroacetate (20µl, 0.1M) was used to dope the analyte solution (20µl) and the resulting mixture was mixed 1:1 with the matrix solution (9-nitroanthracene 0.1M inTHF)). 2µl of the sample preparation was spotted onto the sample slide and the solvents evaporated off in a stream of warm air.

A normal MALDI spectrum was collected in the same way as for PEG and the mass accuracy of each oligomer ion was checked. A silver-adduct at 1207 Da(10 monomer units) was chosen as a suitable parent ion since it was one of the most intense in the polymer distribution.

Ion Gate Tuning

Post-source decay experiments were performed in the same way as described for PEG although poly(styrene) parent ions were easier to tune than the PEG ions since the monomer mass unit of the polymer is larger (104 Da). A 300 ns pulse-width was used and this allowed selection of the parent ion without permitting unwanted neighbouring oligomer ions to pass through the ion gate.

Laser Energies

The best intensities and signal-to-noise values obtained when the laser power was increased as the reflectron voltage was stepped down. Data were collected in the way described previously.

Figure 5.7a shows how the laser energy was increased as the reflectron voltages were decreased for the poly(styrene) PSD spectra. This plot includes measurements made at all reflectron voltages. At each reflectron voltage, the laser power density has an associated error value which represents ≤ 5 % of the total laser power density. **Figure 5.7b** shows how the laser power density function changed increased upto its maximum value and a linear regression of the data set has been performed in the way described for PEG.

Figure 5.8 shows a typical PSD spectrum of the poly(styrene) oligomer ion m /z = 1207 Da collected over 18 reflectron voltages

Figure 5.9 summarises PSD data obtained for the 1207 oligomer ion (Ag+ attached) Assignments of poly(styrene) fragment ions formed by PSD processes were made tentatively. A and B type fragment ions were observed . Series A was formed by the neutral loss of hydrogen plus a number of monomer units, whereas, series B was formed by the loss of the butyl end-group plus a number of monomer units. A third series was detected, labelled Series C in **Figure 5.9.**

Figure 5.7 a

Plot to Show How Average Laser Power Density Increased as the Reflectron Voltage Decreased for Poly(styrene) PSD Data (All Segments)

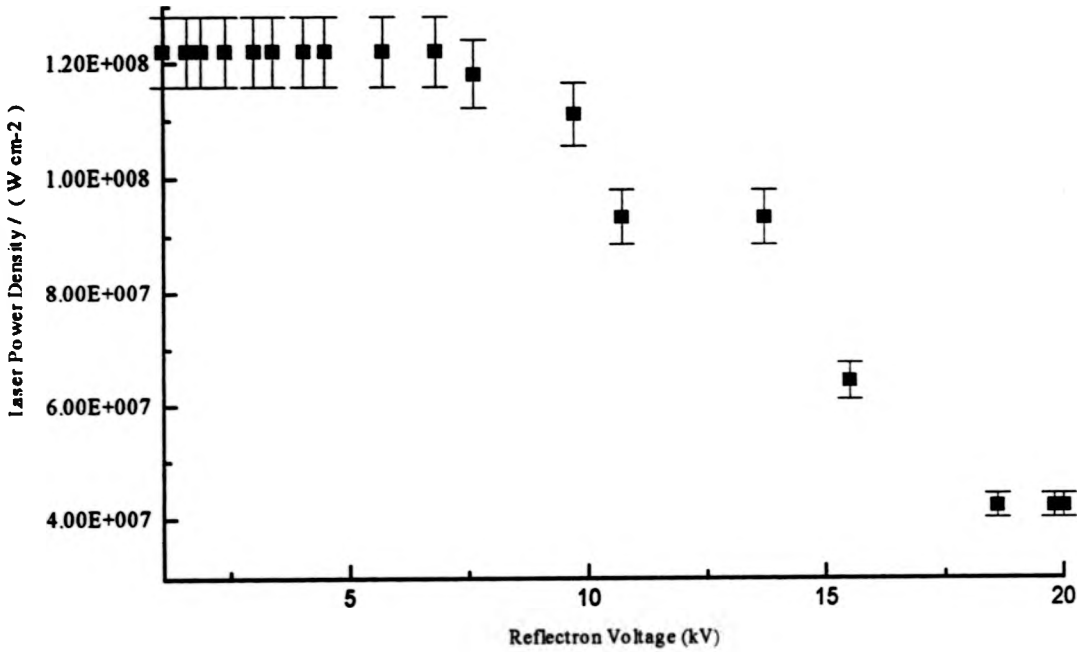

Each error bar represents the maximum possible in the measured laser power density.

Figure 5.7b:
Plot to Show How Average Laser Power Density Increased upto its Maximum Value as the Reflectron Voltage Decreased for Poly(styrene) PSD

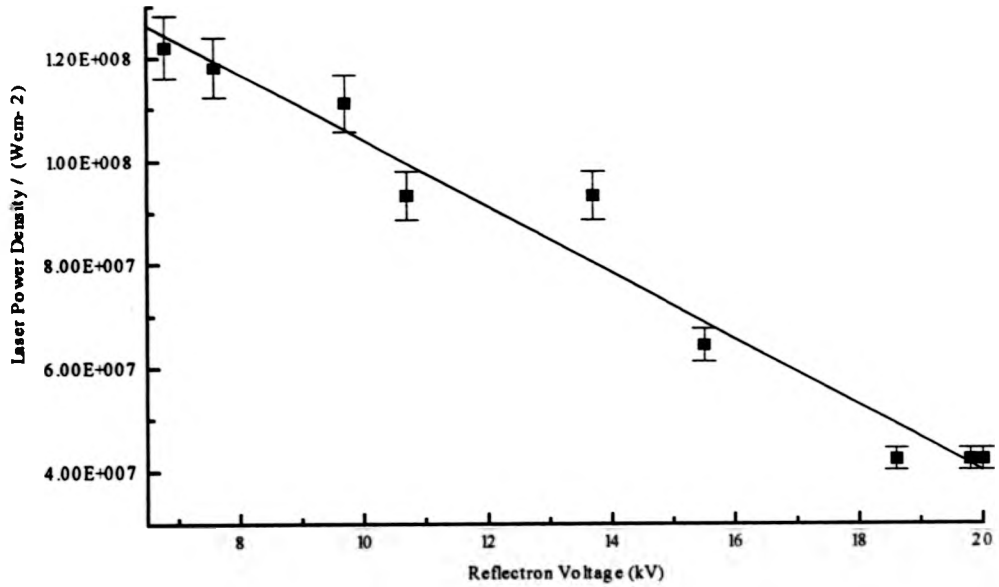

Each error bar represents the maximum possible in the measured laser power density

Linear Regression Statistics

$Y = A + B * X$

A= 1.68E+008 W/cm^2 B=-6.39 x 10^6 Wcm^{-2} kV^{-1}

Figure 5.8

Typical PSD Spectrum of Poly(styrene)

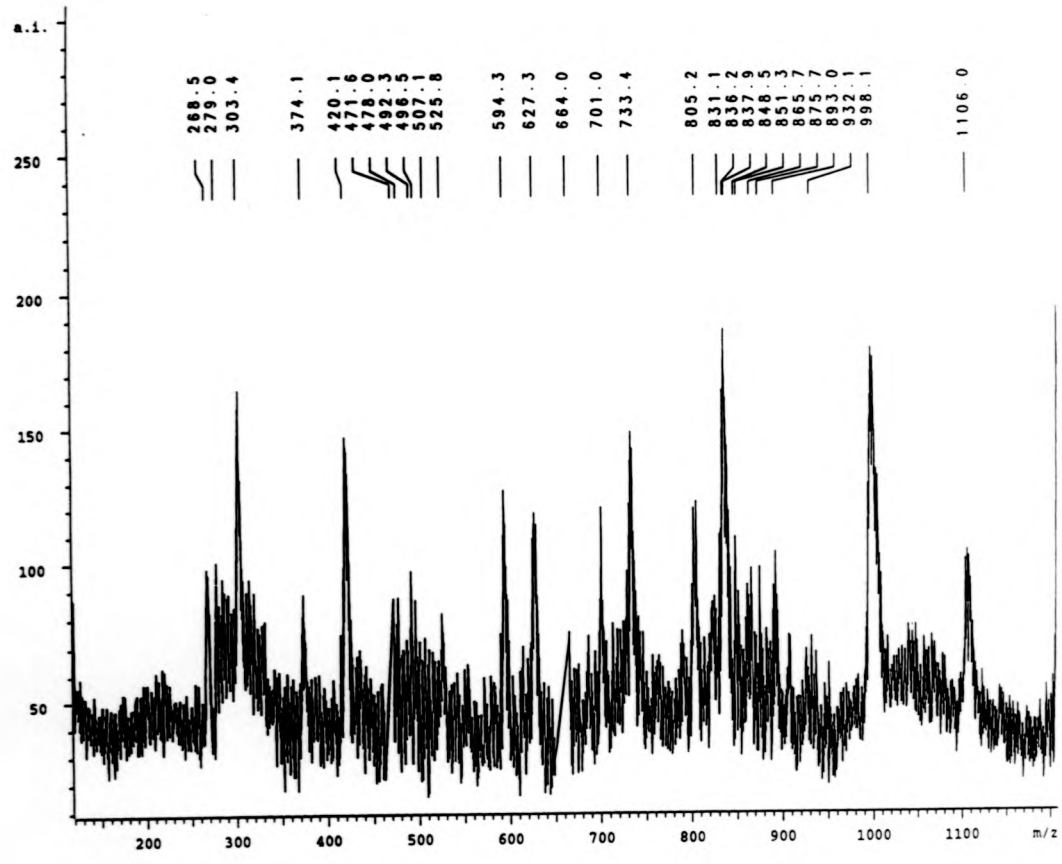

Figure 5.9

Summary of Fragment Ion Masses Observed for a Series of Repeat Experiments Performed on Poly(styrene) m/z= 1207 Parent Ion

Fragment Ion Mass			*Neutral Loss*			*Average Loss*	*Error*	*Assignment*
m1	*m2*	*m3*	*l1*	*l2*	*l3*	*lav*	*std dev*	
1106.7	1105.4	1106.9	100.7	102	100.5	101.1	0.6	A
836.6	837.4	839.4	370.8	370	368	369.6	1.1	B
792.6	790.2		414.8	417.2		416	1.2	A
762.7	764.1	764.2	444.7	443.3	443.2	443.7	0.6	
734.4	733.2	733.2	473	474.2	474.2	473.8	0.5	B
701.3	700.2	699.1	506.1	507.2	508.3	507.2	0.7	C
	628.5	629.5		578.9	577.9	578.4	0.5	B
595.8	594.6	596.8	611.6	612.8	610.6	611.7	0.8	C
553.8	553.8		653.6	653.6		653.6	0	
525.4	526.8	525.9	682	680.6	681.5	681.4	0.5	B
491.4		491.2	716		716.2	716.1	0.1	C
420.7	419.7	422.3	786.7	787.7	785.1	786.5	0.9	B
366	364	366.1	841.4	843.4	841.3	842	0.9	A
303.9	302.5	302.7	903.5	904.9	904.7	904.4	0.6	

Fragment Ion Assignment

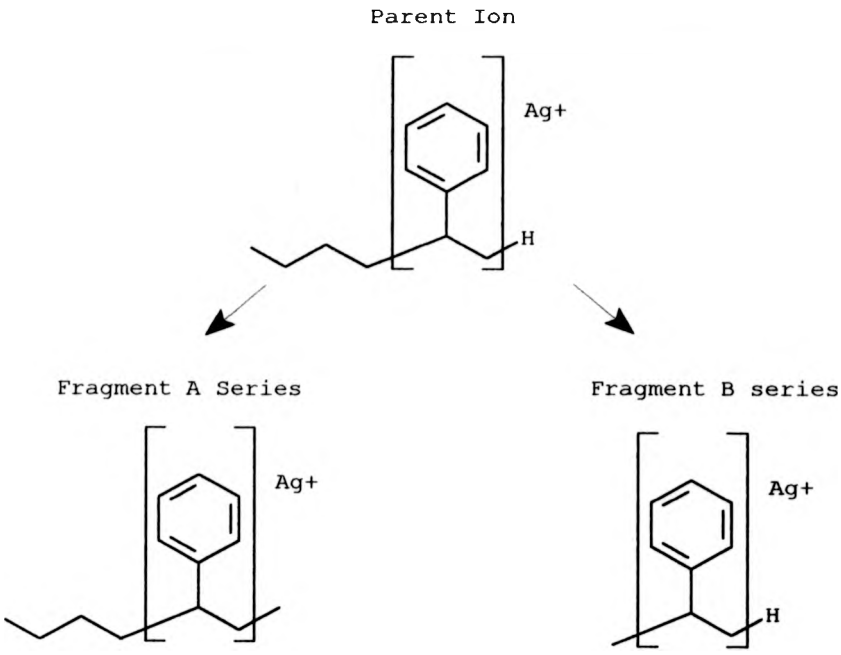

Given the inherent poor resolution of this technique and the problems with mass assignment as described for PEG, it was impossible to assign a structure to series C with any degree of certainty. However, each peak in the series was separated by 104 Da which most probably corresponded to a styrene unit. It is likely that such ions in this series are the products of re-arrangement reactions possibly incorporating a McLafferty Re-arrangement. One of the most intense peaks observed in PSD spectra was at m/z = 303.

Peaks at m/z = 764, 554 and 303 have not been structurally assigned. None of these fragment ions fitted a pattern or a series and have, most likely, resulted from side chain fragmentations followed by re-arrangements.

5.2.3 Poly(isobutylene) Fragment Ion Investigations

Three poly(isobutylene) samples were studied using MALDI-TOF MS and PSD. Their structures are shown in **Figure 5.10b** ; their molecular masses were approximately 1000 Da .

Figure 5.10b

Structures of the Poly(isobutylene) Polymers Studied by PSD

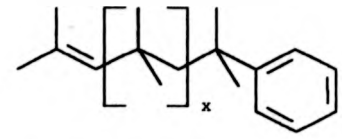

Mono-olefinic Poly(isobutylene)

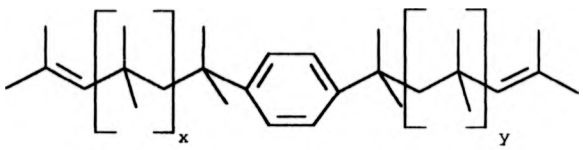

Di-Olefinic Poly(isobutylene)

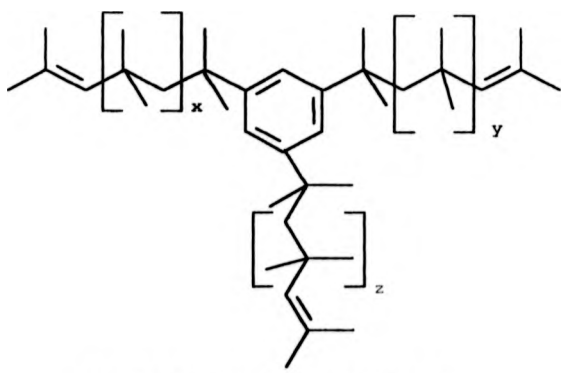

Tri-Olefinic Poly(isobutylene)

PSD analysis required MALDI spectra of high signal-to-noise values to be readily reproduced, and in the case of these samples this meant that special care had to be taken with sample preparation.

PIB Sample Preparation

All three samples were dissolved in THF (3-5 mg per ml) and 100 µl of silver tri-fluoroacetate solution (10^{-1} M in THF) were added to 0.5 ml of polymer solution. The mixture of polymer and silver salt was then mixed in a 1:1 ratio with the matrix solution. (0.1 M 9-nitroanthracene in THF).

The aim of these experiments was to investigate the gas-phase ion chemistry of the species formed by MALDI and to investigate any differences which might occur in their fragmentation patterns. The potential of PSD analysis as applied to synthetic polymers is, therefore,drawn out, and particular attention has been given to the effects of laser power and pressure on the results.

5.2.3.1. Tri-Olefinic PIB Sample

A normal MALDI spectrum was collected and the mass accuracies of each Ag+ adduct was checked. If necessary, a calibration was performed using a PEG standard of similar molecular mass as described previously.

Experimental Conditions

Each PSD spectrum was collected over the full twenty reflectron segments, starting at 20.0kV and decreasing down to 0.68kV. All of the data collected for each individual voltage segment was collected at a constant laser energy. 10 shots were fired before the position of the laser was removed a specific distance along the sample spot. 50 shots of data were collected in each reflectron voltage.

PSD spectra of four oligomer/Ag+ adducts were collected under the conditions stated and compared.

Ion Gate Tuning

Figure 5.11 summaries the conditions under which these spectra were collected.

Figure 5.11

Table Showing the Ion Gate Settings for Each Oligomer Ion Investigated

Mass of adduct	No. of PIB units	Start time (ns)	Pulse width (ns)
867	7	9200	300
923	8	9400	300
979	9	9700	300
1035	10	10000	300

Laser Energies

The same methodology was used for this sample as developed for PEG and poly(styrene) samples, that is, the laser power was increased as the reflectron voltage was stepped down.

Figure 5.12a shows how the laser energy was increased as the reflectron voltages were decreased for tri-olefinic poly(isobutylene) PSD spectra and includes measurements made at all reflectron voltages. **Figure 5.12b** shows how the laser power density function increased upto its maximum value and a linear regression of the data set has been performed in the way described for PEG.

A typical PSD spectrum is depicted in **Figure 5.13 and Figure 5.14** compares the PSD spectra of four tri-olefinic polymer ions containing 7, 8, 9 and 10 PIB units respectively.

Figure 5.15 summarises the fragment ions observed for each of the oligomers studied. Fragment ion assignments are depicted in **Figure 5.16a.** Each series is indicated on a typical PSD spectrum as shown in **Figure 5.16b.**

Figure 5.12a

Plot to Show How Average Laser Power Density Increased as the Voltage Decreased for PSD Analysis of the Tri-Olefinic PIB Sample (All Segments)

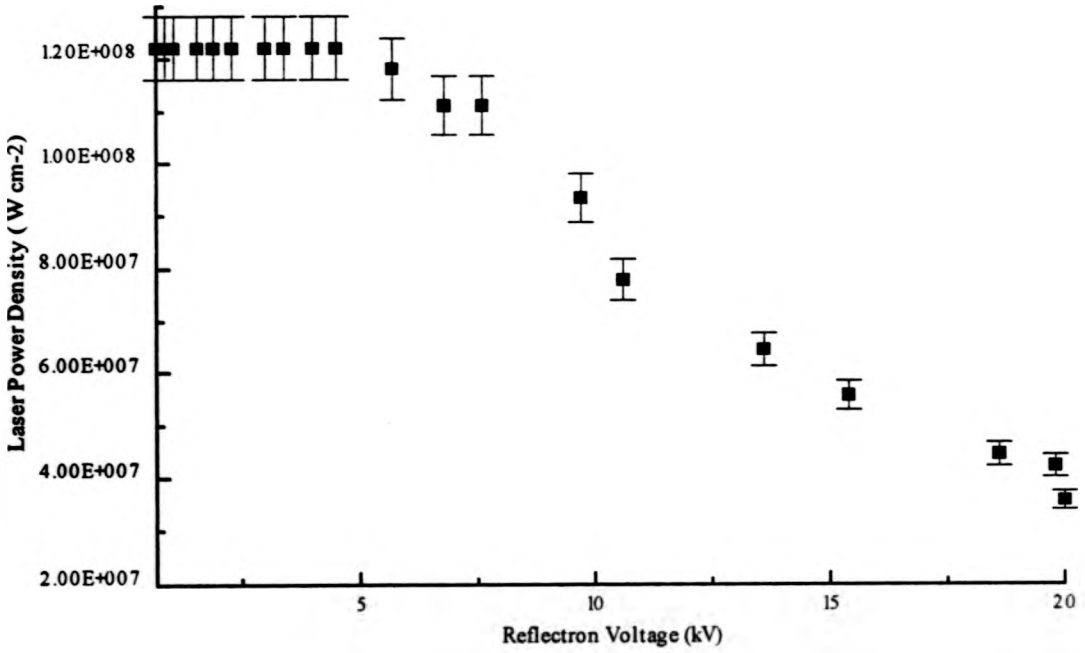

Each error bar represents the maximum possible in the measured laser power density.

Figure 5.12b

Plot to Show How Average Laser Power Density Increased as the Voltage Decreased for PSD Analysis of the Tri-Olefinic PIB Sample

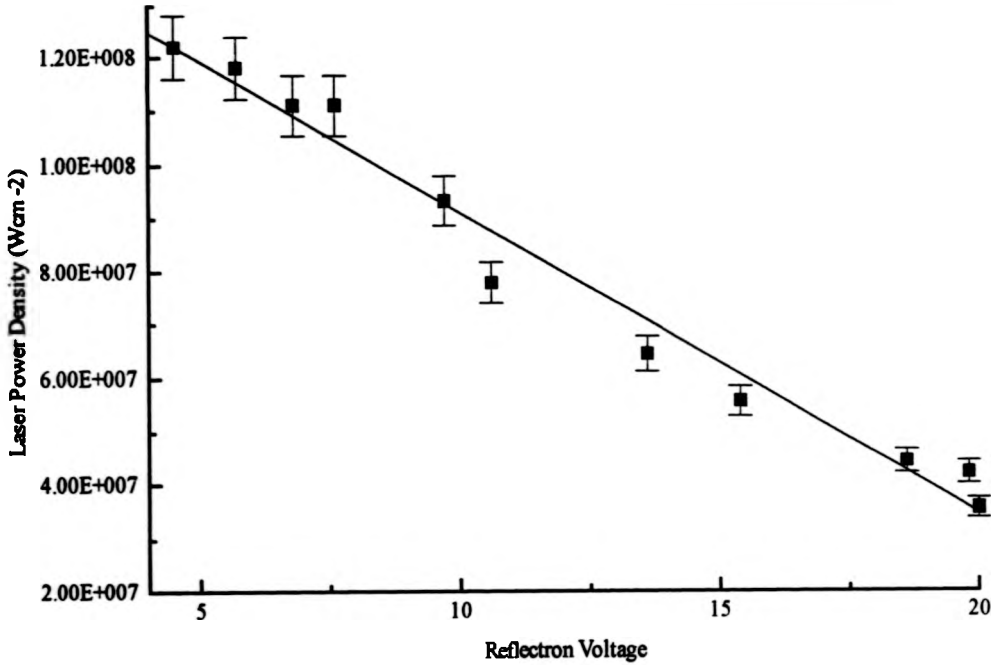

Linear Regression Statistics

$Y = A + B * X$

$A=1.47E+08 W/cm^2$ $B= -5637734 Wcm^{-2} kV^{-1}$

Figure 5.13

PSD Spectrum of the Tri-Olefinic 923.3 Oligomer Ion (Ag+ attached)

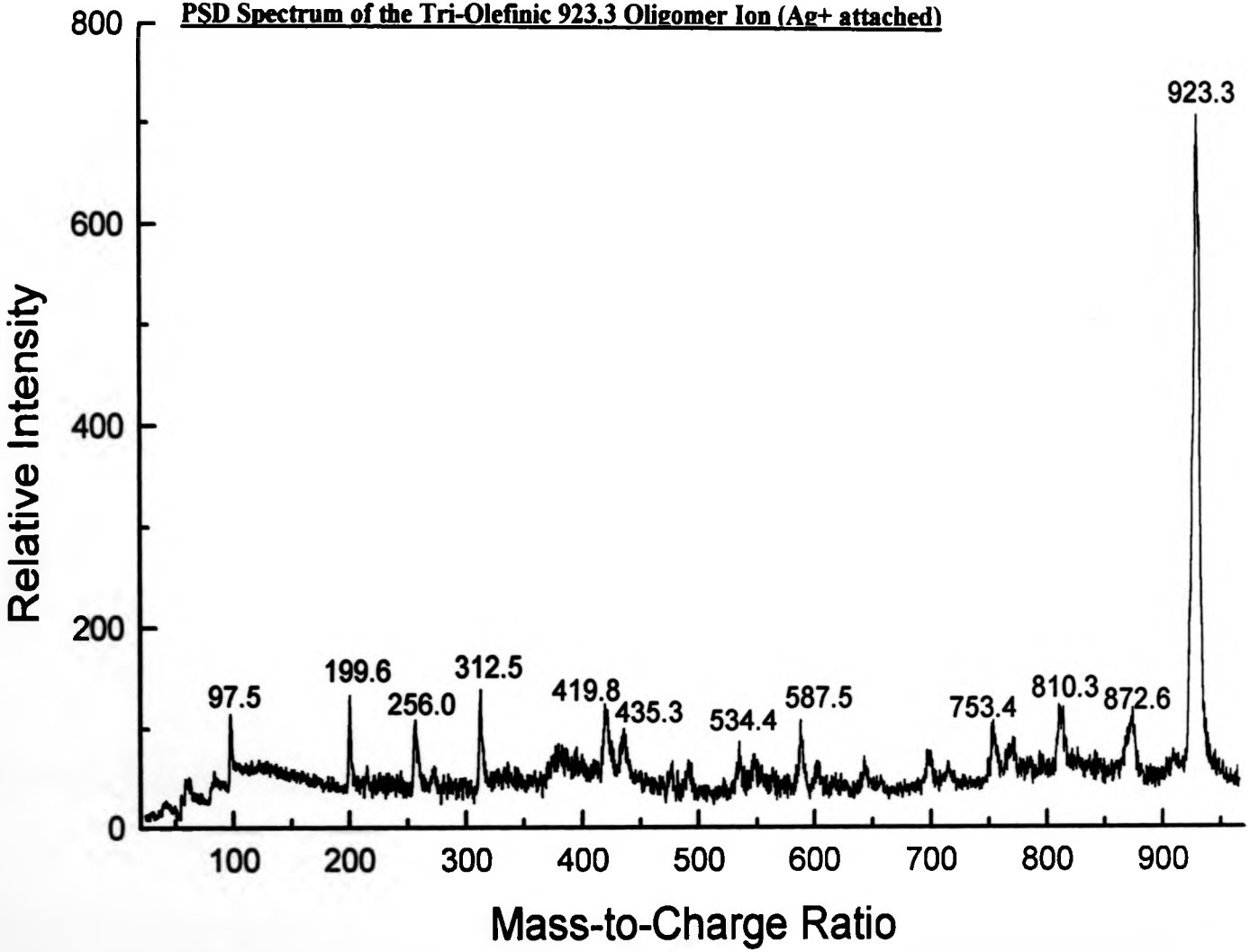

Figure 5.14

Comparison of PSD Spectra for Four Different Molecule Ions from the Tri-Olefinic Sample

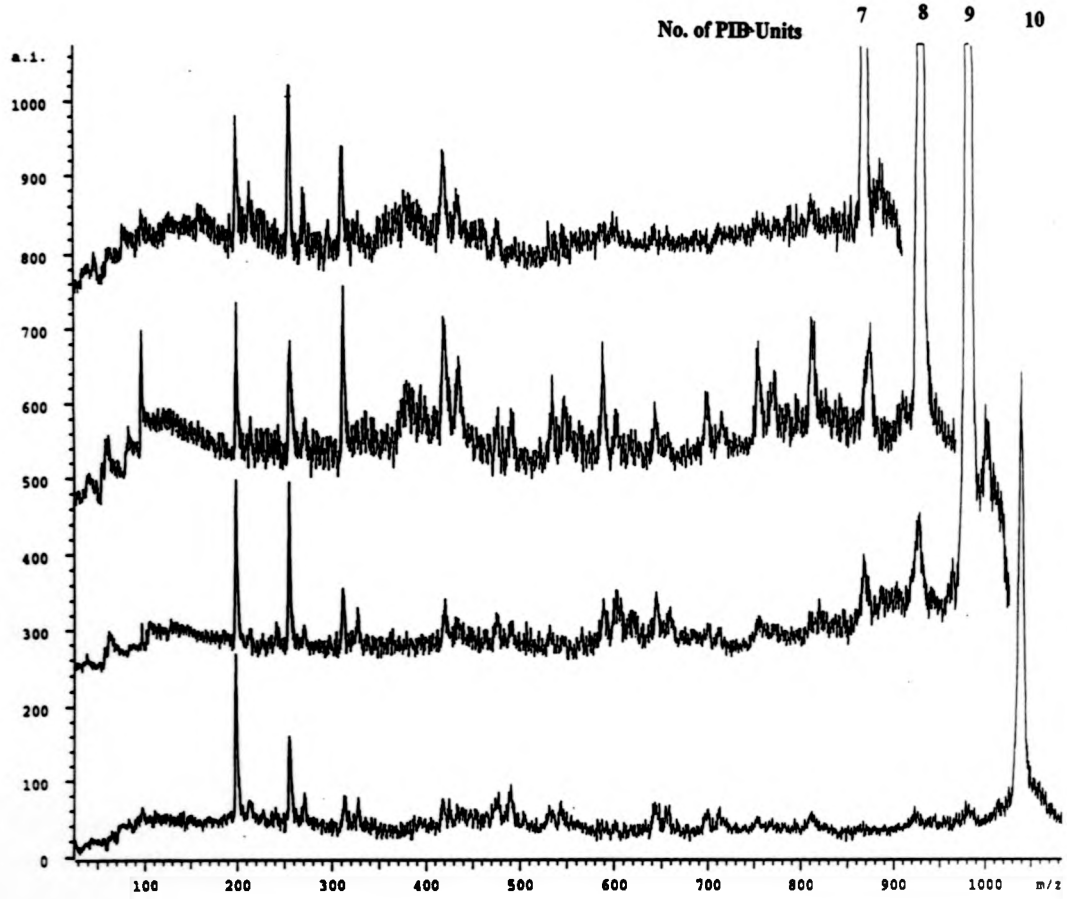

Figure 5.15

Summary of PSD Fragments of Tri-Olefinic PIB Ions

Parent	Fragment	Neutral	Parent	Fragment	Neutral	Parent	Fragment	Neutral	Parent	Fragment	Neutral
1035.4	979.5	55.9	979.4	963.3	16.1						
1035.4	883.1	152.3	979.4	939.8	39.6	923.3	872.6	50.7			
1035.4	868.2	167.2	979.4	926.1	53.3	923.3	810.3	113	867.2	852.6	14.6
1035.4	842.1	193.3	979.4	902.1	77.3	923.3	769.6	153.7	867.2	810.2	57
1035.4	754.8	280.6	979.4	886.3	93.1	923.3	753.4	169.9	867.2	598.3	268.9
1035.4	739.2	296.2	979.4	867	112.4	923.3	696.2	227.1	867.2	529.9	337.3
1035.4	714.4	321	979.4	844.6	134.8	923.3	642.6	280.7	867.2	475.1	392.1
1035.4	697.1	338.3	979.4	818.8	160.6	923.3	601.3	322	867.2	433.5	433.7
1035.4	681.7	353.7	979.4	754.3	225.1	923.3	587.5	335.8	867.2	418.4	448.8
1035.4	658.9	376.5	979.4	712.2	267.2	923.3	547.4	375.9	867.2	376.8	490.4
1035.4	649.2	386.2	979.4	700	279.4	923.3	534.3	389	867.2	367.3	499.9
1035.4	492	543.4	979.4	658.8	320.6	923.3	490.5	432.8	867.2	327.8	539.4
1035.4	333.2	702.2	979.4	644.2	335.2	923.3	477	446.3	867.2	312	555.2
1035.4	271	764.4	979.4	619.3	360.1	923.3	435.3	488	867.2	310.3	556.9
1035.4	199.5	835.9	979.4	603.7	375.7	923.3	419.8	503.5	867.2	271.6	595.6
			979.4	589	390.4	923.3	394.7	528.6	867.2	269.9	597.3
			979.4	565.9	413.5	923.3	379.5	543.8	867.2	255.2	612
			979.4	531.9	447.5	923.3	312.5	610.8	867.2	213.7	653.5
			979.4	507.1	472.3	923.3	271.8	651.5	867.2	199.3	667.9
			979.4	475.3	504.1	923.3	256	667.3	867.2	160.1	707.1
			979.4	432.1	547.3	923.3	246	677.3			
			979.4	420.8	558.6	923.3	198	725.3			
			979.4	327.6	651.8	923.3	97.5	825.8			
			979.4	311.9	667.5						
			979.4	255.5	723.9						
			979.4	242	737.4						
			979.4	199.3	780.1						
			979.4	129.2	850.2						

Figure 5.16a

Structural Assignments of Tri-Olefinic Fragments Ions Observed in PSD Spectra

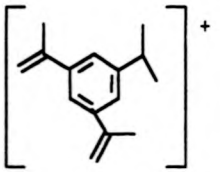

Peak observed at m/z=199, present in all spectra.

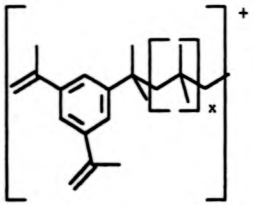

Series A ; These ions belong to a series associated with the base peak and are separated by 56 mass units. Isomers are possible, however, resolution obtained by PSD does not permit unambiguous assignments to be made.

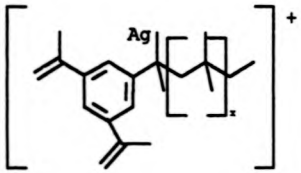

Series B ; Major series observed in PSD spectra which correspond to an end-group unit plus PIB units being lost as neutrals. This species is detected as the silver adduct.

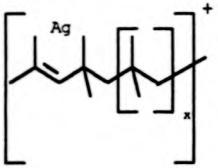

Series C ; Minor series which corresponds to an end-group plus repeat unit ion being formed. This species is detected in the form of a silver adduct.

Figure 5.16b

PSD Spectrum of a Tri-Olefinic Silver Adduct (1035.4, 10 PIB Units) and Assignments

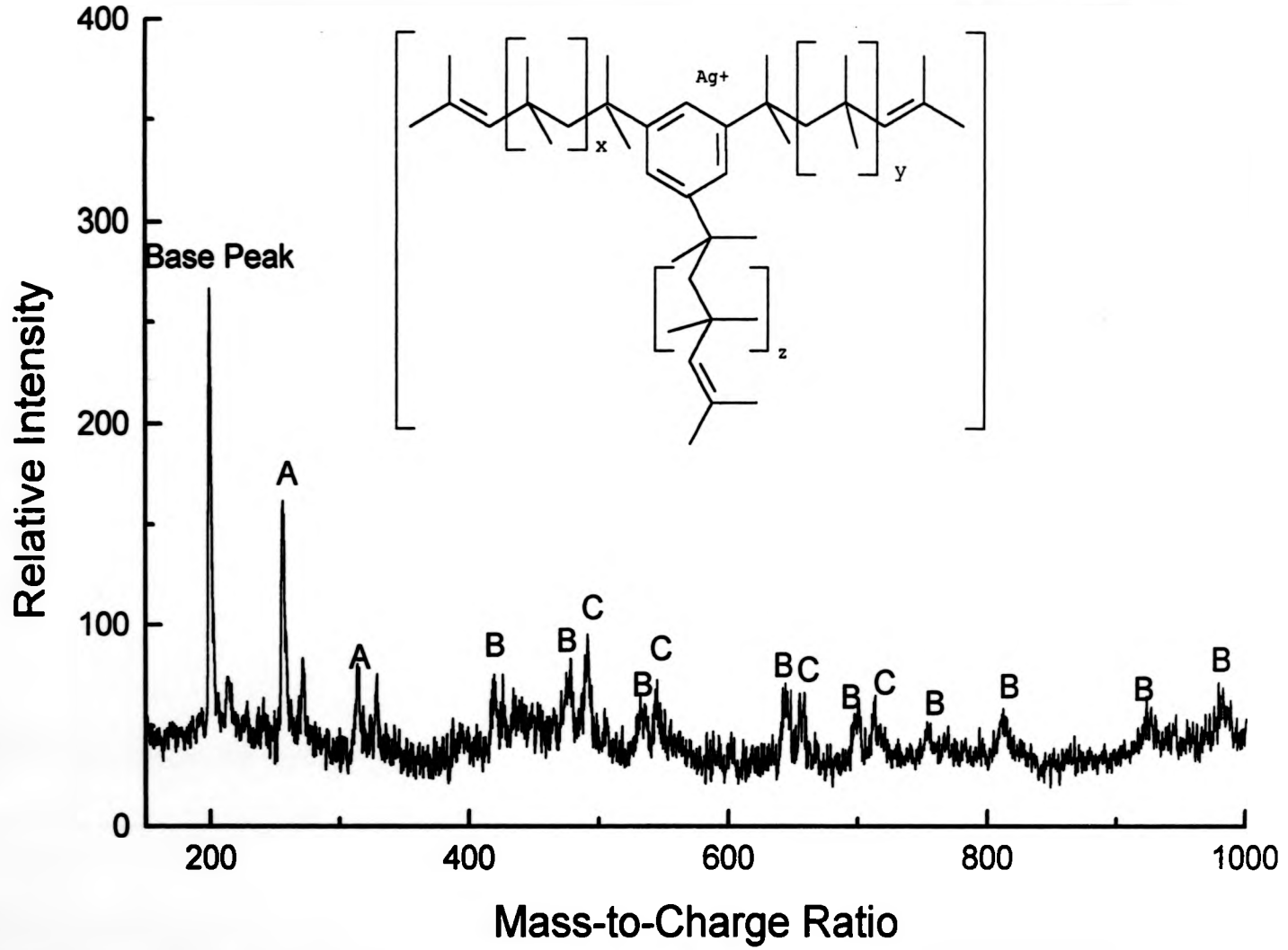

5.2.3.2 Di-Olefinic PIB Sample

A normal MALDI spectrum was collected and the mass accuracies of each Ag+ adduct was checked. A calibration was performed using a PEG standard of similar molecular mass as described previously.

Experimental Conditions

Each PSD spectrum was collected over the full twenty reflectron segments, starting at 20.0kV and decreasing down to 0.68kV. All data for any given segment were collected at a constant laser energy. As the voltage on the reflectron was stepped down, this value was increase as shown in **Figures 5.18a and 5.18b**. 10 shots were fired before the position of the laser was removed a specific distance along the sample spot. 50 shots of data were collected at each reflectron voltage.

PSD spectra of four oligomer/Ag+ adducts were collected under the conditions stated and compared.

Ion Gate Tuning

Figure 5.17 summaries the conditions under which these spectra were collected.

Figure 5.17

Table Showing the Ion Gate Settings for Each Oligomer Ion Investigated

Mass of adduct	No. of PIB units	Start time (ns)	Pulse width (ns)
827	8	9000	300
883	9	9200	300
939	10	9800	300
996	11	10000	300

Laser Energies

The same methodology was used for this sample as developed for PEG and poly(styrene) samples, that is, the laser power was increased as the reflectron voltage was stepped down.

Figure 5.18a as how the laser energy was increased as the reflectron voltages were decreased the di-olefinic poly(isobutylene) PSD spectra and includes measurements made at all reflectron voltages. **Figure 5.18b** shows how the laser power density function increased upto its maximum value and a linear regression of the data set has been performed in the way described for PEG.

A typical PSD spectrum is depicted in **Figure 5.19 and Figure 5.20** compares all four PSD spectra for different molecule ions from the di-olefinic sample.

Figure 5.21 summarises the fragment ions observed for each of the oligomers studied. Fragment ion assignments are depicted in **Figure 5.22a.** Each series is indicated on a typical PSD spectrum as shown in **Figure 5.22b.**

5.2.3.3 Mono-Olefinic PIB Sample

This sample proved to be impossible to analyse using post-source decay techniques. The main problem was the intensities of the parent ions which were up to a factor of 10 weaker than tri-olefinic or di-olefinic parent ions of similar masses.

5.2.4 Effect of Pressure

The pressure, p in the instrument proved to be crucial in determining the quality of PSD data. It was observed that, in general, $1x10^{-6} \geq p \geq 6 \times 10^{-7}$ mbar was required in order to obtain PSD spectra of a reasonable quality. If the pressure in the instrument was outside this range then, either no fragments were detected if the pressure was too low, or if the pressure was too high spectra were too noisy to be able to infer useful structural information. **Figure 5.23** shows how the pressure in the instrument improved during the course of a typical PSD experiment. This meant that only one experiment could be performed before the pressure values were too low.

Figure 5.18a
Plot to Show How Average Laser Power Density Increased as the Reflectron Voltage Decreased for Di-Olefinic PIB PSD Data (All Segments)

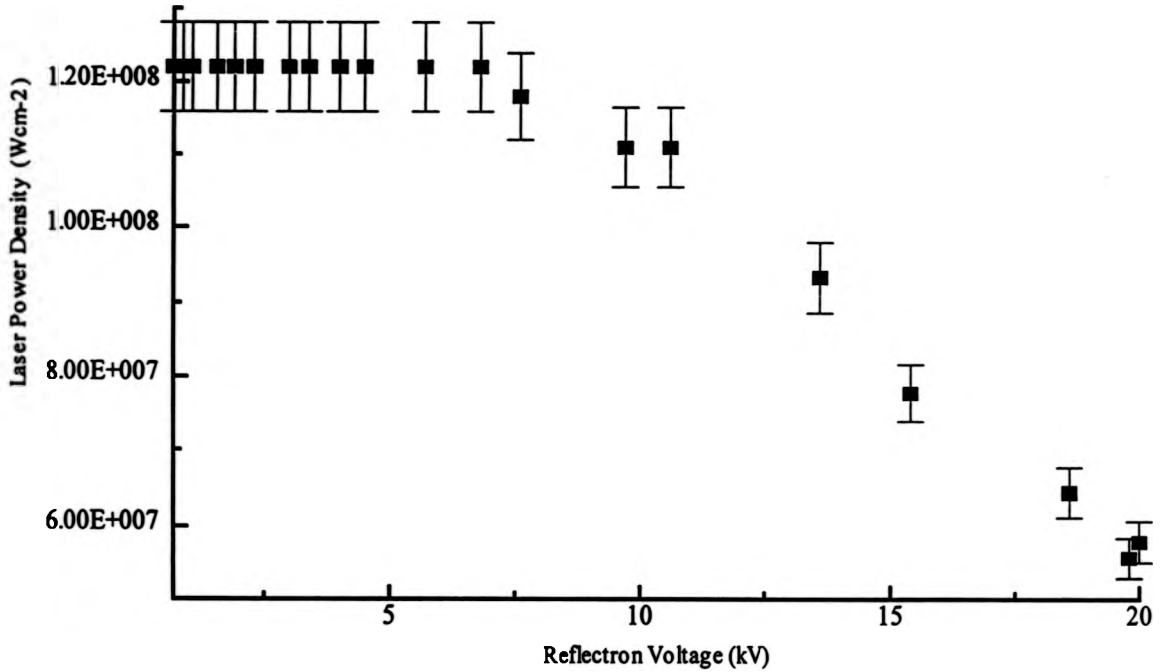

Each error bar represents the uncertainty in the measured laser power density.

Figure 5.18b

Plot to Show How Average Laser Power Density Increased upto its Maximum Value as the Reflectron Voltage Decreased for Di-Olefinic PIB PSD Analysis

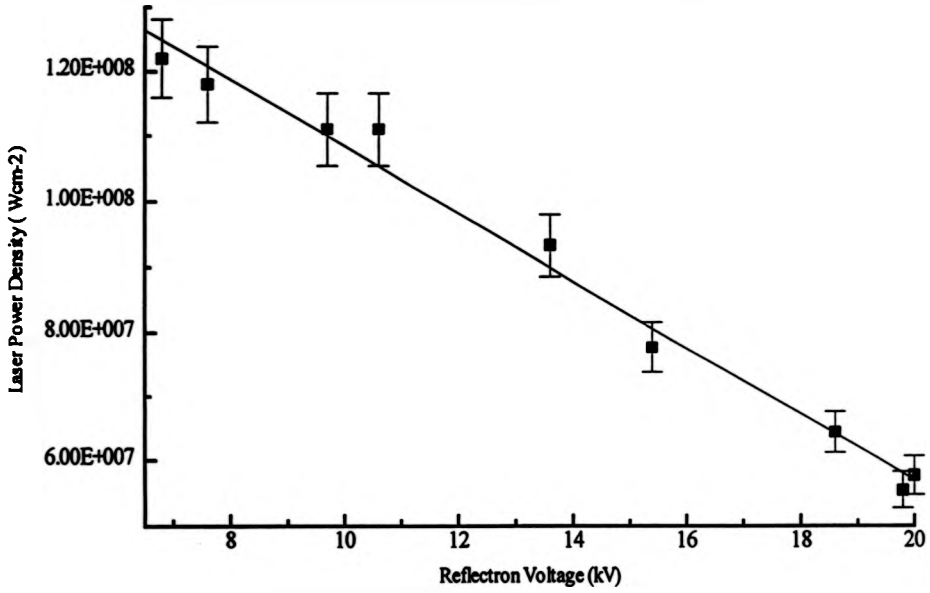

Linear Regression Statistics

$Y = A + B * X$

A= 1.60E+08 W/cm^2 B=-5138387 $Wcm^{-2} kV^{-1}$

Figure 5.19

PSD Spectrum of the Di-Olefinic 939.6 Oligomer Ion (Ag+ attached)

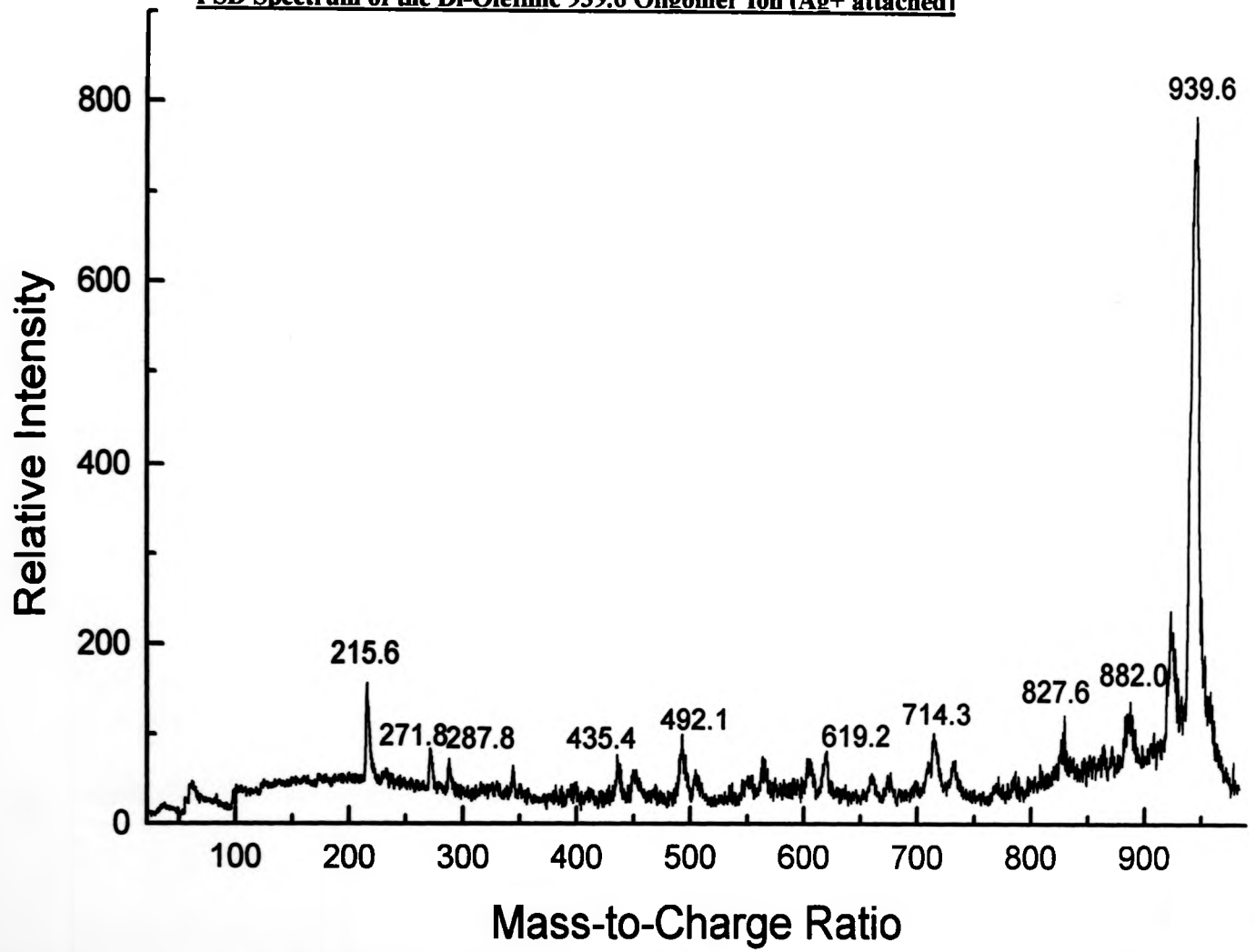

Figure 5.20

Comparison of PSD Spectra for Four Different Molecule Ions from the Di-Olefinic Sample

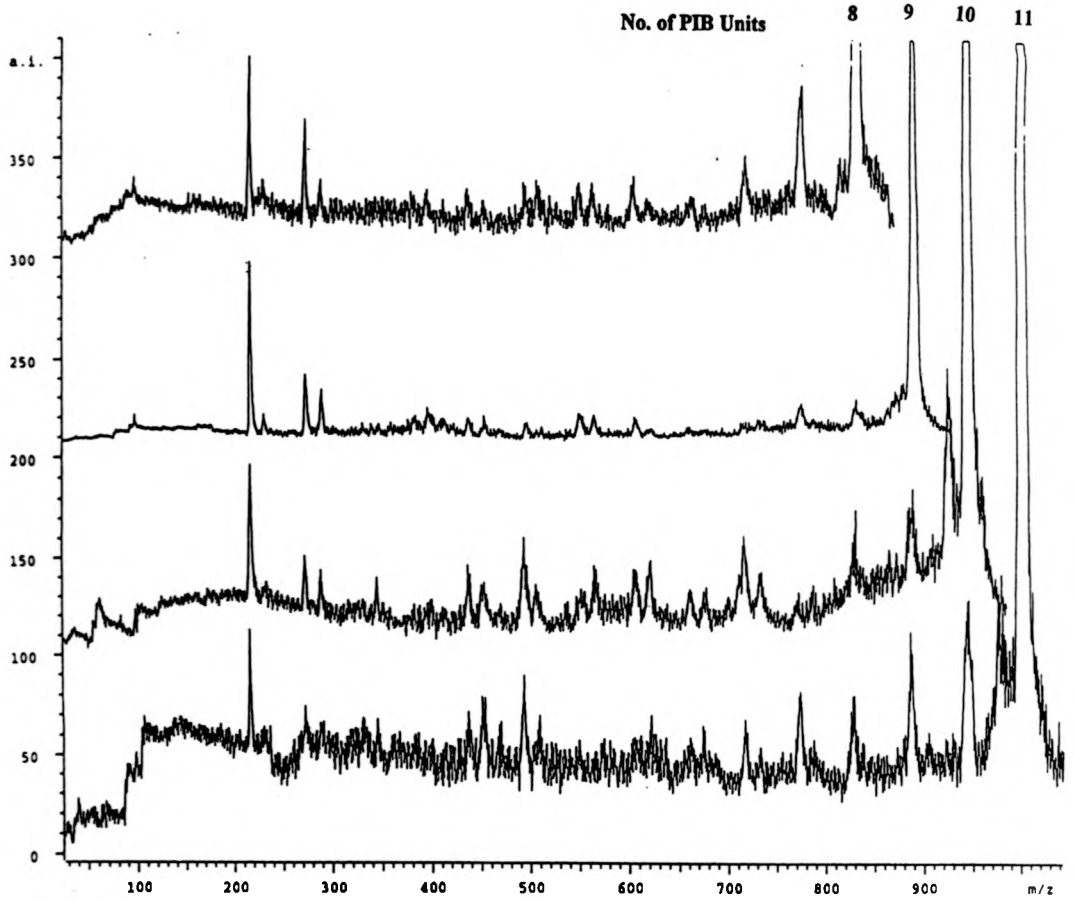

Figure 5.21

Summary of PSD Fragments of Di-Olefinic PIB Ions

Parent	Fragment	Neutral	Parent	Fragment	Neutral	Parent	Fragment	Neutral	Parent	Fragment	Neutral
995.7	974.4	21.3									
995.7	944.2	51.5	939.6	922.7	16.9						
995.7	885.2	110.5	939.6	907.4	32.2	883.5	877.3	6.2			
995.7	828.7	167	939.6	886.5	53.1	883.5	874.8	8.7	827.6	817.8	9.8
995.7	773	222.7	939.6	863.7	75.9	883.5	868.9	14.6	827.6	812.8	14.8
995.7	717.1	278.6	939.6	828.9	110.7	883.5	860.7	22.8	827.6	786.5	41.1
995.7	673.6	322.1	939.6	731.5	208.1	883.5	845.6	37.9	827.6	771.9	55.7
995.7	621.1	374.6	939.6	714.5	225.1	883.5	829.1	54.4	827.6	715.6	112
995.7	508.8	486.9	939.6	619.2	320.4	883.5	800.4	83.1	827.6	602.6	225
995.7	492.6	503.1	939.6	602.7	336.9	883.5	772.3	111.2	827.6	560.8	266.8
995.7	469.6	526.1	939.6	563.2	376.4	883.5	728.6	154.9	827.6	547.3	280.3
995.7	450.5	545.2	939.6	492.1	447.5	883.5	603.1	280.4	827.6	518	309.6
995.7	436.6	559.1	939.6	451.6	488	883.5	562.5	321	827.6	504.8	322.8
995.7	344.7	651	939.6	435.4	504.2	883.5	548	335.5	827.6	491.8	335.8
995.7	331.7	664	939.6	344.1	595.5	883.5	509.5	374	827.6	450.2	377.4
995.7	289.2	706.5	939.6	287.8	651.8	883.5	494.2	389.3	827.6	434.7	392.9
995.7	272.3	723.4	939.6	271.8	667.8	883.5	451.4	432.1	827.6	410.6	417
995.7	215.8	779.9	939.6	215.6	724	883.5	435.6	447.9	827.6	394.4	433.2
						883.5	411.1	472.4	827.6	378.3	449.3
						883.5	407.8	475.7	827.6	287.7	539.9
						883.5	394.5	489	827.6	271.5	556.1
						883.5	382	501.5	827.6	229	598.6
						883.5	374.4	509.1	827.6	214.9	612.7
						883.5	357.7	525.8	827.6	97.1	730.5
						883.5	337.4	546.1			
						883.5	329	554.5			
						883.5	288.1	595.4			
						883.5	272	611.5			
						883.5	229.6	653.9			
						883.5	215.6	667.9			
						883.5	97.4	786.1			

Figure 5.22 a

Structural Assignments of Di-Olefinic Fragments Ions Observed in PSD Spectra

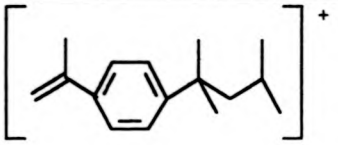

Peak observed at m/z=216, present in all spectra.

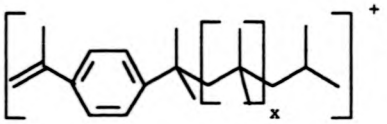

Series A ; These ions belong to a series associated with the base peak and are separated by 56 mass units. Isomers are possible, however, resolution obtained by PSD does not permit unambiguous assignments to be made.

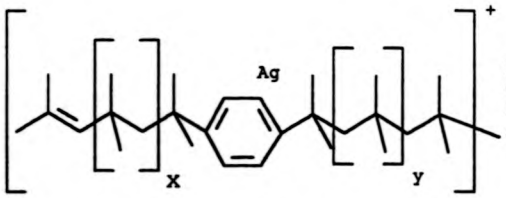

Series B ; Major series observed in PSD spectra which correspond to an end-group unit plus PIB units being lost as neutrals. This species is detected as the silver adduct.

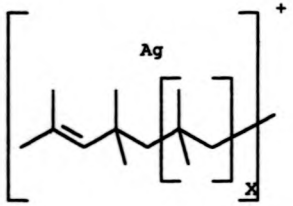

Series C ; Minor series which corresponds to an end-group plus repeat unit ion being formed. This species is detected in the form of a silver adduct.

Figure 5.22b
PSD Spectrum of a Di-Olefinic Silver Adduct (827.6, 8 PIB Units) and Assignments

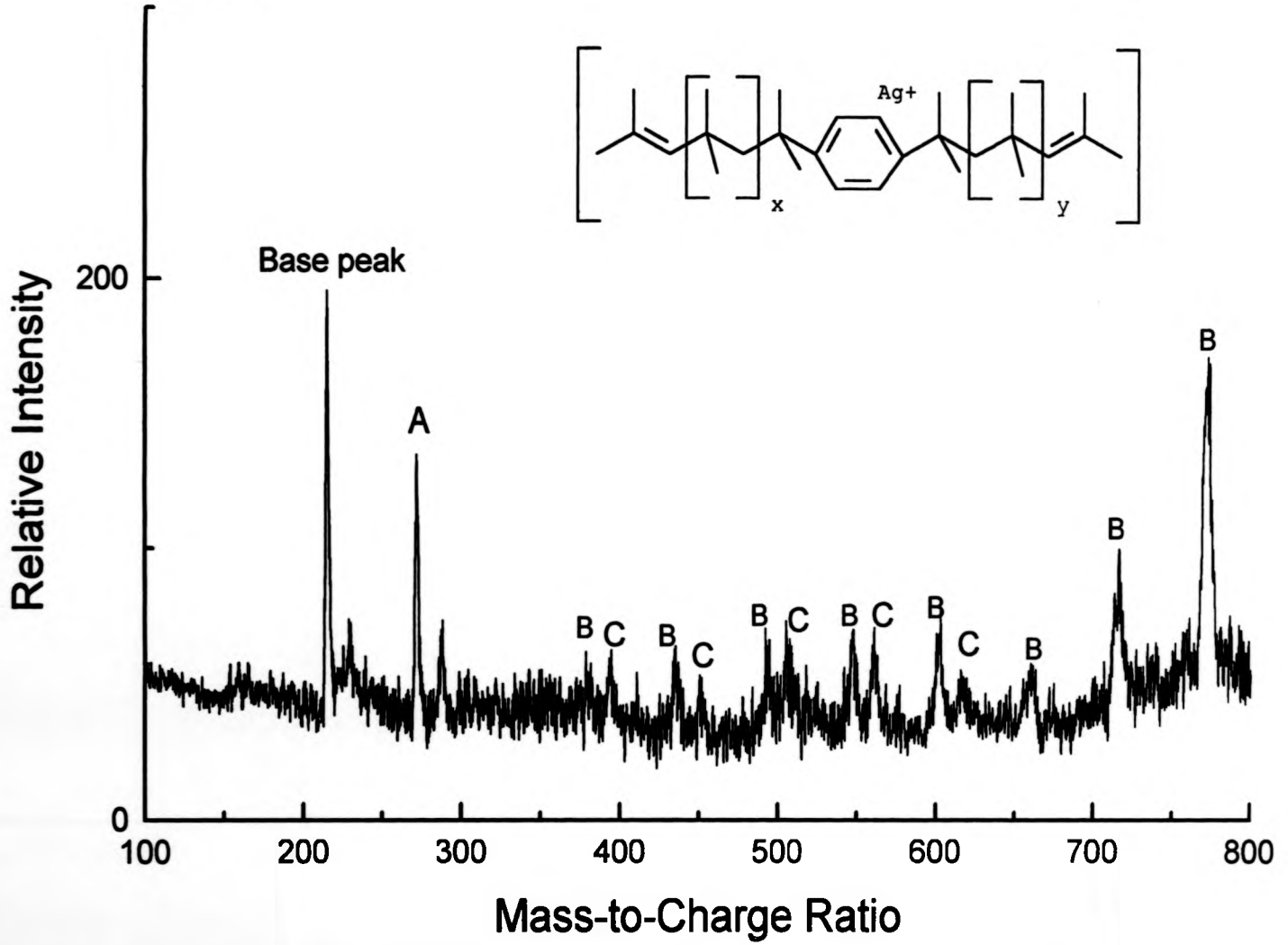

Figure 5.23
Plot to Show How Pressure Decreased During a Typical PSD Experiment

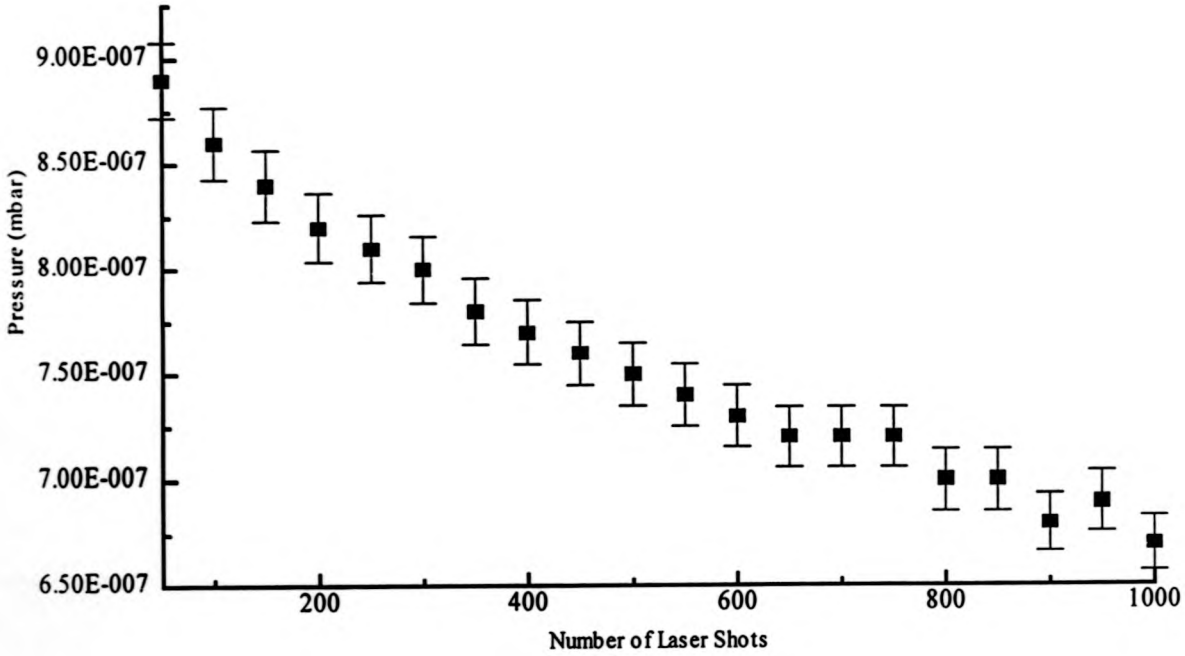

PSD experiments were performed 5 minutes after sample loading.

5.2.5 Reproducibility

The tri-olefinic PIB sample was used to investigate whether peak heights of fragment ions were reproducible. a smple was prepared using 9-nitroanthracene in combination with silver tri-fluroacetate salt addition as described in section 5.17. The sample mixture was used to prepare the required number of sample spots on the same sample slide.

Three experiments were performed on three discrete spots using the same laser energies as plotted in **Figure 5.12.** and were within the experimentally permitted error of ≤ 5 %. These experiments focused on the reproducibility of the three most intense peaks in PSD spectra of tri-olefinic oligomer ions.

An oligomer ion at m/z = 979 (Ag+ attached, 10 PIB units) was selected using the conditions stated in **Figure 5.16**. Repeat experiments were performed at the reflectron voltages for the three most intense peaks present in the PSD spectra of this sample. The masses selected covered segment numbers 9- 12 inclusive and this corresponded to measurements being taken at reflectron voltages of 6.8, 5.7, 4.5 and 4.0 kV.. The pressure p, was in the range $1.0 \times 10^{-6} \geq p \geq 8.0 \times 10^{-7}$ mbar for all of the repeat experiments.

Figure 5.24 shows repeat data collected for the 'base' peaks present in tri-olefinic PSD data.

It can be seen that the signal intensities were highly reproducible, and mass accuracies were approximately the same for each of these spectra.

Figure 5.24

PSD Spectra of Tri-Olefinic PIB with the Three Most Intense Peaks Collected Under the Same Conditions

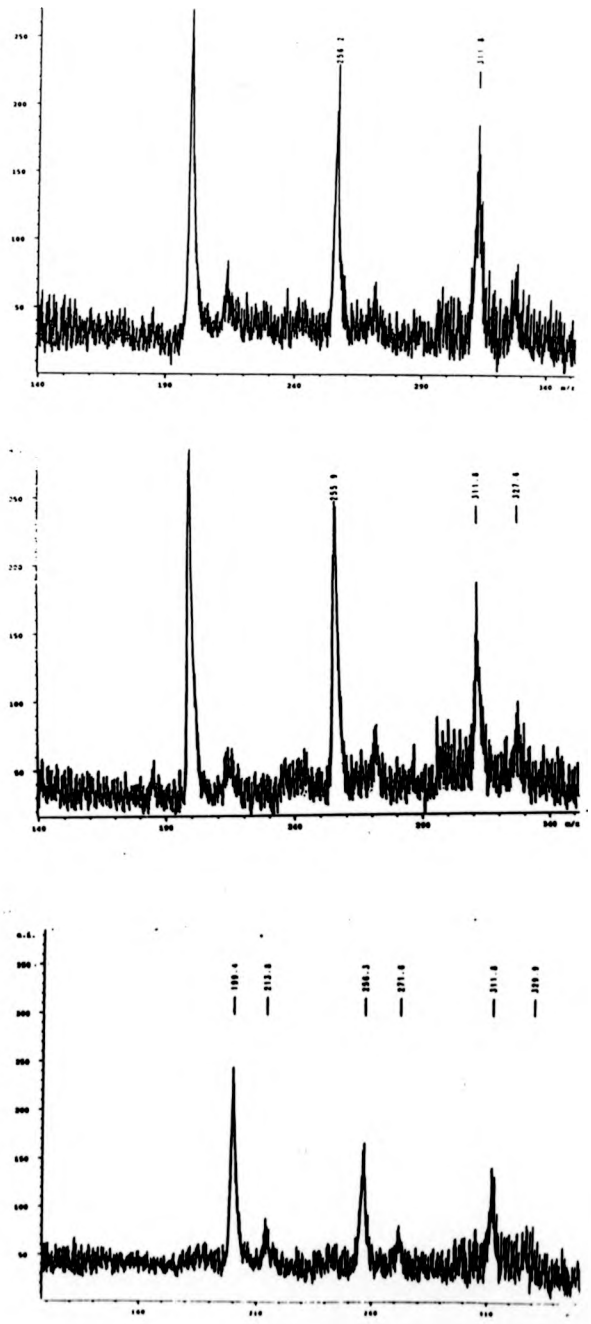

5.3 Post-Source Decay Using a Curved-Field Reflectron

The second part of this chapter is concerned with the investigation of polymers' fragment ion structure using post-source decay analysis on an instrument fitted with a curved-field reflectron.

5.3.1 General Post-Source Decay

All experiments were carried out on a Kratos Kompact IV MALDI-TOF Mass Spectrometer (Kratos Analytical, Manchester, UK) equipped with a nitrogen laser (337nm) and a curved-field reflectron. The accelerating voltage was 20.0kV and the reflectron voltage was set at 20.0kV for all normal MALDI spectra. No variation in the reflectron voltage was necessary for post-source decay experiments owing to the design of the reflectron. All fragment ions were detected using an electron multiplier.

The pressure in the source chamber could not be measured on the Kompact IV as supplied by the manufacturer. A description of special experiments to measure the pressure is given later in this section.

MALDI spectra were generally collected prior to all post-source decay experiments in order to ensure that the mass of the parent ion was known accurately.

Calibration of MALDI spectra was performed using a PEG SEC standard (number average molecular mass = 1470, polydispersity index ≤1.05, Polymer Laboratories, UK.) The average isotope masses of a range of sodium adducts were used over a suitable mass range (700-1600), similar to that of the samples under investigation. Using this calibration procedure, the error in the mass values of PEG ions was less than 0.5 amu.

The PEG SEC standard was prepared in the same way as described in section 5.1.

5.3.1.1 Parent Ion Selection

To acquire post-source decay spectra, a parent ion was selected using software provided by Kratos. The length of the ion gate pulse was dictated by the choice of

parent ion mass range and, in the case of polymers, the mass range was chosen which extended 2-3 mass units either side of the parent ion. For the selection of a PEG oligomer ion, this meant that neighbouring oligomer ions were detected at no more than 4% of the selected parent ion's intensity. Tuning of the ion gate was performed at just above the threshold laser energy of the parent ion.

Data Collection

PSD spectra were collected at a series of constant laser energies, ranging from threshold to up to 50% higher than threshold. In practice, the range of useful laser energies was relatively small since the lowest values resulted in no fragment ions being detected and the highest values resulted in severe distortion of fragment ion peaks.

Each PSD spectrum was collected over 200 laser shots. This is double the number usually collected for a MALDI spectrum of a polymer and was necessary in order to optimise signal-to-noise ratios.

5.3.1.2 Theoretical Calibration of the Curved-Field Reflectron

The calibration of fragments formed by post-source decay was based upon the relationship between the mass of the fragments and the mass of the parent ion provided by the manufacturer. A software defined equation was used to define a calibration curve thus ;

$$M_{ratio} = a + b / M_{app\%} + c \sin \{\Pi/68 * M_{app\%}\} + d /(M_{app\%})^3$$

a, b, c and ***d*** are all dimensionless calibration coefficients

$$M_{ratio} = \textit{apparent mass of fragment ion / actual mass of fragment ion}$$

$$M_{app\%} = \textit{apparent mass of fragment ion / parent ion mass * 100}$$

Figure 5.25 depicts the form of the theoretical calibration curve.

Figure 5.25

Theoretical Curve Used to Calibrate the Curved Field Reflectron for PSD Investigations

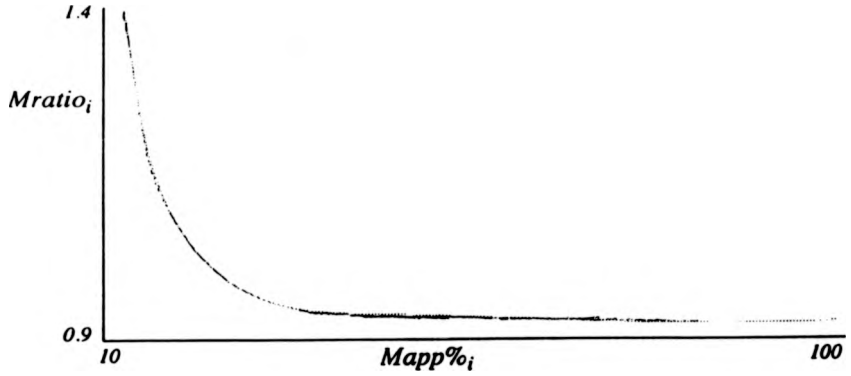

According to the manufacturer's curve[182], as the mass of the fragment ion becomes smaller and its mass as a fraction of the parent ion decreases, the calibration curve becomes sensitive and mass assignment will become less accurate.

In practice, the coefficients were calculated by the software using fragment ions of known apparent and actual masses. The accuracy of the calibration curve depended heavily upon the precise measurement of these values. In practise, a good calibration curve could allow the determination of fragment masses to within 1 amu.

5.3.1.3 Experimental Procedure for PSD Analysis

A standard peptide with a well characterised fragmentation pattern covering a broad mass range was chosen to calibrate the fragment ions focused by the curved-field reflectron. The manufacturer's had set the instrument up so that Angiotensin II could readily be used since the masses of all fragment ions were written into the software.

Calibrant Preparation

An aqueous solution of Angiotensin II (10^{-4}M) was mixed in a 1:1 ratio with a solution of alpha-cyano hydroxycinnamic acid (10^{-1}M in 25 % acetonitrile / 75 % water). 1 µl

of this mixture was spotted onto the stainless steel sample slide and the solvent was slowly dried off in stream of warm air.

Figure 5.26 shows a typical PSD spectrum of Angiotensin II.

Figure 5.27 depicts how software on the Kompact IV instrument correlated incalibrated fragment ions masses with actual fragment mass values.

Figure 5.28 shows a calibration function generated using experimentally derived calibration coefficients. These coefficients are calculated by the software on the Kompact IV instrument and are substituted in the 3rd order polynomial equation outlined in section 5.3.1.2 order to define this calibration curve.

5.3.1.4 Pressure Dependency

According to the manufacturer[182], normal MALDI spectra could only be collected when the pressure in the instrument reached $\leq 5 \times 10^{-6}$ mbar. Pressures of this value or lower triggered a valve system which allowed high potential voltages to be switched on. During the course of initial PSD experiments on this instrument, it was observed that fragment ions of higher intensities were detected when the pressure in the instrument was higher than normal as a result of either venting the instrument or opening the bleed valve. All PSD spectra were subsequently collected under these conditions

5.3.2 Pressure Measurement

The purpose of this experiment was to obtain an approximate value for the pressure in the source region of the Kompact IV instrument which could not be measured on this instrument as supplied by the manufacturer.

Kaufmann and Spengler had noted that residual gas had an effect on the type of fragment ions detected in PSD investigations [111] and so it was important to have an approximate value for this parameter.

Figure 5.26

A typical PSD Spectrum of Angiotensin II.

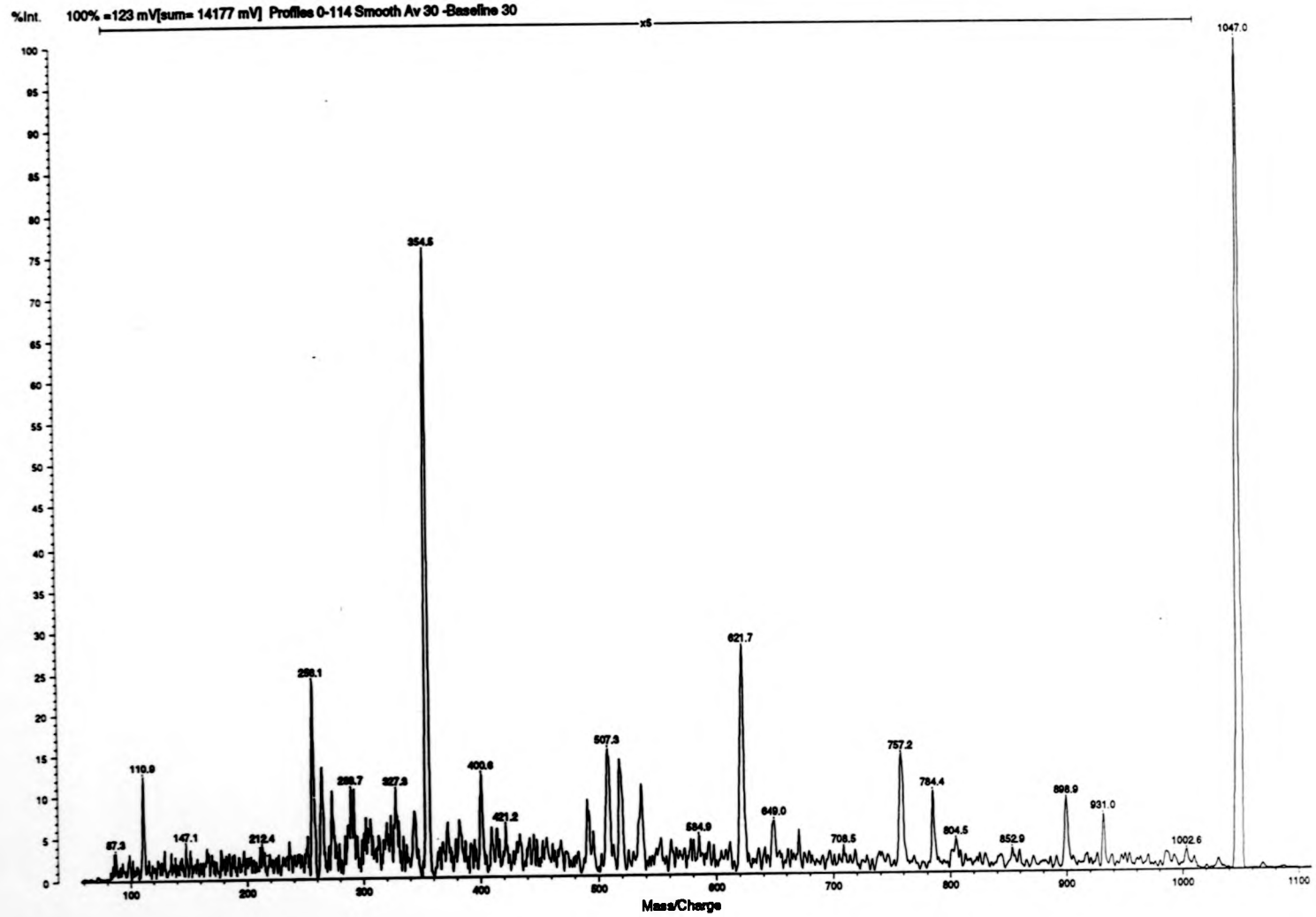

Figure 5.27

How the Apparent Masses of the Fragment Ions of Angiotensin II Corresponded to their Actual Masses

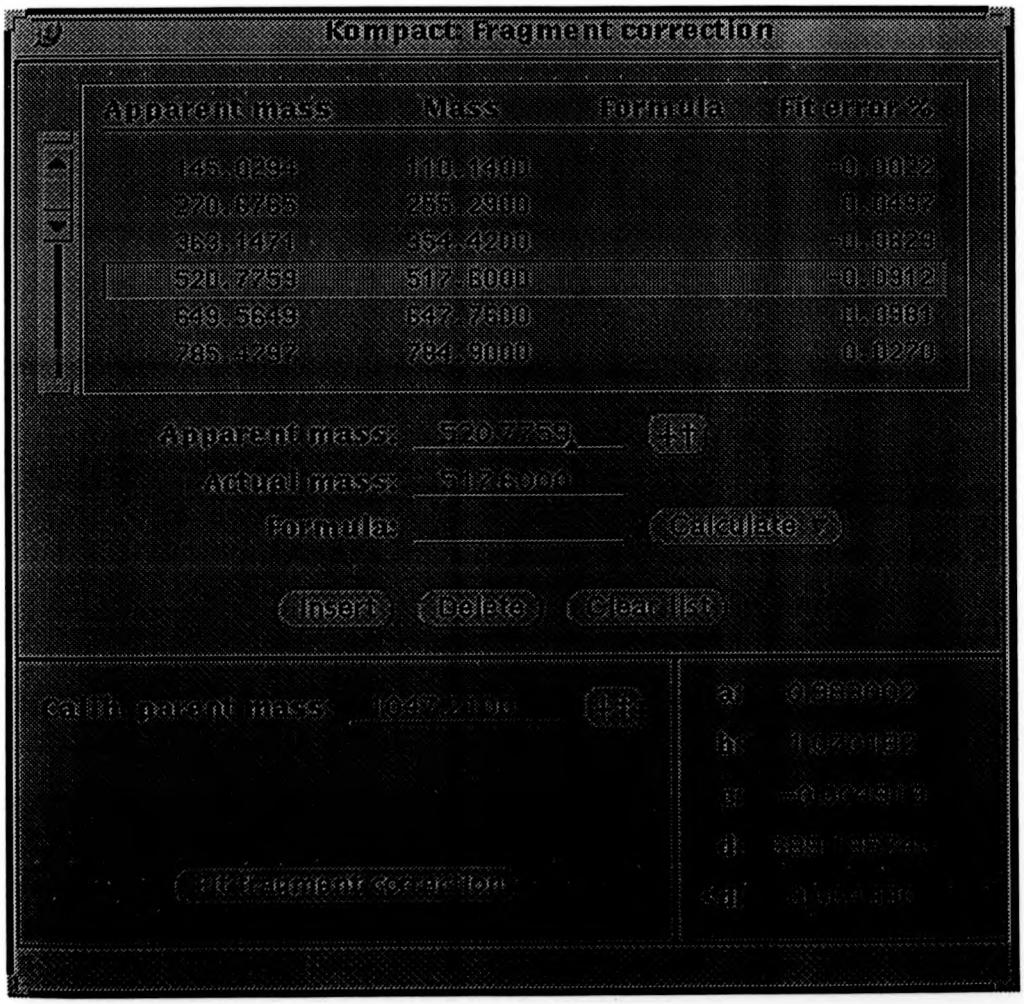

Calibration Function Generated using Experimentally Derived Calibration Coefficients.

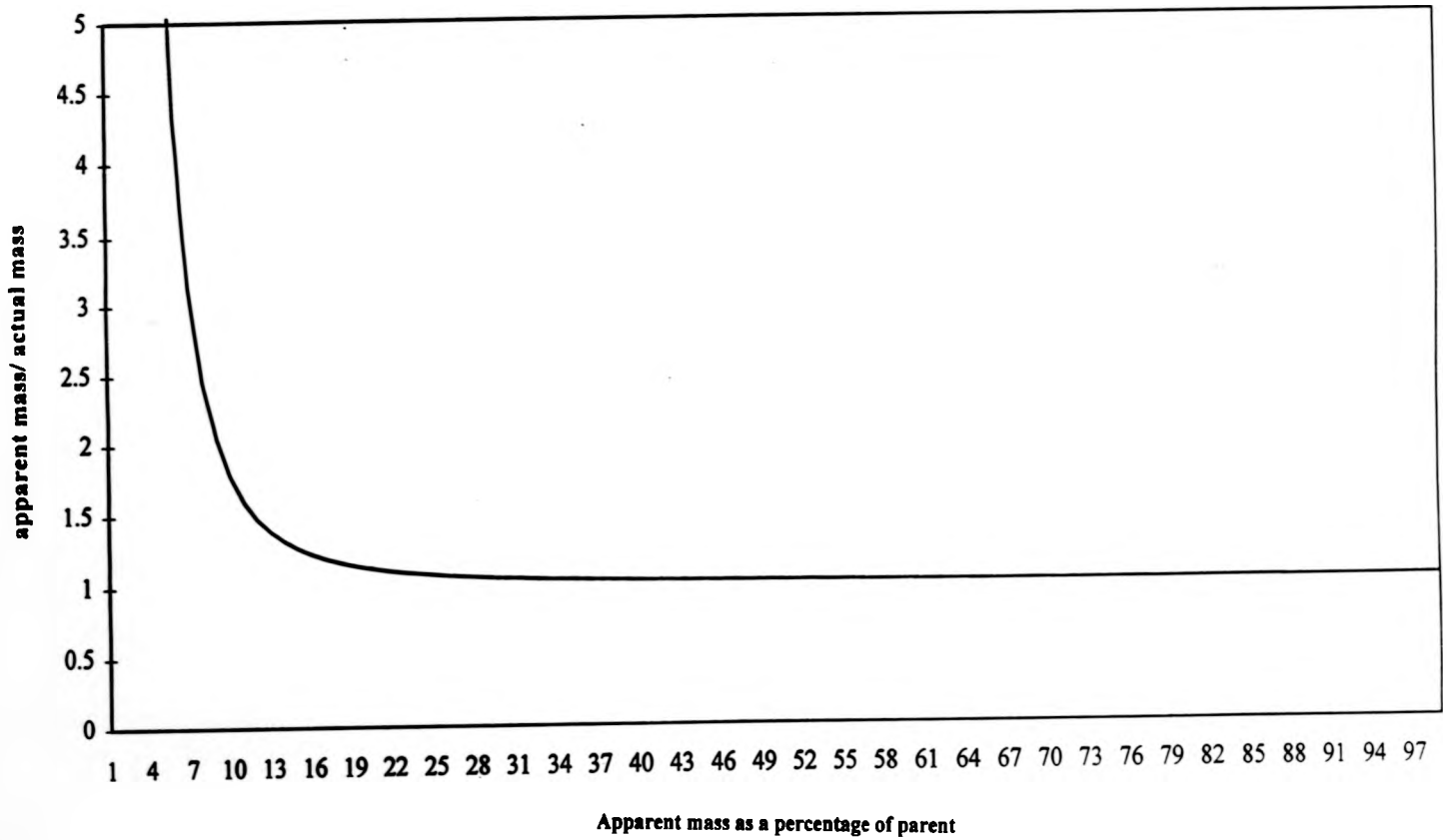

Experimental

The Kompact IV instrument was vented and switched off completely. A stainless steel base plate with an opening of suitable dimensions was fitted in place of the perspex seal that housed the ion source. A series of coupling joints and O-ring seals were used to attach an electronic ion gauge.

A schematic diagram of the experimental set-up is show in **Figure 5.29**

The output from the ion gauge was converted into a chart recorder signal which had previously been calibrated using a standard nitrogen/air mix by the manufacturer. *ref*
The instrument was switched back on and a backing pressure of 7.90×10^{-4} mbar was measured before the turbomolecular pumps started to work again. The pressure decreased at a slow rate and after 72 hours the pressure reached a value of 9×10^{-6} mbar. This value was higher than expected, however, this might be attributed to the additional pumping required to evacuate the extra volume of the coupling parts. or the fact that the residual gas in the instrument consisted mainly of water and would take longer to evacuate. Furthermore, this pressure was by no means the lowest value attainable since the manufacturers quoted a period of upto 2 weeks before absolute pressure could be obtained.

5.3.3 Poly(isobutylene) Fragment Ion Investigations

The three poly(isobutylene) samples depicted in **Figure 5.10** were investigated using MALDI-TOF mass spectrometry coupled with PSD analysis on this instrument. All three samples were prepared using 9-nitroanthracene as the matrix in combination with silver rti-fluoroacetate and care was taken to ensure that MALDI spectra of high signal-to-noise values could be reproduced easily.
The aim of these experiments was to investigate the gas-phase chemistry of the species formed by MALDI and to investigate any differences which may occur in their fragmentation patterns. Results obtained using the curved-field reflectron could,

Schematic Diagram of Apparatus Used to Measure Pressure on the Kompact IV Instrument

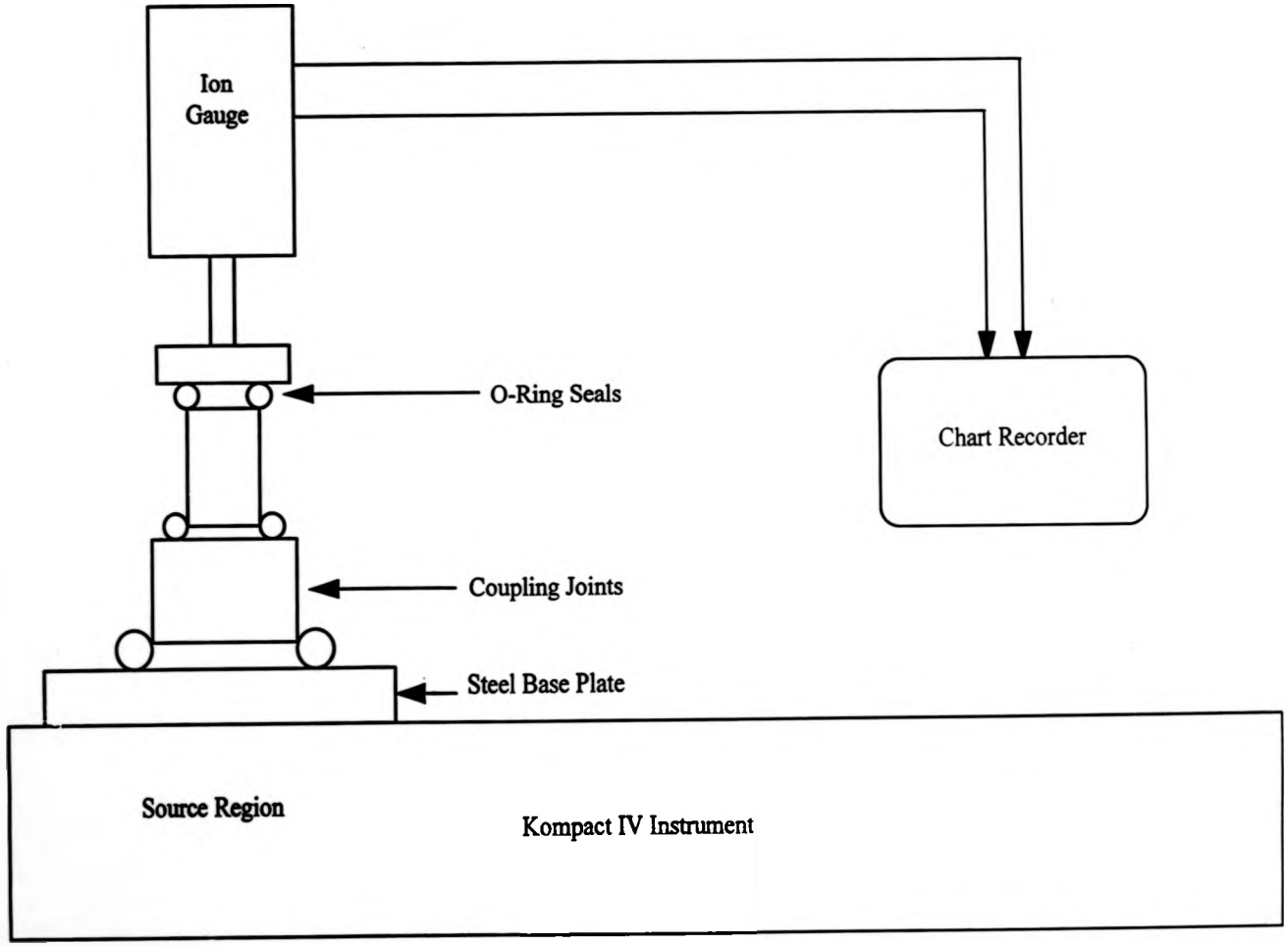

therefore, be compared and contrasted with those detected under slightly different conditions using a two-stage refelectron for the analysis of fragment ions.

A MALDI spectrum was collected and the mass accuracies of each silver adduct was checked. If necessary, a calibration was performed using a PEG SEC standard of similar molecular mass as that of the sample of interest.

Experimental Conditions

Each PSD spectrum was collected over 200 laser shots per sample spot. Each complete spectrum, covering the entire mass range, was collected at a constant laser power. For each oligomer ion, a series of spectra were obtained over a range of laser energies, commencing at just above the threshold energy of the parent ion, thus the effect of laser power on the whole post-source decay spectrum could be observed.

All post-source decay spectra were collected at raised pressures after the instrument had been vented for maintenance work or after the bleed vale had been opened. the pressure had been measured to be approximately 9×10^{-6} mbar. At high laser energies required for PSD analysis, it became increasingly more difficult to successfully accurately select a parent ion of interest. This suggests that ions with high laser energies differing by only 1 monomer mass unit, in this case 56, travel at approximately the same velocity, making it virtually impossible to select one or other as a discrete ion, even if a unit mass was selected as the width of the ion gate. This is because ions which differ by 56 mass units have overlapping kinetic energy distributions owing to the nature to the MALDI process and the pulse duration of the ion gate is not sufficiently short in order to distinguish these ions.

5.3.3.1 Di-Olefinic PIB Sample

Figure 5.30 shows a typical MALDI spectrum of the di-olefinic sample obtained on the Kompact IV instrument. Improved resolution on this instrument compared with that obtained on the Kompact III permitted the unambiguous assignment of a singly-charged silver ion to each polymer.

Figure 5.30

Typical MALDI-TOF Spectrum of the Di-Olefinic PIB Sample Obtained on the Kompact IV Mass Spectrometer

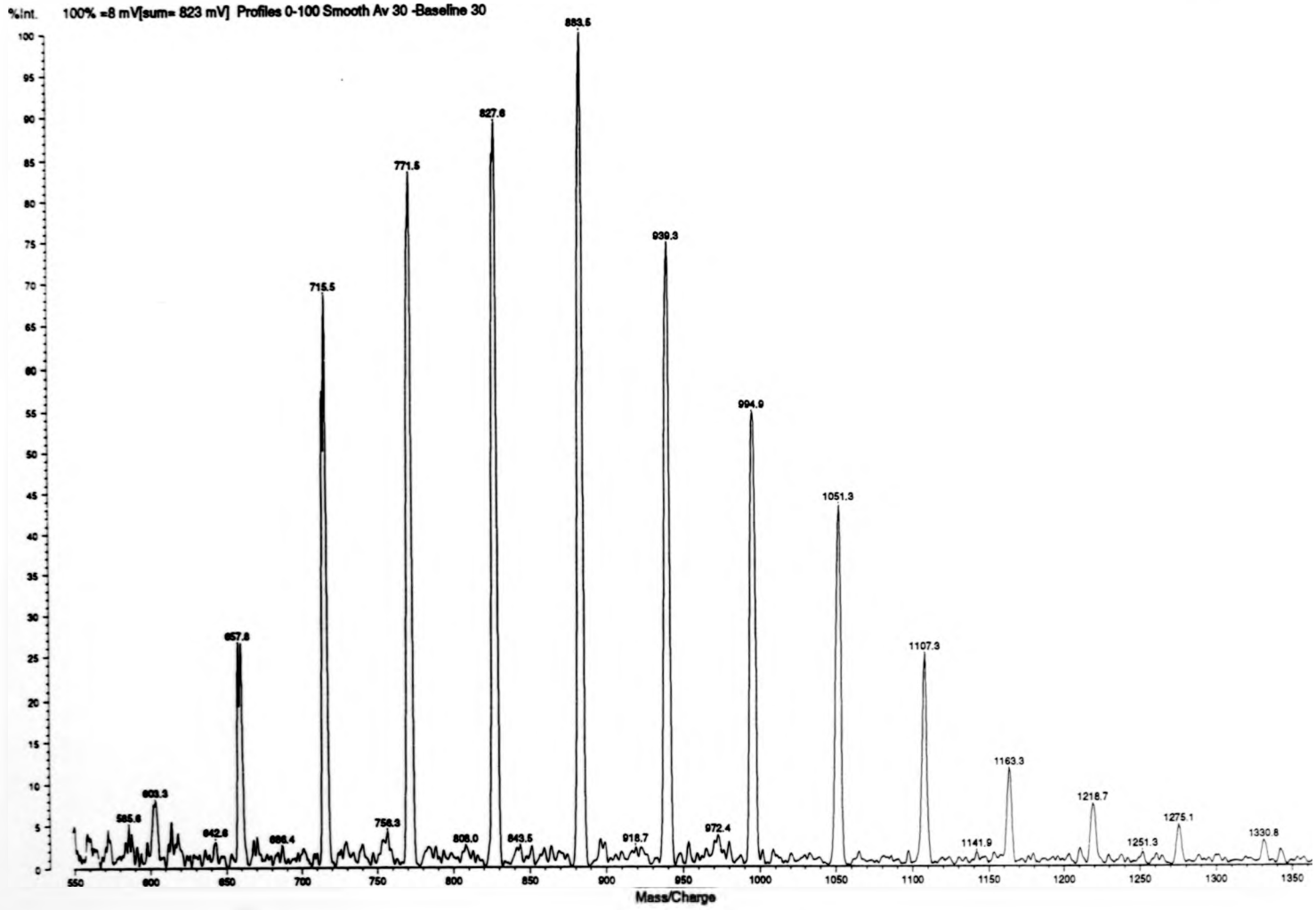

Inset of Silver Isotopic Distribution Associated with Each Oligomer Ion.

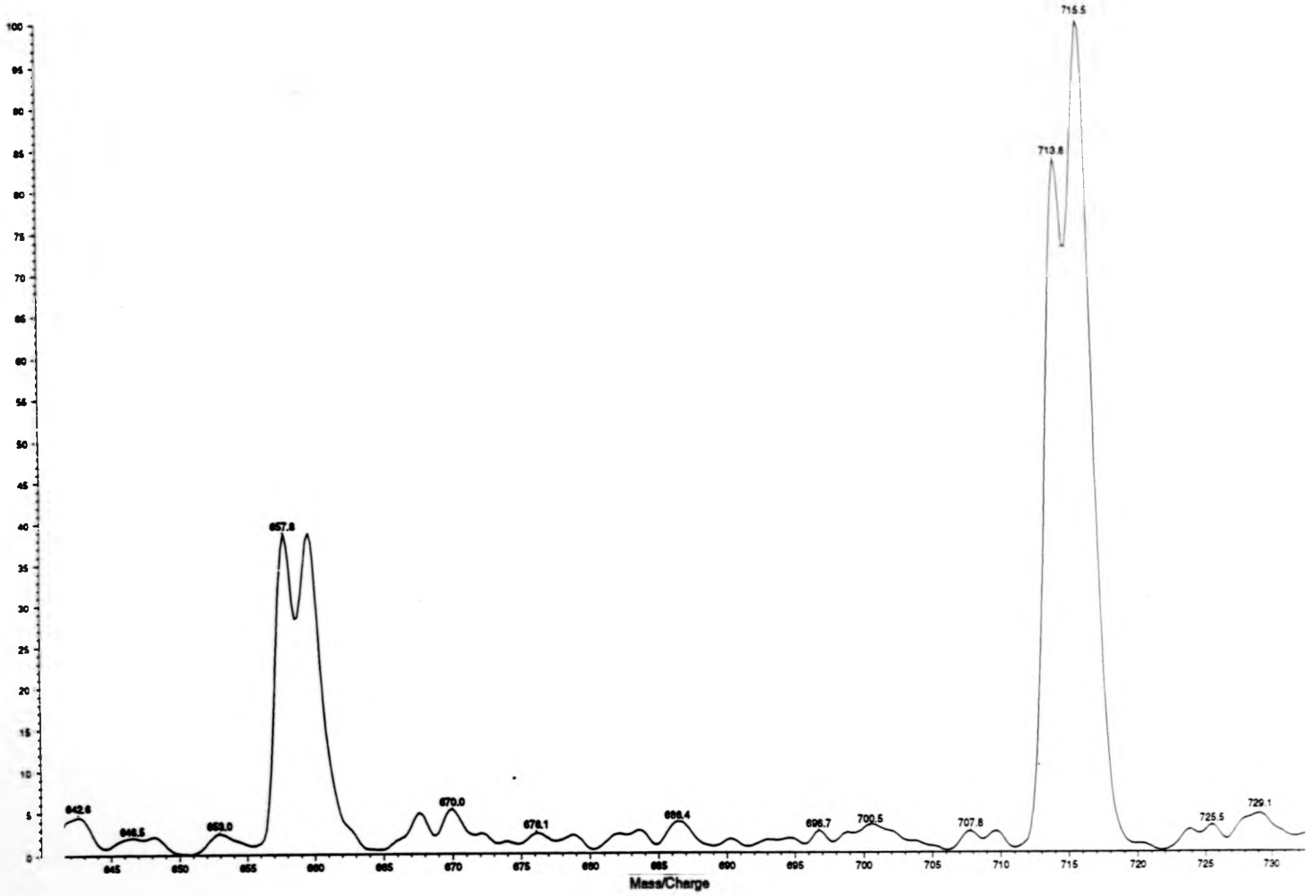

Figure 5.31 clearly shows the 1:1 isotopic distribution associated with the 107 and 109 isotopes of silver.

Laser Energies

The threshold values were measured at software values of 90 and optimum PSD spectra were obtained at software values of 110. These values corresponded to laser power densities of approximately 1.7 and 2 x 10^{7} Wcm^{-2} respectively and were calculated according to the equation defined in section 2.1.1.

Figure 5.32 shows a typical post-source decay spectrum obtained at optimum laser power of a silver attached PIB ion . (939.8, 10 PIB units).

Figure 5.33 depicts the effect of increasing laser power on the quality of the data obtained. As the laser power increases, more fragment ions are detected at the the low mass end of the spectrum. The peaks become broader as the energy increases. At lower energies, the dominant peak in the PSD spectrum is still the parent polymer ion.

Fragmentation Patterns

A total of six silver adducts have been investigated on this instrument, ranging from m/z= 771.8-1051.6, which corresponds to between 7 and 12 PIB units per molecule and their fragmentation patterns were compared. In all cases, the next-lowest mass oligomer ion was consistently higher in intensity than the selected parent ion at the optimum post-source decay laser power. This might be explained by the fact that at higher energies, the ion gate was not as effective at successfully selecting a single polymer ion. However, all oligomer ions fragmented in a similar way hence the series of fragment ions observed from each oligomer ion were the same.

Figure 5.34 shows PSD data obtained for 3 consecutive silver adducts at optimum laser power.

Figure 5.32

Typical PSD Spectrum of a Silver-Attached Di-Olefinic PIB Ion Obtained at Optimum Laser Power.

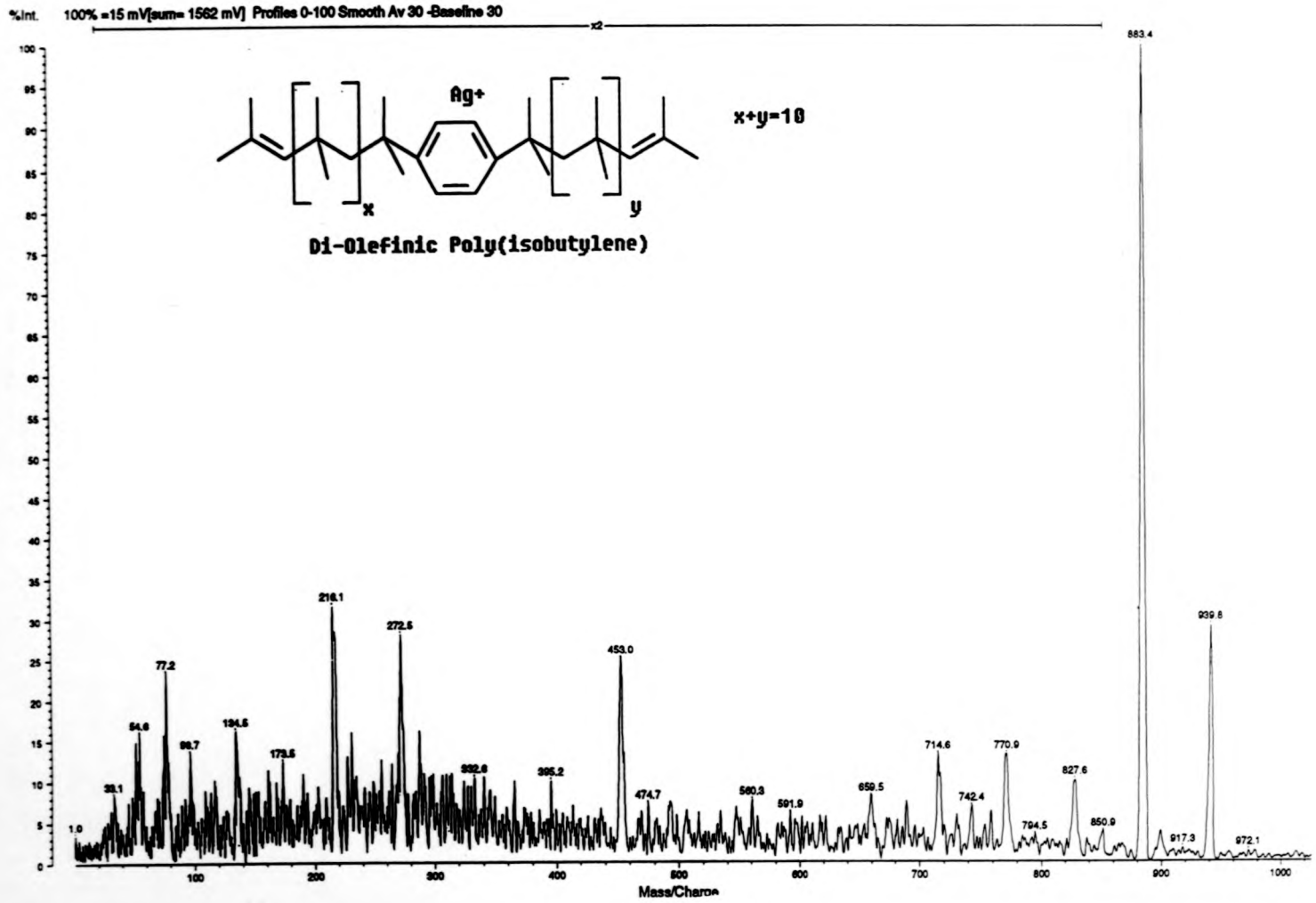

Figure 5.33

Effect of Increasing Laser Power on PSD Spectra

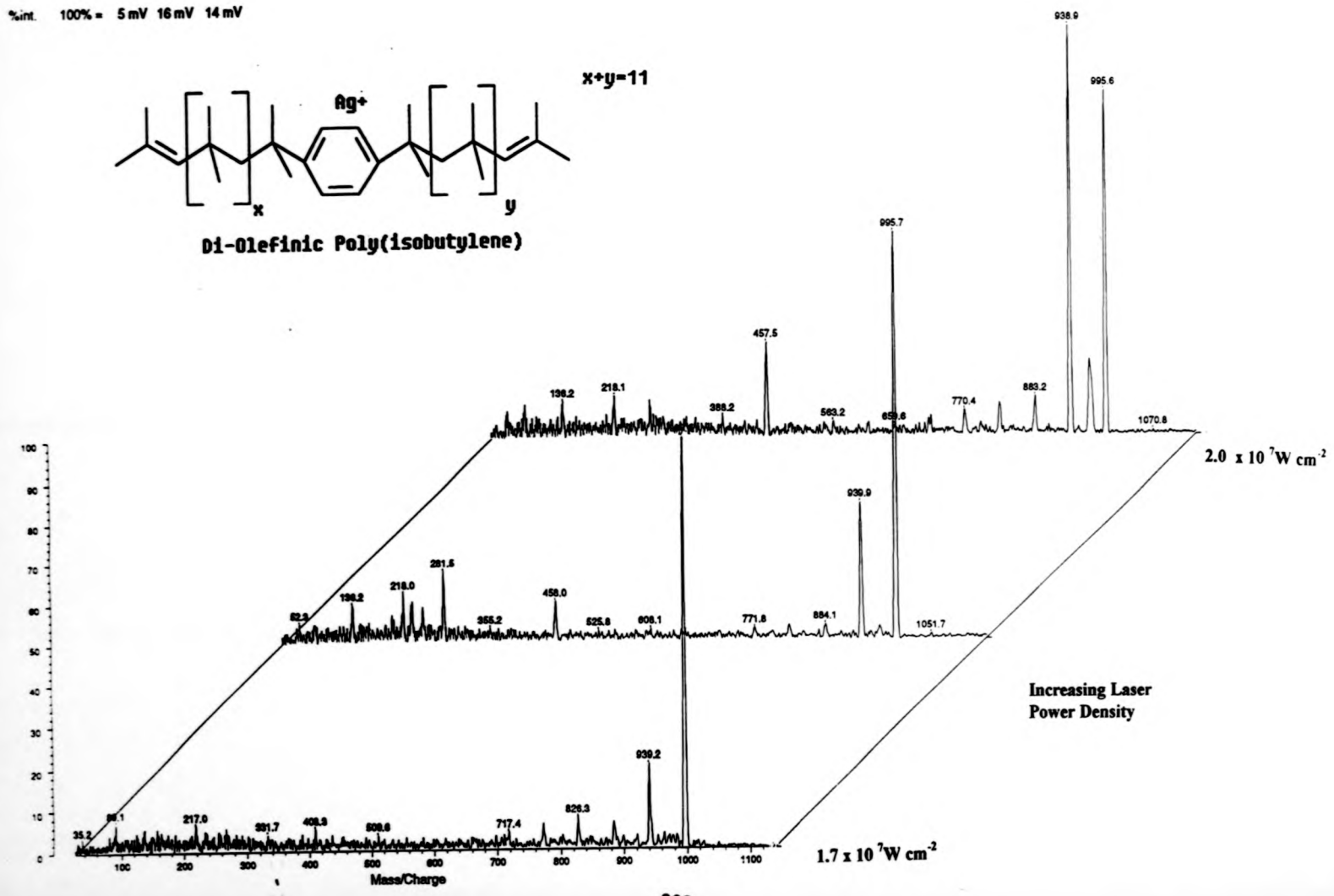

Figure 5.34

PSD Spectra Obtained for Three Consecutive Silver Adducts of the Di-Olefinic Parent Ions at Optimum Laser Power

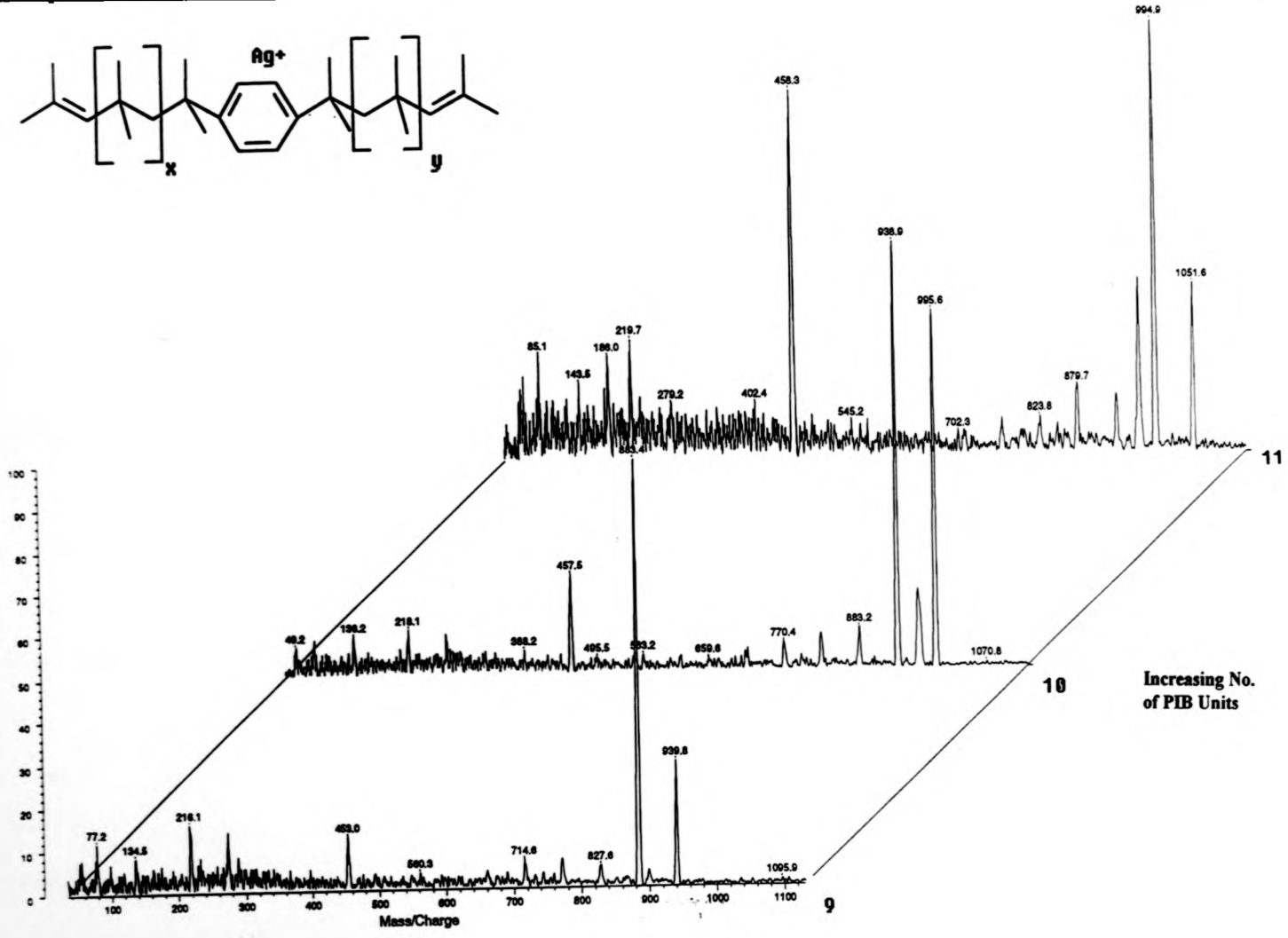

Fragment Ion Assignment

Weak fragment ions in the higher-mass regions were observed which corresponded to a neutral loss of end-group plus PIB units. The silver cation remained attached to the bulk of the polymer chain to form ions of the type ;

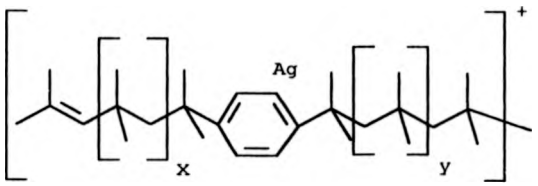

It was impossible to say which of the two PIB polymer chains were unzipping or to postulate the exact the mechanism. Fragment ions of the same type had been observed in PSD spectra collected on the instrument fitted with a two-stage reflectron.

A 'base' peak at m/z=216 was observed and an ion at 56 mass units higher was seen. These fragments were in agreement with previous findings and were tentatively assigned thus:

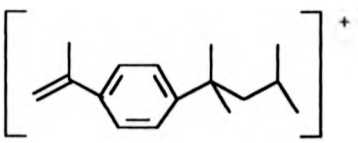

It is conceivable that the ion detected at m/z=216 represented Ag_2+, however, the fact that this peak was not seen in the PSD spectrum of tri-olefinic parent ions suggests that the original assignment was the most likely. Furthermore, the fact that a series is observed at 56 mass units higher supports this assignment.

A peak at m/z=452 is consistently observed in all of the PSD spectra of the di-olefinic sample. This may be assigned as a series C fragment ion which corresponded to the neutral loss of a butyl end-group plus PIB units.

It was observed that not all of the ions detected on the two-stage refelctron instrument were observed in spectra collected on this instrument.

A peak at m/z=77 was seen which may be attributed to an aromatic ring function and the next higher mass peak observed at m/z=134.6 may be attributed to an aromatic ring function with remnants of the polymer chain still attached. All mass assignments and their corresponding structural assignments must be made tentatively, particularly, within this mass range. In general the mass resolution was approximately 100, however, mass assignments where fragment ion mass was ≤ 10% of the parent ion mass had to be made with care because application of the function used to calibrate the curved field reflectron was subject to large errors within this region.

Calibration Difficulties

The calibration function relied upon the accurate mass assignment of each parent ion investigated. This was ensured by calibration with an external calibrant followed by an assignment with the ion gate switched on.

It was observed, however, that for the range of oligomer ions investigated, the masses of fragment ions detected shifted slightly with increased mass of parent ion. This effect was believed to be a problem associated with the calibration function defined by the manufacturer's software. The effect was particularly marked in the middle-mass ranges of the PSD spectrum i.e. at mass-to-charge ratios of 400-500 for parent ions at m/z= 1000

Furthermore, according to the manufacturer's calibration curve, as the mass of the ion becomes smaller and its mass as a fraction of the parent ion decreased, the calibration curve becomes sensitive and mass assignment less accurate as shown in **Figure 5.25.**

One of the most important parameters used in the calibration function was $M_{app\%}$ which is defined as

$$M_{app\%} = \textit{apparent mass of fragment ion} / \textit{parent ion mass} * 100$$

Calibration of the reflectron using a standard compound under normal MALDI conditions, i.e. without the manufacturer's PSD calibration function being applied, allowed a measurement of the apparent masses of fragment ions to be made.

Figure 5.35 shows how the apparent mass of a di-olefinic fragment ion changed with parent ion mass. The fragment ion which was observed to 'shift' with increasing mass of parent ion was the fragment at m/z ≈ 452. In **Figure 5.34** the mass of this ion is seen to increase from 453.0 amu to 458.3 amu as the parent ion increased from 939.8 through to 1051.6.

Tri-Olefinic PIB Results

Laser Energies

Threshold energies were measured at software values of 90 and optimum PSD spectra were obtained at software values of 110. These values were the same as for the di-olefinic sample and corresponded to 1.7 and 2 x Wcm^{-2} respectively, calculated using the same method as described in section 2.1.1

Figure 5.36 shows a typical post-source decay spectrum obtained at optimum laser (software value = 110) power of a silver attached PIB ion. (m/z = 811, 6 PIB units)

Figure 5.37 depicts the effect of increasing laser power on the quality of the spectrum. As in the case of the tri-olefinic samples, as the laser power increases, more fragment ions are detected at the low mass end of the spectrum. The peaks become broader at lower energies. At lower energies, the dominant peak in the spectrum is still the parent polymer ion.

Figure 5.35

Plot to Show How the Apparent Mass of a Di-Olefinic Fragment Ion Varied with Parent Ion Mass

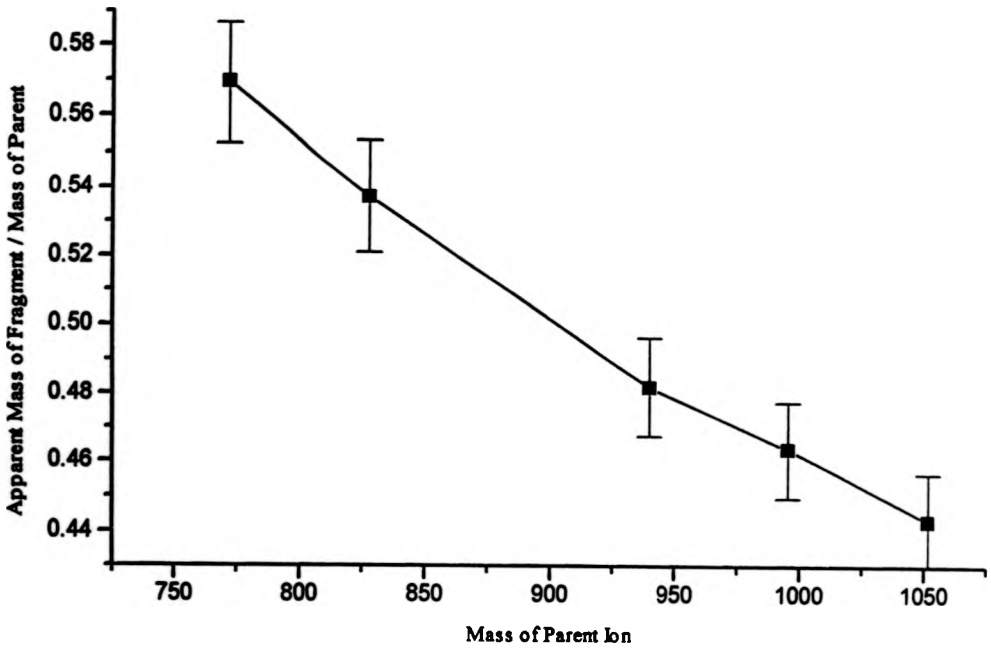

Figure 5.36

Typical PSD Spectrum Power of a Silver Attached Tri-Olefinic PIB Ion Obtained at Optimum Laser.

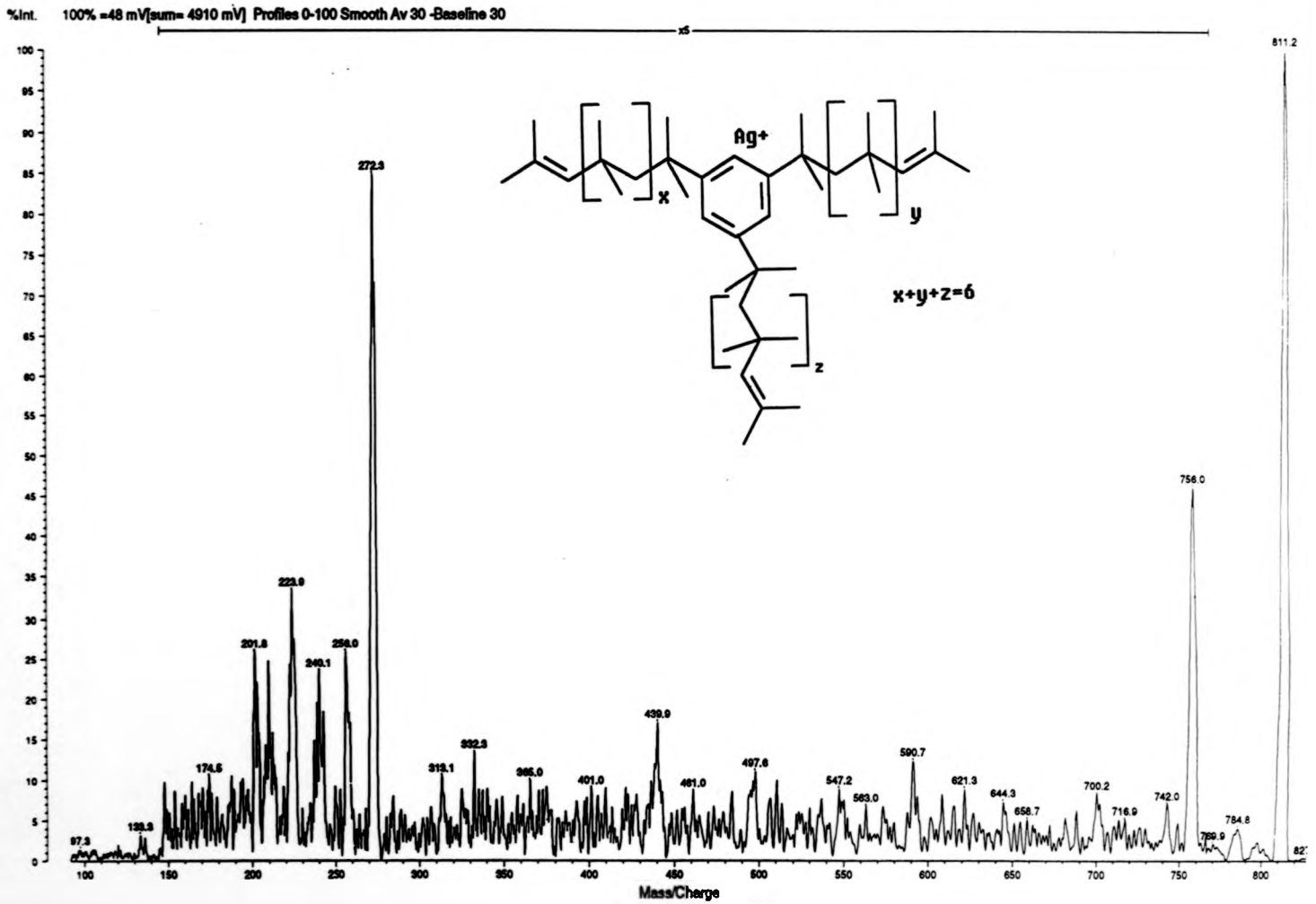

Figure 5.37

Effect of Increasing Laser Power on PSD Spectra

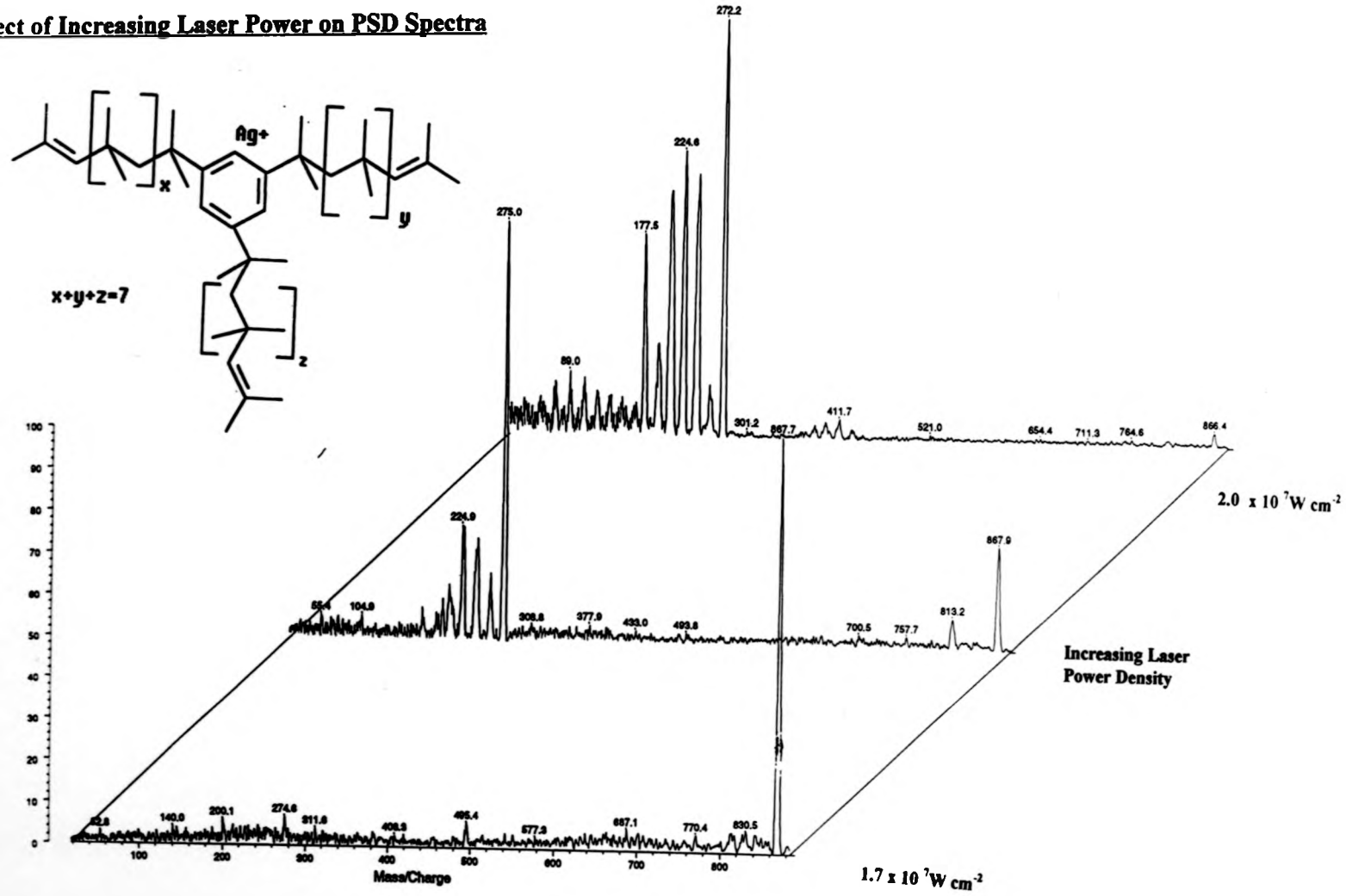

Fragmentation Patterns

A total of five silver adducts have been investigated on this instrument, ranging from m/z= 811.4-1035.8, which corresponds to between 6 and 10 PIB units per molecule and their fragmentation patterns were compared. the same effect on the selection of the parent ion was observed for the tri-olefinic sample as described for the di-olefinic sample in section 5.2.3.1

Figure 5.38 shows PSD data obtained for 3 consecutive silver adducts at optimum laser power. These fragment ions were at m/z = 811.2, 867.9 and 922.8. This corresponded to 6, 7 and 8 PIB units respectively.

Fragment Ion Assignment

Tri-olefinic oligomer ions appeared to fragment more readily than their di-olefinic analogues. Few fragment ions were observed in the middle mass ranges and most oligomers fragmented to form a series of base peaks within the mass range 150-300 Da. It was impossible to say whether any of these fragment ions had been previously observed since the calibration function did not allow an accurate mass assignment to be made.

Calibration Difficulties

The same type of problem occurred as in the di-olefinic sample. For the range of oligomer ions investigated, the mass of fragment ions detected shifted slightly with increased mass of parent ion.. The effect was particularly noticeable for an ion detected where m/z = 270-280.

Figure 5.39 shows how the apparent mass of a fragment ion changed with parent ion mass. The fragment ion which was observed to 'shift' was the fragment at m/z ≈ 272. In **Figure 5.38** the mass of this opn os seen to increase from 271.6 to 277.9 as the parent ion increased from 811.2 to 922.8 amu.

Figure 5.38

PSD Data Obtained for Three Consecutive Silver Adducts of the Tri-Olefinic Parent Ions at Optimum Laser Power

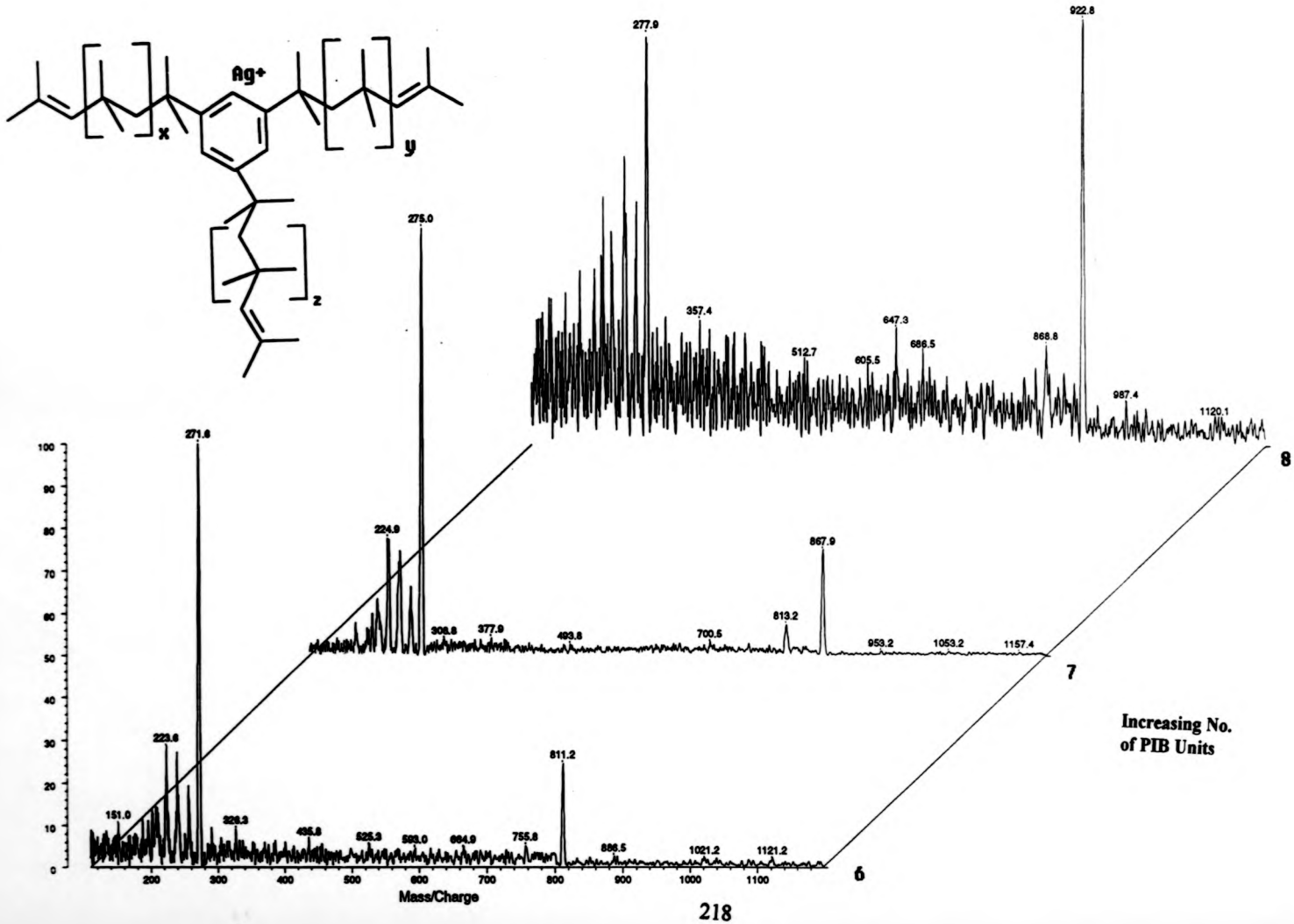

Figure 5.39

Plot to Show How the Apparent Mass of a Tri-Olefinic Fragment Ion Varied with Parent Ion Mass

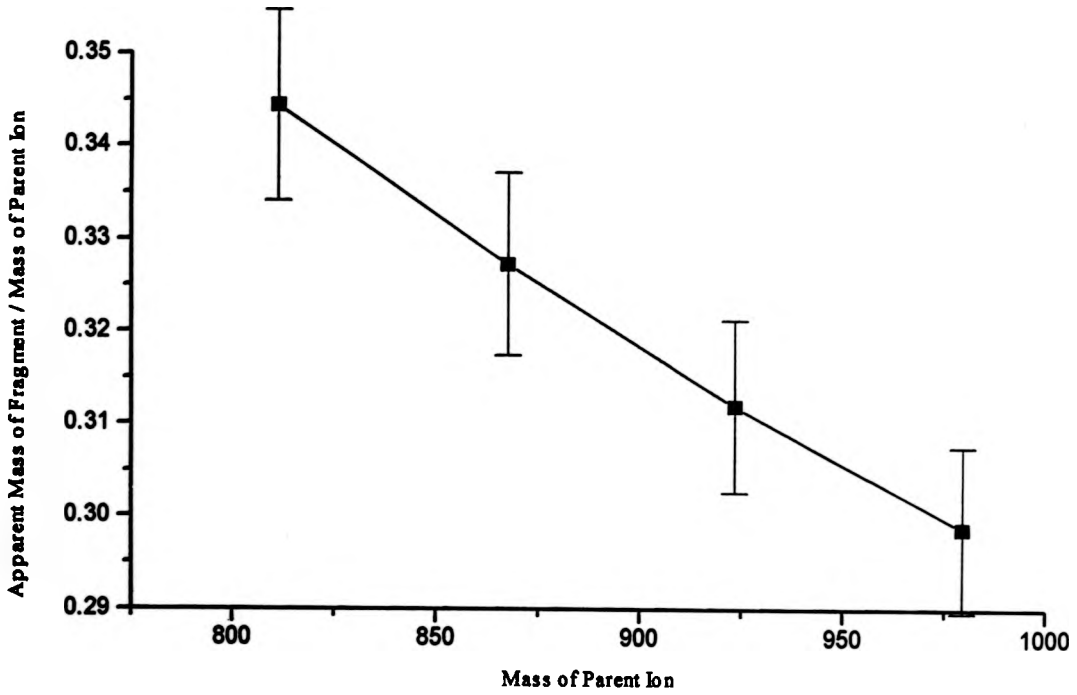

5.3.3.1 Mono-Olefinic PIB Sample

The same difficulties occurred as previously described. MALDI spectra of this sample were generally very hard to obtain and the intensity of the parent ions were too weak to perform post-source decay experiments.

5.3.4 Calibration Reproducibility

The aim of these experiments was to assess whether a set of different standards of varying masses could be used to form a set of calibration curves and to assess whether the post-source decay mass calibration was accurate and reproducible. A series of standard peptides and peptide residues were studied by MALDI-PSD analysis. These compounds were chosen since the mass of all fragment ions could be conveniently predicted using software available on the Kompact IV instrument. These were Substance P, Bradykynin and a set of Bradykynin residues.

Sample Preparation

0.5 µl of alpha-cyano hydroxycinnamic acid (10^{-1}M in 25 % acetonitrile / 75 % water) was spotted onto a stainless steel sample slide and the solvent was slowly dried off in stream of warm air to form a layer of matrix material. 0.5 µl of an aqueous solution of peptide (10^{-4}M) was spotted on top of this layer and allowed to dry in air.

Each peptide was analysed by MALDI and then post-source decay analysis was performed to investigate the types of fragment ions formed. **Figure 5.40** shows typical MALDI spectra of the standards investigated. The amino-acid sequence of the peptide was used to calculate the accurate masses of all possible fragment ions and these values were used to assess a standard calibration curve obtained under standard calibration conditions.

The apparent masses of all fragment ions were measured by not applying the manufacturer's PSD calibration software and these values could be used to generate a new PSD calibration file, unique to the peptide of interest.

Figure 5.41 summarises the peptides investigated and the strongest fragments ions used to calibrate the spectrum. The fragments used for calibratrion purposes were all generated by a separate peptide program. These peaks were chosen because of their high intensities.

It was discovered that calibration curves generated for each peptide were not interchangeable, that is the most accurate data was obtained when unique calibration curves, specific to a peptide or a peptide residue, were used. This meant that a combination of poor resolution and an inaccurate calibration function made it virtually impossible to analyse fragment ions of an unknown type on this instrument.
All calibration functions generated shifted fragment ions of poly(isobutylene) in the same way described earlier. Furthermore, even if the calibration was carried out at the same laser power as the PIB samples shifts in fragment ions were also observed.

Peptide Ion Chemistry

All of the spectra generated by post-source decay analysis lacked of x, y and z fragment types of ions. All PSD spectra are dominated by a and b type ions.

Laser Energies

Threshold energies were measured at software values of 70 and optimum PSD spectra were obtained at software values of 90. These values were calculated using the equations defined in secrion 2.1.1 and corresponded to actual laser power densities of $9.0x10^6$ and $1.7x10^7$ W/cm^{-2} respectively. Both of these values are lower than laser power density values measured for any polymer sample.

PSD spectra of each of the peptides investigated are shown in **Figure 5.42.**

Figure 5.40

MALDI Spectra of Standard Peptides - All spectra were averaged over 200 laser shots (software laser power = 70)

a) Substance P

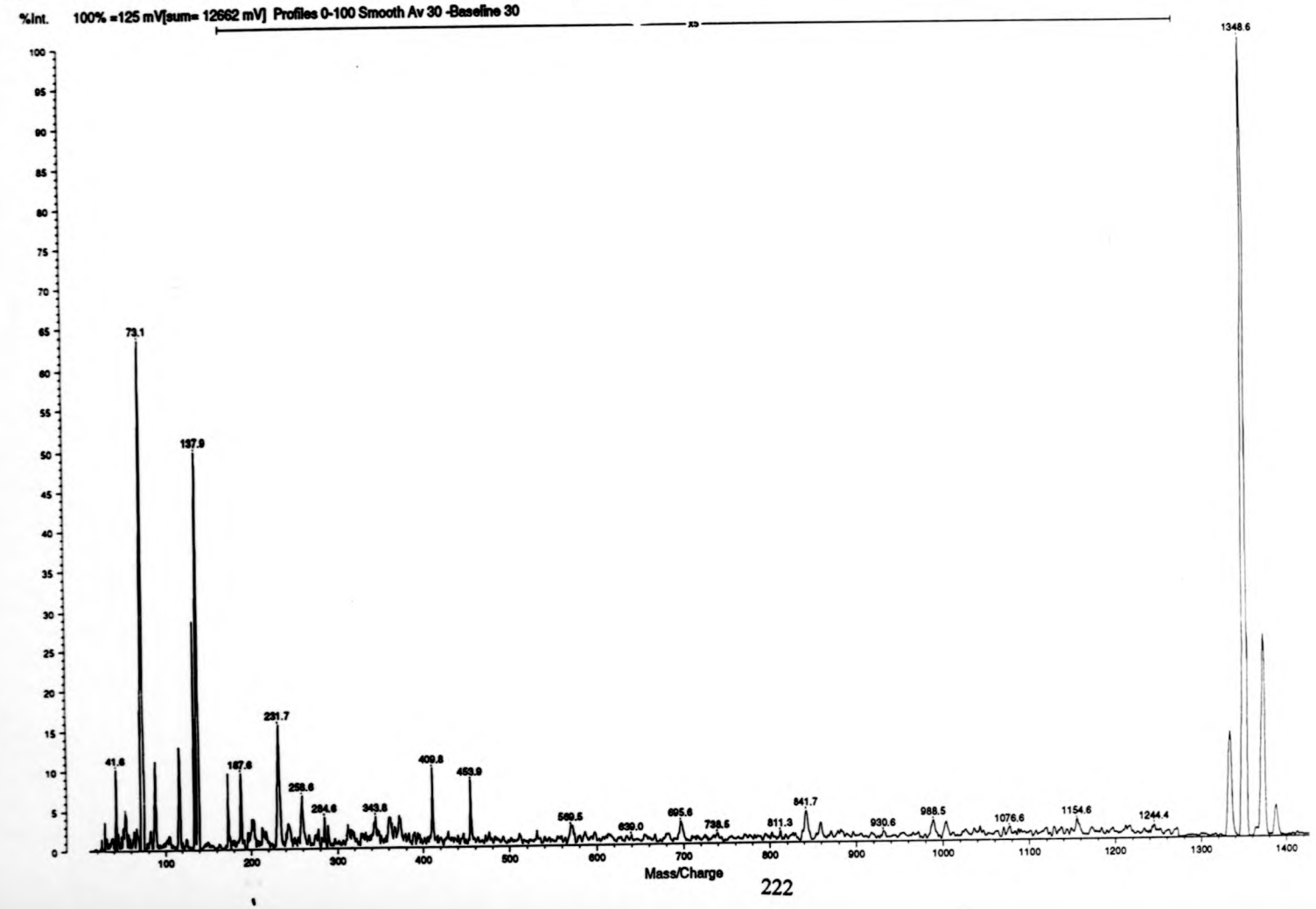

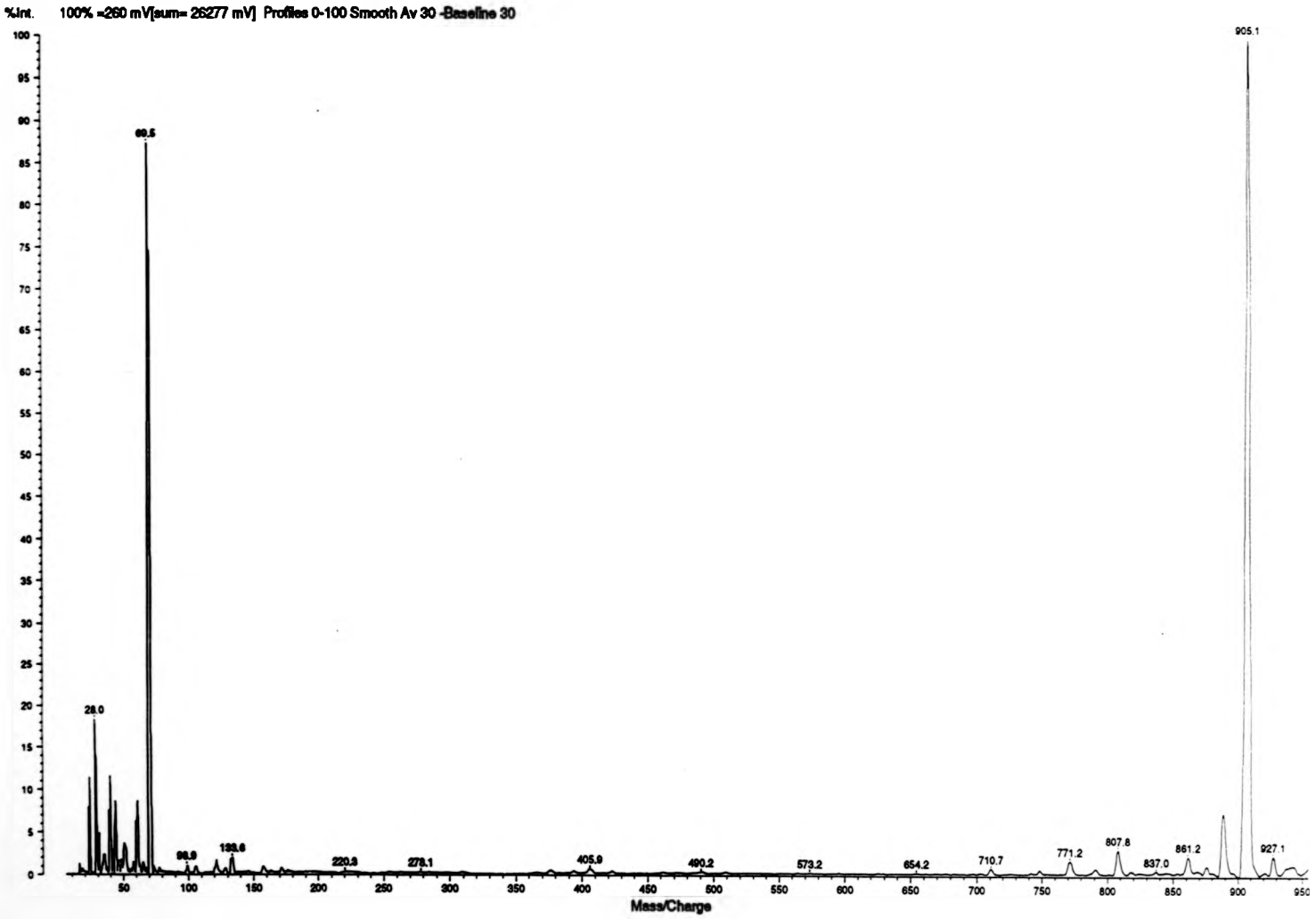
%Int.
100% =260 mV[sum= 26277 mV] Profiles 0-100 Smooth Av 30 -Baseline 30
905.1
88.5
28.0
Mass/Charge

c) Bradykynin

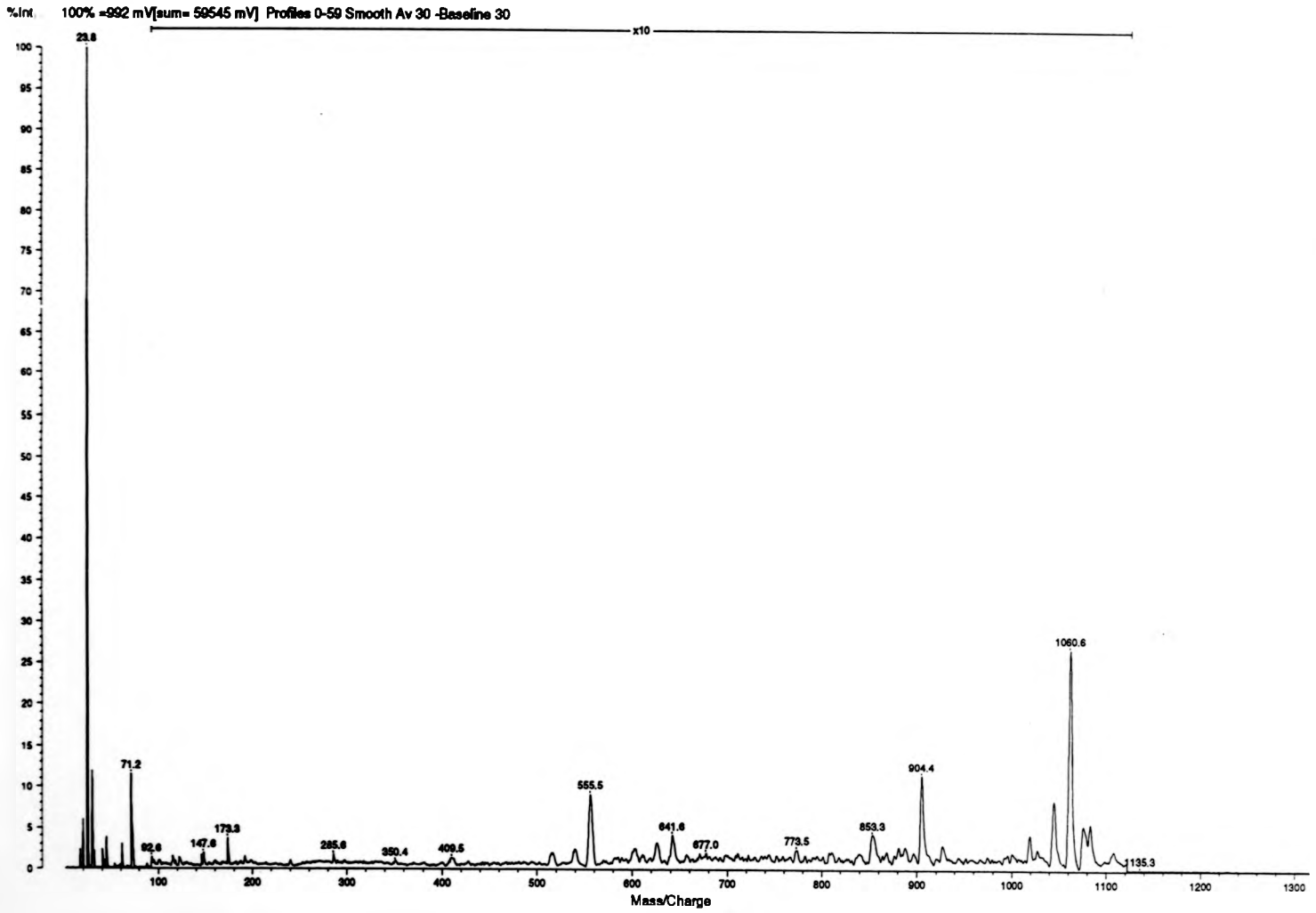

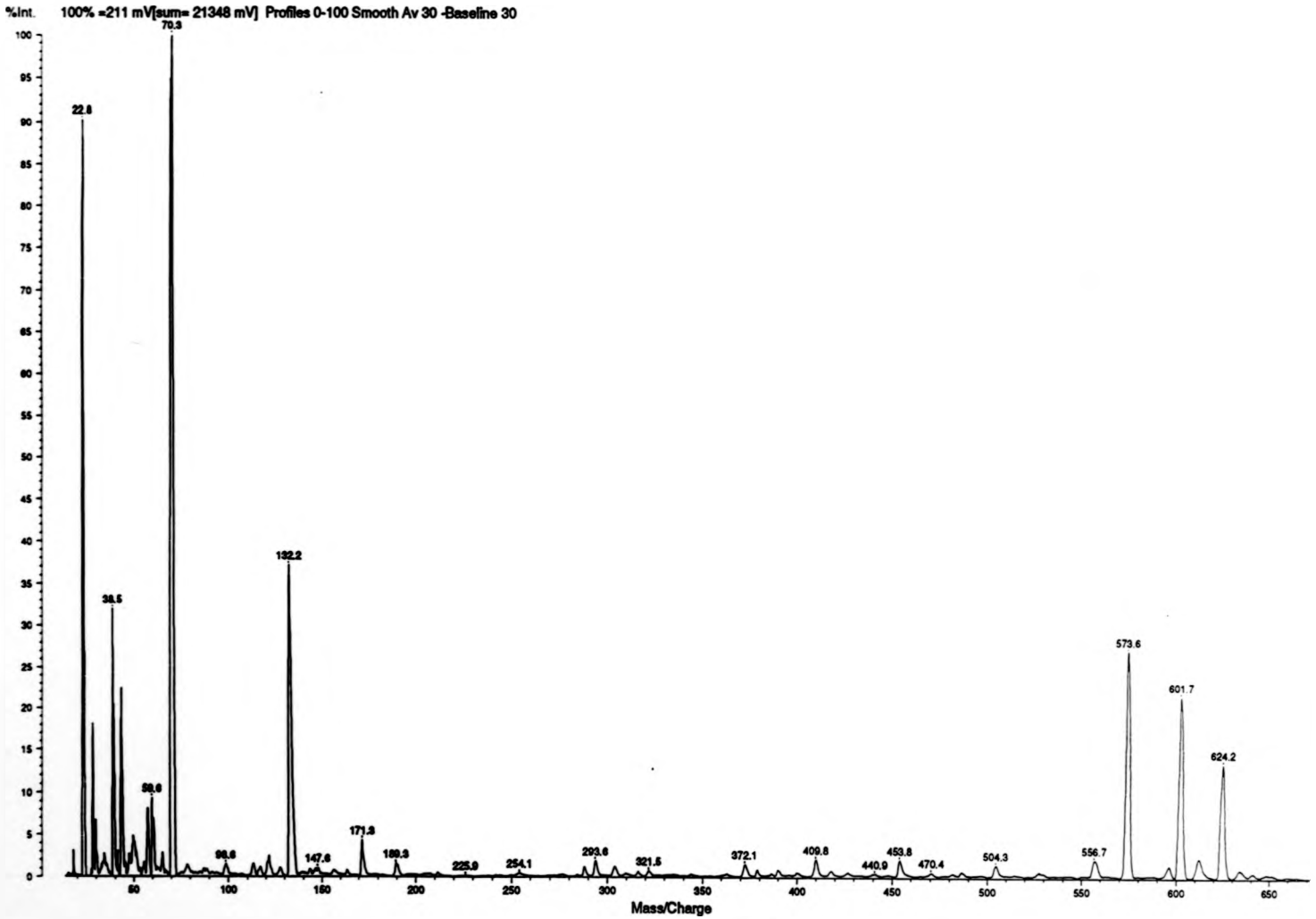
%Int.
100% =211 mV[sum= 21348 mV] Profiles 0-100 Smooth Av 30 -Baseline 30
70.3
22.8
38.5
58.6
132.2
98.6
147.6
171.8
189.9
225.9
254.1
293.6
321.5
372.1
409.8
440.9
453.8
470.4
504.3
556.7
573.6
601.7
624.2
Mass/Charge

e) Bradykynin Residue 572.7

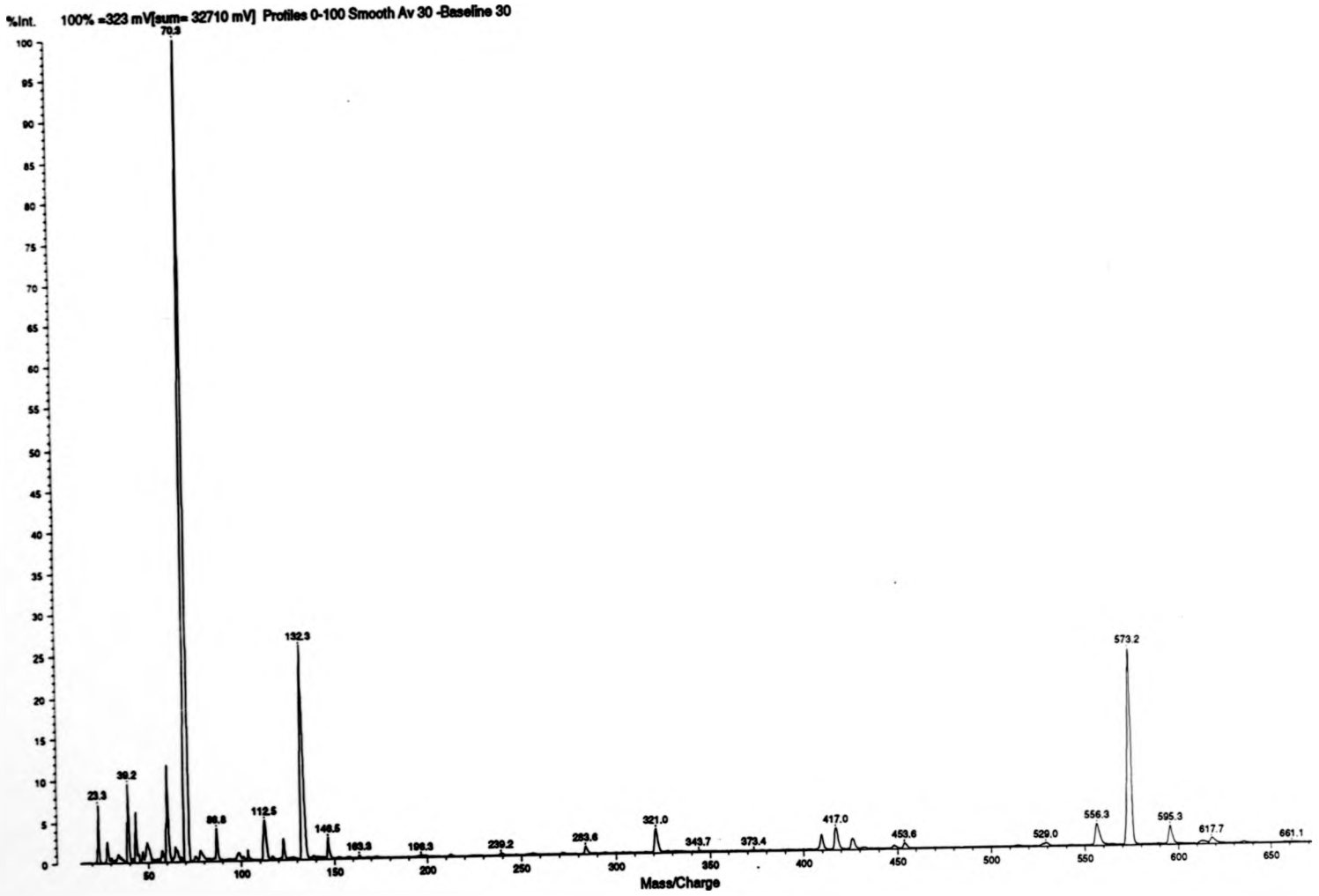

Figure 5.41
Summary of Peptide Fragment Ions Investigated by PSD

Name	[M+H]+	Sequence	Laser Power Density*	Fragments Used for Calibration
Substance P	1348.67	RPKPQQFFGL	1.70E+07	a" : 228.32, 356.50
			8.00E+06	a-17: 112.19, 209.30, 562.73
				b": 256.33, 384.51
				b-17: 237.31
				i : 86.16
Bradykynin	1060.23	RPPGFSPFR	1.70E+07	a: 859.03
			8.00E+06	a-17: 112.19, 510.65, 597.73
				b: 887.04
				c:570.68
				y : 903.4
				z : 305.36, 402.48
Bradykynin Residues	904.04	RPPGFSPF	1.70E+07	a-17: 112.19, 209.30, 306.42,
			8.00E+06	501.65, 597.73
				b: 157.20, 887.04, 254.31, 408.48
				b-17: 140.20, 237.31, 391.48
	600.68	PPGFSP	1.70E+07	a: 70.12, 167.23, 224.29, 555.66
			8.00E+06	b: 195.24, 252.30, 399.47, 486.55
				b-17 : 235.30
				c: 113.14
	572.67	RPPGF	1.70E+07	a: 129.19, 323.42
			8.00E+06	a-17: 112.19, 209.30
				b: 157.20, 254.31, 555.66
				b-17: 237.31

All fragment ions used for calibration purposes were calculated using software avilable on the Kompact IV Instrument
* Laser power density values quoted are in W cm^{-2}.

Figure 5.42

PSD Spectra of Standard Peptides - All spectra were averaged over 200 laser shots (software laser power = 90)

a) Substance P

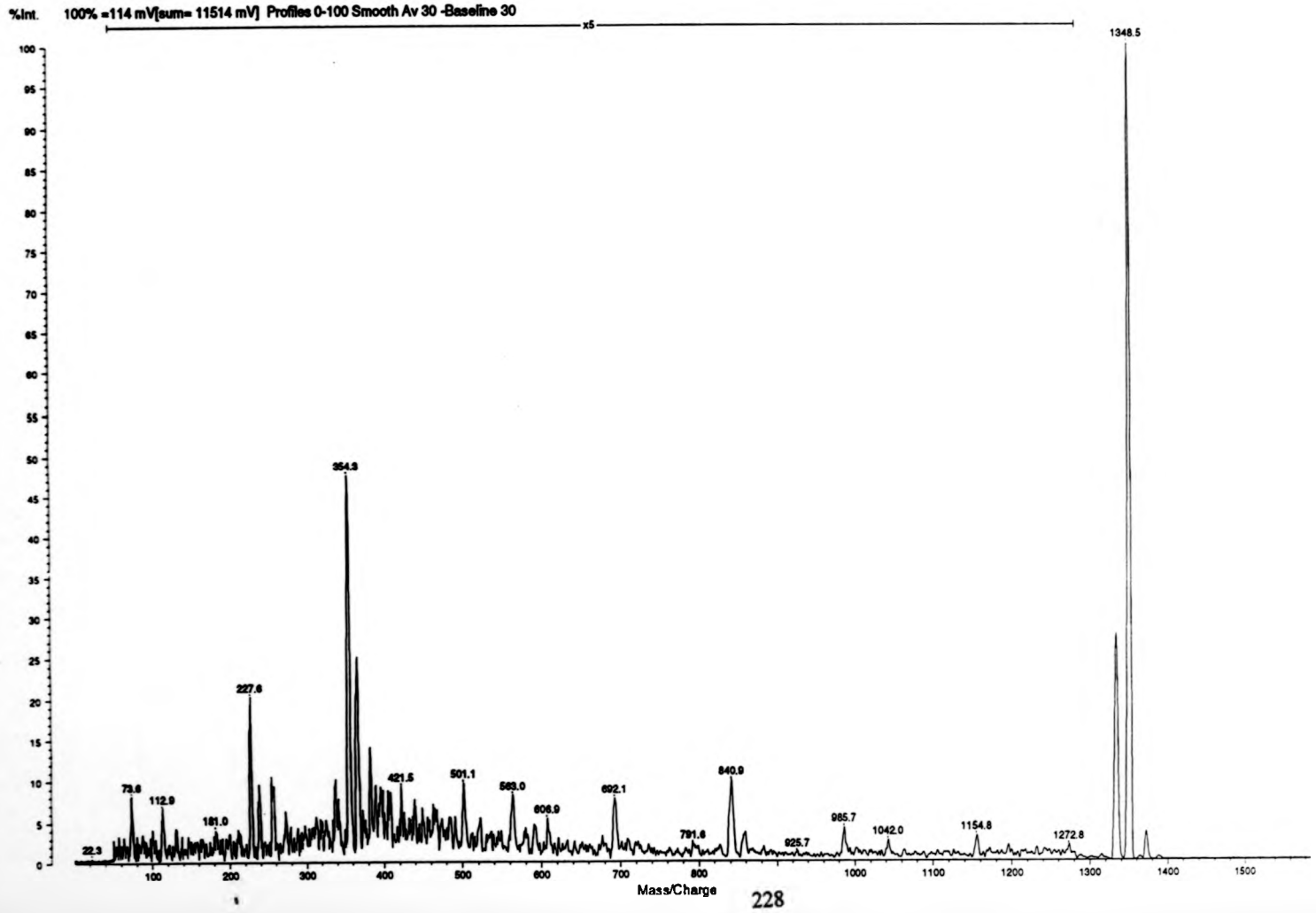

b) Bradykynin Residue 904

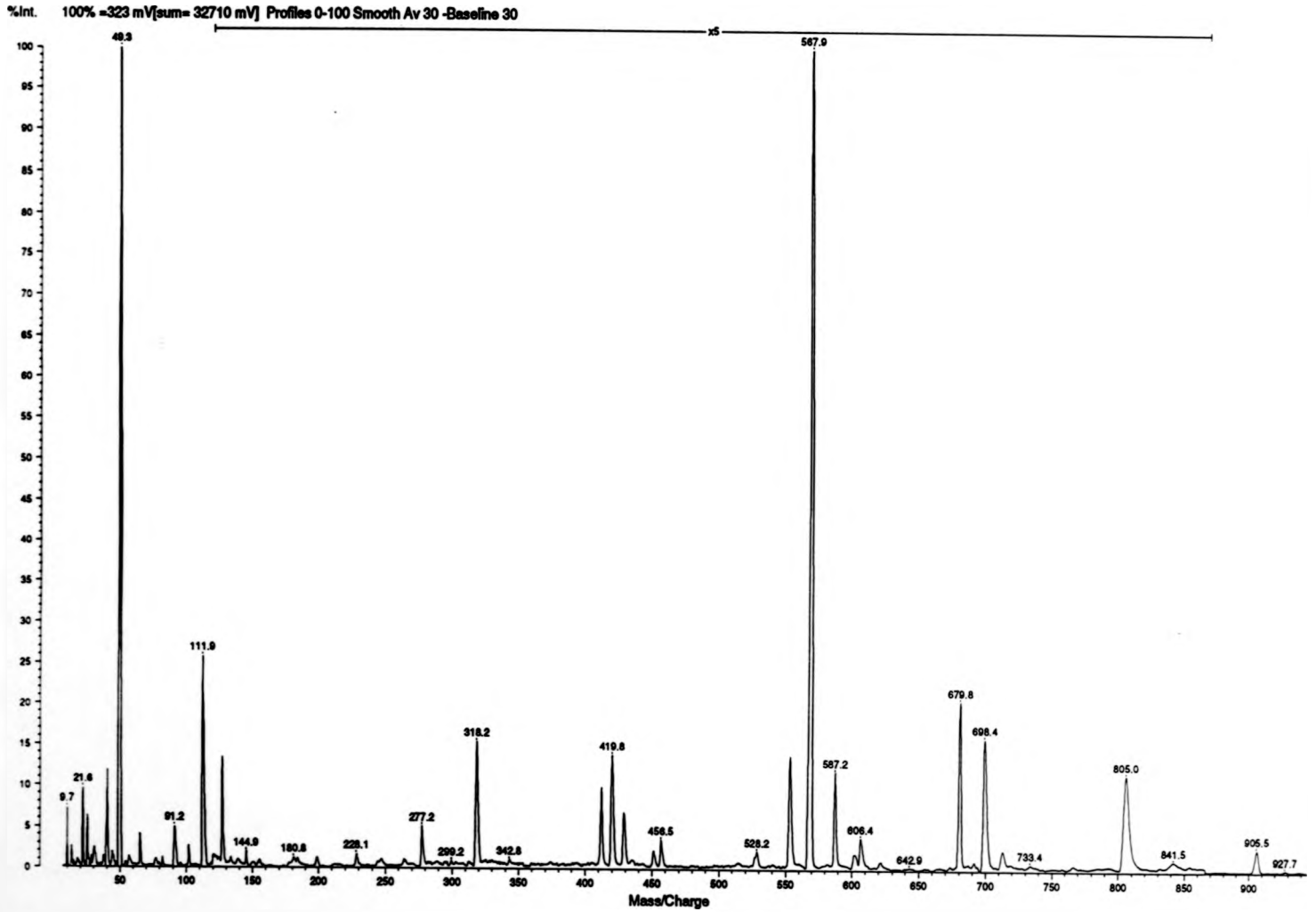

c) Bradykynin

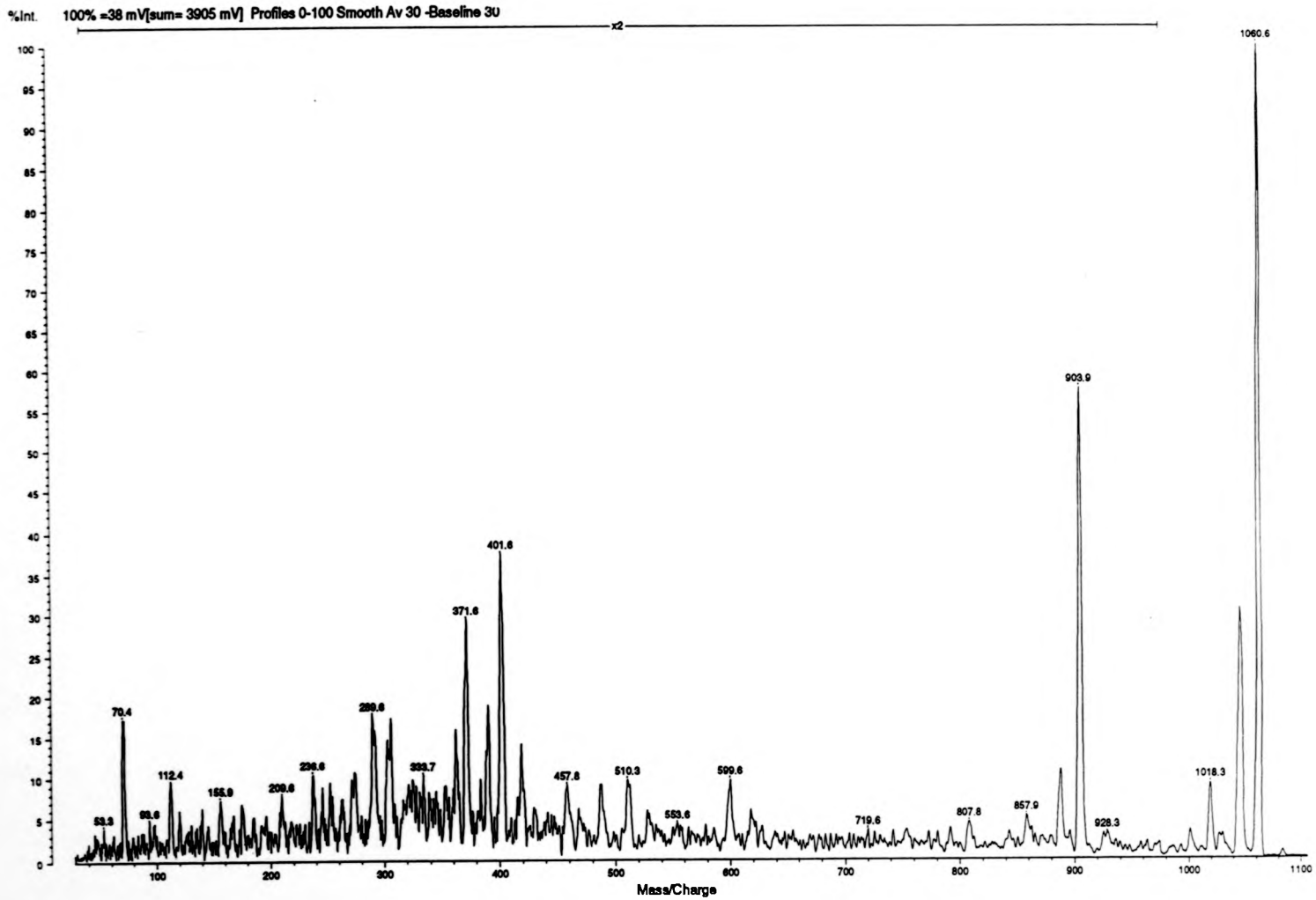

d) Bradykynin Residue 600.7

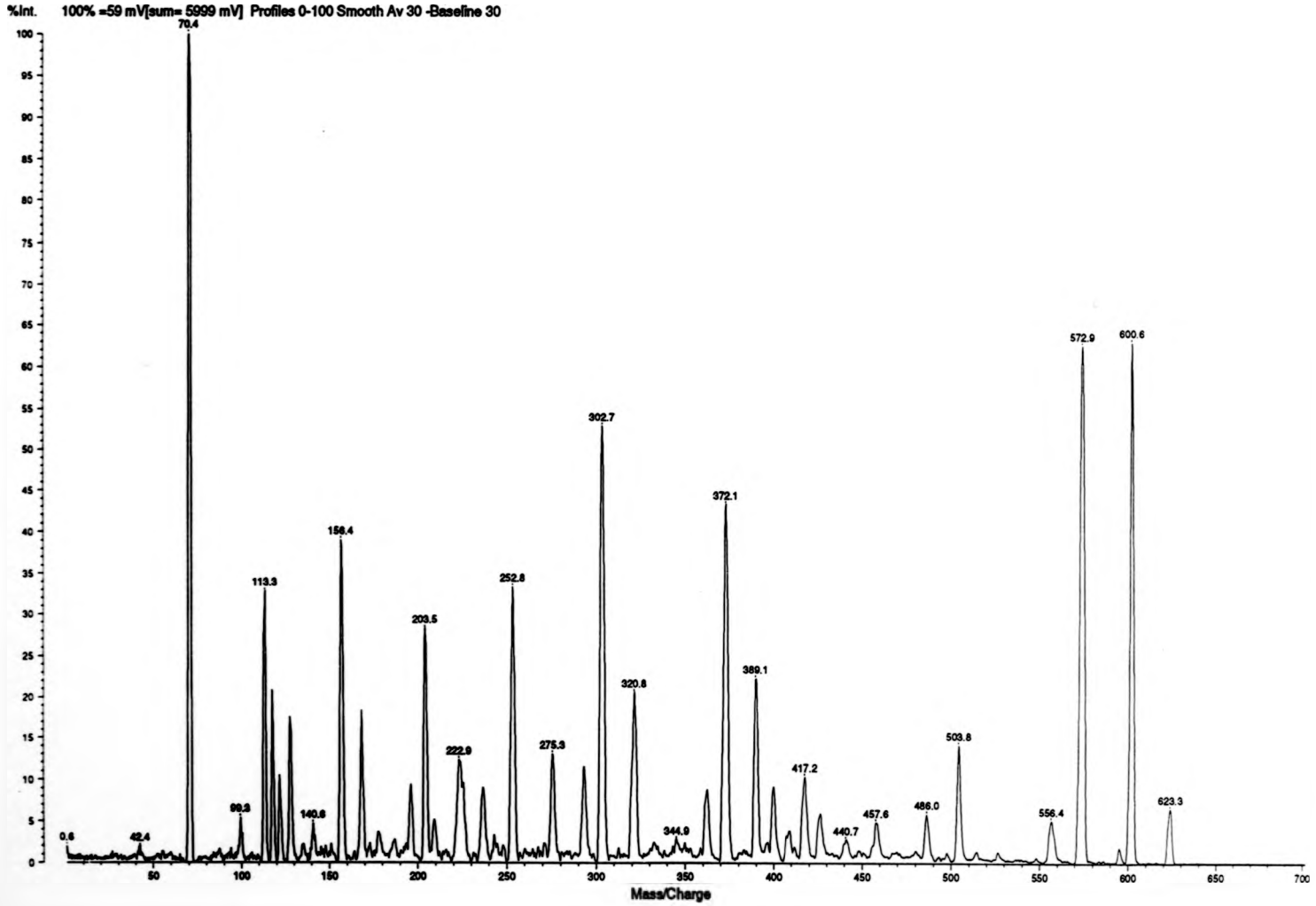

e) Bradykynin Residue 572.7

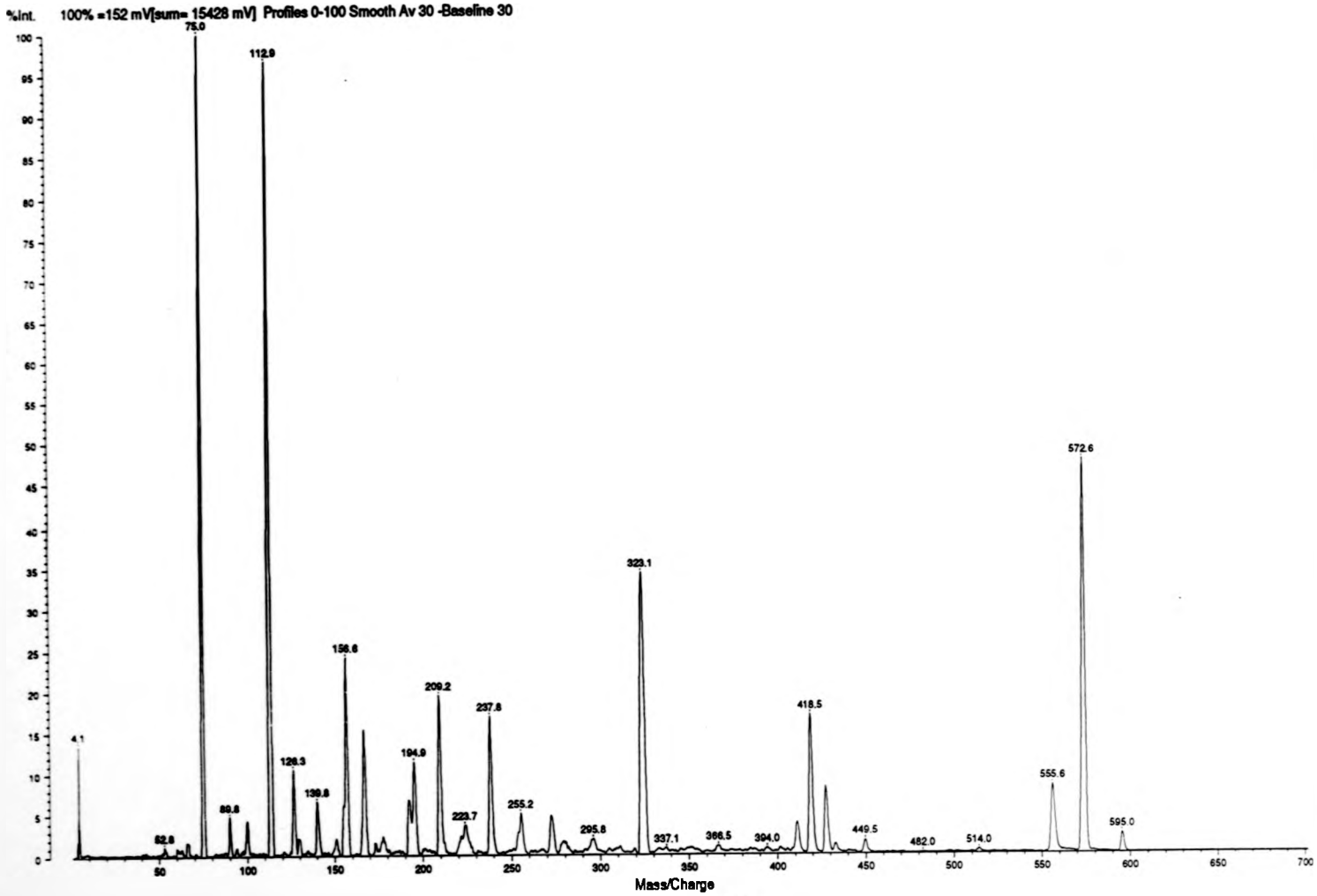

5.4 Discussion of Ion Chemistry

A brief discussion of the ion chemistry involved in MALDI is presented. Chapter 7 discusses these results in more detail in relation to conclusions drawn from other experiments.

5.4.1 Post-Source Decay Conditions

In general, all results were limited by the resolution and difficulties involved in calibrating reflectrons used to analyse fragment ions formed by post-source decay processes. Laser powers and pressure values were both crucial in determining the amount and type of fragment ions detected. Any variations between the data sets obtained from two instruments might be attributed to differences in these parameters. In general , PSD measurements were carried out higher laser powers and at lower pressures on the Biflex instrument, upto a factor of 10 difference in both cases.

Laser power quoted for the Biflex instrument were measured, whereas, those quoted for the Kompact IV instrument have been calculated, based upon a set of equations and reasonable assumptions. Laser powers may have been slightly lower than those quoted since degradation of the laser has not been taken into account in these calculations. The laser power range of the Kompact IV instrument was, however, lower than that available on the Biflex instrument.

Pressure on the Biflex instrument was measured directly during the course of a post-source decay experiment and this was measured to be in the range 1×10^{-6}- 5.0×10^{-7} mbar. If the pressure was allowed to decrease further the amount of fragment ions detected decreased significantly. The pressure on the Kompact IV instrument was measured indirectly and this had the disadvantage of increasing the volume to be evacuated. Furthermore, this measurement was made over the source region, not in the

time-of-flight region as in the Biflex instrument. A pressure of 9.0 x 10^{-6} mbar was measured. The backing pressure was approximately 7.8 x 10^{-4} mbar.

The pressure measurements were higher than those supplied by the manufacturer who had quoted an absolute pressure of ~6.0 x 10^{-7} mbar after pumping down the instrument over a minimum period of a week. These values could be verified indirectly by measuring a potential difference across two test points on the instrument. This method was regularly used throughout all PSD experiments and all measurements were found to be agreement with the values quoted by the manufacturer.

5.4.2 Ion Chemistry

PEG and PS were briefly investigated by post-source decay analysis in order to optimise suitable conditions. Both PEG and PS were ionised by MALDI to form adducts of the type [M+X+] where X = Na+ for PEG and X=Ag+ for PS. The threshold energies for these polymers were typically, 6.0x10^{6} Wcm^{-2} and 8 x$10^{6}Wcm^{-2}$ for PEG and PS respectively. Using the two-stage reflectron for the analysis of fragment ions formed by post-source processes meant that laser powers had to be increased as the reflectron voltage was stepped down at a rate of 6.21 x$10^{-2}Wcm^{-2}kV^{-1}$ and 6.39 x 10^{-6} $Wcm^{-2}kV^{-1}$ for PEG and PS respectively.

Both sets of oligomers fragmented in a similar way under these conditions. All fragment ions detected were cation attached and two main fragment ion series were observed:

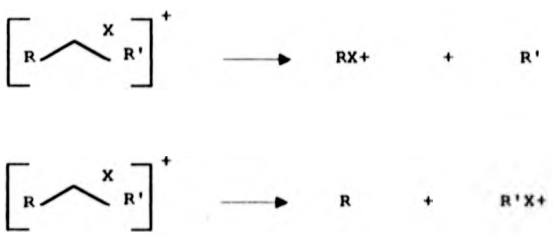

R'X+ and RX+ are the two main fragment ion series detected.

To summarise, both PG and PS required relatively low energies to form gaseous ions by MALDI but post-source decay processes required a significantly higher amount of energy in order to form the fragment ions described.

Poly(isobutylene) Fragment Ions

The threshold energies of the di-olefinic PIB sample and the tri-olefinic PIB sample were measured to be approximately 3.5×10^{7} Wcm^{-2} and this value was in agreement with measurements made on the other instrument. These values were higher than the threshold energy values of PEG and PS. Furthermore, the rate of increase of laser power with respect to the reflectron voltage in order to detect fragment ions was lower than that measured for PEG and PS, however, the formation and detection of low mass fragment ions of all types of polymer required laser powers in excess of 10^{8} Wcm^{-2}

The more highly-branched tri-olefinic sample fragmented more than the di-olefinic analogue under the same conditions. In general, more fragments were seen in the Biflex data and this was more than likely because these measurements were made at significantly higher laser powers.

The same types of fragment ions were detected in sets of data obtained from the two instruments for the di-olefinic PIB sample. In the case of the tri-olefinic PIB sample, there was a distinct lack of fragment ions detected in the mass range 300-700 although a set of base peaks were observed which were similar in structure to those detected on the other instrument. It was not possible to assign accurately these peaks owing to calibration difficulties but the most probable assignments were presented earlier and these are in agreement with other data sets.

Peptide Fragment Ions

The types of peptide fragmentation observed are in agreement with those published. The main observation was that MALDI post-source decay spectra were dominated by fragment ions of the type a, b, a-17 and b-17.

Peptide threshold energies were lower than those measured for polymers. This may be explained by the use of alpha-cyano hydroxy cinnamic acid as the matrix material in the analysis of peptides which is a so-called 'hot' matrix, said to encourage ion and fragment ion formation.

In general the types of ions detected by post-source decay processes are of the same type as those detected by low-energy CID experiments. on the Kompact IV instrument pressure was upto a factor of ten times higher and laser powers were up to a factor of ten times lower than on the Bruker instrument. It is, therefore, more likely that the fragmentations on the Kompact IV instrument were induced by collisions, whereas, on the Bruker instrument the more likely fragmentation process is unimolecualr decay as a result of excitation in the source by laser irradiation.

CHAPTER SIX

Field Desorption Mass Spectrometry and Emitter Activation Experiments

6.1 Introduction

Field desorption mass spectrometry (FD-MS) was initially reported in 1969[15a] and was the first desorption ionisation method to be used in mass spectrometry.[16,26,27,28] FD-MS is a variation of field ionisation mass spectrometry (FI-MS). In FD-MS samples are loaded directly onto an emitter whereas in FI-MS a gaseous sample is passed over an activated emitter.

FD-MS has been applied to the analysis of many different types of polymers and has many advantages over conventional ionisation methods.[136,137,139,140] Information on the repeat unit, the end-group and the number-average and mass-average molecular masses may be readily obtained since FD-MS gives the molecular mass of each individual polymer chain in the sample. Such data can help considerably in the determination of the polymer's composition and can throw light on the initiation, propagation and termination processes which are involved in the synthesis of polymers.

FD-MS is a particularly gentle ionisation method which results in very little or no fragmentation of large polymeric species and has the advantage of being particularly well-suited to non-polar analytes, in contrast to other techniques such as liquid secondary ion mass spectrometry, electrospray ionisation (ESI) and matrix-assisted laser desorption/ionisation (MALDI), FD-MS is routinely used in the analysis of petroleum products.

FD-MS has been effectively applied to determining the molecular mass statistics of a wide range of polymer standards including PEG[141], poly(styrene)[133,134], and poly(butadiene)[137] All data were in good agreement with those obtained by conventional methods such as SEC. More recently, polydisperse poly(ethylene) samples of low mass distributions have been investigated using FD-MS and data obtained showed poor agreement with SEC measurements[192].

Despite its obvious advantages, the growth and popularity of FD has been somewhat restrained. This may be attributed to the sudden success of matrix-assisted laser desorption/ionisation and the inherent difficulties involved in performing field desorption experiments.

One of the main disadvantages of FD is its reliance on the use of emitters. The preparation of good quality emitters with reproducible parameters has remained crucial to the success of FD. The emitter growing procedure is a particularly tedious and time-consuming method which requires special equipment and precious materials.

Many different methods have been used to obtain field desorption emitter wires, all based on the artificial production of sharp tips of conductible materials. The most widely used techniques have included electrochemical etching of thin-wire foils for field ionisation experiments[30,31], high-temperature and high-rate activation of tungsten wires in benzonitrile vapours by production of microneedles[28,33] or electrochemical activation by metal dendrites[32,34]. Recent work by Kosevich has described a new type of graphite emitter which was simply formed by fracturing a graphite rod.[35]

Despite these continuous efforts to develop faster and less complex alternative procedures, the use of benzonitrile as an activating agent has consistently resulted in the growth of emitter wires which have offered the best performance in terms of durability of the microneedles when subjected to chemical attack or thermal or mechanical stress[28].

Chan and co-workers developed a controlled method for the whole activation procedure of emitter wire growth.[199] Both indene and benzonitrile were investigated as suitable activating agents, although only emitters activated with benzonitrile were found to be suitable for use in FD experiments. Furthermore these emitter were made by growth of carbonaceous microneedles on 25 μm tungsten wire as opposed to 10μm which has generally been used. This has meant these emitters were particularly robust. The control program written by Chan [191] was specifically designed to grow emitter wires for use on a large-scale mass spectrometer and these emitters differed in dimensions from those required to perform field desorption experiments on the four-sector instrument. In this chapter, a series of experiments are described which were part of an attempt to grow successfully emitters on 25μm tungsten wire for use on the four-sector instrument.

The overall aim of this work was to study non-polar polymers such as poly(isobutylene) and poly(ethylene) by field desorption mass spectrometry and to investigate fragmentation patterns of these polymers using low-energy and high-energy collision-induced dissociation experiments. Experiments performed using these techniques would provide invaluable medium-to-high resolution data concerning molecular mass statistics, repeat units and end-group information which are not available by other means.

6.2 Emitter Activation Experiments

All experiments were carried out on the field desorption emitter activation unit using a computer controlled procedure written by Chan as described in chapter 2.
Emitters used on the four-sector instrument were composed of nichrome posts mounted on a ceramic base with 5mm separation between posts. This distance was shorter than the computer program had originally been designed for.

A general methodology was followed before the computer program could be activated and this is described below.

6.2.1 General Preparation

25μm diameter tungsten wire was spot welded to the top of the support posts with sufficient tension to produce a straight wire. Welds which resulted in the flattening of the wire into a leaf shape were required since these produced wires of a minimum resistance and such welds could be checked under a powerful magnifying glass for consistency. Batches of five emitters were loaded into the vacuum chamber and care was taken to ensure that all emitters were level so that they were positioned exactly 2 mm from a grounded counter electrode made from stainless steel. After each activation procedure, the counter electrode could be removed and cleaned to removal carbon deposits. This surface was periodically sand-blasted to remove any lingering deposits. Benzonitrile (Aldrich Chemicals) was leaked into the vacuum chamber via a needle valve. It was degassed by freezing with liquid nitrogen and then allowing the liquid to thaw and freeze and by pumping away evolved gases. This thaw-freeze cycle was repeated three times or more or until no more gases evolved and this was checked by observing the pressure readings on a Pirani gauge. The chamber was repeatedly flushed with gaseous nitrogen to ensure that no oxygen, detrimental to the whole activation procedure, was present in the vacuum chamber and left to pump down overnight until the pressure reached a minimum value of 4×10^{-4} Torr.

6.2.2 Computer Controlled Experiments

Carburisation Procedure

A constant power of ~ 0.19W per emitter wire was used in a benzonitrile pressure of 1×10^{-2} mbar for 40 minutes to pre-activate or carburise the emitter wires. This process converted tungsten into tungsten carbide and, in general, the total resistance of the wires increased to between 5 and 6 Ohms. The emitter wires glowed during this

process since a wire temperature of ~ 1600K was required for carburisation. This process was controlled by the computer program. After successful carburisation, the computer program was paused in order to obtain the correct pressure settings required for the second part of the process, activation.

In general, if sufficient care was taken in preparing the emitter wires, the computer program worked well for this part of the emitter growing process.

Activation Procedure

This process took a total of 48 hrs and had previously been completely automated using a pre-set power-resistance isotherm for the activation of larger FD emitter wires. The computer program used the following experimental values which had been established by manual activation experiments. For the first 4 hours, the high potential was held at 14kV at a constant power of ~ 0.15 W. This ensured that the carburisation process was complete and allowed the initiation of growth of carbon deposits as protrusions. During the next 6 hours, the high potential was decreased gradually to 10kV, which, in theory, would allow the enlargement of carbon protrusions along the length of the tungsten wire. Over the next 15 hours, the high potential was set to decrease steadily to a value of 6kV. These conditions would allow the micro needles to grow and branch on the protrusions. The final stage of the activation procedure took place after 25 hours and involved the elongation of the micro needles at a constant potential of 6kV.

This computer controlled power-resistance isotherm removed the necessity for constant manual adjustment of the current since the resistivity of the emitters changed during the activation period. However, repeated attempts to grow emitters using this computer controlled program failed. In general, the emitters consistently broke during the first 2-3 hours of the activation process.

Figure 6.1 shows the power-resistance isotherm followed by the computer program. The position at which typical emitter breakage occurred is labelled.

Figure 6.1

Power-resistance isotherm followed by the computer controlled activation program

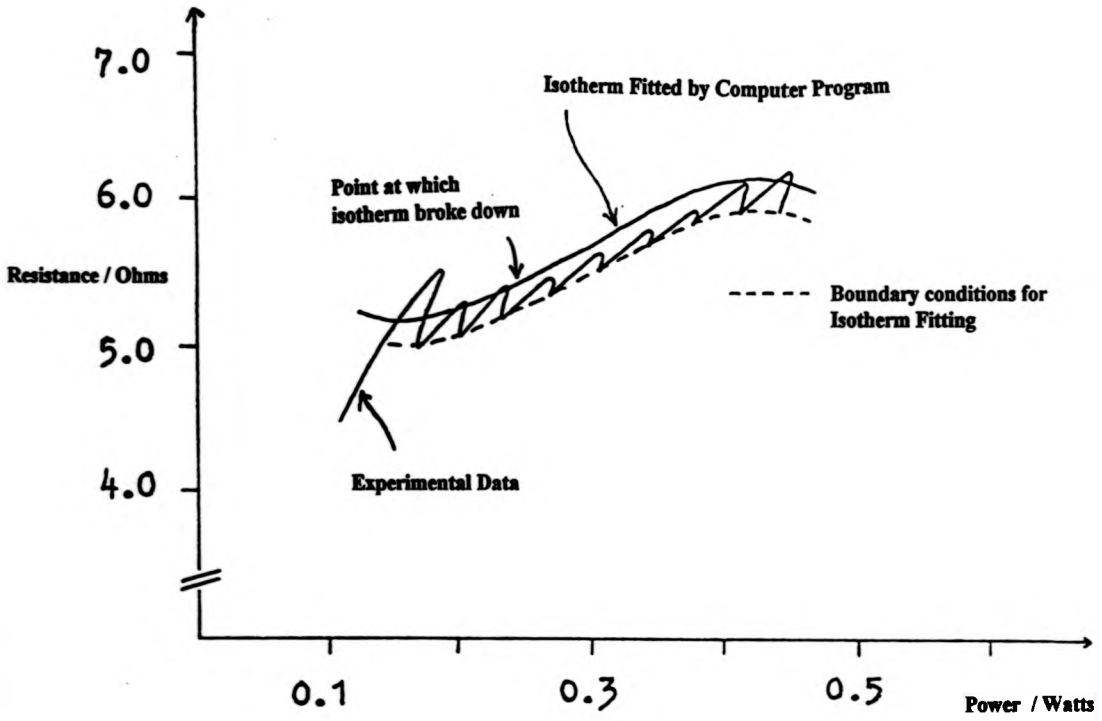

6.2.3 Manual Emitter Activation Experiments

The same preparation procedure was followed for these experiments up and including the automated carburisation process. Experimental activation data quoted by Chan was used to give an indication of the experimental parameters required for successful emitter activation **Figure 6.2** shows typical parameters used to attempt manual emitter activation.

Manual experiments of this kind yielded emitters of poor quality. The main problem was that the carbon micro needles were unevenly deposited along the length of the tungsten wire, furthermore, the needles were typically short in length.(10-20μm) It was clear from these experiments that the computer program needed to be completely re-worked using fresh experimental data obtained by from manual experiments, optimising the conditions under which these specific emitter wires could be activated.

6.3 Field Desorption Mass Spectrometry

A brief set of experiments were carried out on the four-sector instrument. Emitters were provided by Mr. P. M. Lloyd. Liquid-secondary ion mass spectrometry(L-SIMS) was initially performed using caesium iodide to calibrate and tune the instrument.
Cholesterol was chosen as a suitable standard with which to optimise L-SIMS conditions and then attempt field desorption experiments since it is well-characterised and field desorption/ionisation of this compound was reported to be relatively straightforward.

The molecular structure of cholesterol is shown in **Figure 6.3 and Figure 6.4** shows a L-SIMS spectrum of cholesterol obtained on the four-sector instrument (using thioglycerol as the liquid matrix)

Figure 6.2

Typical parameters used to attempt manual emitter activation.

Time (hrs)	High Potential (kV)	Emitter Heating Current (V)
0.5	14.0	0.9
2.5	14.0	0.9
4.5	14.0	1.0
6.5	13.5	0.9
8.5	12.5	0.9
10.5	11.5	1.0
12.5	10.4	1.0
14.5	9.6	1.0
16.5	8.8	1.0
18.5	8.0	1.0
20.5	7.2	1.1
22.5	6.4	1.2
24.5	6.0	1.2
26.5	6.0	1.3
28.5	6.0	1.3
30.5	6.0	1.3
32.5	6.0	1.4
34.5	6.0	1.3
36.5	6.0	1.3
38.5	6.0	1.3
40.5	6.0	1.3
42.5	6.0	1.3
44.5	6.0	1.3
46.5	6.0	1.4
48.5	6.0	1.5

Figure 6.3

Molecular Structure of Cholesterol

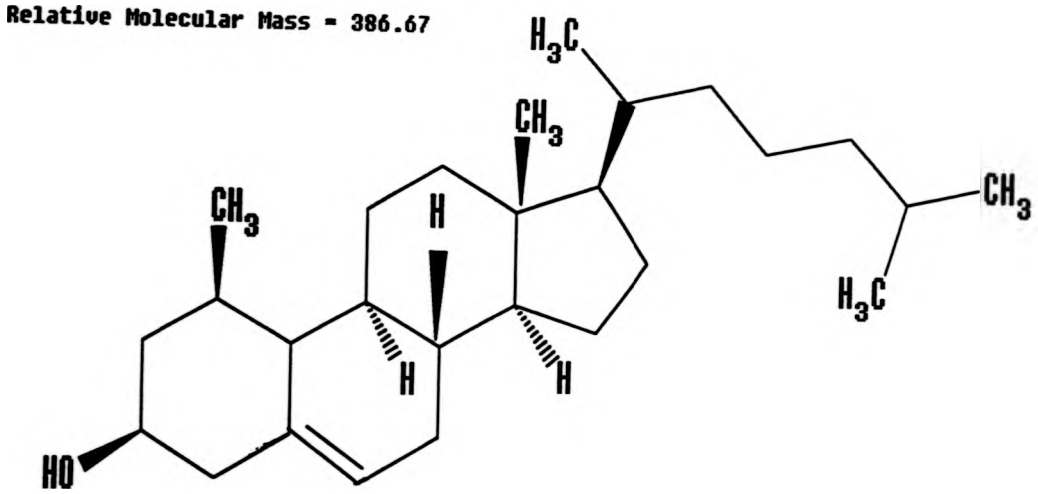

Figure 6. 4

L-SIMS Spectrum of Cholesterol

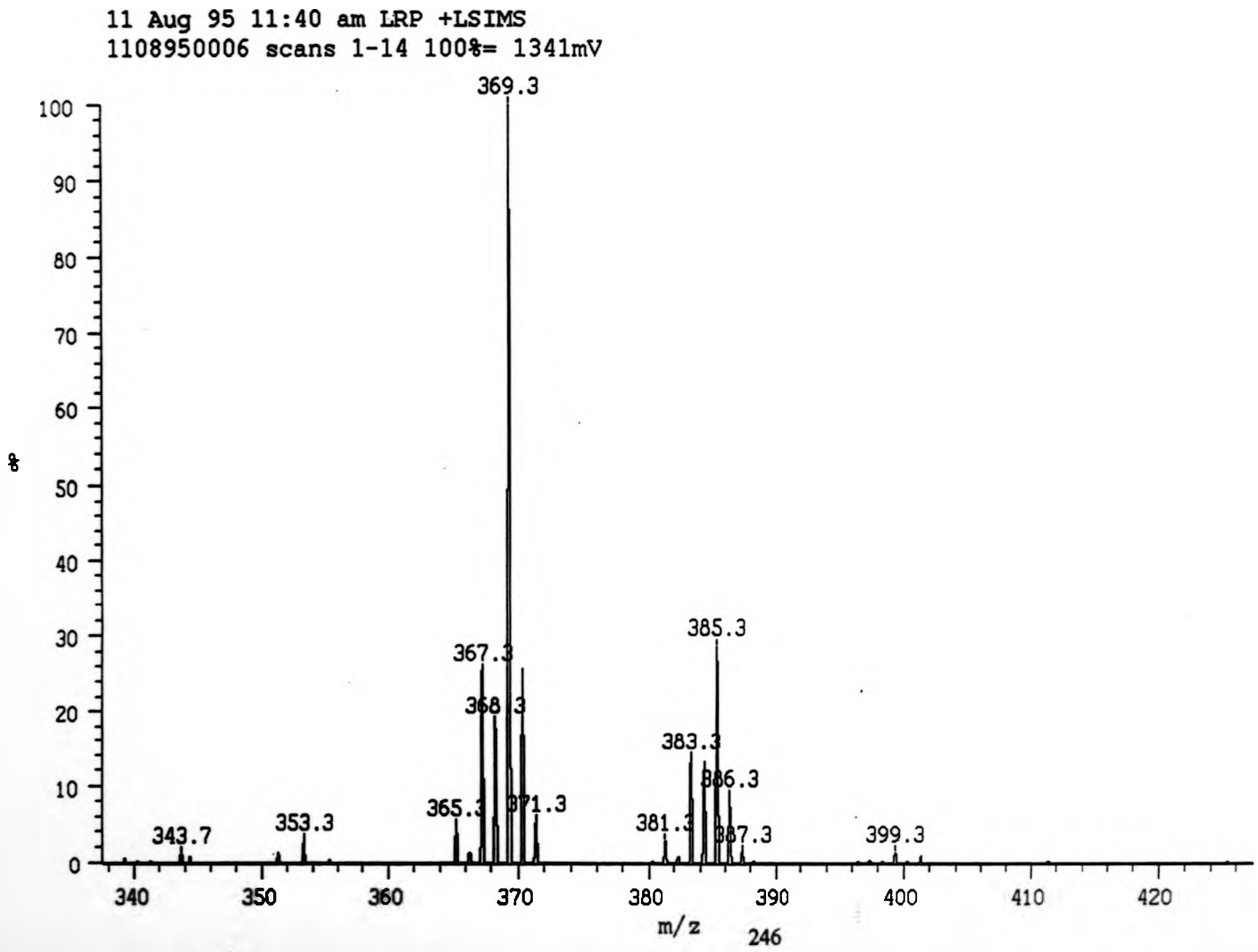

6.3.1 Sample Preparation and Emitter Loading

Samples were placed in a small glass dish and dissolved in ~ 5µl of a suitable spectroscopic grade solvent. In the case of cholesterol, acetone was used as the solvent. FD emitters were repeatedly dipped into this solution and excess solvent was evaporated between dippings by drying in a stream of warm air. Between each dipping, emitters were checked for sufficient quantities of sample deposited on the microneedles and also for an even coating under a powerful magnifying glass. Excess solvent was removed from the top of the emitter posts by careful washing with solvent.

The emitter-counter electrode distances were set by insertion of an unactivated emitter base perpendicular to the normal positioning of the probe into the source chamber until it reached the counter electrode. The required distance was set by retracting the probe using a micrometer attached to the probe handle. Since the emitter was mounted onto a probe tip, it was not possible to correct misalignment in the z and y directions caused by variation in the emitter bases.

6.3.2 Emitter Heating and Desorption of Samples

Emitters were heated using a constant current supply and the emitter heating current (EHC) was manually adjusted gradually until the total ion current (TIC) measured at the counter electrode increased. The most stable ion currents and successful experiments resulted when the EHC was increased over a period of about an hour. Typical EHC value for cholesterol was measured to be 60mV.

Figure 6.5 shows a typical FD spectrum of cholesterol obtained under these conditions.

The mass spectrum obtained using the field desorption source was observed to be weak. Ion optical modelling of this source by Makarov using the SIMION program had revealed a series of problems as described in chapter 2.

Figure 6.5

Typical Spectrum of Cholesterol Obtained by FD-MS

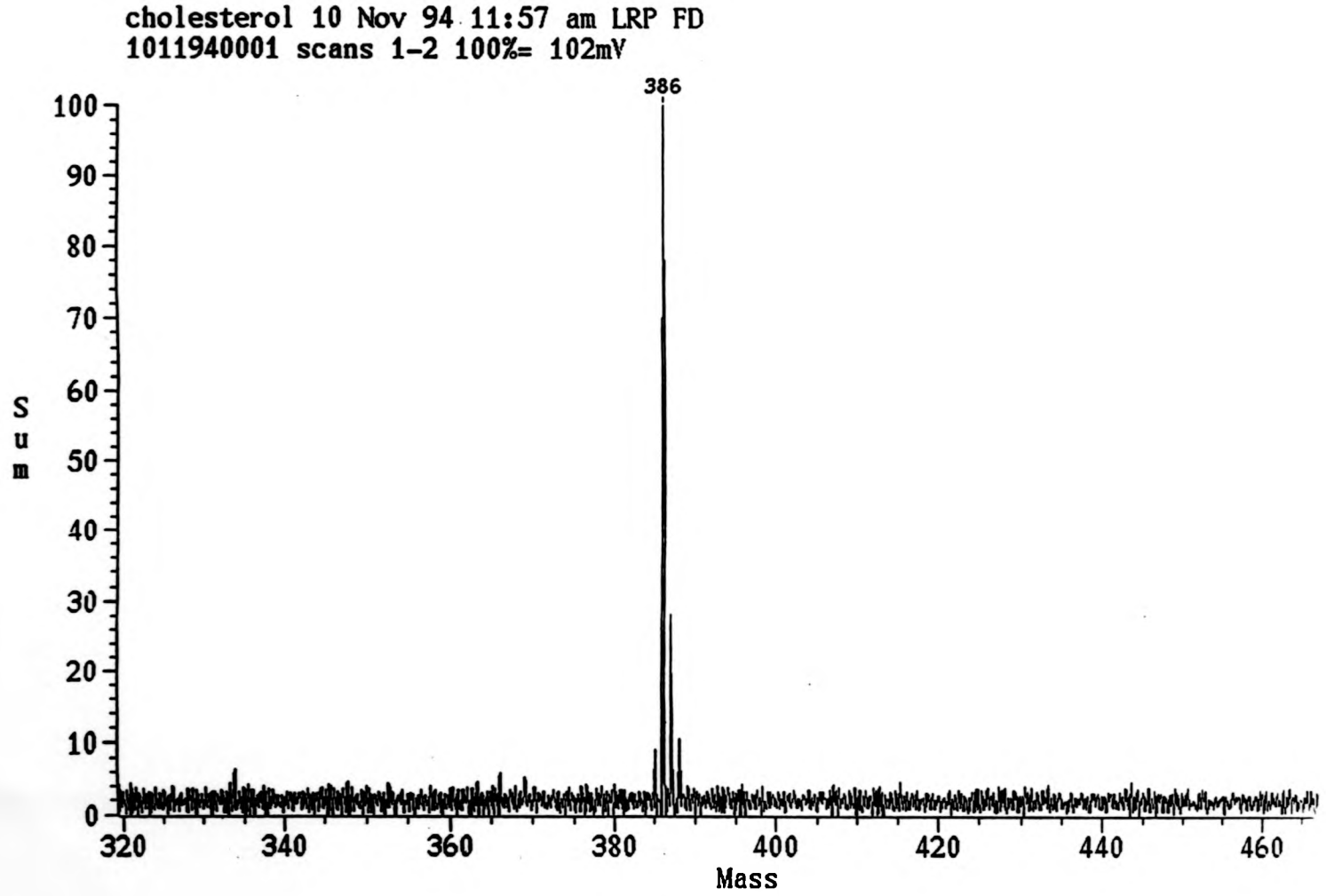

6.4 Conclusions

The difficulties encountered in repeated attempts to perform successfully field desorption mass spectrometry have briefly been described. The determining factor in these experiments' failure was the lack of a regular supply of suitable emitter wires. The problems with the computer controlled program have been described and the main conclusion is that extensive research on optimum emitter growing conditions would have been required. The fact that the program failed consistently in the same position may give some indication as to the type of adjustments needed. Flaws in the field desorption ions source have also been revealed. Further modifications may have to be made in order to obtain optimum total ion current values needed to perform tandem mass spectrometry experiments.

CHAPTER SEVEN

Conclusions and Further Work

7.1 Matrix-Assisted Laser Desorption/Ionisation of Synthetic Polymers

7.1.1 Hydrocarbon Polymers

Matrix-assisted laser desorption/ionisation has successfully been applied to the analysis of a range of synthetic polymers, including poly(ethylene glycol)(PEG), poly(methyl methacrylate)(PMMA) and poly(styrene)(PS). Choice of matrix material was shown to be crucial in such experiments. Essentially polar polymers such as PEG and PMMA have been investigated using similarly polar matrices, in particular, 2, 5 DHB has proved to be an effective matrix in such experiments. PEG and PMMA species were detected as alkali-cation adducts. The effect of cation concentrations on measuring resolution and mass distributions are subjects for present debate and research. In the experiments performed on a range of PMMA standards, it was observed that oligomers of different sizes had different affinities for different types of alkali-metal cations. Oligomers of higher masses had greater affinity for potassium cations than sodium cations. Theories which might account for such observations focus on the relative sizes of cations compared with polymer chains[200] and the gas-phase kinetics of the cation attachment process[156]. Cation addition has proved to be extremely useful in the analysis of synthetic polymer and most sample preparation methods rely on doping to enhance signal-to-noise values and intensities of polymer distributions. Hydrocarbon polymers such as poly(styrene) have been shown to interact favourably with transition metal cations, whereas, more polar moieties such as PEG possess higher affinities for alkali-metal cations. These observations have so far been discussed in terms of hard soft acid base (HSAB) Theory[153] No investigations have been carried out on the gas-phase chemistry involved in the polymer cation interaction.

The aim of early experiments was the successful analysis of hydrocarbon polymers, such as poly(ethylene) and poly(isobutylene) by MALDI-TOF mass spectrometry. The physical nature of such polymers and their incompatibility with most of the matrices in common use made investigations in this area difficult. Experiments which have been performed are described in chapter three. 9-Nitroanthracene, an essentially non-polar matrix, was successfully applied to the analysis of poly(isobutylene) polymers containing an aromatic ring function up to molecular masses of ~ 1000 Da. Silver cation addition was critical in obtaining MALDI spectra. Research by Hercules and colleagues has shown that silver cation addition was required in the analysis of poly(butadiene) using secondary ion mass spectrometry (SIMS).[201] Furthermore, poly(isobutylene) samples possessing no phenyl function proved to be impossible to analyse under the same conditions. All species were detected as [M + Ag +], M being the molecule ion. The observation that the ability to obtain MALDI data was dependent on end-group functions is in agreement with experiments performed by Waterson and co-workers[202] who has shown that a direct link exists between the nature of end-group function on poly(methyl methacrylate) and ability to obtain MALDI data. Recent research on matrices and sample preparation has investigated the possibility of using electron transfer reagents such as coumarin dyes[203]. Such matrices might be useful in the analysis of hydrocarbon polymers Research by Belov and Myatt is investigating a different approach which relies on the gas-phase interactions of metal cations with neutral polymer species.[204]

Poly(isobutylene) samples analysed are, to date, the most non-polar investigated by MALDI-TOF mass spectrometry .More recent work has shown that azo-compounds are also effective cationisation materials for the analysis of synthetic polymers by MALDI including poly(styrene)[205]. Danis and co-workers have reported a sample preparation method for the analysis of ' hydrocarbon' polymers based on silver cation addition.[206] The fact that 9-nitroanthracene in combination with silver cationisation also works well for a range of more polar polymers such as poly(sulfides) has shown

that phenyl functions were not essential for successful analysis, however, sulfur functions are well-known for their strong interactions with silver and this might be a determining factor.

To conclude, progress has been made in the analysis of hydrocarbon polymers by MALDI-TOF mass spectrometry, however, much more research needs to be performed to understand and control the fundamental ion chemistry involved in the MALDI process so that this technique may be applied to difficult classes of compounds such as inorganic salts and hydrocarbon polymers.

7.1.2 Molecular Mass Calculations

Molecular mass statistics obtained by MALDI-TOF mass spectrometry for a range of PS and PMMA polymers with narrow poly(dispersity) indices have been shown to be in good agreement with those derived form size exclusion chromatography (SEC) measurements[195]. PS was analysed using 9-nitroanthracene in combination with silver cation addition, whereas, PMMA was investigated using 2,5 DHB only. The same sample preparation used for PS was applied to PIB analysis, however, it was observed that molecular mass data derived from MALDI-TOF mass spectrometry measurements were in poor agreement with those derived from SEC and those quoted by the manufacturer. Statistics quoted from MALDI were often up to 15% lower than expected even though these samples had a low poly(dispersity) index value (≤1.1). This observation was surprising since it has been generally accepted with both polymer and mass spectrometry communities that polymers of low poly(dispersity) values compare well between mass spectrometry and SEC. SEC data measured at Warwick may be considered to be less accurate than normally expected and this may be attributed to the lack of suitable calibration standards. Poly(sulfide) were analysed by MALDI-TOF mass spectrometry and a set of molecular mass statistics were derived from these data. These statistics showed poor agreement with values calculated from

SEC, however, this may be attributed to the fact that these polymers have high poly(dispersity) index values (≥2).

The reasons why polymers of broad mass distributions are under represented in MALDI spectra were unclear. Montaudo and Spickermann both claim to have separately developed experimental methods to overcome such problems and involve measuring the intensities of salt clusters or fractionating the polymer into units of mass distributions[170,171,172,173]. Instrumental parameters were certainly in no part to blame, and McEwen[167] has recently summarised the factors involved The fundamental understanding of the MALDI process required to overcome the difficulties involved in the analysis of high mass polymers of broad mass distributions is still lacking and more research is required before polymer chemists may rapidly and accurately obtain absolute molecular mass statistics from MALDI data.

7.2 Post-Source Decay Investigations

Fragment ions detected in post-source decay (PSD)experiments were typical of those obtained by mass analysed kinetic energy and low-energy collision induced decomposition (CID) experiments using field desorption/ionisation.

Data obtained for PS and PEG were in agreement with those derived from FD experiments of this type[139,140,142]. Such observations suggest that the type of post-source decay processes which may occur were typically unimolecular decay decompositions or resulted from low-energy collisions between parent ions and residual gas molecules or a combination of reactions. Furthermore, pressure measurements on both instruments showed that PSD ions could only be detected within specific pressure ranges. The observation that the intensities of fragment ions increased with the use of collision gases supports this conclusion.

Pressure values were up to a factor of ten lower on the Bruker instrument than on the Kompact IV. It may, therefore, be tentatively suggested that ions detected using this instrument were more likely to be products of predominantly unimolecular decay processes. This theory is supported by the observation that laser powers of up to a factor of ten higher were needed to detect PSD ions and this observation might be attributed to the relatively high amounts of internal energies required to encourage molecule ions to fall apart within the time scale of these experiments.

Both PIB samples fragmented in the same way under these conditions, forming fragment ions of the same type. Silver ions were not detected as discrete species in either case. It may be inferred that the majority of ions observed were products of unimolecular decay processes. Low-energy CID experiments have been recently performed on electrospray-generated silver I complexes of peptides by Li and co-workers[206] . The main observations were that a multitude of silver-containing product ions dominated the spectra and that changing end-groups on the peptide from a carboxylate to an amide altered the types of product ions seen, Furthermore, no discrete silver clusters were detected. These findings are in agreement with the experiments performed on PIB silver adducts and suggest that low energy CID is a contributing process in the formation of fragment ions.

Experiments on the Kompact IV mass spectrometer were carried out at significantly higher pressures and up to a factor of ten lower laser powers. PIB fragment ions were of the same type as those detected on the Bruker instrument. In general, these fragment ions were lower intensities, although, at lower masses, m/z = 100-200, fragment ions were much more intense. Unfortunately, owing to the calibration difficulties with the manufacturer's software, it was not possible to assign structures to these fragments, however, it may be inferred that these ions were the products of predominantly low-energy CID processes rather than unimolecular decay reactions.

PSD investigations carried out on a set of standard peptides showed that mainly a and b type ions were formed under such conditions. These observations are in agreement with general opinion that PSD reactions are low-energy processes.[116]

In the case of PIB polymers, an interesting set of further experiments would have been to compare fragment ions obtained under PSD conditions with other low-energy and high-energy CID methods. Unimolecular decay decompositions at background pressures could also be investigated using the MIKES technique. Such experiments would require the successful application of field desorption/ionisation coupled with four-sector tandem mass spectrometry analysis.

To conclude, it has been demonstrated that polymer adducts formed by MALDI do undergo fragmentation processes in the field-free regions of a time-of-flight mass spectrometer. Fragmentation pathways were observed to depend on both laser powers and pressures. PEG and PS fragmented by low-energy processes such as unimolecular decay and collision-induced decomposition reactions and the ions detected by PSD wee the same as those detected in low-energy CID experiments using field desorption as the ionisation method. The resolution obtained for these experiments was low and, in terms of molecular structure assignment, this method would be unsuitable for the characterisation of end-groups or side chains. Higher resolution experiments such as MALDI-FT-ICR would be more suited to solving such problems.

PIB samples up to m/z =1000 have been shown to fragment readily under PSD conditions. Some structural information was obtained but this was limited by the inherent low resolution of these experiments. It was possible, however, to differentiate between polymers with two and three side-chains. The mono-olefinic PIB sample could not be investigated by such experiments since the relative intensities of parent ions were too weak.

These experiments have shown that PSD could prove to be a useful method in studying the relative stabilities of polymer ions formed by MALDI. Laser energies measured in this thesis suggest that PEG and PS adducts were more stable in the gas phase than PIB silver adducts since the amount of energy required to induce fragmentation was lower in the case of the latter.

7.3 Conclusions

This work has shown that MALDI-TOF MS has been and will continue to be an extremely useful method for the analysis of synthetic polymers. Hydrocarbon polymers still remain a challenge for the mass spectrometrist but developments in sample preparation and methodologies may allow the application of MALDI to the analysis of these compounds. PSD analysis of polymers was shown to be of limited use for structural investigations, however, such experiments may be more useful in fundamental studies as a way of investigating relative stabilities of complexes and ions formed in the gas phase.

REFERENCES

1. Thomson, J. J. and Thomson, G. P. ; *'Conduction of Electricity through Gases,' CUP, Cambridge*, **2**, (1933) ref. to Goldstein, *E.; Berl. Monat*, **284**, (1876).

2. Beynon, J. H. and Morgan, R. P. ; *Int. J. Mass Spectrom. Ion Phys.*, **27**, 2 (1948) ref. to *Wien, W., Verh. Phys. Gesell.*, **17**, (1898).

3. Thomson, J. J. and Thomson, G. P. ; *'Conduction of Electricity through Gases,' CUP, Cambridge*, **2**, 267 (1933).

4. Thomson, J. J. and Thomson, G. P. ; *'Conduction of Electricity through Gases,' CUP, Cambridge*, **1**, 246, (1933).

5. Munson, M. S. B. and Field, F. H. ; *J. Am Chem Soc.*, **88**, 2621 (1966).

6. Munson, M. S. B. and Field, F. H. ; *Anal. Chem.*, **49**, 722A, (1977).

7. Busch, K. L. and Cooks, R. G.; *Science*, **218**, 247, (1982).

8. Lafortune, F., Beavis, R., Tang, X., Standing, G. and Chait, B. T. ; *Rapid Commun. Mass Spectrom.*, **1**, 114, (1987).

9. Barber., M., Bordoli, R. S., Elliot, G. J., Sedgewick, R. D. and Tyler, A. N. ; *J. Chem. Soc. Commun.*, **7**, 328, (1981).

10. McNeal, C. J. and MacFarlane, R. D. ; *J. Am Chem. Soc.*, **103**, 325, (1981).

11. Barber, M., Bordoli, R. S., Elliot, G. J., Sedgwick, R. D., Tyler, A. N. ; *Anal. Chem.* **54**, 645A, (1982).

12. Barber., M., Bordoli, R. S., Elliot, G. J., Sedgwick, R. D., Tyler, A. N., Green, B. N., Parr, V. C. and Gower, J. L. ; *Biomedical Mass Spectrom.*, **9**, 11, (1982).

13. MacFarlane, R. D. and Torgerson, D. F. ; *Science*, **191**, 920, (1976).

14. McNeal C. J. ; *Anal. Chem.*, **54**, 43A, (1982).

15a. Beckey, H. D. ; *Int. J. Mass Spectrom. Ion Phys.* ; **2**, 500, (1969).

15b. Robertson, A. J. B., Viney, B. W. and Warrington, M ; *Bri. J. Appl. Phys.*, **14**, 278, (1963).

16. Prokai, L. (ed) ; *'Field Desorption Mass Spectrometry, ' Marcel Dekker, New York*, (1990).

17. Yamashita, M. and Fenn, J. B. ; *J. Phys. Chem.*, **88,** 4451, (1984).

18. Fenn, J., Mann, M., Meng, C. K. and Wong, S. F. ; *Mass Spectrom. Rev.*, **9**, 37, (1990).

19. Posthumus, M. A., Kstemaker, P. G., Meuzelaar, H. L. C. and Ten Neuer de Brauw., M. C. ; *Anal. Chem.* **50**, 985, (1978).

20. Karas, M. and Hillenkamp, F ; Benninghoven , A. (ed) *Ion Formation from Organic Solids, Springler Series in Chemical Physics*, 25, *Springler-Verlag, New York,* (1983).

21. Karas, M. and Hillenkamp, F. ; *Anal. Chem.* **60,** 2299, (1988).

22. Busch, K. L. ; *J. Mass Spectrom.* **30**, 233, (1995).

23. Kauer, S., Hollander, D., Hass, R. and Burlingame, A. L. ; *J. Am Chem. Soc.*, **197,** 38, (1989).

24. Muller, E. W. ; *Z. Physik,* **131**, 136 (1951).

25. Inghram, M. G. and Gomer, R. ; *J. Chem. Phys.* ; **22,** 1279, (1954).

26a. Beckey, H. D., Hilt, E., and Schultern, H. R. ; *J. Phys. E. Sci.*, **6,** 1043, (1973).

26b. Beckey, H. D., Hendricks, A. and Winkler, H. U. ; *Int. J. Mass Spectrom. Ion Phys.*, **3**, 9, (1970).

27. Beckey, H. D., Bloching, S., Migahed, M. D., Ochterbeck, E. and Schulten H. R. ; *Int. J. Mass Spectrom. Ion Phys.*, **8**, 169, (1971).

28. Migahed, M. D. and Beckey, H. D. ; *Int. J. Mass Spectrom. Ion Phys.*, **7,** 1 (1971).

29. Rabrenovic, M., Ast, T. and Kramer, V. ; *Int. J. Mass Spectrom. and Ion Proc.*, **37,** 297, 1981.

30. Hellal, A. I., Zahram, N. F. and Badaway, W. A. *; Egypt. J. Phys.*, **15,** 175, (1984).

31. Zahram, N. F., Hellal, A. I. and Badaway, W. A. ; *Indian., J. Technol.*, **21,** 478, (1983).

32. Matsuo, T., Matsuda, H, and Karatuse, I. ; *Anal. Chem.*, **51,** 69, (1979).

33. Linden, H., Hilt, E. and Beckey, H. D. ; *J Phys. E; Sci. Instr.*, **11,** 1033, (1978).

34.Lehmann, W. D. and Fischer, R. ; *Anal. Chem.*, **53**, 743, (1981).

35.Kosevich, M. V. and Shelkovsky, V. S. ; *Rapid Commun. Mass Spectrom.*, **7**, 805, (1993).

36.Prokai, L. (ed) ; *'Field Desorption Mass Spectrometry, ' Marcel Dekker, New York,* (1990). ref. to Gomer, R., *J. Chem. Phys.*, **31,** 341, (1959).

37.Derrick, P. J.; *Fresenius, Z. Anal. Chem.* ; **234**, 486, (1986).

38.Prokai, L. (ed) ; *' Field Desorption Mass Spectrometry, ' Marcel Dekker, New York,* (1990). ref. to Rollgen, F. W., Giessmann, U., Wong, S. S. and Okuyama, F. ; *Proceedings of 32nd ACMC and Allied Topics, Boston, USA,* (1983), 513.

39. Tanaka, K., Waki, H., Ido, Y., Akita, S., Yoshida, Y. and Yoshida, M. ; *Rapid Commun. Mass Spectrom.*, **2** 151, (1988).

40. Karas, M. Bachmann, D., Bahr, U. and Hillenkamp. F. ; *Int. J. Mass Spectrom. Ion. Proc.* **78**, 53, (1987).

41. Karas, M., Ingendoh, A., Bahr, U. and Hillenkamp, F. ; *Biomass Envir. Mass Spectrom.*, **18,** 841, (1989).

42. Karas, M., Bachmann, D. and Hillenkamp. F. ; *Anal. Chem.*, **57,** 2935, (1985).

43 Karas, M. and Hillenkamp, F. ; *Adv. Mass Spectrom.*, **11A**, 354, (1988).

44.Solouki, T., Gillig, K. J. and Russell, D. H.; *Anal. Chem.*, **66,** 1583, (1994).

45.Solouki, T., Gillig, K. J. and Russell, D. H. ; *Rapid. Commun. Mass Spectrom.* ; **8,** 26, (1994).

46. Dogruel, Nelson, R. W., Williams, P. ; *Rapid. Commun. Mass Spectrom.* ; **10**, 801 (1996)

47. Dubois, F., Knochenmuss, R., Steenvoorden, R. J. J. M., Breuker, K. and Zenobi, R. ; *Eur. Mass Spectrom.*, **2,** 167-172, 1996.

48. Yau, P. Y., Chan, T. W., Cullis, P. G., Colburn, A. W and Derrick, P. J. ; *Chem. Phys. Lett.*, **202**, 93, (1993).

49. Driesewerd, K., Schurenberg, M., Karas, M. and Hillenkamp, F., ; *Int. J. Mass Spectrom. and Ion Proc.* ; **141**, 127, (1995).

50.Karas, M., Bachmann, D., Bahr, U. and Hillenkamp, F. ; *Int. J. Mass Spectrom. Ion Proc.* **78,** 53, (1987).

51. Karas, M., Bahr, U., Ingendoh, A., Nordhoff, E., Stahl, B., Strupat, K. and Hillenkamp, F. ; *Anal. Chimica. Acta,* **241**, 175, (1990).

52.Ehring, H., Karas, M. and Hillenkamp. F. ; *Org. Mass Spectrom.*, **27**, 472, (1992).

53. White, M. A. and Russell, D. H ; *Proceedings of the 39th ASMS Conference on Mass Spectrometry and Allied Topics, Nashville, Tennssee, May19-24,* (1991).

54. Gimon, M. E., Preston, L. M., Solouki, White, M. A. and Russell, D. H. ; *Org, Mass Spectrom. Lett. ;* **27**, 827, (1992).

55. Hillenkamp, F., Bahr, U., Karas, M. and Spengler, B. ; *Scanning Microscopy Supplement,* **1**, 33, (1987).

56. Figueroa, I. D., Campo, K. K. and Russell, D. H. ; *Proceedings of the 45th ASMS Conference on Mass Spectrometry and Allied Topics ; Palm Springs, California,* . (1997).

57. Sumner, L. W., Gray, J. P., Kirkpatrick, J. R. and Russell, D. H. ; *Proceedings of the 45th ASMS Conference on Mass Spectrometry and Allied Topics ; Palm Springs, California,* (1997).

58. Lard, C. M. and Kinsel, G. R. *; Proceedings of the 45th ASMS Conference on Mass Spectrometry and Allied Topics ; Palm Springs, California,* (1997).

59. Grigorean, G., Carey, R. and Amster, J.; *Eur. Mass Spectrom.*, **2,** 139-143, (1996).

60. Bolkermann, V., Spengler, B and Kaufmann, R. ; *Eur. Mass Spectrom.*, **1,** 81-93, (1995).

61. Beavis, R. C. and Chait, B. T. ; *Rapid Commun. Mass Spectrom.*, **3,** 12, (1989)

62. Karas. M., Hillenkamp, F, Beavis, R. C. and Chait, R. C. ; *Anal. Chem.*, **63,** 1193A, (1991).

63. Beavis, R. C., Chaudhary, T. and Chait, B. T. ; *Org. Mass Spectrom.*, **27**, 156, (1992).

64. Cordero, M. M., Cornish, T. J. and Cotter, R. J. ; *Rapid. Commun. Mass Spectrom.*, **9**, 1356, (1995).

65. Brown, R. S., Carr, B. L and Lennon, J. J ; *J. Am. Soc. Mass Spectrom.*, ; **7**, 225, (1996).

66. Fong, J. and Brown, R. S.; *Proceedings of the 45th ASMS Conference on Mass Spectrometry and Allied Topics ; Palm Springs, California,* (1997).

67. Brune, D. C. and Jeung, J. ; *Proceedings of the 45th ASMS Conference on Mass Spectrometry and Allied Topics ; Palm Springs, California,* (1997).

68a. Alimpiev, S. S., Mlynski, V. V., Belov, M. E. and Nikiforov, S. M. ; *Anal. Chem.*, **67,** 181, (1995).

68b. Belov, M. E., Alimiev, S. S., Mlynski, V. V., Nikiforov, S. M. and Derrick, P. J.; *Rapid. Commun. Mass Spectrom.*, **9,** 1431, (1995).

69.Berkenkamp, S., Karas, M. and Hillenkamp, F. ; *Proc. Nat. Acad. Sci. of United States of America*, **93**, 4003, (1996).

70. Strupat, K., Karas, M. and Hillenkamp, F. ; *Int. J. Mass Spectrom. and Ion Proc.*, **111,** 89, (1991).

71. Bahr, U, Deppe, A, Kara, M. and Hillenkamp. F. and Giessmann, U., ; *Anal. Chem.* **64,** 22, 2866, (1992).

72.Karas, M, Ehring, H., Nordhoff, E., Stahl, B., Strupart, K., Hillenkamp, F., Grehl, M., Krebs, B ; *Org. Mass Spectrom.*, **28**, 1496, (1993).

73. Danis, P. O. and Karr, D. E. ; *Org. Mass Spectrom.* ; **28**, 923, (1993).

74. Juhasz, P. and Costello, C. E. ; *Rapid Commun. Mass Spectrom.*, **7**, 346, (1993).

75. Montaudo, G., Montaudo, M. S., Puglisi, C., Samperi, R. ; *Rapid Commun. Mass Spectrom.*, **8**, 1011 (1994).

76. Juhasz, P., Costello, C. E., Biemann, K. ; *J. Am. Soc. Mass Spectrom.*, **4**, 399, (1996).

77. Liu, H. M. D. and Schulegger, U. P.; *Rapid Commun. Mass Spectrom.*, **10,** 870 (1996).

78. Zollner, P., Schmid, E. R., Allmaier, G. ; *Rapid Commun. Mass Spectrom.*, **10,** 1278, (1996).

79.Michalak, L. M, Fischer, K. J., Alderdice, D. S., Jardine, D. R. and Willett, G. D. ; *Org. Mass Spectrom. Lett.*, ; **29**, 512, (1994).

80.McCarley, T. D., R. L. McCarley and Limbach, P. A. ; *Proceedings of the 45th ASMS Conference on Mass Spectrometry and Allied Topics ; Palm Springs, California*, (1997).

81a. Overburg, A., Karas, M., Bahr, U., Kaufmann, R. and Hillenkamp, F.; *Rapid Commun. Mass Spectrom.*, **4**, 293, (1990).

81b. Overburg, A., Karas, M. and Hillenkamp, F.; *Rapid Commun. Mass Spectrom.*, **5**, 128, (1991).

82. Constantin, E. and Schnell, A. ; *'Mass Spectrometry', Ellis Horwood, London, reprinted* (1991).

83. Chapman, J. R. ; *'Practical Organic Mass Spectrometry,' John Wiley and Sons Ltd., Reprinted June 1995*

84. Wiley, W. C. and I. H. MacLaren, ; *Rev. Sci. Instr.*, **26**, 1150, (1955).

85. Koster, C., Castoro, J. A., Wilkins, C. L. ; *J. Am Soc. Mass Spectrom.*, **114**, 7572, (1992).

86. McLafferty, F. W. ; *Acc. Chem. Res.*, **27**, 379, (1994).

87. Herzog, R. ; *Z. Phys.* **89**, 447, (1934).

88. Mattauch, J. and Herzog, R. ; *Z Phys.*, **89**, 786, (1934).

89. Lewis, R. and Beyer, N. ; *Adv. Mass Spectrom.*, **2**, 198, (1963).

90. Johnson, E. G. and Nier, A. O. ; *Phys. Rev.*, **10**, (1953).

91. Guilhaus, M. ; *J. Mass Spectrom.*, **30**, 1519, (1995).

92. Stephens, W. E. ; *Phys. Rev.*, **69**, 691, (1946).

93. Beavis, R. C. and Chait, B. T. ; *Anal. Chem.*, **62**, 1836, (1990).

94. Spengler, B., Kirsch, D., Kaufmann, R., Karas, M. Hillenkamp, F. and Giessmann, U ; *Rapid Commun. Mass Spectrom.*, **4**, 301, (1990).

95.Mamyrin, B. A.; USSR Patent # **198**, 034 (1966).

96. Mamyrin, B. A., Karataev, V. I., Shrikk, D. V. and Zagulin, V. A. ; *Sov. Phys. JETP*, **37**, 45 (1973).

97. Karataev, V. I., Mamyrin, B. A. and Schnikk, D. V. ; *J. Tech. Phys.*, **16,** 1498, (1971).

98. Kinsel, G, R., Mowry, C. D., McKown, P. J. and Johnston, M. V. ; *Int. J. Mass Spectrom., Ion Proc.* ; **91**, 157, (1991).

99. Comisatow, M. and Marshall, A. G. ; *Chem. Phys. Lett. ;* **25,** 282, (1974).

100. Miranker, A., Robinson, C. V., Radford, S. E., Alpin, R. T. and Dobson, C. M. ; *Science,* **262**, 896, (1993).

101. Cody, R. B., Burnier, R. C. and Freiser, B. S. ; *Anal. Chem.*, **54**, 96, (1982).

102. Chen, L., Wang, T.-C, Ricca, T. L. and Marshall, A. G. ; *Anal. Chem.*, **59,** 449 (1991).

103. Aston, F. W. ; *Proc. Cambridge, Philos., Soc.*, **19**, 317, (1919)

104. Mattauch, J. and Lichtblau, H. ; *Phys. Zeit.*, **40,** 16, (1939).

105. Hipple, J. A., Fox, F. E. and Cordon, E. U. ; *Phys. Rev.*, **69, 47,** (1946).

106. Sheil, M. M. and Derrick, P. J. ; *Org. Mass Spectrom.*, **23,** 429, (1988).

107. Bradley, C. D. ; *PhD Thesis, University of Warwick, United Kingdom,* (1992).

108. Cooper, H. ; *PhD Thesis, University of Warwick, United Kingdom,* (1995).

109. Moseley, J. ; PhD Thesis, *University of Warwick, United Kingdom,* (1996).

110. Spengler, B., Kirsch, D. and Kaufmann, R ; *Rapid Commun. Mass Spectrom.*, **5,** 198, (1991).

111. Spengler, B., Kirsch, D. and Kaufmann, R. ; *J. Phys. Chem.*, **96**, 9678, (1992).

112. Raptakis, E. ; *PhD Thesis, University of Warwick, United Kingdom,* (1996).

113. Cornish, T. J. and Cotter, R. J. *; Proceedings of the 43rd. ASMS Conference on Mass Spectrometry and Allied Topics. Atlanta, USA,* 133, (1995)

114. Cordero, M. M., Cornish, T. J. and Cotter R. J. ; *Rapid Commun. Mass Spectrom.*, **9,** 1356, (1995).

115. Rouse, J. C., Yu, W. and Martin, S. A. ; *J. Am. Soc. Mass Spectrom.* ; **6, 822,** (1995).

116. Jai-nhukan, J. and Cassday, C. J. ; *Rapid Commun. Mass Spectrom.*, **10, 1678,** (1996).

117. Osprina, M., Powell, D. H., Sapp, L., Deslow, N. and Yost, R. A. ; *Proceedings of the 45th ASMS Conference on Mass Spectrometry and Allied Topics ; Palm Springs, California,* (1997).

118. Talbo, G. and Mann, M. ; *Rapid Commun. Mass Spectrom.* ; **10**, 100, (1996).

119. Yamagaki, T., Ishizuka, Y., Kawabata, S. and Nakanishi, H ; *Rapid Commun. Mass Spectrom.*, **10,** 1887, (1996).

120. Jai-nhukan, J. and Cassday ; C. J. *Proceedings of the 45th ASMS Conference on Mass Spectrometry and Allied Topics ; Palm Springs, California,* (1997).

121. Chaurand, P., Kaufmann, R., Lutzenkirchen and Spengler, B ; *Proceedings of the 45th ASMS Conference on Mass Spectrometry and Allied Topics ; Palm Springs, California,* (1997).

122. Bowdler, A. R., Demetriades, N., Humphrey, P. and Resch, M. ; *Proceedings of the 45th ASMS Conference on Mass Spectrometry and Allied Topics ; Palm Springs, California,* (1997).

123. Kaufmann, R., Spengler, B. and Lutzenkirchen, F. ; *Rapid Commun. Mass Spectrom. Mass Spectrom.*, **7,** 902, (1993).

124. Kaufmann, R., Kirsch, D. and Spengler, B ; *Int. J. Mass Spectrom., Ion Proc. ;* **131,** 355, (1994.)

125. Kaufmann, R., Kirsch, D., Tourmann, J. L., Machold, J., Hucjo, Ulkin, Y. and Tsetlin, V ; *Eur. Mass Spectrom.*, **1,** 313, (1995).

126 Medhihadszky, K. F., Adams, G. W., Burlingame, A. L, Bateman, R. H and Green M. R. ; *J. Am. Soc., Mass Spectrom.*, **7,** 1, (1996).

127. Jackson, A. T., Yates, H. T., Scrivens, J. H., Critchley, G., Brown, J., Green, M.R. and Bateman, R. H. ; *Rapid Commun. Mass Spectrom.*, **10,** 1668 (1996).

128. Elias, H. G., *' An Introduction to Polymer Science, ' 1st. Ed., Weiheim,* (1997).

129. Challa, G., *' Polymer Chemistry, ' Ellis Horwood,* (1993).

130. Medinavera, M. ; *J. Anal. and Appl. Pyrol.*, **36,** 27, (1996).

131. Wiley, R. H. and Cook, Jr., J. C. ; *J. Macromol. Sci. Chem.* ; **10,** 811, (1976).

132. Matsuo, T., Matsuda, H. and Katakuse, I. ; *Anal. Chem.*, **51,** 1329, (1979).

133. Craig, A. G., *PhD. Thesis, University of New South Wales, Austrailia,* (1984).

134. Craig, A. G. and Derrick, P. J. ; *Aust. J. Chem.*, **39**, 421, (1986).

135. Lattimer, R. P. and Schulten, H. R. ; *Int. J. Mass Spectrom. Ion. Phys.*, **52**, 105, (1983).

136. Lattimer, R. P., Harmon, D. J. and Hansen, G. E. ; *Anal. Chem.*, **52**, 1808, (1980).

137. Craig, A. J., Cullis, R. P. and Derrick, P. J. ; *Int. J. Mass Spectrom., Ion Proc.*, **38**, 397, (1981).

138.Jardine, D. R., Nekula, S., Thang-Thong, N., Haddad, P. R., Derrick, P. J, Grespos, E. and O' Donnell, J. H. ; *Macromol.* **19**, 1770, (1986).

139.Craig, A. G. and Derrick, P. J. ; *J. Am Chem. Soc.* ; **107**, 6707, (1985).

140 Cullis, A. G. and Derrick, P. J. ; J. *Chem. Soc. Chem. Commun*, **89**, (1985).

141.McCrae, C. E. and Derrick, P. J.; *Org. Mass Spectrom.*, **18**, 321, (1983).

142.Agma, M. ; *PhD. Thesis, University of New South Wales, Austrailia*, (1989.)

143. Van Breeman, R. B., Huang, C.-H. and Burngardner, C. L ; *Anal. Chem.*, **##**, 2577, (1991).

144. Hope, F. W. ; *PhD. Thesis, University of New South Wales, Austrailia*, (1988).

145. Kukuli, D., Davis, T. P., Suddaby. K. G. and Haddleton, D. M. ; *J. Polymer Sci. Part A. - Polymer Chem.*, **35**, 859, (1997).

146.Dunclaf, D. J., Wade, H. J., Waterson, C. Derrick, P. J., Haddleton, D. M. and McCamley, A. ; *Macromol.* **29**, 6399, (1996).

147.Haddleton, D. M., Hunt, K. H. and Crossman, M. C. ; *Macromol. Symp.*, **107**, 1022, (1996).

148. Haddleton, D. M., Topping, C., Hastings, J. J. and Suddaby, K. G. ; *Macromol. Chem. and Phys.*, **197**, 3027, (1996).

149. Montaudo, G., Montaudo, M. S., Puglisis, C., Samperi, F., Spassky, N., Leborgne, A. and Wisniewski, M. ; *Macromol.*, **29**, 6461, (1996).

150. Montaudo, G., Montaudo, M. S., Puglisi, C., Samperi, F. and Sepulchro, M. ; *Macromol. Chem. and Phys.*, **197**, 2615, (1996).

151. Pasch, H., Rode, K., Glahary, R. and Braun, D. ; *Ang. Makromol. Chemie*, **241**, 95, (1996).

152. Spickermann, J., Rader, H. J., Mullen, K., Muller, B., Gerle, M., Fischer, K. and Schimdt, M. ; *Macromol. Rapid, Comm.*, **17**, 885, (1996).

153. Llenes, C. F. and O'Malley, R. M. ; *Rapid Commun. Mass Spectrom.*, **6**, 564 (1992).

154. Mowat, I. A. and Donovan, R. J. ; *Rapid. Commun. Mass Spectrom.*, **9**, 82, (1995).

155. Fong, W. Y. K., *3rd. Year Project Report, 'Interactions of Organic Polymers,'* March, (1994).

156. Scrivener, E., Fong, K. W., Lloyd, P. M., Maloney, D. R., Eason, M., Cox, A., Haddleton, D. M. and Derrick, P. J ; *Unpublished results.*

157. Von Helden, G. T., Wytterbach and T., Bowers ; M. T. ; *Science*, **267**, 1483, (1995).

158. Von Helden, G. T., Wytterbach and T., Bowers ; M. T ; *Int. J. Mass Spectrom. Ion Proc.*, **146**, 349, (1995).

159. Wong, C. K. L. and Chan, T. W. D. ; *Rapid. Commun. Mass Spectrom.*, **5**, 513, (1997).

160. Deery, M. J., Jennings, K. R., Jasieczek, C. B., Haddleton, D. M., Jackson, A. T., Yates, H. T. and Scrivens, J.H. ; *Rapid. Commun. Mass Spectrom.*, **11**, 57, (1997).

161. Humphrey, P., Kimber, M., Paulus, G., Resch, M., and Tanaka, K. ; *Proceedings of the 45th ASMS Conference on Mass Spectrometry and Allied Topics ; Palm Springs, California*, (1997).

162. Jackson, A. T., Yates, H. T., Lindsay, C. I., Didler, Y., Segal, J. A., Scrivens, J. H., Critchley, G. and Brown, J. ; *Rapid. Commun. Mass Spectrom.*,**11**, 520, (1997).

163. Mowat, I. A. and Donovan, R. J. ; *Rapid. Commun. Mass Spectrom.*,**11**, 89, (1997).

164. Axellson, J. Scrivener, E., Haddleton, D. M. and Derrick, P. J. ; *Macromol.* **29**, 8875, (1996).

165. Axelsson, J. and Reimann, C. T. ; *Nucl. Instr. and Meth.* **B 88,** 131, 1994.

166. Axelsson, J. and Reimann, C. T. ; *Nucl. Instr. and Meth.* **B 88,** 499, 1994.

167. McEwen, C. N., Jackson, C. T. and Larsen, B. S., *Int. J. Mass Spectrom. and Ion Proc.*, **160,** 387, (1997).

168. Jackson, C., Larsen, B., and McEwen, C. ; *Anal. Chem.*, **68,** 1303, (1996).

169. Burger, H. M., Muller, H. M., Seebach, D., Bornsen, K., Schar, M. and Widmer, H. M. ; *Macromol.*, **26,** 4783, (1993).

170. Martin, K., Spickermann, J., Rader, H. J. and Mullen, K. ; Rapid. Commun. Mass Spectrom., 10, 1471, (1996).

171. Spickermann, J., Martin, K., Rader, H. J., Muller, K., Schlaad, H., Muller, A. H. E., and Kruger, R. P. ; *Eur. Mass Spec.* **2,** 161, (1996).

172. Montaudo, M. S., Puglisi, C. and Samperi, F. ; *Rapid, Commun. Mass Spectrom.*, **9,** 453, (1995).

173. Montaudo, G., Scamporrino, E., Vitalini, D. and Mireo, P. ; *Rapid. Commun. Mass Spectrom.* ; **10,** 1551, (1996).

174. Hogan, J. D., Laude, D. A. J. ; *Anal. Chem.*, **64,** 763, (1992).

175. Day, M., Castoro, J. A., Wilkins, C. L. ; *Anal. Chem.*, **67,** 1575 (1995).

176. de Koster, C. G., Duursma, M. C., van Rooij, G. J., Heeren, R. M. A., Boon J. J., *Rapid Commun. Mass Spectrom.*, **9,** 957, (1995).

177. Van Rooij, G. J, Duursma, M. C., Heeren, R. M. A., Boon, J. J. de Koster, C. G ; *J. Am. Soc. Mass Spec.*, **7,** 449, (1996).

178. Sric, D., Martinovic, S., Pasa-Tolic, L., Kezele, N., Kazazic, L., Shevchenko, S. M., Klaisine, L ; *Rapid. Commun. Mass Spectrom.*, **10,** 580, (1996).

179. Cromwell, E. F., Reihs, K., de Vries, M. S., Ghaderi, S., Wehdt, H. R. and Hunziker, H. E. ; *J. Phys. Chimie.*, **97,** 4720, (1993).

180. Kahr, M. S. and Wilkins, C. L. ; *J. Am. Soc. Mass Spectrom.* ; **4,** 453, (1993).

181. Campana, J. E., Sheng, L.-S., Shew, S. L. and Winger, B. E. ; *Trends Anal. Chem.*, **13,** 239, (1994).

182. Kratos Analytical, Wharfside. Trafford Wharf Road, Manchester, UK.

183. Davis, S. C., Neumann, G. M., and Derrick, P. J. ; *Anal. Chem.*, **59**, 1360, (1987).

184.Davis, S. C. ; *PhD. Thesis, University of New South Wales, Austrailia, (*1988*).*

185. Westman, A., Demirev, P., Huth-Fehre, T., Bielawski, J. and Sundqvist, B. U. R. ; *Int. J. Mass Spectrom. Ion. Proc.*, **130**, 107, (1994).

186.Vorm, O., Roepstorff, P. and Mann, M ; *Anal. Chem.*, **66**, 3281, (1994).

187. Perera, I. K., Perkins, J. and Kantartzoglou, S. ; *Rapid. Commun. Mass Spectrom.*, **9**, 180, (1995).

188. Allwood, D. A., Perera, I.K., Perkins, J., Dyer, P. E. and Oldershaw, G. A. ; *Appl. Surf. Science*, **103**, 3, (1996).

189. Xiang, F. and Beavis, R. C. ; Rapid. Commun. Mass Spectrom., **8**, 199, (1994).

190. Axellson, J., Hoberg, A-M, Waterson, C., Myatt, P., Shield, G.L., Varney, J. E., Haddleton, D. M. and Derrick, P. J. ; *Rapid. Commun. Mass Spectrom.*, **11**, 209, (1997).

191.Chan, T-W.D and Derrick, P. J. ; *MSc. Thesis, University of Warwick, UK. (1989)*

192. Evans, W. J., Decoster, D. M. and Greaves, J., *J. Am. Soc. Mass Spectrom.*, **7**, 1070, (1996).

193. Varney, J. E., Lloyd, P. M. and Derrick, P. J. ; *Poster Presented at 21st BMSS Meeting, Manchester, (1995).*

194. Lehrle, R. S. and Sarson, D ; *Rapid Commun. Mass Spectrom.*, **9**, 91 (1995).

195. Lloyd, P. M., Suddaby, K. G., Varney, J. E., Scrivener, E., Derrick, P. J. and Haddleton, D. M ; *Eur. Mass Spectrom.*, **1**, 293, (1995).

196. Schriemer, D. C., Whittal, R. M. and Li, L. ; *Macromol.*, **30**, 1955, (1997).

197. Mahon, A, Kemp, T. J., Buzy, A. and Jennings, K, R, J. ; *Polymer*, **37**, 531, (1996).

198. Mahon, A, Kemp, T. J., Buzy, A. and Jennings, K, R, J. ; *Polymer*, **38**, 2337, (1996).

199. Chan, T. W. D, Colburn, A. W., Alderdice, D. S. and Derrick, P. J. ; *Int. J. Mass Spectrom. and Ion Proc.*, 491, (1991).

200. Humphries, P and Bowdler. A. R ; *Proceedings of the 45th ASMS Conference on Mass Spectrometry and Allied Topics ; Palm Springs, California,* (1997).

201.Hittle, H. R. and Hercules, D. M. ; *Surf. and Interface Anal.*, **21**, 217 (1994).

202. Waterson, C. ; *Personal Communication*

203. Perera, I. K., Kartartzoglou and S , Dyer, P. E., ; *Rapid. Commun. Mass Spectrom.*,, (1996).

204.P. Myatt, *Personal Communication.*

205.Liu, H. M. D. and Schlunegger. U. P. ; *Rapid. Commun. Mass Spectrom.*, **10**, 483, (1996).

206. Danis, P. O., Karr, D. E., Xoing, Y. and Owens, K. G. ; *Rapid Commun. Mass Spectrom.*, 10, 862, (1996).

207. Li, H., Lee, V., Siu, M. And Guevremont, R. ; *Proceedings of the 45th ASMS Conference on Mass Spectrometry and Allied Topics ; Palm Springs, California,* (1997).

208. Shriver, D. F., Atkins, P. W. and Langford, C. H.; *Inorganic Chemistry,* Oxford University Press, 1st Edition, (1990).

DX

210241